

Application of a supercritical carbon dioxide extraction unit

Extraction of *Iris germanica* L. and *Rosmarinus officinalis* L.

Dissertation

zur Erlangung des Grades

Doktor der Naturwissenschaften (Dr. rer. nat.)

Fakultät für Chemie und Pharmazie

Universität Regensburg



vorgelegt von

Alexander Wollinger

aus Hengersberg

Februar 2016

Promotionsgesuch eingereicht am: 29.02.2016

Promotionskolloquium am : 13.04.2016

Die Arbeit wurde angeleitet von Prof. Dr. Werner Kunz, Lehrstuhl für Physikalische und Theoretische Chemie II der Universität Regensburg.

Promotionsausschuss:

Vorsitzender:	Prof. Dr. Henri Brunner
1. Gutachter:	Prof. Dr. Werner Kunz
2. Gutachter:	Prof. Dr. Frank-Michael Matysik
3. Prüfer:	Prof. Dr. Hubert Motschmann

Acknowledgment

Diese Doktorarbeit entstand in der Zeit von November 2012 bis April 2016 am Lehrstuhl für Physikalische und Theoretische Chemie II der Universität Regensburg unter der Betreuung von Prof. Dr. Werner Kunz. An dieser Stelle möchte ich mich herzlich bei allen bedanken, die mich während der Anfertigung dieser Arbeit unterstützt haben.

Zuerst gebührt mein Dank Herrn Prof. Dr. Werner Kunz für die Möglichkeit, diese Doktorarbeit mit dem interessanten und abwechslungsreichen Thema „Pflanzenextraktion“ an seinem Lehrstuhl für Physikalische Chemie anfertigen zu können. Vielen Dank auch für die vielen Ideen, Ratschläge und Hilfestellungen während der letzten Jahre.

Außerdem möchte ich mich bei Prof. Dr. Frank-Michael Matysik bedanken, der die Aufgabe als Zweitgutachter übernimmt. Des Weiteren danke ich Prof. Dr. Hubert Motschmann, dass er als Drittprüfer eintritt sowie Prof. Dr. Henri Brunner für die Übernahme des Vorsitzes meines Promotionskolloquiums.

Besonderer Dank geht an meine beiden „Extraktionskollegen“ und Freunde Theresa Höß und Dr. Marcel Flemming. Vielen Dank für die tolle Zeit im Labor, die unzähligen Diskussionen und vor allem die unvergesslichen Dienstreisen. Im Einzelnen danke ich Theresa für die Korrektur der Doktorarbeit und die hilfreichen Kommentare.

Außerdem danke ich Dr. Julien Marcus für die Einführung in Statistische Versuchsplanung, das Übersetzen von französischen E-Mails und Paper sowie für die Korrektur der Doktorarbeit. Merci beaucoup.

Weiterhin möchte ich Dr. Didier Touraud für die zahlreichen und guten Ideen für diese Doktorarbeit danken. Merci.

Vielen Dank an meine Kollegen für die wissenschaftliche Hilfe und die super Atmosphäre am Lehrstuhl. Dankeschön an Vroni, Julien, Auriane, Stefan, Lydia, Theresa, Andreas S., Julian, Gabriel, Tatjana, Tini, Marcel, Claudia, Andreas N., Käthe, Damian, Sebastian, Tobi sowie allen anderen Lehrstuhlmitgliedern.

Außerdem möchte ich den Studenten Johannes Schwarz, Lukas Wirth, Neslihan Aslan, Christian Mayer, Ramona Höflinger, Lukas Koch, Michael Peer danken, die mich im Rahmen ihrer Bachelorarbeit im Labor unterstützt haben, sowie den Forschungspraktikanten Franz Schermer und Alexander-Anton Dietz. Besonderer Dank gebührt Elodie Perrin, mit deren Hilfe ich die ersten Extraktionsversuche durchgeführt habe.

Bei der Firma Phytotagante, insbesondere bei Jamal Chahboun, bedanke ich mich für die Irisrhizome und Rosmarinblätter.

Weiterhin bedanke ich mich bei den Mitarbeitern der Firma Separex Romain Polanz, Anne-Lise Humbert, Jeremy Lagrue und Guillaume Tisserant für die tolle Unterstützung und hilfreichen Tipps bei der Bedienung und Reparatur der Extraktionsanlage. Merci beaucoup pour votre aide et soutien.

Für die Unterstützung und Hilfestellungen in Sachen HPLC- und GC-Analyse bedanke ich mich herzlichst bei Prof. Dr. Jörg Heilmann sowie Josef Kiermaier.

Ein ganz besonderes Dankeschön gilt meinem Freund Christian für die alltägliche Unterstützung und Aufmunterung während der Zeit zur Anfertigung dieser Arbeit. Vielen Dank auch für die zahlreichen und großartigen Fotos, die ich in dieser Arbeit verwenden kann.

Im Besonderen danke ich meinen Eltern für die mentale und finanzielle Unterstützung während des Studiums und der Doktorarbeit. Vielen Dank, dass ihr immer an mich geglaubt habt. Ohne euch hätte ich es nicht so weit geschafft.

Regensburg, 29.02.2016

Wollinger Alexander

Abstract

This dissertation deals with the investigation and optimization of new and existing extraction methods in regard to the principles of “green extraction” and “green chemistry”. The thesis consists of three major topics. In the first part, the application of a supercritical fluid extraction unit is described, whereas in the second part the unit is used to extract odorants from iris (*Iris germanica* L.) rhizomes. The third part deals with the extraction and application of antioxidants from rosemary (*Rosmarinus officinalis* L.) leaves.

Over the last years, new sustainable and green extraction methods became more and more important. Supercritical fluid extraction (SFE) with carbon dioxide is an alternative technique to conventional methods for plant extraction. The first topic deals with the planning and installation of a new supercritical fluid extraction unit. In detail, this unit was purchased from Separex/France and is a major part of the new research topic “plant extractions” at the “Institute of Physical and Theoretical Chemistry” of the University Regensburg. This device enables extractions with supercritical carbon dioxide up to 1,000 bar and 150 °C. Also pressurized solvent extraction with water, ethanol, and other solvents up to 400 bar and 250 °C, are feasible. In addition, a combination of both techniques can be performed. Furthermore, the fractionation of the extract can be achieved by two separators. The construction with the different components of the extraction unit is described in Chapter 5. This section is considered to be a handbook and instruction manual for the handling of the unit for future PhD students. Besides, some troubles with the unit and the corresponding troubleshooting will be described.

The main aim of the second part of this thesis was the establishment of a new extraction method to obtain iris butter, the essential oil of iris rhizomes. Supercritical fluid extraction with carbon dioxide was used as an alternative technique to conventional extraction methods. The research was focused on a fast, selective, and environmentally friendly extraction of irones, the main odorants in iris rhizomes. Preliminary experiments by SFE showed that the extraction of irones from iris rhizomes is a very complex process. For this reason, a design of experiments (DoE) was used in order to investigate the importance and best values of several extraction parameters on the irone yield. In detail, the extraction time, the flow of CO₂, and both the temperature and pressure in the extraction vessel, the first separator, and the second separator of SFE were investigated. However, the result of DoE showed that the extraction of irones by SFE is not exhaustive and selective enough. Only one third of the actual irone content in the rhizomes were extracted. For this reason, the parameters obtained by DoE were used as the basis of further experiments in order to improve the extraction efficiency and selectivity. It was determined that an extraction pressure of 100 bar and a temperature of 60 °C increase significantly the selectivity of irone extraction from iris rhizomes. In fact, SFE-extracts were obtained which contain up to 30% of irones. This is

three times the amount compared to conventional iris butter obtained by steam distillation. The only disadvantage of this procedure is the non-exhaustive extraction efficiency of irones. Further attempts to enhance the irone yield were not successful. In addition, appropriate methods to determine the residual moisture and irone content of iris rhizomes are described.

The third part of this thesis deals with antioxidant compounds in rosemary leaves. The importance of natural sources of antioxidants has significantly increased in the last years. The reason is that artificial antioxidants are prohibited as food additives because of the potential toxic and carcinogen properties. The main antioxidants in rosemary are rosmarinic acid (water soluble) and carnosic acid (not water soluble). First investigations were performed in order to determine the influence of hydro distillation on these antioxidants. Hydro distillation is a common way to extract essential oil from rosemary leaves. It was found that large amounts of antioxidants get lost during hydro distillation. On the one hand, antioxidants, especially rosmarinic acid, are solubilized in the hydro distillation water residue. The antioxidant activity in the residual water, determined by radical scavenging experiments with DPPH, reaches a maximum value after 2.5 h of hydro distillation. On the other hand, the long exposure of heat during distillation also influences the residual antioxidants, especially carnosic acid, in the leaves. Actually, 76% of the initial rosmarinic acid and 36% of the initial carnosic acid get lost during hydro distillation. In regard to the concept of biorefinery, it would be desirable to see the hydro distillation water residue as co-product of the extraction and not as waste product. Therefore, this residue was taken and introduced in different microemulsions. It was shown that the hydro distillation water residue can enhance the antioxidant activity of drinkable microemulsions. Thus, this antioxidant water residue can be an alternative to common antioxidants, like ascorbic acid, in conventional beverages. In the final part of the rosemary chapter, an alternative green extraction method of antioxidants from rosemary leaves is presented. In particular, micellar extractions with different salts of fatty acids were performed. It is shown that almost the total amount of rosmarinic acid and three-quarter of the water insoluble carnosic acid can be extracted by means of a 4 wt% sodium myristate within 5 min. In addition, an alternative processing method of the extract was invented in order to recover selectively the carnosic acid. This is the first process used to obtain carnosic acid by extractions of rosemary leaves with aqueous solutions.

To sum up, two new green extraction methods were established for the extraction of odorants from iris rhizomes and antioxidants from rosemary leaves. In addition, an approach is presented to valorize the hydro distillation water residue of rosemary leaves. These methods enhance the extraction techniques in regard to the principles of green extraction and biorefinery.

Zusammenfassung

Diese Doktorarbeit handelt über die Erforschung neuer und die Optimierung bestehender Extraktionsverfahren im Hinblick auf die Grundsätze von grüner Extraktion und Bioraffinerie. Diese Arbeit ist dabei in drei große Themengebiete gegliedert. Im ersten Teil werden der Aufbau und die Anwendung einer Anlage zur Extraktion mit überkritischen Lösungsmitteln beschrieben. Im zweiten Teil wird diese Anlage dazu verwendet, um Duftstoffe aus Rhizomen der Schwertlilie (*Iris germanica* L.) zu extrahieren. Der dritte Teil beschäftigt sich dagegen mit der Gewinnung und Anwendung von Antioxidantien aus Rosmarinblättern (*Rosmarinus officinalis* L.).

In den letzten Jahren wurde die Bedeutung von neuen nachhaltigen und grünen Extraktionsverfahren immer wichtiger. Die Extraktion von Inhaltsstoffen aus Pflanzen mit Hilfe von überkritischem Kohlenstoffdioxid ist eine alternative Methode zu herkömmlichen Extraktionsverfahren. Das erste Thema dieser Doktorarbeit befasst sich mit der Planung und Installation einer neuen erworbenen Hochdruckextraktionsanlage. Das Gerät wurde von der Firma Separex/Frankreich hergestellt. Diese soll ein wichtiger Bestandteil des neuen Forschungsgebiets "Pflanzenextraktionen" am "Institut für Physikalische und Theoretische Chemie" der Universität Regensburg werden. Mit Hilfe der Anlage ist es möglich Extraktionen mit überkritischem Kohlendioxid bis zu 1.000 bar und 150 °C durchzuführen. Außerdem ermöglicht sie Lösungsmittlextraktionen mit Wasser, Ethanol oder anderen Lösungsmitteln bis zu einem Druck von 400 bar und einer Temperatur von 250 °. Darüber hinaus kann auch eine Kombination beider Verfahren durchgeführt werden. Weiterhin kann mit Hilfe von zwei Separatoren eine Fraktionierung des Extrakts erreicht werden. Der Aufbau und die verschiedenen Komponenten der Extraktionsanlage sind in Kapitel 5 beschrieben. Dieser Abschnitt soll dabei als Bedienungsanleitung für den Umgang mit der Anlage dienen, vor allem für zukünftige Doktoranden. Außerdem werden einige Probleme mit dem Gerät und die entsprechende Fehlerbehebungen beschrieben.

Im zweiten Abschnitt dieser Arbeit wird eine neue Extraktionsmethode zur Gewinnung von Iris Butter, dem ätherischen Öl von Irisrhizomen, beschrieben. Dazu wird die Extraktion mit überkritischem Kohlenstoffdioxid als Alternative zu herkömmlichen Extraktionsverfahren verwendet. Das Ziel dabei war die Hauptduftstoffe in Irisrhizomen, nämlich Irone, auf eine schnelle, selektive und umweltfreundliche Weise zu extrahieren. Jedoch zeigten bereits Vorversuche, dass die Extraktion von Ironen aus den Rhizomen mit überkritischem CO₂ ein sehr komplexer Vorgang ist. Aus diesem Grund, wurde die Statistische Versuchsplanung angewandt, um die Wichtigkeit und die besten Werte von mehreren Extraktionsparametern auf die Ironausbeute zu bestimmen. Im Einzelnen wurden der CO₂-Fluss, die Extraktionszeit und jeweils der Druck und die Temperatur in der Extraktionszelle und den beiden Separatoren untersucht. Jedoch zeigten die Ergebnisse, dass die Extraktion von Ironen mit

überkritischem CO₂ nicht vollständig und selektiv genug ist. Es konnte nur ein Drittel des aktuellen Irongehalts in den Rhizomen extrahiert werden. Um die Extraktionseffizienz und Selektivität zu verbessern wurden weitere Versuche auf Basis den zuvor bestimmten Parameter, durchgeführt. Es konnte festgestellt werden, dass ein Extraktionsdruck von 100 bar und einer Temperatur von 60 °C die Selektivität der Ironextraktion deutlich steigert. Tatsächlich enthalten die CO₂-Extrakte bis zu 30% Irone. Das ist die dreifache Menge im Vergleich zu herkömmlicher Iris Butter, die durch Wasserdampfdestillation gewonnen wird. Der einzige Nachteil dieses Extraktionsverfahren ist weiterhin die nicht vollständige Extraktion von Ironen. Weitere Versuche, um die Extraktionseffizienz zu steigern, waren nicht erfolgreich.

Der dritte Teil dieser Doktorarbeit befasst sich mit Antioxidantien aus Rosmarinblättern. Die Bedeutung natürlicher Quellen von Antioxidanten hat in den letzten Jahren stark zugenommen. Der Grund dafür ist, dass künstliche Antioxidanten, aufgrund ihrer potentiell toxischen und karzinogenen Eigenschaften, als Nahrungsmittelzusatz verboten wurden. Die wichtigsten Antioxidanten in Rosmarin sind Rosmarinsäure (wasserlöslich) und Carnosolsäure (nicht wasserlöslich). Zuerst wurde der Einfluss von Hydrodestillation auf die beiden Antioxidanten untersucht. Normalerweise wird dieses Verfahren für die Extraktion des ätherischen Öls von Rosmarin eingesetzt. Jedoch wurde herausgefunden, dass eine große Menge an Antioxidantien während der Destillation verloren gehen. Einerseits werden Antioxidanten, vor allem Rosmarinsäure, in dem wässrigen Rückstand gelöst. Die antioxidative Wirkung dieses Restwassers erreicht einen Maximalwert nach einer Destillationszeit von 2.5 h. Andererseits, reduziert die lange Hitzeeinwirkung die Konzentration von Antioxidantien, vor allem Carnosolsäure, in den Blättern. Tatsächlich gehen 76% an Rosmarinsäure und 36% Carnosolsäure während der Hydrodestillation verloren. In Bezug auf das Konzept von Bioraffinerie wäre es erstrebenswert den wässrigen Rückstand der Destillation als Nebenprodukt und nicht Abfallprodukt zu sehen. Aus diesem Grund wurde dieser Rückstand dazu verwendet die antioxidative Stärke in Mikroemulsion zu initialisieren bzw. zu erhöhen. Der Destillationsrückstand könnte somit als Alternative zu konventionellen Antioxidanten, wie z.B. Ascorbinsäure, in Getränken eingesetzt werden. Im letzten Abschnitt des Rosmarin-Kapitels wird ein alternatives grünes Extraktionsverfahren von Antioxidantien aus Rosmarin vorgestellt. Dabei handelt es sich um eine mizellare Extraktion mit Hilfe von verschiedenen Fettsäuresalzen. Es wird gezeigt, dass nahezu die komplette Menge an Rosmarinsäure und dreiviertel der nicht wasserlöslichen Carnosolsäure mit einer 4 Gew%-igen wässrigen Natriummyristatlösung innerhalb von 5 min extrahiert werden kann. Zusätzlich wurde eine alternative Aufarbeitungsmethode des Extrakts entwickelt, um einen hohen Anteil an Carnosolsäure zu erhalten. Dies ist das erste beschriebene Verfahren, in dem selektiv Carnosolsäure mit Hilfe von wässrigen Lösungen extrahiert werden kann.

Table of contents

1	Introduction.....	1
2	Extraction methods	3
2.1	General information	3
2.2	Mechanical expression	4
2.3	Steam and hydro distillation	4
2.3.1	Procedure	4
2.3.2	Microwave-assisted distillation (MAD).....	5
2.4	Solvent extraction	6
2.4.1	Maceration and correlated techniques	6
2.4.2	Percolation and Soxhlet extraction	7
2.4.3	Selection of solvent	8
2.4.4	Alternative solvents	11
2.4.4.1	Ionic liquids (ILs)	11
2.4.4.2	Surfactants	11
2.4.4.3	Hydrotropes.....	12
2.4.5	Enhancement of solvent extraction	13
2.4.5.1	Microwave-assisted extraction (MAE).....	13
2.4.5.2	Ultrasound-assisted extraction (UAE).....	13
2.5	Supercritical fluids.....	14
2.5.1	Supercritical state	14
2.5.2	Physical properties	15
2.5.3	Applications	17
2.5.4	Supercritical fluid extraction (SFE)	18
2.5.4.1	Procedure of SFE.....	18
2.5.4.2	Extraction	19
2.5.4.3	Separation.....	20
2.5.4.4	Advantages & disadvantages compared to conventional techniques.	21
2.5.4.5	Applications.....	22
2.5.4.6	Alternatives to carbon dioxide	22
2.6	References.....	23
3	Microemulsions	29
3.1	Definition and properties.....	29
3.2	Classification.....	29
3.3	Salt effects.....	30

3.4	Characterization	32
3.5	Applications	32
3.6	References.....	33
4	Analysis methods	35
4.1	Chromatography in general.....	35
4.1.1	Separation mechanisms.....	35
4.1.2	Chromatographic separation	35
4.1.3	Chromatogram.....	37
4.2	High-performance liquid chromatography (HPLC)	38
4.2.1	Procedure	38
4.2.2	Stationary phase	39
4.2.3	Mobile phase	40
4.2.4	Detectors	41
4.3	Gas chromatography (GC).....	41
4.3.1	Procedure	41
4.3.2	Injector.....	42
4.3.3	Stationary phase	43
4.3.4	Mobile phase	43
4.3.5	Detectors	44
4.4	Determination of antioxidant activity.....	44
4.5	References.....	45
5	Supercritical fluid extraction unit „LAB SFE 100mL – 4368“	47
5.1	General information	47
5.2	Engineering plan	48
5.3	Instrumentation	49
5.3.1	Cabinet and pressure cylinder.....	49
5.3.2	Chiller	50
5.3.3	CO ₂ pump	50
5.3.4	Cosolvent pump	52
5.3.5	Extraction vessel and oven	52
5.3.6	Pressure regulators.....	54
5.3.7	Separators	55
5.3.8	Computer and control software	56
5.3.9	Other components	57
5.4	Operation manual.....	58
5.4.1	Preparations	58

5.4.2	General procedure of SFE	59
5.5	Troubleshooting.....	63
5.5.1	Plugging in pipe	63
5.5.2	Leakage of pipe adapters	64
5.5.3	Leakage of back pressure regulation valve	64
5.6	Summary of maximum operating conditions.....	65
5.7	References.....	65
6	Extraction of <i>Iris germanica</i> L.	67
6.1	Introduction	67
6.2	Fundamentals: <i>Iris germanica</i> L.	68
6.2.1	Ingredients of rhizomes.....	70
6.2.2	Extraction methods	73
6.2.3	Iris butter.....	75
6.3	Experimental section	77
6.3.1	Plant material and iris butter	77
6.3.2	Residual moisture	77
6.3.3	Extraction methods	78
6.3.3.1	Macerations.....	78
6.3.3.2	Ultrasound-assisted extraction	78
6.3.3.3	Soxhlet extractions	79
6.3.3.4	Supercritical carbon dioxide extraction	79
6.3.4	Oxidation process	80
6.3.5	Analysis methods.....	80
6.3.5.1	Gas chromatography (GC)	80
6.3.5.2	High-performance liquid chromatography (HPLC)	81
6.3.5.3	Thin-layer chromatography (TLC).....	82
6.4	Results & discussion.....	82
6.4.1	Analytical method development	82
6.4.1.1	HPLC	83
6.4.1.2	GC	87
6.4.1.3	TLC.....	91
6.4.2	Characterization of iris rhizomes	92
6.4.2.1	Residual moisture	92
6.4.2.2	Actual irone content.....	95
6.4.2.3	Maximum irone content	98
6.4.2.4	Summary.....	99
6.4.3	Ultrasound-assisted extraction.....	100

6.4.4	Extraction with sc-CO ₂	102
6.4.4.1	Comparison of iris butter and CO ₂ extract	102
6.4.4.2	Preliminary experiments	104
6.4.4.3	Design of experiments (DoE).....	108
6.4.4.4	Static pressure during SFE with the best parameters of DoE	118
6.4.4.5	Dynamic pressure during SFE with the best parameters of DoE	120
6.4.4.6	Influence of filling capacity, particle size, and flow direction.....	123
6.4.4.7	Extractions with ethanol as cosolvent	124
6.4.4.8	Enhancement of selective extraction of irones.....	126
6.4.4.9	Extractions with pretreatment of rhizomes	129
6.4.4.10	Extractions with myristic acid as “cosolvent”	131
6.5	Conclusion	132
6.6	References	136
7	Extraction of <i>Rosmarinus officinalis</i> L	141
7.1	Introduction	141
7.2	Fundamentals: <i>Rosmarinus officinalis</i> L	142
7.2.1	Ingredients	143
7.2.2	Extraction methods	145
7.3	Experimental section	146
7.3.1	Plant material	146
7.3.2	Residual moisture	146
7.3.3	Extraction methods	147
7.3.3.1	Soxhlet extractions	147
7.3.3.2	Hydro distillation	147
7.3.3.3	Steam distillation	148
7.3.3.4	Infusion and percolation	148
7.3.3.5	Micellar extraction	148
7.3.3.6	Alternative processing of the extract.....	150
7.3.3.7	Removal of myristic acid from the extract	150
7.3.4	Analysis methods.....	151
7.3.4.1	Gas chromatography (GC)	151
7.3.4.2	High-performance liquid chromatography (HPLC)	151
7.3.4.3	DPPH assay	153
7.3.5	Microemulsions	154
7.3.5.1	Ternary phase diagram	154
7.3.5.2	Conductivity measurements	154
7.3.5.3	DPPH assay	155

7.4	Results & discussion	155
7.4.1	Analytical method development	155
7.4.1.1	HPLC	156
7.4.1.2	GC	163
7.4.2	Characterization of rosemary leaves	165
7.4.2.1	Residual moisture	165
7.4.2.2	Content of antioxidants.....	166
7.4.2.3	Content of essential oil	168
7.4.2.4	Summary.....	168
7.4.3	Extraction of essential oil	169
7.4.3.1	Yield of essential oil.....	169
7.4.3.2	Content of camphor in essential oil.....	170
7.4.4	Influence of hydro distillation on antioxidants	172
7.4.4.1	Content of antioxidants in hydro distillation water residues.....	172
7.4.4.2	Content of antioxidants in the residual leaves after hydro distillation	173
7.4.5	Antioxidant activity of hydro distillation water residues	176
7.4.5.1	Calibration	176
7.4.5.2	Reference substances.....	176
7.4.5.3	Soxhlet extracts.....	179
7.4.5.4	Hydro distillation water residues	179
7.4.6	Antioxidant activity of hydro distillation water residues in microemulsions	181
7.4.6.1	System SDS/1-pentanol/ <i>n</i> -dodecane/water	181
7.4.6.2	Antioxidant activity of some essential oils	188
7.4.6.3	System TWEEN 60/ethanol/essential oil/water	190
7.4.7	Extraction with sodium myristate.....	195
7.4.7.1	Adjustment of extraction procedure	195
7.4.7.2	Influence of extraction time and solid-liquid ratio	197
7.4.7.3	Influence of concentration of sodium myristate	198
7.4.7.4	Influence of pH value and base	199
7.4.7.5	Influence of particle size and ultrasound-assisted extraction	201
7.4.7.6	Extraction with best parameters	202
7.4.7.7	Alternative surfactants	203
7.4.7.8	Alternative extraction method	205
7.4.7.9	Selective extraction of carnosic acid	205
7.4.7.10	Regeneration of the extract	208
7.5	Conclusion	209
7.6	References	212

8	Conclusion	217
A	Definition of technical terms and natural compounds	219
	List of figures	223
	List of tables.....	233
	List of publications	235
	Declaration	237

1 Introduction

The economic impact of extracts derived from plants has grown considerably in the last years due to the consumer demand for products from natural sources. Plant-based extracts are especially requested in food, nutritional supplements, flavors/fragrances, cosmetics, and in the pharmaceutical industry. Typical raw materials for the extraction of natural products are leaves, flowers, rhizomes, roots, seed, branches, bark, seed, and fruits. Since the 1990s, the demand of natural products, essential oils, plant extracts, or chemicals from natural plants is steadily growing. In respect to this, the average trading volume of herbal extracts amounted to about 6.7 billion € in Europe and about 17.5 billion € worldwide in 2003. The annual growth rates for nutraceuticals and pharmaceuticals by industrial product extraction are about 6 to 8%. In order to manage the growing demand of plant-based extracts and products, the development of new processes and ingredients has to be accelerated. In addition, existing production techniques need to be optimized with respect to energy, solvent consumption, and solvent selection [1-3].

Therefore, the concept and principles for green extraction of natural products was established. "Green extraction" is based on the discovery and development of new extraction techniques, which will reduce the energy consumption, enable the use of alternative solvents derived from renewable natural products, and ensure a safe and high quality extract. An additional approach for green extraction is the concept of biorefinery. It is defined as "the sustainable processing of biomass into a spectrum of marketable products and energy". This means that the entire range of plant compounds is used in an integrated approach, thus valorizing the value of by-products. Thereby, each ingredient of the plant can be extracted and used for the production of green fuels, building materials, cosmetics, and others [4-6].

In detail, the common method to obtain the essential oil from plant materials is steam distillation. However, this process is very energy consuming, long-lasting, and the high temperature may reduce the quality of the final extract. An alternative technique is solvent extraction. A major drawback of this method is the use of often toxic or highly flammable solvents, like *n*-hexane or acetone. Solvent extraction is also used to obtain other plant compounds, for example antioxidants, polyphenols, or flavonoids. It has to be considered that the final extract can contain a residual amount of the extraction solvent. The drawbacks linked to these techniques led to the establishment of new alternative extraction processes, which should replace the common methods. In particular, suitable methods for green extraction are microwave-assisted distillation, supercritical fluid extraction, sub-critical water extraction and solvent extraction with new nontoxic and green solvents [4-8].

The aim of this thesis is to invent new extraction methods and optimize existing extraction methods in regard to the principles of green extraction and biorefinery. For this reason, the

extraction of plant material, in particular iris rhizomes, with supercritical carbon dioxide was investigated. Another approach was the optimization of an existing extraction method, i.e. the steam distillation of rosemary leaves. Thereby, an application of the distillation waste water was sought. Furthermore, micellar extraction, an alternative green method, was investigated in order to obtain antioxidants from rosemary leaves.

A short explanation and definition of technical terms and plant compounds are presented in Appendix A (page 219 et sqq.).

References

- [1] O. Sticher, *Nat. Prod. Rep.*, **2008**, 25, 517-554.
- [2] M. Kassing, U. Jenelten, J. Schenk, and J. Strube, *Chem. Eng. Technol.*, **2010**, 33, 377-387.
- [3] H.J. Bart and S. Pilz, *Industrial Scale Natural Products Extraction*, **2011**: Wiley.
- [4] F. Chemat, M.A. Vian, and G. Cravotto, *Int. J. Mol. Sci.*, **2012**, 13, 8615-27.
- [5] F. Chemat and J. Strube, *Green Extraction of Natural Products*, 1. ed, **2015**, Weinheim: Wiley-VCH Verlag GmbH & Co. KGaA.
- [6] N. Rombaut, A.-S. Tixier, A. Bily, and F. Chemat, *Biofuels, Bioprod. Bioref.*, **2014**, 8, 530-544.
- [7] M.D. Luque de Castro, M.M. Jiménez-Carmona, and V. Fernández-Pérez, *Trends Anal. Chem.*, **1999**, 18, 708-716.
- [8] F. Chemat and M.A. Vian, *Alternative Solvents for Natural Products Extraction*, **2014**, Berlin, Heidelberg: Springer-Verlag.

2 Extraction methods

2.1 General information

The history of the extraction of natural products dates back to Mesopotamian and Egyptian times, where production of perfumes or pharmaceutically active oils and waxes was a major business [1]. The increasing interest in plants and their metabolites made it necessary to expand and modify the traditional extraction techniques. Nowadays, plant-based extracts are requested in food, flavor, cosmetics, and in the pharmaceutical industry. Moreover, the consumer demand for products from natural sources increases continuously [1-3].

In general, the extraction of compounds from a solid plant matrix can be regarded as a five-stage process:

1. Desorption of the compound from the active site of the plant matrix.
2. Diffusion into the matrix itself.
3. Solubilization of the analyte in the extractant.
4. Diffusion of the compound in the extractant.
5. Collection of the extracted compounds.

Ideally, the extraction process is exhaustive, fast, simple, and inexpensive. Conventional extraction techniques include maceration, Soxhlet extraction, percolation, and steam/hydro distillation. These methods present major drawbacks, for example long extraction times, large amount of organic solvents, unsatisfactory extraction efficiencies, and potential degradation of labile compounds. For this reason, new extraction techniques were developed in recent years with significant advantages. These new processes include supercritical fluid extraction (SFE), microwave-assisted extraction (MAE), ultrasound-assisted extraction (UAE), and pressurized-liquid extraction (PLE) [2]. Moreover, major advantages are e.g. the reduction of solvent consumption, the decrease of the extraction time, and the improvement in extraction efficiency and selectivity. The extraction techniques are in conformity with the concept of “green extraction” [4-6]. The six principles of “green extraction” are [4]:

1. Innovation by selection of varieties and use of renewable plant resources.
2. Use of alternative solvents (principally water or agro-solvents).
3. Reduction of energy consumptions by energy recovery and using novel processes.
4. Production of co-products instead of waste (principle of biorefinery).
5. Reduction of unit operations (favor safe, robust, and controlled techniques).
6. Aim for a non-denatured and biodegradable extract without contaminants.

The following chapters are considered to give an overview of conventional and alternative extraction methods.

2.2 Mechanical expression

A common way to extract vegetable oils from seeds is mechanical expression. This method is suitable for plant materials with high oil contents. It is the more economic technique compared to solvent extraction, but over 5 wt% of the oil can remain in the raw material. Nonetheless, mechanical expression has relatively low initial and operational costs. In addition, the extracted oil is free of solvent residues and thus has a higher overall quality [7]. Mechanical expression is for example used for the extraction of citrus oil. Therefore, peels from lemons, oranges or tangerines are abraded and pressed out. These extracts resemble closely the original oil of the plant material as they are not exposed to heat during the extraction process. However, high temperatures must be avoided as thermal degradation of some compounds can be induced, which results in a modified scent of the extract [8, 9].

2.3 Steam and hydro distillation

Hydro and steam distillation are traditional methods to extract volatile compounds, especially essential oils, from plants. However, the extraction procedure of both techniques is slightly different [5].

2.3.1 Procedure

The procedure of steam and hydro distillation is shown in Figure 2.1. Regarding the hydro distillation, the plant material and water are mixed together in a flask. Subsequently, this suspension is heated until boiling. In the case of steam distillation, the steam is generated separately and then guided through the plant material.

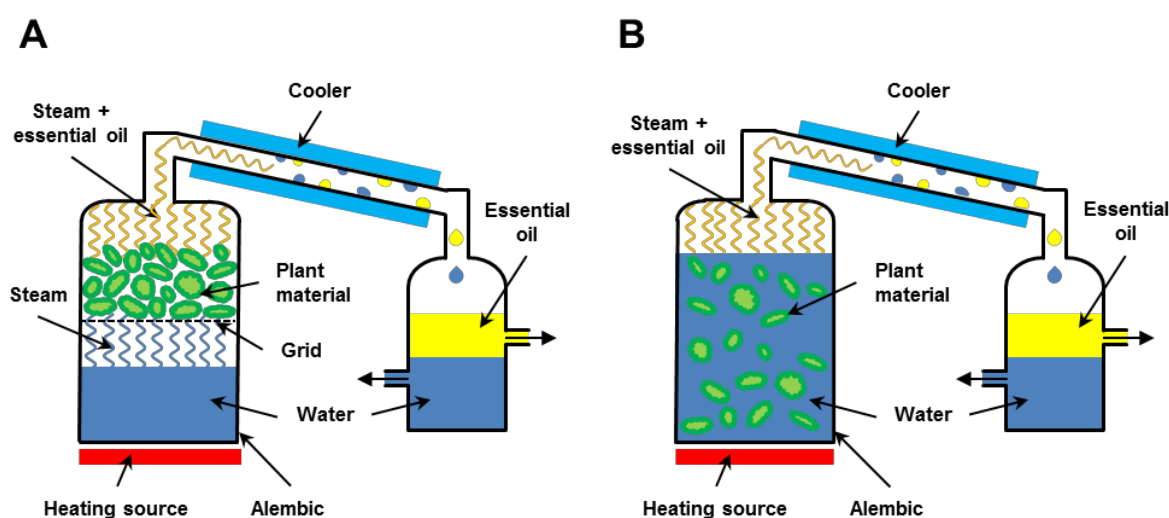


Figure 2.1: Procedure of (A) steam and (B) hydro distillation of plant material to obtain the essential oil.

In general, the steam takes the essential oil along to the condenser. There, the vapor is liquefied and a water/oil mixture is gained. Subsequently, the mixture is collected in a separator, where a two phase system is observed. There, water is the lower phase and the upper phase represents the essential oil. Afterwards, the essential oil can be recovered [5, 10]. The distilled and condensed water phase is called hydrosol. If this hydrosol is recycled and re-used to carry out another steam or hydro distillation the process is called cohobation [11].

The techniques of steam and hydro distillation merely work because of the coexistence of two immiscible liquids (water and essential oil). The basic principle is that the immiscible compounds form low-boiling azeotropes. The pressure within the distillation system can be described by means of Raoult's law, which is given in equation (2.1).

$$p = x_1 p_1^* + x_2 p_2^* \quad (2.1)$$

where p = total pressure of the system; p_1^* , p_2^* = saturation steam pressures of the compounds; x_1, x_2 = mole fractions of compounds.

In a good approximation, a very low solubility of the essential oil in the water phase is assumed. Thus, the involved substances are not mixed within the vapor phase. Thereby, both mole fractions are equal to one. That is why the resulting vapor pressure of the system is equal to the sum of the vapor pressures of the pure compounds. Consequently, the boiling point of the mixture is below the boiling points of both, water and essential oil at atmospheric pressure. For this reason, the essential oil can be extracted without reaching the boiling point of the single compounds [5, 12, 13].

One of the disadvantages of steam and hydro distillation is that the essential oils can undergo chemical alteration. Additionally, heat-sensitive compounds can easily be destroyed. For this reason, the quality of the essential oil extracts can be extremely impaired. Moreover, the scent of the extract is more akin to a cooked aroma, rather than a fresh fruit or vegetable flavor [8, 14]. A further drawback is the high-energy and time consumption during steam and hydro distillation [15].

2.3.2 Microwave-assisted distillation (MAD)

Microwave-assisted distillation (MAD) is a recently developed method to extract essential oil from plant materials. MAD can be an alternative technique for steam and hydro distillation [16].

Microwave-assisted distillation is performed by putting fresh plant material in a beaker placed in a microwave reactor. However, no additional water or solvent is necessary. The microwave radiation causes the heating of the water in the raw material. This results in the bursting of plant cells, releasing the contained essential oil. In addition, steam is produced *in*

situ from water included in the plant matrix. The released essential oil is transported by the generated steam to a condenser at the top of the microwave oven. The vapor is subsequently condensed obtaining a two phase system (essential oil and water). Finally, the excessive water is redirected to the plant material in the microwave oven [16]. A further development of this extraction technique is called Microwave Hydrodiffusion and Gravity (MHG). This process is performed in an “upside down” microwave alembic. The plant material is also heated by microwave radiation, but the extract drops out of the reactor by gravity. In difference to MAD, this method can be used to extract additionally non-volatile compounds like pigments or antioxidants [7, 15, 16].

These microwave-assisted extraction methods have major advantages compared to traditional techniques. In general, the total extraction time can be significantly reduced. Moreover, the energy consumption and CO₂ emission is decreased and a lower amount of waste water is produced [16].

Nonetheless, whether these technologies can economically be transferred to the manufacturing scale is questionable, since the technical complexity of applying microwaves in a large-scale equipment is high [1]. Currently, pilot microwave reactors with a feeding volume up to 75 L are feasible [17].

2.4 Solvent extraction

Solvent extraction is the most widely used technique for plant extractions. The principle is based on the transfer of the compound from the sample to an organic solvent [8]. It is a very important operation in numerous industries, such as the chemical, biochemical, food, cosmetics and the pharmaceutical industries [7]. Several techniques to perform solvent extraction are described in the following sections. In addition, the selection of an appropriate solvent for plant extractions and new developed solvents is discussed.

2.4.1 Maceration and correlated techniques

Maceration describes the soaking of a solid plant material in a solvent at room temperature for a defined time. Thus, the solid is just in contact with the solvent without any motion. Typically, the extraction time is long, whereas the efficiency is poor. This can be explained by the fact that maceration is a process which induces equilibrium of the compound concentrations in the plant material and the extraction solvent. This means that the extraction takes place until a maximum concentration of the extracted compounds is reached in the solvent. However, depending on the solubility properties, a significant amount of the desired components may remain in the plant material. For a complete extraction the repeated addition of fresh solvent is required, which can result in a high solvent consumption. Maceration is especially used in the case of fragile molecules because of the mild extraction

conditions. If macerations are carried out at a constant elevated temperature, the method is called **digestion**. Thereby, the establishment of the equilibrium can be enhanced [1, 7, 18].

Another modification of maceration is called **immersion**. To this purpose, the plant material is immersed in a solvent, while the mixture is stirred. This procedure ensures a very intense contact between the phases [1].

A further extraction technique is **infusion**. Here, the solid is immersed in a heated solvent without boiling, followed by the cooling of the suspension. The most prominent example of infusion is the preparation of tea. In the case of a boiling solvent the extraction technique is called **decoction**. However, these methods are only feasible for non-thermo sensitive compounds. Nonetheless, this is a very fast and sometimes inevitable extraction method [7].

2.4.2 Percolation and Soxhlet extraction

In contrast to the previous described techniques, **percolation** is a method for the exhaustive extraction of compounds from plant materials. To this purpose, the solid plant material is stacked as a fixed bed while fresh solvent passes through. Generally, this process is driven by gravity from the top to the bottom. Furthermore, adequate extraction efficiencies can be achieved by recycling the extraction solvent and passing it several times through the plant bed. It should be pointed out that a constant flow of the solvent has to be ensured. An advantage of this technique is the relatively low mechanical stress on the solid material. Moreover, no additional filtering step is required, as the extract is relatively free of solid particles. The most prominent example of percolation is the preparation of coffee [1, 7, 18].

Another exhaustive method to extract compounds using a suitable solvent is the **Soxhlet extraction**. In general, this technique is performed in lab scale in order to determine the total content of compounds that can be dissolved in the used solvent. A sketch of the Soxhlet apparatus is presented in Figure 2.2.

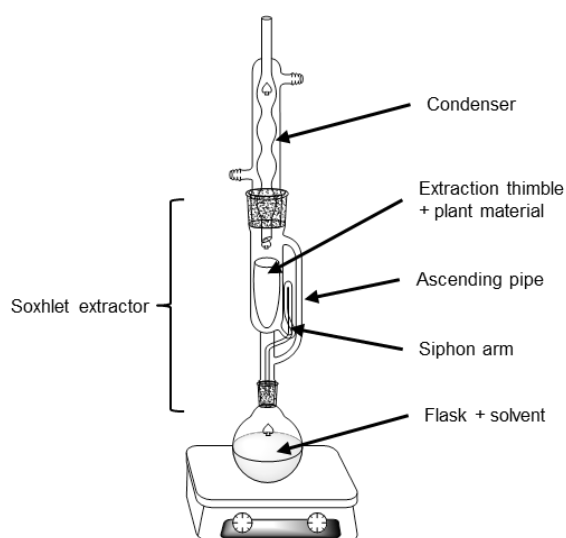


Figure 2.2: Sketch of a Soxhlet extraction apparatus for the exhaustive extraction of plant material.

Preliminary, the solid plant material to be extracted is filled in a porous extraction thimble, mostly consisting of cellulose fibers. Afterwards, the thimble is placed in the chamber of the Soxhlet extractor. The solvent in the bottom flask is then heated to boiling. The vapor fumes through an ascending pipe to a condenser. There, the pure solvent condenses, drops into the extraction thimble and comes into contact with the plant material. Once a certain amount of solvent has been collected, the chamber is emptied through a special siphon arm. The extract solution flows back into the bottom flask. Subsequently, a new extraction cycle starts automatically. With this process, the plant material is extracted several times with fresh solvent until, theoretically, all soluble components are extracted. The extracted compounds are collected and concentrated in the bottom flask. Nonetheless, not all of the soluble compounds may be extractable due to adsorptive or chemisorptive forces in the plant matrix. Degradation of the components may also occur in the bottom flask, as the solvent is kept at its boiling temperature for several hours [1, 8, 18, 19].

2.4.3 Selection of solvent

The selection of an appropriate solvent is the most important parameter of solid-liquid extractions. The choice of the solvent often follows the principle “like extracts like”. This means that the extraction efficiency is based on the polarity of both, the target compound and the solvent. Plant ingredients can be classified into five main chemical groups: fats, essential oils (terpenes) sugars, polyphenols, and glycosides. Figure 2.3 presents these ingredients and their corresponding suitable extraction solvent in dependence of their polarity [1, 3].

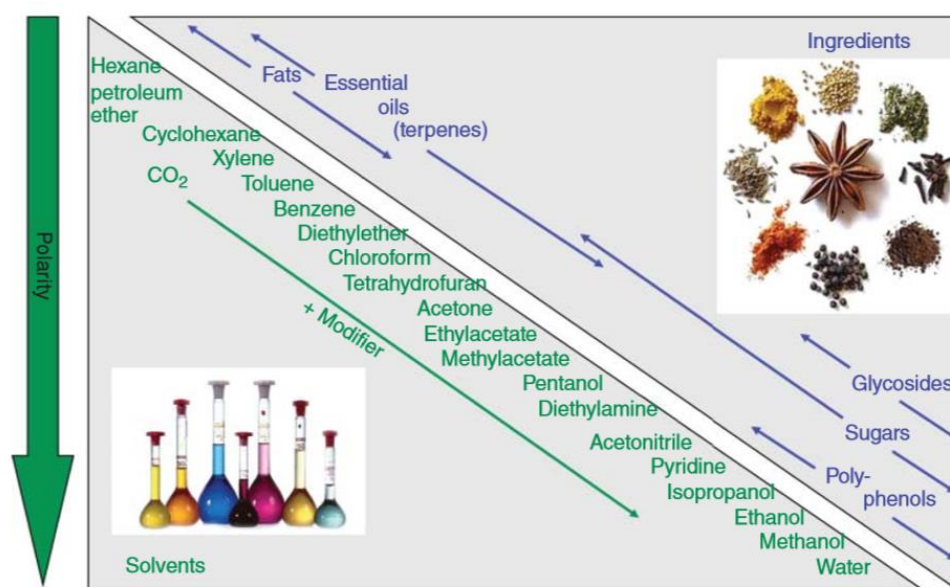


Figure 2.3: Selection of solvents which are suitable for different plant ingredients [7].

In addition, the concept of solubility parameters can be used to make first predictions of the solubilization behavior. There are different models for the solubility of a compound in a solvent. The first approach was introduced by Hildebrand [20], who introduced the Hildebrand solubility parameter δ , according to equation (2.2).

$$\delta = \left(\frac{E_{coh}}{V_m} \right)^{1/2} \quad (2.2)$$

where δ = Hildebrand solubility parameter; E_{coh} = cohesion energy density; V_m = molar volume.

The cohesion energy density is the difference between the enthalpy of evaporation and the energy of the ideal gas according to equation (2.3).

$$E_{coh} = \Delta H_{vap} - RT \quad (2.3)$$

where E_{coh} = cohesion energy density, ΔH_{vap} = evaporation enthalpy; R = gas constant; T = temperature.

It is shown that the Hildebrand parameters can easily be determined by this equation. According to this model, two components are miscible if the values of solubility parameters δ are equal. The concept is very simple and can easily be adapted to multicomponent systems. Therefore, mean values of the δ parameters, the volume, and the composition of the mixtures have to be calculated. However, this concept often works only for so-called regular mixtures and small molar volumes. The approach often fails, if strong interactions are present, involving polar interactions and/or hydrogen bonds [3, 7, 20].

A further development of these solubility parameters was approached by Hansen [21]. He introduced the Hansen solubility parameters, which are the most prominent ones and still widely used in industry. Thereby, the Hildebrand parameter δ is divided into three parts, which include dispersion and permanent dipole interactions and hydrogen bonding. According to this concept, two components are miscible if the values of the three parameters are similar. However, this concept should only be used for making first predictions on the solubility of a compound in a solvent [7, 21].

Additionally, new methods to estimate the solubility or rather extraction efficiency of a compound with a certain solvent were established. These methods include the perturbed-chain statistical associating fluid theory (PC-SAFT) [22], the COSMO-RS theory [23] or the (modified) UNIFAC model [24]. These concepts are more suitable for the prediction of solubility properties compared to Hildebrand or Hansen solubility parameters. Nonetheless, there can still be big deviations for the estimated solubility behavior of a compound due to the complex matrices present in botanical raw materials [3].

Besides the solubility, which is a key feature in obtaining a crude solvent extract of plants, there are additional criteria for solvent selection [1, 8]:

- **Selectivity:** A high selectivity of the solvent enables the reduction of purification steps of the extract to obtain the target compound.
- **Recoverability:** The solvent should be easily recovered to obtain the crude extract. Solvents with low boiling points are preferred in order to remove it easily and prevent the loss or degradation of compounds.
- **Viscosity:** Highly viscous solvents reduce the mass transfer efficiency and can lead to difficulties with pumping or dispersion.
- **Surface tension:** A low surface tension of the solvent promotes the wetting of the plant material. This ability is very important since the solvent must penetrate the plant matrix.
- **Thermal and chemical stability:** The solvent should be thermal and chemical stable in order to facilitate the recycling, for example the solvent recovery in an evaporator.
- **Corrosivity:** Corrosive solvents can increase equipment costs.
- **Availability and costs:** The solvent should be readily available. However, not the price of the solvent is important, but the costs of inevitable losses during the process.
- **Toxicity and flammability:** Especially for food processing only nontoxic solvents will be taken into consideration. In general, any associated hazard with the solvent will require extra safety measures. For this reason, aliphatic solvents are preferred to aromatic or halogenated ones.
- **Environmental impact:** The solvent should be environmentally friendly and compatible with downstream process steps in order to minimize losses due to evaporation, solubility and carryover. Additionally, a full removal of the solvent from the residual plant material should be achieved.

Especially, the last two aspects gained more and more importance in recent years. Therefore, the HSE (health, safety and environment) profile of the solvent must also be taken into account. A classification in regards of flammability, toxicity, and the HSP profile of traditional and alternative organic solvents is presented in literature [25, 26]. Currently, there is a strong tendency towards the use of “green” extraction solvents and agents which are in conformity with the concept of “green extraction” [4-6].

An example for a new alternative solvent is 2-methyltetrahydrofuran (MeTHF). This solvent was recently considered to be a green alternative for the petroleum-based *n*-hexane in extraction processes. MeTHF is a biodegradable and plant derived solvent. It is produced by hydrogenation of products obtained from carbohydrate fractions of hemicellulose from various feedstocks. This solvent is in accordance with several principles of green chemistry and sustainable or green extraction [27].

2.4.4 Alternative solvents

Besides the traditional organic solvents, new classes of solutions can be used to extract active compounds from plant material. These solutions include ionic liquids, surfactants and hydrotropes. The following sections should give a short overview of these new extraction methods.

2.4.4.1 Ionic liquids (ILs)

Ionic liquids (ILs) are defined as solvents that consist solely of ions including at least one organic ion. They are liquid below a temperature of 100 °C, which is notably the result of the poor coordination of the ions. The chemical and physical properties of ILs can be tuned by the application respectively variation of the cations and anions [28, 29]. Particularly, it is possible to design highly selective solvents [30].

Ionic liquids are often proposed as green solvents due to their low or negligible volatility. This is especially beneficial, because processes can be designed without the emission of volatile organic compounds [31, 32]. A minor drawback of ILs is the high viscosity compared to common solvents used in extraction processes. In addition, ionic liquids are only suitable in plant extraction if they are nontoxic, relatively pure, and not expensive [7].

Recently ionic liquids were for example successfully applied for the extraction of the biopolymer suberin from cork without destroying its structure. To this purpose, choline hexanoate was used, which is a nontoxic and biodegradable ionic liquid [33, 34].

2.4.4.2 Surfactants

Surfactants are amphiphilic compounds consisting of a hydrophilic part and a lipophilic part. On the one hand, the hydrophilic part has a polar group with an affinity for polar solvents particularly water. On the other hand, the lipophilic part consists of a long hydrocarbon chain with at least eight carbon atoms, which has an affinity for nonpolar substances. Due to the amphiphilic structure surfactants are able to reduce the surface tension of water allowing easier spreading. In addition, surfactants reduce the interfacial tension between two liquids [35, 36].

Surfactants can be classified in four main groups according to the species and charge of the hydrophilic head group. The head group of anionic surfactants is negatively charged, which can for example exist of a carboxylate-, sulfate- or sulfonate-group. Known anionic surfactants are sodium dodecyl sulfate (SDS) or conventional soaps (alkali salts of fatty acids). Furthermore, cationic surfactants have a positive charged head group, like quaternary ammonium compounds. Amphoteric (zwitterionic) surfactants exhibit both ionic head groups, like amino acids. Finally, a polar nonionic head group is present in nonionic surfactants. They

are mainly polyoxyethylene (EO) or polyoxypropylene (PO) glycol alkyl ethers. The water solubility depends strongly on the number of EO or PO units [35, 36].

A characteristic property of surfactants is the formation of small spherical aggregates at a certain concentration in aqueous solutions. These aggregates are called micelles. Thereby, the long alkyl chains are grouped in the center of the micelle, whereas the polar head groups are orientated to the water phase. The point at which this aggregation takes place is called critical micellar concentration (CMC). This behavior allows the solubility of more hydrophobic compounds in aqueous solutions. Micelles provide a pseudo-organic phase enabling the transfer of hydrophobic compounds to the inside of the micelle. In addition, there are two important points for surfactants in aqueous solutions. On the one hand, the Krafft temperature is defined as the minimum temperature at which a solid surfactant gets soluble in an aqueous medium. On the other hand, the cloud point is defined as the temperature at which micelles of nonionic surfactants are no longer stable and a two phase system is formed [7, 35, 36].

Usually, nonionic surfactants are mainly reported for the extraction of plant materials. This is a consequence of the special processing method after extraction. The extraction technique is also called “cloud point extraction”. For this purpose, the target compounds are preliminary recovered from the plant matrix by micellar extraction. In a second step the system is brought into the two-phase region above the cloud point. Here, the concentration and purity of the extracted hydrophobic substances increases. The target substance is either concentrated in the surfactant-rich phase or in the water phase depending on its polarity [7, 37-39].

However, the solvent recovery and product removal from the extract is still worthy of improvement. Economically feasible processing methods have to be developed for the extraction of natural compounds from plant. The back extraction of compounds can probably be avoided if the extract solution with the active compound is directly used as an ingredient for secondary products, (e.g. cosmetic creams) [1].

2.4.4.3 Hydrotropes

Hydrotropes are, just like surfactants, amphiphilic compounds consisting of a hydrophilic part and a lipophilic part. However, the hydrophobic part is typically too small and bulky to form micelles. Hydrotropes are usually anionic compounds, which are composed of an aromatic ring substituted by a sulfate-, sulfonate- or carboxyl-group. The most prominent substance is sodium xylene sulfonate (SXS). Hydrotropes can increase the solubility of water insoluble compounds in an aqueous solution. The concentration of the hydrotrope needs to exceed the minimal hydrotropic concentration (MHC) to enhance the solubility of a solute. The formation of certain aggregates above the MHC such as micellization is probable. The value of a MHC is usually quite higher than the CMC [36, 40, 41].

For this reason, aqueous hydrotrope solutions can be used for the selective extraction of non-water soluble phytochemicals from plant materials. Hydrotropes destroy the phospholipid bilayer and penetrate through the cell wall into the inner structures. The target compound is released and solubilized in the aqueous hydrotrope solution. After a certain time, the aqueous extract solution is diluted below the MHC of the hydrotrope. Thus, the solubility of the extracted compound decreases and it precipitates. Subsequently, the target compound can be easily recovered by a suitable separation technique. This extraction and processing methods implement a high purity of the desired compound [41-46].

2.4.5 Enhancement of solvent extraction

There are different techniques to accelerate and enhance the previously described extraction methods. Microwave- and ultrasound-assisted extractions are two promising techniques, which will be described in the following sections.

2.4.5.1 Microwave-assisted extraction (MAE)

In recent years, microwave-assisted extraction (MAE) has been intensively studied and successfully applied in solid–liquid extractions of plant materials. Microwave radiation can be used for the fast extraction of several classes of plant compounds [16].

To this purpose, the plant material is immersed in an organic solvent, which must not absorb microwave radiation, such as *n*-hexane. More precisely, the solvent must have a low dielectric constant, which makes it relatively transparent for microwave radiation. Microwaves affect directly the water in the cells of the plant matrix. These cells are ruptured by the caused high pressure in the cell, releasing the plant compound. The substance is dissolved in the organic solvent and can be further processed [6, 7, 16, 47]. Extractions can also be performed with a solvent which absorbs microwave radiation. However, strong heating must be avoided in order to prevent thermal degradation of the plant compounds. A binary solvent mixture is usually used for extraction processes, containing only one solvent which absorbs microwaves [1].

Microwave-assisted extraction has several advantages compared to traditional techniques. First of all, compounds can be extracted more selectively and more rapidly. In addition, MAE enables equal or even better extraction yields by a minimal sample manipulation. Furthermore, the consumption of energy and organic solvents is reduced [1, 2, 7].

2.4.5.2 Ultrasound-assisted extraction (UAE)

Another technique to enhance the extraction efficiency is ultrasound-assisted extraction (UAE). The most common tools for UAE are ultrasonic baths, ultrasonic probes, and

cavitating tubes. The efficiency of the technique can be explained by the phenomenon of cavitation [6, 7].

Preliminary, the plant material is immersed in a solvent and ultrasound is applied to the sample. Fundamentally, two different effects of ultrasound on the cell walls can be described. On the one hand, sonication can easily destroy the thin skin of glandular plant cells releasing the cellular content into the surrounding solvent. On the other hand, ultrasound can also accelerate the swelling and hydration of plant matrices, which results in an enlargement respectively disruption of the plant cell walls. This behavior improves the mass transfer rate, resulting in an increase of the extraction efficiency [1, 6, 7, 48].

The advantages of ultrasound-assisted extraction are the shortening of extraction time and the enhancement of extraction efficiencies. In addition, the energy and solvent consumption can be reduced compared to conventional techniques [6, 48-50].

2.5 Supercritical fluids

The occurrence of a supercritical state was for the first time observed by Baron Cagniard de la Tour in 1822. Thereby, a pure substance was trapped in a molten glass vessel and subsequently heated. It was observed visually that the boundary between the liquid and gaseous phase disappeared, obtaining one visual phase [51]. The term “critical point” was introduced by T. Andrews about half a century later [52]. Only a few years later, the first experimental evidence has been provided by Hannay and Hogarth in 1879 that supercritical fluids enhance the solubility of solids. In addition, they were able to show that the dissolving power of a supercritical fluid (SCF) is depending on the pressure [53]. This tunable solvation power is the basis of modern-day research in the sector of supercritical fluids, for example supercritical fluid extraction (SFE).

In the following sections, supercritical fluids are described with respects to their characteristics and physical behavior. The main focus will be on supercritical dioxide and its application in supercritical fluid extraction.

2.5.1 Supercritical state

In general, pure chemical substances can exist in different states of aggregation, depending on the prevailing pressure and temperature conditions. Figure 2.4 presents the phase diagram of carbon dioxide (CO_2). By means of this diagram, it can be realized what state of the substance is present under a given pressure and temperature.

Particularly, four different regions are present, in which the substance occurs as a single phase: solid (s), liquid (l), gaseous (g) and supercritical (sc). Here, the pressure and the temperature can be changed without the occurrence of a phase transition. These areas are

limited by lines at which the compound is in equilibrium with two different phases. The sublimation curve represents the pressure and temperature conditions under which the solid and gaseous states are present at the same time. The coexistence of the solid and liquid phase is represented by the melting curve, whereas the vaporization curve indicates the equilibrium of the gaseous and liquid states. The intersection of these three curves is called triple point. Here, the substance is in equilibrium with the solid, liquid, and gaseous state [13].

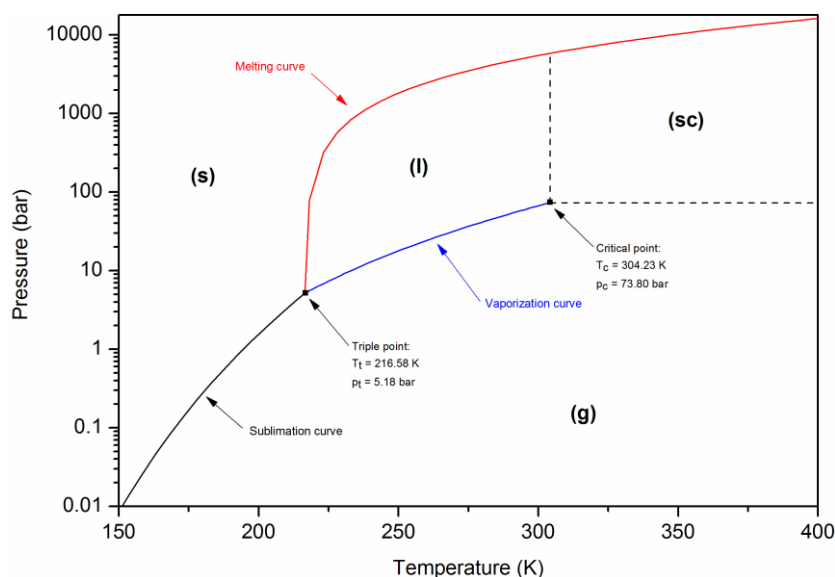


Figure 2.4: Phase diagram of carbon dioxide. Data from [54-57].

Furthermore, the point at which the vaporization curve ends is called "critical point". It is characterized by the critical temperature T_c and critical pressure p_c . By exceeding these critical values, the phase boundary between the liquid and gas vanishes and both phases cannot be distinguished anymore. In this area, the substance is in a state, which is designated as "supercritical". Moreover, it is possible to transfer a supercritical fluid to a solid state, but only at very high pressures [13]. In addition, critical opalescence can be observed before reaching the supercritical state [58]. The critical point of carbon dioxide is at $\Theta_c = 31.1 \text{ }^\circ\text{C}$ and $p_c = 73.8 \text{ }^\circ\text{C}$ [55].

2.5.2 Physical properties

The physical properties of supercritical fluids vary over a wide range depending on pressure and temperature. These properties are in general between those of gases and liquids. In detail, the densities of supercritical fluids can reach the values of liquids, whereas viscosities are similar to those of gases. Moreover, the diffusion coefficients are intermediate between those of gases and liquids. Precise values of density, viscosity, and the diffusion coefficient are summarized in Table 2.1.

Table 2.1: Physical properties of solvents in different states of aggregation [59].

Solvent	Density $\rho / \text{g cm}^{-3}$	Viscosity $\eta / \text{Pa s}$	Diffusion coefficient $D / \text{cm}^2 \text{s}^{-1}$
Gas ^a	$6 \cdot 10^{-4} - 2 \cdot 10^{-3}$	$1 \cdot 10^{-5} - 3 \cdot 10^{-5}$	0.1 - 0.4
Critical fluid ^b	0.2 - 0.5	$1 \cdot 10^{-5} - 3 \cdot 10^{-5}$	$7 \cdot 10^{-4}$
Supercritical fluid ^c	0.4 - 0.9	$3 \cdot 10^{-5} - 9 \cdot 10^{-5}$	$2 \cdot 10^{-4}$
Liquid ^a	0.6 - 1.6	$2 \cdot 10^{-4} - 3 \cdot 10^{-3}$	$2 \cdot 10^{-6} - 2 \cdot 10^{-5}$

^a $p = 1 \text{ bar}$, $\Theta = 25 \text{ }^\circ\text{C}$. ^b $p = p_c$, $\Theta = \Theta_c$. ^c $p = 4p_c$, $\Theta \approx \Theta_c$

The density of supercritical fluids is comparable to liquids, but it is strongly depended on pressure and temperature. The density of the supercritical fluid can be varied above the critical values without the occurrence of a discontinuity. It is fundamental that the solubility of a substance is strongly influenced by the density of the supercritical fluid. Thus, it is possible to adjust continuously the solvation power of the supercritical fluid by varying the temperature respectively pressure. In detail, this means that increasing the pressure at a constant temperature results in an increased solubility of the compound due to the rising density [60, 61].

The relative dielectric constant ϵ_r and thus the polarity of the solvent also affects the solubility of substances in supercritical fluids. The dielectric constant of carbon dioxide can be slightly increased with pressure from a value of 1.0 at 20 bar up to 1.6 at 300 bar and 40 °C [62]. The modification of the dielectric constant at different conditions can be better demonstrated with water. The dielectric constant of liquid water is 78.4 at ambient conditions. However, supercritical water ($\Theta_c = 373.9 \text{ }^\circ\text{C}$ and $p_c = 220.6 \text{ }^\circ\text{C}$) shows a dielectric constant of 2 near the critical point. Thus, water is a polar solvent at ambient conditions and a more or less nonpolar solvent in the supercritical state [63, 64].

The diffusion coefficient and viscosity represent the transport properties of the supercritical fluid which affect the mass transfer rate. In general, the viscosity of a supercritical fluid is similar to the gaseous state. On the other hand, the diffusion coefficient is at least one order of magnitude higher compared to liquid solvents. This means that the diffusion of a substance through a supercritical fluid will occur at a faster rate than that obtained in a liquid solvent. This behavior implies that a solid will dissolve more rapidly in a supercritical solvent. In addition, the surface tension is lowered, which enhances the penetration of a supercritical fluid into a micro-porous solid structure, like a plant matrix. The diffusion coefficient and the viscosity can be varied by the applied pressure and temperature. In detail, the viscosity increases with rising pressure, causing a decrease of the diffusion coefficient. This effect is

less pronounced at high pressure values, as the density becomes less sensitive to the pressure. In contrast, the diffusion coefficient generally increases with an isobaric increase of the temperature. However, changing the temperature at a constant solvent density has only a small effect on the diffusion [65].

2.5.3 Applications

These special and tunable physical properties of the supercritical fluids induced the invention of several technical applications.

Supercritical fluid chromatography (SFC) is a separation method in which a solvent is used in its supercritical state as mobile phase. It can be considered as an intersection between gas chromatography (GC) and liquid chromatography (LC). The stationary phase consists either of a capillary column or packed column. The transport velocity or separation efficiency depends on the distribution of the substances between the mobile and stationary phase. The solvent power of the mobile phase can be varied by the density of the supercritical fluid. In addition, an organic solvent can be added in order to modify the mobile phase and facilitate the separation of the compounds. The separation efficiency can be enhanced by varying the pressure and temperature of the supercritical fluid. The importance of SFC is based on the fact that it permits the separation of compounds which are usually not processed by LC or GC. An advantage of SFC is the easy removal of the mobile phase from the separated compounds. However, a disadvantage is that strongly polar and ionic molecules are not soluble in supercritical fluids [65-67].

In addition, supercritical fluids can be used as solvent in chemical synthesis. In detail, hydrogenations, oxidations, radical reactions, enzymatic reactions, polymerization, and several other reactions can be performed in supercritical fluids [65, 68, 69]. Supercritical carbon dioxide can also be used to dry hydrogels, in order to obtain aerogels. In detail, aerogels are lightweight materials with outstanding textural properties (i.e. high surface area and open porosity) consisting of silica. Aerogels are obtained from wet gels by using the supercritical drying process. By means of this method, it is feasible to avoid the pore collapse phenomenon and keep the porous texture of the wet material intact [70-72].

Further applications of supercritical fluids are for example dyeing [73, 74], impregnation [75, 76] and the preparation of fine particles ("supercritical fluid precipitation") [77].

In particular, the most important application of supercritical solvents is the supercritical fluid extraction, which will be described in the following section.

2.5.4 Supercritical fluid extraction (SFE)

Supercritical fluid extraction (SFE) is an interesting alternative technique to conventional solid-liquid extractions with organic solvents. Amongst all supercritical fluids, carbon dioxide is the most common and suitable solvent in SFE [2].

This fact is a consequence of several advantages which offers CO₂ in comparison to other supercritical fluids. First of all, carbon dioxide exhibits moderate critical conditions. The critical point of carbon dioxide is at a critical temperature of 31.1 °C and a pressure of 73.8 bar [55]. Consequently, thermal degradation of natural compounds during the extraction process can be avoided [2].

Carbon dioxide shows only a low toxicity which results in a safer handling of the solvent. Actually, the maximum workplace concentration (MAC value) of CO₂ is 9 g/m³. Carbon dioxide is also an environmental friendly and biocompatible solvent. In particular, the concentration of CO₂ in the atmosphere is 0.03% by volume and it can be degraded by photosynthesis of plants. Moreover, carbon dioxide is relatively chemical inert and non-flammable [78].

A further advantage of carbon dioxide is its low price (values of \$ 0.05-3 kg⁻¹) [65, 79, 80]. In addition, CO₂ is available in large quantities and high purity. Carbon dioxide can be recovered as by-product in the exhaust gases of power plants or the chemical industry, for example in the production of lime, hydrogen, ammonia, and ethylene oxide. Also subterranean natural sources from active or extinct volcanoes are feasible. The crude gas of the chemical processes contains more than 95% of carbon dioxide. After the deposition of gaseous impurities and moisture, the carbon dioxide is compressed and exhibits a purity of at least 99%. The liquefaction of the gas is performed at pressures between 14 and 20 bar and temperatures of -40 to -25 °C [81]. This liquefied carbon dioxide, with a vapor pressure of 57.29 bar at 20 °C, is used directly in supercritical fluid extraction [82].

2.5.4.1 Procedure of SFE

Supercritical fluid extraction of plant materials consist of two main steps. Initially, the extraction process itself, followed by the separation of the solvent from the extract [66]. A simplified flow scheme of a SFE unit is presented in Figure 2.5. By means of this scheme, the procedure of SFE is explained.

The process steps are the following. Preliminary, the high pressure extraction vessel is filled with the plant material. Liquid carbon dioxide is supplied from a storage tank and guided through a condenser in order to ensure the liquid state of the solvent. CO₂ is compressed and transported by a pump (mainly piston pump) to a heat exchanger in order to reach the desired process conditions. Afterwards, the supercritical carbon dioxide passes through the extraction vessel, usually from the bottom to the top. Here, the mass transfer of the solutes

into the fluid solvent takes place. A second pump can be used to add an organic solvent in order to influence the extraction efficiency. Furthermore, the pressure in the vessel is adjusted by a back pressure regulation valve. The loaded supercritical fluid is transported to the separation vessel, where the extract is precipitated by adjusting the temperature and the pressure. Generally, the carbon dioxide gets gaseous in this step and exits the separator. Finally, the exhausted CO_2 can be recycled by liquefaction in a condenser and can be recirculated by the pump [1, 2, 66].

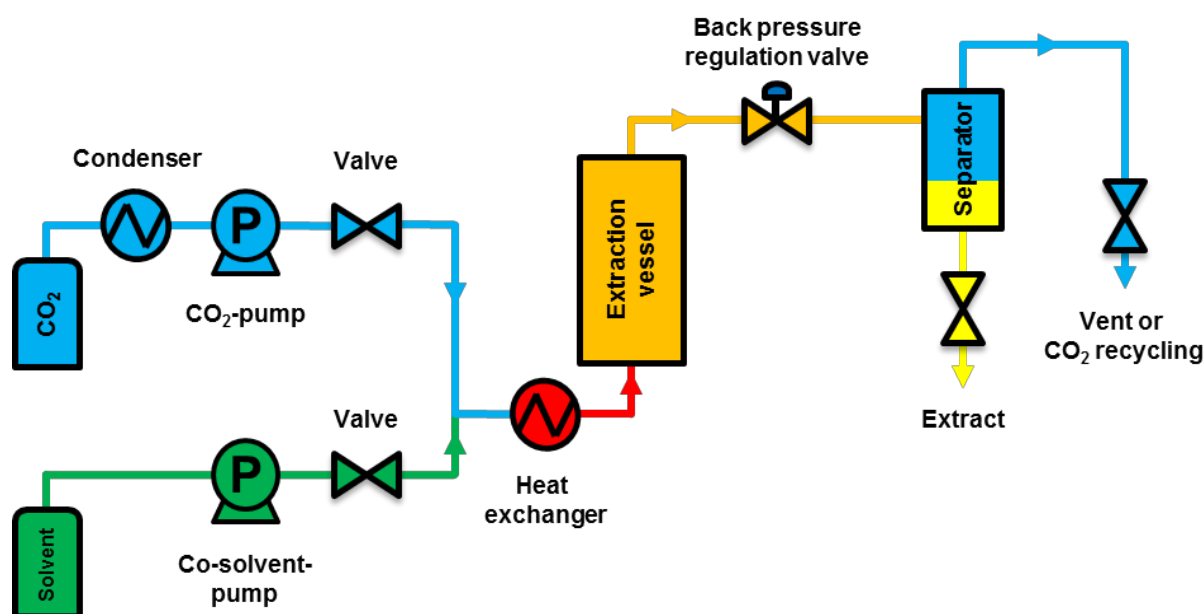


Figure 2.5: Simplified flow scheme of a supercritical fluid extraction unit with the most important sections.

2.5.4.2 Extraction

Extractions with supercritical carbon dioxide are especially applied for the recovery of volatile (e.g. essential oil) and/or nonpolar (e.g. fats, waxes) compounds from plant materials. There are many variables which have to be considered in order to optimize the extraction yield and selectivity of SFE. These parameters include the values of pressure, temperature, extraction time, solvent flow rate, particle size, packing density, and the addition of a cosolvent [47, 83-85]. In the following, a few general statements regarding these variables for plant extractions are discussed.

First of all, the pressure and temperature in the extraction vessel are the most important parameters in SFE. By means of them, the density and thus the solubility of the target compound can be adjusted. In general, it can be stated that the extraction of volatile compounds is more favorable at low densities ($\sim 0.3 \text{ g/mL}$) respectively pressures (100 bar). Otherwise, higher densities ($\sim 0.8 \text{ g/mL}$) of carbon dioxide enhance the extraction of by-

products with a high molecular weight, e.g. fatty acids, triglycerides, or waxes. Thus, the selectivity of supercritical is impaired [83-85].

However, in most cases of plant extractions, the diffusion of the target compound out of the matrix is usually the limiting step [86]. This limit can be avoided either by increasing the temperature and thus the volatility of the compound, or at high solvent densities. In order to achieve a good selectivity SFE, it is significant to control the solvent density carefully [83].

The solubility of the target compound can also be limited by the nonpolar character of carbon dioxide. Consequently, an (polar) organic solvent, called modifier or entrainer can be added to the supercritical carbon dioxide in order to enhance the solvating properties. Volatile polar solvents such as ethanol, methanol, acetone, or acetonitrile are preferred as cosolvent [2]. At least, 17 different modifiers in SFE of natural products have been studied [87]. Among all the modifiers, methanol is the most commonly used cosolvent for SFE because of its polar properties and good miscibility with CO₂. Usually, the extraction of polar compounds can be increased. However, the selectivity of the extraction process gets impaired due to the enhanced extraction of by-products [83].

Generally, longer extraction times increase the extraction yield of most of the compounds. Thereby, it has to be distinguished between static (no solvent flow) and dynamic (constant solvent flow) extraction. It has been shown that a preliminary static extraction step can enhance the extraction yield, as the sample-solvent contact is improved [84, 88].

The flow rate of the supercritical carbon dioxide through the extraction vessel has also a strong influence on the extraction efficiency. In fact, slow flow rates enhance the penetration of the plant matrix. However, if the mass transfer of the target compound in the supercritical fluid is low, the yield is not influenced by the solvent flow rate [84, 85].

As a general rule it can be asserted that decreasing the particle size of the plant material results in a higher surface area, which facilitates the extraction. However, excessive grinding of the solid may hinder the extraction due to re-adsorption of the target compounds on the matrix surface [84, 88].

Finally, a detailed discussion of the influences of different parameters on the extraction yield and selectivity of SFE is presented in chapter 6.4.4. There, SFE was performed in order to extract selectively odorants from iris rhizomes.

2.5.4.3 Separation

The second main step of SFE is the separation of the extract from the solvent. The development respectively application of an appropriate collection technique for the target compound is mandatory. To this purpose, three different separation approaches are commonly used in supercritical fluid extraction [66, 83-85].

Liquid-solvent collection is technically simple and has been the most widely used technique for natural products. Therefore, the supercritical carbon dioxide loaded with the extract is guided through a solvent and depressurization of the supercritical fluid is performed directly in the collecting solvent (e.g. ethyl acetate, acetone) [83, 84]. A major disadvantage of this method is the additional recovery of the extract from the solvent.

Another technique for the separation of extracts from the supercritical fluid is the solid-phase trapping method. It is performed by depressurization of the supercritical carbon dioxide and the extract prior to the trap. Subsequently, the target compound is directly collected from the gas phase. Suitable sorbents include silica gel, glass, or stainless steel beads. After SFE, the extract can be recovered from the trap with a suitable organic solvent. A major advantage of this method is that the selectivity of the extraction can be improved by selective trapping coupled with selective elution of the target compound. However, the solvent has to be removed in order to obtain the crude extract [66, 83, 84].

Furthermore, the collection of the extract in an empty vessel is another separation method. For this technique, the solvating power and thus the density of the supercritical fluid need to be decreased. This can be achieved either by increasing the temperature or decreasing the pressure in the separator. In addition, a fractionation of the extract can be realized by two or more separators, which are connected in series and operated at different conditions. The major advantage of this technique is that the crude extract precipitates and can be recovered without the addition of an organic solvent [66, 85].

2.5.4.4 Advantages & disadvantages compared to conventional techniques

SFE with carbon dioxide has several advantages compared to conventional extraction techniques. In detail, the extraction time can be significantly reduced compared to traditional solvent extraction or steam distillation. Typically, SFE is performed within a few tens of minutes, whereas solvent extractions or steam distillation is carried out for several hours respectively days. Moreover, the solvent power of the supercritical fluid can be adjusted by the solvent density, which leads to a higher selectivity regarding the target compound. Supercritical fluid extraction with carbon dioxide is performed at low extraction temperatures, which prevents the degradation of volatile, thermal labile or oxygen-sensitive compounds. The scent of a SFE extract is comparable to the original odor of the plant material, whereas extracts of steam distillation can exhibit a rather different and “cooked” aroma. A further advantage of SFE compared to solvent extraction, is the use of carbon dioxide, which is a non-flammable and non-toxic solvent. CO₂ can be easily removed by depressurization obtaining the crude extract without any residual solvent. Thus, no further processing, like the evaporation of an organic solvent, is needed [8, 47, 83, 84]. Finally, the energy consumption of supercritical fluid extraction is significantly lower compared to traditional extraction methods. In detail, about 0.8 kWh are consumed during SFE to obtain 1 kg of plant extract.

However, approximately 8 kWh are consumed in solvent extraction and 10-30 kWh in steam distillation to obtain the same amount of extract [89]. Concluding, SFE is an alternative method for plant extraction in regards to the principle of “green extraction” [5, 6]

Nonetheless, supercritical fluid extraction with carbon dioxide has some minor disadvantages. In detail, CO₂ can only be used to extract more or less nonpolar compounds. However, this can be overcome by using modifiers like methanol or ethanol. Additionally, the development of an extraction procedure is very time consuming in order to find the best extraction conditions and balance the temperature, pressure, and solvent flow rate for each type of plant. Further drawbacks of SFE are the high engineering requirements and investment costs of the extraction unit due to the high required pressures. Finally, carbon dioxide can react with water and form carbonic acid or amine groups in order to form amidocarbonic acids and carbamates which can cause damage of the unit parts [1, 8, 90].

2.5.4.5 Applications

Supercritical fluid extraction of natural products from plants with carbon dioxide has become one of the most important application areas [83].

One of the best-known application of SFE is the decaffeination of coffee beans [91]. The process is based on a patent of K. Zosel developed in 1970 at the Studiengesellschaft Kohle mbH (Mülheim) [92]. By means of this method, green coffee beans are extracted with supercritical carbon dioxide at a temperature of 40-80 °C and a pressure of 200-300 bar [93]. It is noteworthy that caffeine can be removed in a highly selective way. In addition, compounds are not lost that contribute to the typical coffee aroma after roasting. The main advantage of this technique is that no residual solvent is remaining in the coffee beans. Formerly, toxic chlorofluorocarbons (dichloromethane, trichloroethylene) were used as solvent for the decaffeination of coffee beans. In addition, the decaffeination of tea leaves can also be performed with supercritical carbon dioxide [91].

Another application of SFE is the extraction of volatile essential oils or active compounds (antioxidants, flavonoids, etc.) from plants [83-85, 94-99]. For example, the company FLAVEX (Rehlingen/ Germany) distributes a large number of different natural extracts obtained by SFE with carbon dioxide of plants like rosemary, oregano, ginger, hop, cinnamon, iris, pepper, and juniper berry [100].

2.5.4.6 Alternatives to carbon dioxide

An alternative solvent for carbon dioxide in SFE is supercritical dinitrogen monoxide (N₂O). This fluid is a polar solvent and thus it is better suited for the extraction of polar compounds. However, N₂O has been shown to cause violent explosion when used for samples containing

a high amount of organic compounds. For this reason, this supercritical fluid should only be used when absolutely necessary and is not suitable for plant extractions [84, 101, 102].

In addition, the application of water in SFE is not suitable due to the high critical point. Indeed, the supercritical state of water is reached at temperatures above 374 °C and pressures beyond 221 bar [84]. These extreme conditions cause the degradation and oxygenation of natural products [103]. For this reason, water can only be applied for extraction processes below its critical temperature. This technique is called subcritical or superheated water extraction, in which water is maintained at the liquid state by pressurization at temperatures between 100 and 374 °C. In fact, water is a polar solvent at ambient conditions with a relative dielectric constant of $\epsilon_r = 78.4$. However, this parameter can be changed in a wide range by adjusting the temperature and pressure of the solvent. The dielectric constant of water at 250 °C and 40 bar exhibits a value of $\epsilon_r = 27$. This value is comparable to ethanol at ambient conditions and enables the extraction of low-polar compounds [47]. Superheated water was successfully applied for the extraction of essential oils [104-114] and active compounds (e.g. antioxidants) [115, 116] from different plants.

2.6 References

- [1] H.J. Bart and S. Pilz, *Industrial Scale Natural Products Extraction*, **2011**: Wiley.
- [2] O. Sticher, *Nat. Prod. Rep.*, **2008**, 25, 517-554.
- [3] M. Kassing, U. Jenelten, J. Schenk, and J. Strube, *Chem. Eng. Technol.*, **2010**, 33, 377-387.
- [4] F. Chemat, M.A. Vian, and G. Cravotto, *Int. J. Mol. Sci.*, **2012**, 13, 8615-27.
- [5] F. Chemat and J. Strube, *Green Extraction of Natural Products*, 1. ed, **2015**, Weinheim: Wiley-VCH Verlag GmbH & Co. KGaA.
- [6] N. Rombaut, A.-S. Tixier, A. Bily, and F. Chemat, *Biofuels, Bioprod. Bioref.*, **2014**, 8, 530-544.
- [7] F. Chemat and J. Strube, *Green Extraction of Natural Products: Theory and Practice*, **2015**, Weinheim: Wiley-VCH.
- [8] D.J. Rowe, *Chemistry and Technology of Flavors and Fragrances*, **2005**, Oxford: Blackwell Publishing Ltd.
- [9] E.R. Chamorro, S.N. Zambón, W.G. Morales, A.F. Sequeira, and G.A. Velasco, *Study of the Chemical Composition of Essential Oils by Gas Chromatography*, in *Gas Chromatography in Plant Science, Wine Technology, Toxicology and Some Specific Applications*, D.B. Salih, Editor. **2012**, InTech: Rijeka, Shanghai.
- [10] C. Boutekedjiret, F. Bentahar, R. Belabbes, and J.M. Bessiere, *Flavour Fragr. J.*, **2003**, 18, 481-484.
- [11] S. Catty, *Hydrosols: the next aromatherapy*, **2001**, Rochester: Healing Arts Press.
- [12] E. Stahl and W. Schild, *Pharmazeutische Biologie (Drogenanalyse II: Inhaltsstoffe und Isolierungen)*, **1981**, Stuttgart, New York: Gustav Fischer.

- [13] P.W. Atkins and J. de Paula, *Physikalische Chemie*, 4. ed, **2006**, Weinheim: Wiley-VCH.
- [14] V. Illés, H.G. Daood, S. Pernecki, L. Szokonya, and M. Then, *J. Supercrit. Fluids*, **2000**, 17, 177-186.
- [15] N. Bousbia, M. Abert Vian, M.A. Ferhat, E. Petitcolas, B.Y. Meklati, and F. Chemat, *Food Chem.*, **2009**, 114, 355-362.
- [16] F. Chemat and G. Cravotto, *Microwave-assisted Extraction for Bioactive Compounds: Theory and Practice*, **2012**: Springer US.
- [17] A. Filly, X. Fernandez, M. Minuti, F. Visinoni, G. Cravotto, and F. Chemat, *Food Chem*, **2014**, 150, 193-8.
- [18] P.H. List and P.C. Schmidt, *Technologie pflanzlicher Arzneizubereitungen*, **1984**: Wissenschaftliche Verlagsgesellschaft.
- [19] K. Schwetlick, *Organikum*, 23. ed, **2009**, Weinheim: Wiley VCH.
- [20] J.H. Hildebrand and R.L. Scott, *The solubility of nonelectrolytes*, **1950**: Reinhold Pub. Corp.
- [21] C.M. Hansen, *Hansen Solubility Parameters: A User's Handbook*, 2. ed, **2007**, Boca Raton: CRC Press.
- [22] J. Gross and G. Sadowski, *Ind. Eng. Chem. Res.*, **2001**, 40, 1244-1260.
- [23] A. Klamt, *J. Phys. Chem.*, **1995**, 99, 2224-2235.
- [24] J. Gmehling, B. Kolbe, M. Kleiber, and J. Rarey, *Chemical Thermodynamics for Process Simulation*, **2012**, Weinheim: Wiley-VCH.
- [25] L. Moity, M. Durand, A. Benazzouz, C. Pierlot, V. Molinier, and J.-M. Aubry, *Green Chem.*, **2012**, 14, 1132-1145.
- [26] M. Durand, V. Molinier, W. Kunz, and J.M. Aubry, *Chemistry*, **2011**, 17, 5155-64.
- [27] F. Chemat and M.A. Vian, *Alternative Solvents for Natural Products Extraction*, **2014**, Berlin, Heidelberg: Springer-Verlag.
- [28] R.D. Rogers and K.R. Seddon, **2003**, 856, i-v.
- [29] A. Stark and K.R. Seddon, *Ionic Liquids*, in *Kirk-Othmer Encyclopedia of Chemical Technology*. **2007**, John Wiley & Sons, Inc.: Hoboken.
- [30] F. Favre, H. Olivier-Bourbigou, D. Commereuc, and L. Saussine, *Chem. Commun.*, **2001**, 1360-1361.
- [31] B. Tang, W. Bi, M. Tian, and K.H. Row, *Journal of chromatography. B, Analytical technologies in the biomedical and life sciences*, **2012**, 904, 1-21.
- [32] P. Wasserscheid and T. Welton, *Ionic Liquids in Synthesis*, **2008**: Wiley.
- [33] R. Ferreira, H. Garcia, A.F. Sousa, M. Petkovic, P. Lamosa, C.S.R. Freire, A.J.D. Silvestre, L.P.N. Rebelo, and C.S. Pereira, *New J. Chem.*, **2012**, 36, 2014.
- [34] R. Ferreira, H. Garcia, A.F. Sousa, C.S.R. Freire, A.J.D. Silvestre, L.P.N. Rebelo, and C. Silva Pereira, *Ind. Crop. Prod.*, **2013**, 44, 520-527.
- [35] M.J. Rosen and J.T. Kunjappu, *Surfactants and Interfacial Phenomena*, **2012**, Weinheim: Wiley-VCH.
- [36] D.F. Evans and H. Wennerström, *The Colloidal Domain: Where Physics, Chemistry, Biology, and Technology Meet*, **1999**, Weinheim: Wiley-VCH.
- [37] H. Tani, T. Kamidate, and H. Watanabe, *Anal. Sci.*, **1998**, 14, 875-888.

- [38] F.H. Quina and W.L. Hinze, *Ind. Eng. Chem. Res.*, **1999**, 38, 4150-4168.
- [39] K.-Y. Jeon and J.-H. Kim, *Biotechnol. Bioprocess Eng.*, **2007**, 12, 354-358.
- [40] P. Bauduin, A. Renoncourt, A. Kopf, D. Touraud, and W. Kunz, *Langmuir : the ACS journal of surfaces and colloids*, **2005**, 21, 6769-75.
- [41] P.P. Dongre, D.M. Kannur, V. Kosambiya, and B.D. Desai, *IJPSR*, **2011**, 2, 730-734.
- [42] J. Nagarajan, W.W. Heng, C.M. Galanakis, R.N. Ramanan, M.E. Raghunandan, J. Sun, A. Ismail, T. Beng-Ti, and K.N. Prasad, *Sep. Sci. Technol.*, **2016**.
- [43] G. Raman and V.G. Gaikar, *Langmuir : the ACS journal of surfaces and colloids*, **2003**, 19, 8026-8032.
- [44] G. Raman and V.G. Gaikar, *Ind. Eng. Chem. Res.*, **2002**, 41, 2966-2976.
- [45] S.P. Mishra and V.G. Gaikar, *Ind. Eng. Chem. Res.*, **2009**, 48, 8083-8090.
- [46] S.P. Mishra and V.G. Gaikar, *Ind. Eng. Chem. Res.*, **2004**, 43, 5339-5346.
- [47] M.D. Luque de Castro, M.M. Jiménez-Carmona, and V. Fernández-Pérez, *Trends Anal. Chem.*, **1999**, 18, 708-716.
- [48] F. Chemat, H. Zill e, and M.K. Khan, *Ultrasonics sonochemistry*, **2011**, 18, 813-35.
- [49] T. Allaf, V. Tomao, K. Ruiz, and F. Chemat, *Ultrasonics sonochemistry*, **2013**, 20, 239-46.
- [50] Y. Li, A.S. Fabiano-Tixier, V. Tomao, G. Cravotto, and F. Chemat, *Ultrasonics sonochemistry*, **2013**, 20, 12-8.
- [51] C.C.d.I. Tour, *Ann. Chim. Phys.*, **1822**, 21, 127-132.
- [52] T. Andrews, *Philos. Trans. R. Soc. London*, **1869**, 159, 575-590.
- [53] J.B. Hannay and J. Hogarth, *Proc. Roy. Soc.*, **1879**, 29, 324-326.
- [54] ChemicalLogic, *Carbon Dioxide Phase Diagram - Sublimation, Saturation and Melting Line*, Cited: 06.02.2016, Available from: <http://www.chemicallogic.com/Pages/DownloadPhaseDiagrams.aspx>.
- [55] National Institute of Standards and Technology (NIST), *Carbon dioxide - Phase change data*, Cited: 06.02.2016, Available from: <http://webbook.nist.gov/cgi/cbook.cgi?Name=carbon+dioxide&Units=SI&TP=on>.
- [56] J.D. Grace and G.C. Kennedy, *J. Phys. Chem. Solids*, **1967**, 28, 977-982.
- [57] A. S., B. Armstrong, and K.M. de Reuck, *International Thermodynamic Tables of the Fluid State- Carbon Dioxide*, Vol. 3, **1976**, Oxford, New York: Pergamon Press Ltd.
- [58] M. Moldover, *J. Chem. Phys.*, **1974**, 61, 1766-1778.
- [59] G. Brunner, *Chem. Ing. Tech.*, **1987**, 59, 12-22.
- [60] A. Birtigh and G. Brunner, *Chem. Ing. Tech.*, **1995**, 67, 829-835.
- [61] T. Clifford, *Fundamentals of Supercritical Fluids*, **1999**, New York: Oxford University Press.
- [62] T. Moriyoshi, T. Kita, and Y. Uosaki, *Ber. Bunsen. Ph. Chem.*, **1993**, 97, 589-596.
- [63] W.J. Ellison, K. Lamkaouchi, and J.M. Moreau, *J. Mol. Liq.*, **1996**, 68, 171-279.
- [64] D.P. Fernández, A.R.H. Goodwin, E.W. Lemmon, J.M.H. Levelt Sengers, and R.C. Williams, *J. Phys. Chem. Ref. Data*, **1997**, 26, 1125.
- [65] P.G. Jessop and W. Leitner, *Chemical Synthesis Using Supercritical Fluids*, **2008**, Weinheim: Wiley-VCH.

- [66] G. Brunner, *Gas extraction: an introduction to fundamentals of supercritical fluids and the application to separation processes*, **1994**, Darmstadt: Steinkopff.
- [67] C. Bicchi, P. Rubiolo, M. Fresia, F. David, and P. Sandra, *Phytochem. Anal.*, **1996**, 7, 37-41.
- [68] R.S. Oakes, A.A. Clifford, and C.M. Rayner, *J. Chem. Soc., Perkin Trans. 1*, **2001**, 917-941.
- [69] C. Blattner, *Biocatalysis using lipase immobilised in organogels in supercritical carbon dioxide*, Ph.D. Thesis, **2005**, Institute of Physical and Theoretical Chemistry at University of Regensburg
- [70] C.A. García-González, M.C. Camino-Rey, M. Alnaief, C. Zetzl, and I. Smirnova, *J. Supercrit. Fluids*, **2012**, 66, 297-306.
- [71] P.H. Tewari, A.J. Hunt, and K.D. Lofftus, *Mater. Lett.*, **1985**, 3, 363-367.
- [72] L. Kocon, F. Despetis, and J. Phalippou, *J. Non-Cryst. Solids*, **1998**, 225, 96-100.
- [73] E. Bach, E. Cleve, and E. Schollmeyer, *Rev. Progr. Color.*, **2002**, 32, 88-102.
- [74] M. van der Kraan, M.V. Fernandez Cid, G.F. Woerlee, W.J.T. Veugelers, and G.J. Witkamp, *J. Supercrit. Fluids*, **2007**, 40, 470-476.
- [75] J.N. Hay and K. Johns, *Surf. Coat. Int.*, **2000**, 83, 106-110.
- [76] I. Kikic and F. Vecchione, *Curr. Opin. Solid State Mater. Sci.*, **2003**, 7, 399-405.
- [77] J.W. Tom and P.G. Debenedetti, *Journal of Aerosol Science*, **1991**, 22, 555-584.
- [78] A.F. Holleman and N. Wiberg, *Lehrbuch der anorganischen Chemie*, 102. ed, **2007**, Berlin: Walter de Gruyter.
- [79] J. Eastoe, *Curr. Opin. Colloid Interface Sci.*, **2003**, 8, 267-273.
- [80] E.L.V. Goetheer, M.A.G. Vorstman, and J.T.F. Keurentjes, *Chem. Eng. Sci.*, **1999**, 54, 1589-1596.
- [81] Air Liquide Deutschland GmbH, *Kohlendioxid - Ohne CO₂ kein Leben, keine Zivilisation, keine Zukunft*, Cited: 11.02.2016, Available from: <https://www.airliquide.de/inc/dokument.php/standard/911/kohlendioxid.pdf>.
- [82] Berndt Wischnewski, *peace software - Calculation of thermodynamic state variables of carbon dioxide at saturation state, boiling curve*, Cited: 11.02.2016, Available from: http://www.peacesoftware.de/einigewerte/co2_e.html.
- [83] Q. Lang and C.M. Wai, *Talanta*, **2001**, 53, 771-782.
- [84] S.M. Pourmortazavi and S.S. Hajimirsadeghi, *J. Chromatogr. A*, **2007**, 1163, 2-24.
- [85] E. Reverchon, *J. Supercrit. Fluids*, **1997**, 10, 1-37.
- [86] W.K. Modey, D.A. Mulholland, and M.W. Raynor, *J. Chromatogr. Sci.*, **1996**, 34, 320-325.
- [87] W.K. Modey, D.A. Mulholland, and M.W. Raynor, *Phytochem. Anal.*, **1996**, 7, 1-15.
- [88] K.D. Bartle, A.A. Clifford, S.B. Hawthorne, J.J. Langenfeld, D.J. Miller, and R. Robinson, *J. Supercrit. Fluids*, **1990**, 3, 143-149.
- [89] P. Pellerin *Comparing extraction by traditional solvents with supercritical extraction from an economic and environmental standpoint*, in *International Symposium on Supercritical Fluids* **2003**: Versailles, France.
- [90] W. Leitner, *Top. Curr. Chem.*, **1999**, 206, 107-132.

- [91] M. McHugh, V. Krukonis, and H. Brenner, *Supercritical Fluid Extraction: Principles and Practice*, **1994**, Stoneham: Butterworth-Heinemann.
- [92] K. Zosel, *Verfahren zur Entcoffeinierung von Kaffee*, **1970**, Patent, P 2005293.1.
- [93] H. Garloff, H. Lange, and R. Viani, *Kaffee*, in *Lebensmitteltechnologie: Biotechnologische, chemische, mechanische und thermische Verfahren der Lebensmittelverarbeitung*, R. Heiss, Editor. **1991**, Springer Berlin Heidelberg: Berlin, Heidelberg. 358-370.
- [94] B. Diaz-Reinoso, A. Moure, H. Dominguez, and J.C. Parajo, *J Agric Food Chem*, **2006**, 54, 2441-69.
- [95] A.K. Genena, H. Hense, A. Smânia Junior, and S.M.d. Souza, *Ciênc. Tecnol. Aliment.*, **2008**, 28, 463-469.
- [96] O. Celiktas, E. Bedir, and F. Sukan, *Food Chem.*, **2007**, 101, 1457-1464.
- [97] M.T. Tena, M. Valcarcel, P.J. Hidalgo, and J.L. Ubera, *Anal. Chem.*, **1997**, 69, 521-6.
- [98] C. Bicchi, A. Binello, and P. Rubiolo, *Phytochem. Anal.*, **2000**, 11, 236-242.
- [99] A.N. Giannuzzo, H.J. Boggetti, M.A. Nazareno, and H.T. Mishima, *Phytochem. Anal.*, **2003**, 14, 221-3.
- [100] *Produktindex*, Cited: 12.02.2016, Available from: <http://www.flavex.com/naturextrakte/produkte/produktindex/>.
- [101] N. Alexandrou, M.J. Lawrence, and J. Pawliszyn, *Anal. Chem.*, **1992**, 64, 301-311.
- [102] D.E. Raynie, *Anal. Chem.*, **1993**, 65, 3127-3128.
- [103] S. Minett and K. Fenwick, *European Water Management*, **2001**, 4, 54-56.
- [104] M.Z. Ozel, F. Gogus, and A.C. Lewis, *Food Chem.*, **2003**, 82, 381-386.
- [105] F. Gogus, M.Z. Ozel, and A.C. Lewis, *Flavour Fragr. J.*, **2006**, 21, 122-128.
- [106] A.A. Clifford, A. Basile, and S.H.R. Al-Saidi, *Fresenius J. Anal. Chem.*, **1999**, 364, 635-637.
- [107] M. Khajenoori, A.H. Asl, F. Hormozi, M.H. Eikani, and H.N. Bidgoli, *Journal of Food Process Engineering*, **2009**, 32, 804-816.
- [108] B. Jayawardena and R.M. Smith, *Phytochem. Anal.*, **2010**, 21, 470-2.
- [109] R. Soto Ayala and M.D. Luque de Castro, *Food Chem.*, **2001**, 75, 109-113.
- [110] M.Z. Ozel and H. Kaymaz, *Anal. Bioanal. Chem.*, **2004**, 379, 1127-33.
- [111] M.M. Jiménez-Carmona, J.L. Ubera, and M.D. Luque de Castro, *J. Chrom. A*, **1999**, 855, 625-632.
- [112] A. Basile, M.M. Jiménez-Carmona, and A.A. Clifford, *J. Agric. Food Chem.*, **1998**, 46, 5205-5209.
- [113] A. Ammann, D.C. Hinz, R.S. Addleman, C.M. Wai, and B.W. Wenclawiak, *Fresenius J. Anal. Chem.*, **1999**, 364, 650-653.
- [114] R.M. Smith, *J. Chrom. A*, **2002**, 975, 31-46.
- [115] E. Ibanez, A. Kubatova, F.J. Senorans, S. Caverro, G. Reglero, and S.B. Hawthorne, *J. Agric. Food Chem.*, **2003**, 51, 375-82.
- [116] A. Cvetanović, J. Švarc-Gajić, P. Mašković, S. Savić, and L. Nikolić, *Ind. Crop. Prod.*, **2015**, 65, 582-591.

3 Microemulsions

3.1 Definition and properties

The occurrence of a microemulsion was for the first time observed by J. H. Schulman and T. P. Hoar in 1943. Thereby, water, alkali soaps, and oil were mixed with an alcohol or a non-ionized amphiphilic compound obtaining an optically transparent and thermodynamically stable solution [1]. However, the term “microemulsion” was introduced by Schulman *et. al.* in 1959 for such systems [2]. In addition, microemulsions are isotropic solutions formed spontaneously (without any energy input required) and exhibit a relatively low viscosity [3].

In general, microemulsions consist of two immiscible liquids, usually water and an aliphatic hydrocarbon (oil), and an ionic or nonionic surfactant. However, some systems require the addition of a cosurfactant, which are mostly medium chained alcohols. The cosurfactant molecules are arranged between the surfactant molecules and decrease the rigidity of the interfacial film. This behavior prevents any possible organization of the single molecules. The surfactant and cosurfactant molecules optimize the occupied area in the interfacial film and help decreasing the direct contact of water and oil. This results in extremely low interfacial tensions with values of 10^{-2} to 10^{-3} mN/m. Moreover, the addition of a cosurfactant to the microemulsion can even further decrease the interfacial tension to a value of 10^{-5} mN/m. In comparison, the interfacial tension of the two immiscible solvents water and *n*-hexane is 51.4 mN/m [4-7].

Apart from this, microemulsions can also be formed in supercritical carbon dioxide consisting of water, carbon dioxide, and surfactant. Thereby, carbon dioxide acts as nonpolar “oil phase”. In addition, mostly fluorocarbon surfactants are used in these types of microemulsions [8-11].

3.2 Classification

Microemulsions are dispersed systems in which a liquid phase (dispersed phase) is distributed in another liquid phase (continuous phase). These solutions are structured and can be classified in three different types depending on the oil and water content. In detail, oil-in-water (o/w) microemulsions are formed at high water contents, where water is the continuous phase and oil the dispersed phase. These microemulsions consist of well-defined droplets with diameters from 5 to 100 nm. For this reason, microemulsions are optically transparent as these particles are too small to scatter visible light. The interfacial film between the two nanoscopically immiscible “phases” is stabilized by a monolayer consisting of surfactants and cosurfactants. Furthermore, water-in-oil (w/o) microemulsions are formed

at high oil contents. Here, oil is the continuous and water the dispersed pseudo-phase [4, 12]. A schematic representation of these two types of microemulsions is shown in Figure 3.1.

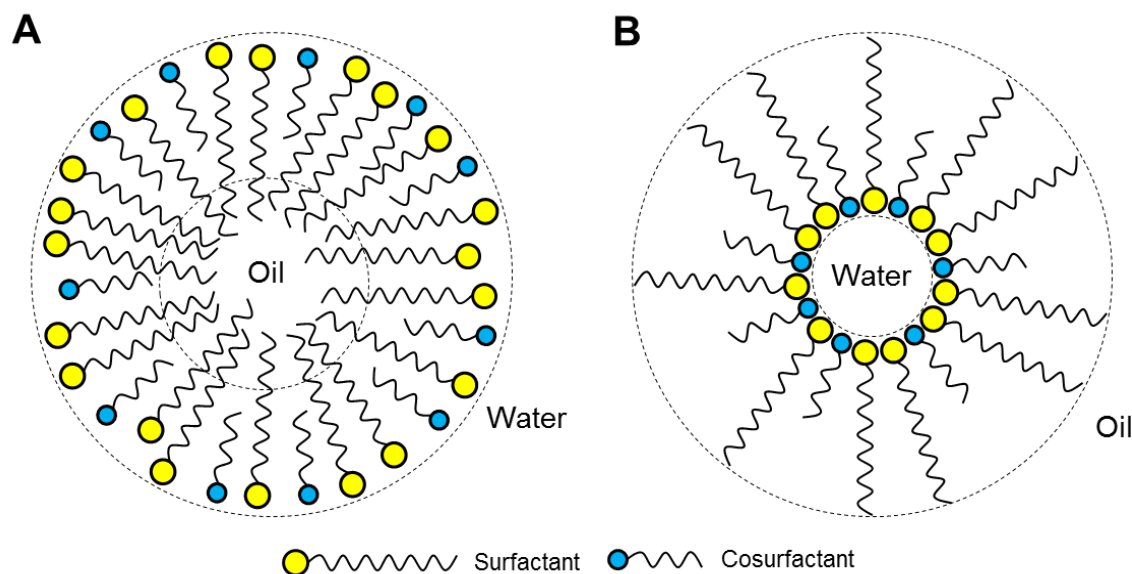


Figure 3.1: Schematic representation of nanodroplets formed in (A) o/w-microemulsions and (B) w/o-microemulsions. Adapted from [13].

The third structure type is called bicontinuous microemulsion. In general, these structures appear at intermediate ratios of oil to water (near 50/50), thus between the formation of o/w- and w/o-microemulsions. Here, isotropic sponge-like structures are present, in which oil and water domains are intertwined and interconnected. These networks are still stabilized by an interfacial film of surfactants and cosurfactants [11, 14, 15].

Often, abbreviations are used to describe the different types of microemulsions, i.e. L1 phase (o/w-microemulsion), L2 phase (w/o-microemulsion) and L3 phase (bicontinuous microemulsion) [16]. In addition, a (pseudo-) ternary phase diagram (Gibbs' triangle) is used to plot the compositions of oil, water, and surfactant (+cosurfactant) at which microemulsion domains occur. However, parameters like the temperature, pressure, type of oil, type of surfactant, and the ratio of surfactant to cosurfactant have to be kept constant [11].

3.3 Salt effects

Besides cosurfactants, the addition of a salt also influences the formation of microemulsions as the physical properties of amphiphilic molecules are strongly influenced. In 1888, F. Hofmeister investigated the effect of salts on the solubility of proteins in water. He discovered that some ions are able to precipitate proteins in water ("salting-out") and other ions enhance their solubilization ("salting-in"). Typically, cations and anions can be ordered according to

the “Hofmeister Series” which is presented in Figure 3.2. All ions on the left side of the series tend to “salt-out” proteins and are also called kosmotropic ions, while the ions on the right side tend to “salt-in” proteins and are also called chaotropic ions. A dividing line between kosmotropic and chaotropic ions is often drawn at the chloride anion and the sodium cation [17-19].

<i>weakly hydrated soft (low charge density)</i>	Cations										<i>strongly hydrated hard (high charge density)</i>		
	$\text{N(CH}_3)_4^+$	NH_4^+	Cs^+	Rb^+	K^+	Na^+	Li^+	Mg^{2+}	Ca^{2+}				
	kosmotropic = “salting-out”						chaotropic = “salting-in”						
	SO_4^{2-}	HPO_4^{2-}	OAc^-	cit^-	OH^-	Cl^-	Br^-	NO_3^-	ClO_3^-	BF_4^-	I^-	ClO_4^-	SCN^-
<i>strongly hydrated hard (high charge density)</i>	Anions										<i>weakly hydrated soft (low charge density)</i>		
surface tension ↑											surface tension ↓		
solubility hydrocarbons ↓											solubility hydrocarbons ↑		
protein denaturation ↓											protein denaturation ↑		
protein stability ↑											protein stability ↓		

Figure 3.2: A typical ordering of cations and anions in “Hofmeister Series” with their most important properties and effects. Adapted from [19].

In general, kosmotropic cations are weakly hydrated soft ions with a low charge density, whereas, kosmotropic anions are strongly hydrated hard ions with a high charge density. These ions tend to increase the structure and surface tension of water, but decrease the solubility of hydrocarbons in water. In the case of proteins, kosmotropic ions enhance their stability in aqueous solutions, which leads to a decrease of denaturation. Consequently, the proteins are precipitated i.e. “salted-out”. On the contrary, chaotropic ions tend to break the structures of water and decrease its surface tension. In addition, the solubility of hydrocarbons in water is increased and hence, they adsorb at the interface, which leads to the “salting-in” effect. Chaotropic anions are weak hydrated soft ions with a low charge density, whereas chaotropic cations are strongly hydrated hard ions with a high charge density. These effects can also be used to customize the formulation of microemulsions [19-21].

3.4 Characterization

Various methods are known to investigate the microstructures (w/o, o/w, and bicontinuous) of microemulsions.

Conductivity measurements are an easy and suitable method to determine these microemulsion domains. To this purpose, the specific conductivity κ is measured as a function of the water content in the microemulsion. Typically, the conductivity shows a bell-shaped evolution with increasing water content. This behavior is well-known and can be explained by the percolative conduction phenomenon. Starting with a w/o-microemulsion, the electrical conductivity is nearly zero. Here, oil is the continuous phase, but water and conducting ions are trapped in spherical droplets. Thus, no or only a slight charge transfer can occur. By increasing the water content, a non-linear increase of the conductivity can be observed until the so-called percolation threshold is reached. Here, interlinking and clustering processes start occurring. Subsequently, the conductivity increases linearly until a maximum value is reached. This leads to the formation of channels until bicontinuous microemulsions are present. A further increase of the water content leads to a decrease of conductivity, which is due to the formation of o/w-microemulsion. The further decrease of the conductivity can be explained by dilution effects [14, 22-26]. A common conductivity curve with percolative behavior is presented in Figure 7.23 (p. 184).

In addition, anti-percolative systems show a different behavior of the conductivity, as the merging of droplets is prevented by a rigid interfacial film. As a consequence, the conductivity of such systems exhibits only low values [27].

More sophisticated methods to characterize and investigate the structures of microemulsions include dynamic light scattering (DLS) [28, 29], small angle neutron scattering (SANS) [30], small-angle x-ray scattering (SAXS) [11, 16], NMR [11], freeze fracture electron microscopy (FFEM) [31], or cryo-scanning electron microscopy [32].

3.5 Applications

The unique properties of microemulsion led to of multiple applications of microemulsions in different sectors.

The interest of microemulsions in the pharmaceutical industry has grown in the past decades. Here, microemulsions can be used as drug delivery systems by incorporating a wide range of drug molecules. Especially, o/w microemulsions can be used to enhance the solubility of hydrophobic drugs and incorporate them into the nonpolar oil phase. In addition, the drug absorption in the body can be enhanced by the increasing membrane permeability [33-35].

Furthermore, microemulsions can be used to extract natural compounds from plants. However, this is a rather poorly studied field of microemulsions. The applications include the extraction of vegetable oils from oilseeds [36], β -carotene from carrots [37], or nicotine from tobacco waste [38].

Further applications of microemulsions include the formulation of cosmetics [38], detergents [3], and food products [39], as well as the oil recovery from porous soils [40], the water remediation [41], or the cleanup of soils [42].

3.6 References

- [1] T.P. Hoar and J.H. Schulman, *Nature*, **1943**, 152, 102-103.
- [2] J.H. Schulman, W. Stoeckenius, and L.M. Prince, *J. Phys. Chem.*, **1959**, 63, 1677-1680.
- [3] P. Kumar and K.L. Mittal, *Handbook of Microemulsion Science and Technology*, **1999**, New York: Taylor & Francis.
- [4] D.F. Evans and H. Wennerström, *The Colloidal Domain: Where Physics, Chemistry, Biology, and Technology Meet*, **1999**, Weinheim: Wiley-VCH.
- [5] P.G. De Gennes and C. Taupin, *J. Phys. Chem.*, **1982**, 86, 2294-2304.
- [6] S.H. Chen and R. Rajagopalan, *Micellar Solutions and Microemulsions: Structure, Dynamics, and Statistical Thermodynamics*, **1990**, New York: Springer-Verlag.
- [7] A. Goebel and K. Lunkenheimer, *Langmuir : the ACS journal of surfaces and colloids*, **1997**, 13, 369-372.
- [8] J.L. Fulton and R.D. Smith, *J. Phys. Chem.*, **1988**, 92, 2903-2907.
- [9] K. Jackson and J.L. Fulton, *Langmuir : the ACS journal of surfaces and colloids*, **1996**, 12, 5289-5295.
- [10] C. Blattner, *Biocatalysis using lipase immobilised in organogels in supercritical carbon dioxide*, Ph.D. Thesis, **2005**, Institute of Physical and Theoretical Chemistry at University of Regensburg
- [11] K. Holmberg, *Handbook of Applied Surface and Colloid Chemistry*, Vol. 1-2, **2002**, Weinheim: Wiley-VCH.
- [12] D. Myers, *Surfactant Science and Technology*, 3. ed, **2006**, Hoboken: John Wiley & Sons.
- [13] U. Pfüller, *Mizellen - Vesikel - Mikroemulsionen: Tensidassoziate und ihre Anwendung in Analytik und Biochemie*, **1986**, Berlin, Heidelberg: Springer-Verlag
- [14] M. Clausse, J. Peyrelasse, J. Heil, C. Boned, and B. Lagourette, *Nature*, **1981**, 293, 636-638.
- [15] L.E. Scriven, *Nature*, **1976**, 263, 123-125.
- [16] J. Marcus, *Study of surfactant-free microemulsions and microemulsions with fatty acid salts* Ph.D. Thesis, **2015**, Institute of Physical and Theoretical Chemistry at University of Regensburg
- [17] F. Hofmeister, *Arch. Exp. Pathol. Pharmacol.*, **1888**, 24, 247-260.

- [18] W. Kunz, J. Henle, and B.W. Ninham, *Curr. Opin. Colloid Interface Sci.*, **2004**, 9, 19-37.
- [19] W. Kunz, *Specific Ion Effects*, **2010**, Singapore: World Scientific Publishing.
- [20] W. Kunz, *Curr. Opin. Colloid Interface Sci.*, **2010**, 15, 34-39.
- [21] E. Leontidis, *Curr. Opin. Colloid Interface Sci.*, **2002**, 7, 81-91.
- [22] M.L. Klosek, D. Touraud, and W. Kunz, *Green Chem.*, **2012**, 14, 2017.
- [23] M. Sahimi, *Applications of Percolation Theory*, **1994**, London: Tayler & Francis.
- [24] M. Dvolaitzky, M. Lagues, J.P. Le Pesant, R. Ober, C. Sauterey, and C. Taupin, *J. Phys. Chem.*, **1980**, 84, 1532-1535.
- [25] B. Lagourette, J. Peyrelasse, C. Boned, and M. Clausse, *Nature*, **1979**, 281, 60-62.
- [26] M. Laguës, *J. Phys. Lett.*, **1979**, 40, 331-333.
- [27] T.N. Zemb, *Colloids Surf. A*, **1997**, 129-130, 435-454.
- [28] M.J. Hou, M. Kim, and D.O. Shah, *Journal of Colloid and Interface Science*, **1988**, 123, 398-412.
- [29] M. Tomsic, M. Bester-Rogac, A. Jamnik, W. Kunz, D. Touraud, A. Bergmann, and O. Glatter, *J. Colloid Interface Sci.*, **2006**, 294, 194-211.
- [30] H. Endo, M. Mihailescu, M. Monkenbusch, J. Allgaier, G. Gompper, D. Richter, B. Jakobs, T. Sottmann, R. Strey, and I. Grillo, *J. Chem. Phys.*, **2001**, 115, 580.
- [31] S. Burauer, L. Belkoura, C. Stubenrauch, and R. Strey, *Colloids Surf. A*, **2003**, 228, 159-170.
- [32] C. Note, J. Ruffin, B. Tiersch, and J. Koetz, *Journal of Dispersion Science and Technology*, **2007**, 28, 155-164.
- [33] M.J. Lawrence and G.D. Rees, *Advanced Drug Delivery Reviews*, **2000**, 45, 89-121.
- [34] P.P. Constantinides, J.P. Scalart, C. Lancaster, J. Marcello, G. Marks, H. Ellens, and P.L. Smith, *Pharmaceutical Research*, **1994**, 11, 1385-1390.
- [35] P.P. Constantinides, *Pharmaceutical Research*, **1995**, 12, 1561-1572.
- [36] A.D. Gadhav, *International Journal of Research in Engineering and Technology*, **2014**, 03, 147-158.
- [37] S. Roohinejad, *Extraction of β -carotene from carrot pomace using microemulsions and pulsed electric fields*, Ph.D. Thesis, **2014**, at University of Otago
- [38] C. Solans and H. Kunieda, *Industrial Applications of Microemulsions*, **1996**, New York: Marcel Dekker.
- [39] N. Garti, *Curr. Opin. Colloid Interface Sci.*, **2003**, 8, 197-211.
- [40] D.O. Shah and R.S. Schechter, *Improved Oil Recovery by Surfactant and Polymer Flooding* **1977**, New York: Academic Press.
- [41] J.H. Harwell, D.A. Sabatini, and R.C. Knox, *Colloids Surf. A*, **1999**, 151, 255-268.
- [42] S. Wellert, M. Karg, H. Imhof, A. Steppin, H.J. Altmann, M. Dolle, A. Richardt, B. Tiersch, J. Koetz, A. Lapp, and T. Hellweg, *J. Colloid Interface Sci.*, **2008**, 325, 250-8.

4 Analysis methods

4.1 Chromatography in general

Chromatography is a technique to separate different compounds. In order to quantify and qualify the separated compounds, the process has to be coupled with a suitable detection method.

The Russian botanist M. Tswett is considered to be the discoverer of chromatography. In 1906, he described at first the separation of leaf pigments (chlorophylls and xanthophyll) by means of a packed column. Thereby, a leaf extract was passed with petroleum through a glass column, which was filled with powdery calcium carbonate. The observation of different colored sections on the column led to the neologism “chromatography”. The name consists of the Greek words *chroma* for “color” and *graphein* for “writing” [1, 2].

The principle of chromatography is based on the transition of the compound to be separated between two immiscible phases. To this purpose, the sample mixture is dissolved in a mobile phase (liquid, gas, supercritical fluid) and passes through a stationary phase. A separation of the mixture can be achieved due to dissimilar interactions of the compounds with the stationary phase [2]. In general, chromatography can be divided in three major techniques depending on the state of aggregation of the mobile phase: liquid chromatography (LC), gas chromatography (GC) and supercritical fluid chromatography (SFC) [3].

4.1.1 Separation mechanisms

The separation of the single compounds is based on different mechanisms. First of all, distribution processes are occurring if a liquid mobile and a liquid stationary phase are used. The separation depends on the dissimilar solubility of the analyte in the two liquids. In general, if the partition equilibrium of the analyte is higher in the stationary phase, the lower is the velocity of the analyte through the separation column. Another mechanism of chromatography is based on adsorption processes. Here, the compounds interact with the surface of the stationary phase due to their polarities. The transport velocity of a compound through the separation column is mainly depended on two factors: the affinity of the substance to the stationary phase and the ability of the mobile phase to oust the substance from the stationary phase. In addition, chromatography can be based on ionic interactions and exclusion processes due to the charge respectively size of the analyte [4].

4.1.2 Chromatographic separation

The chromatographic separation is based on the continuous transition of the substances between the stationary and mobile phase. This phase transition serves the adjustment of the

equilibrium concentration of a compound in the mobile and stationary phases. However, the establishment of the equilibrium is disturbed by the continuous transport of the mobile phase. Thus, the distance in a chromatography column can be divided in numerous theoretical separations stages.

The separation mechanism in a chromatography column can be described as sequence of numerous adsorption and distribution processes. In general, the separation efficiency is the greater the more theoretical plates are present in the column. The efficiency is depending on the length of the column, the particle size, the packing density, and surface properties of the stationary phase. In addition, the theory of theoretical plates can be described by the Van Deemter equation (Figure 4.1). Here, a relation between the height of a theoretical plate H and the linear velocity u of the mobile phase is drawn. In detail, the height of a theoretical plate consists of three different terms, which are depending on the velocity of the mobile phase [3, 4].

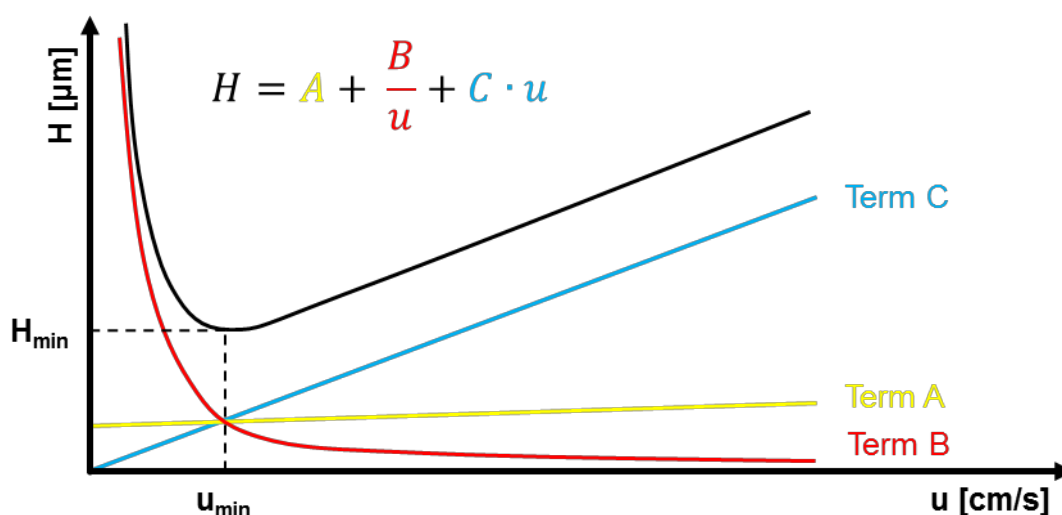


Figure 4.1: Presentation of the curve according to the equation of Van Deemter depending on the height of a theoretical plate H and the linear velocity u of the mobile phase.

The term A is called Eddy-diffusion or turbulent diffusion. This effect results from the geometry of the solid particles (stationary phase) and is based on the dispersed flow of the analyte around the particles. Thus, the distance of the analytes through the column is (statistically) distributed. However, the Eddy-diffusion is not influenced by the linear velocity of the mobile phase and thus exhibits a constant value for a given column. Furthermore, the term B characterizes the longitudinal diffusion of the analytes in the mobile phase. This means that the analytes are not only moved in the flow direction of the mobile phase, but can also induce an own mobility in all directions. The diffusion coefficient of the mobile phase has a major influence on the B-term. The longitudinal diffusion is reciprocally proportional to the

linear velocity. Moreover, the mass transfer between the stationary and mobile phase is described by the term C . In the case of a liquid stationary phase, the distribution equilibrium of the analyte is dominant. A small film thickness of the stationary phase results in a high diffusion coefficient and thus the mass transfer is enhanced. On the other hand, if the stationary phase consists of solid particles, the mass transfer of the analyte is depending on adsorption and desorption processes. The C -term increases linearly with the velocity of the mobile phase [2, 3, 5].

In principle, the aim of chromatography is the effective separation of compounds within short analysis times. To this purpose, a minimum value of the theoretical plate height H is desirable. In general, this can be achieved by a small particle size or a low film thickness of the stationary phase (influences A - and C -term). In addition, a homogenous distribution of the particle size and packing density of the stationary phase is preferable (influences B -term). Moreover, a small diameter of the column enhances the separation efficiency (influences A - and B -term) [2].

However, several additional parameters influence the separation efficiency. In particular, the adsorption of compounds on the stationary phase can be decreased by increasing the temperature of the column. The selectivity of the separation column can be influenced by the polarity of the stationary phase. A sufficient separation can be achieved if the substances are differently retained on the column [4].

4.1.3 Chromatogram

The result of a chromatographic separation is recorded by a chromatogram, where the signal of a detector is plotted against the analysis time. A general chromatogram is presented in Figure 4.2.

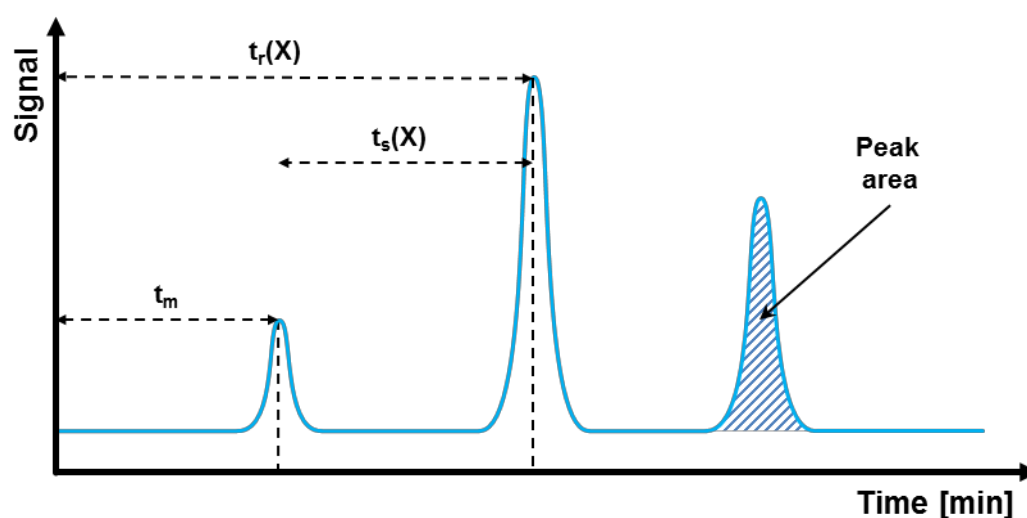


Figure 4.2: General chromatogram with the retention times of the mobile phase (t_m), the total (t_r) and net (t_s) retention time of a compound X and the integrated area of a peak.

The time at which a certain compound is eluted and thus detected is called retention time. The minimum time that a non-retaining compound requires to be transported from the injector to the detector is called permeation time (t_m). This means that all other compounds in the analysis sample will reside in the system for at least the same time. The separation of the substances is due to the fact that the substances interact with the stationary phase and thus elute at different total retention times (t_r). In addition, the net retention time (t_s) refers to the duration of stay of a compound in the stationary phase. The retention time of a peak is the main qualitative results that can be used for the assignment of different substances. This can be controlled by the injection of a reference compound and the subsequent elution under the exact same chromatographic conditions [4].

In addition, the chromatogram can be used to make quantitative statements of a selected analyte. To this purpose, the peak needs to be integrated, because the peak area is proportional to the amount of substance. However, a suitable calibration method is necessary to calculate the concentration of the analyte in the sample. This can be done by analyzing calibration samples with different concentrations of the pure analyte [4].

4.2 High-performance liquid chromatography (HPLC)

High-performance liquid chromatography (HPLC) is a separation method where solid particles are used as stationary phase and organic solvents as mobile phase. The separation process is performed at high pressures (up to 400 bar) due to the small size and high packing density of the stationary phase. This leads to an improvement of the separation efficiency compared to conventional liquid chromatography techniques [2].

In order to examine a sample by HPLC, it has to be assured that the substance to be analyzed is adequately soluble in a suitable solvent. If this condition is fulfilled, HPLC analyses are mainly performed for nonvolatile and thermally unstable compounds. In addition, analytes with a high molecular weight are often analyzed by HPLC, especially in the sector of bio-analytics [6].

4.2.1 Procedure

A simplified scheme of a typical HPLC system with the most important unit parts is shown in Figure 4.3. The separation process is described in the following. First of all, one or more organic solvents are supplied by a storage vessel and subsequently transported through a degasser in order to remove residual gases. Afterwards, the solvents are mixed at an atmospheric pressure and further transported by the solvent pump. The sample to be analyzed is introduced with a defined volume to the system by a manual sampling loop or Autosampler. The mixture is transported to the column with a constant flow rate of the solvent. Here, the separation of the different compounds takes place at a constant

temperature value. Subsequently, the isolated compounds can be identified by a suitable detector, which generates an electrical signal obtaining the final chromatogram [2, 7].

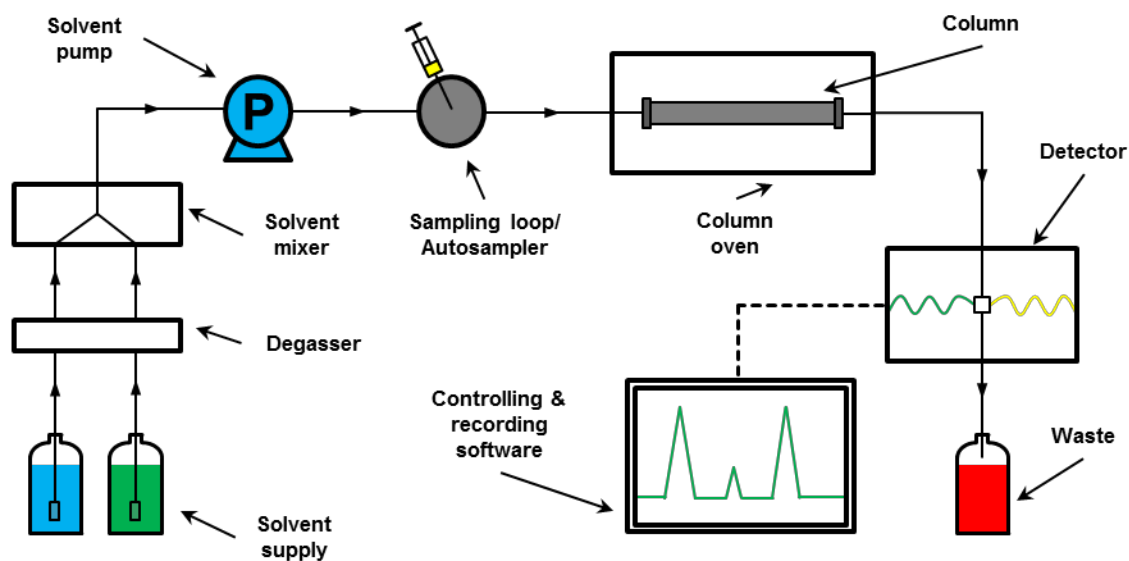


Figure 4.3: Simplified scheme of a high-performance liquid chromatography (HPLC) system.

4.2.2 Stationary phase

In general, it can be distinguished between two main types of stationary phases. In normal phase chromatography (NP-HPLC), polar porous particles like aluminum oxide or silica gel are used as stationary phase. Normal phases are predominantly used to separate nonionic and nonpolar to medium polar substances. The retention of the compounds increases with increasing polarity.

Another technique is the reversed phase chromatography (RP-HPLC). Here, the silanol groups of silica gel particles are chemically modified with nonpolar alkyl chains. Principally, the hydrophobic chain consists of linear octyl (RP-8) or octadecyl (RP-18) groups. In addition, free silanol groups of the particles, can be modified by short chain alkyl groups in order enhance the nonpolar character of the phase. This technique is called “end-capping”. Reversed phase chromatography is the most common separation technique in HPLC analyses. It can be used for the separation of amino acids, peptides, proteins, and other biogenic compounds. The analytes are retarded with their increasing hydrophobic character, thus the retention increases with decreasing polarity of the compound.

Usually, the diameter of the spherical solid particles is between 2 and 15 μm . However, the trend towards smaller particles increased in the past years. Solid particles with a mean diameter of 1.5 μm increase significantly the separation efficiency. However, HPLC units are required which can endure or rather produce high pressure values. This technique is called ultra-high performance liquid chromatography (UHPLC) [6, 7].

4.2.3 Mobile phase

The choice of an appropriate solvent as mobile phase is mandatory in HPLC analyses. In general, the solvent selection is depending on the stationary phase (RP or NP) in order to adjust the separation and recovery of the compounds. The polarities of the mobile and stationary phase are decisive for the separation efficiency. To this purpose, the eluotropic series was investigated, which is shown in Table 4.1. Here, different solvents are order by the increasing eluting power for normal-phase chromatography. Consequently, it is valid that a polar solvent is a good eluent, whereas a nonpolar mobile phase is weak a eluent in NP-HPLC [7].

Table 4.1: Eluotropic series for common HPLC solvents, arranged by increasing eluting power with silica gel as stationary phase. Adapted from [3].

Solvent	Eluting power ϵ_0	UV-cut off λ / nm
Hexane	0.00	210
Chloroform	0.26	245
Tetrahydrofuran	0.35	220
Acetonitrile	0.50	200
Ethanol	0.68	210
Methanol	0.73	220
Water	≥ 1.00	≤ 200

However, the eluotropic series in reversed-phase chromatography is vice versa. Here, the mobile phase consists mainly of relatively polar solvents which are miscible with water, like acetonitrile or methanol. Thus, the eluting power of the mobile phase decreases by increasing the polarity of the solvent [7].

The selection of a solvent for a mobile phase is also depending on the UV-cut-off wavelength. The adsorption of a solvent increases significantly below the given values (see Table 4.1). Also, proper degassing by ultrasound under vacuum or purging with an inert gas like helium of the mobile phase is necessary in order to avoid the formation of gas bubbles in the HPLC system [7].

There are two different elution techniques in HPLC analyses. The first method is the isocratic elution, where the composition of the mobile phase is not changed during the separation process. The eluents are previously mixed in the required ratio. Thus, the eluting power of the mobile phase is constant. The second technique is gradient elution. Here, the composition or the eluting power of the mobile phase is changed during the separation

process. By means of this technique, shorter analysis times of strongly retarding substances can be achieved. A further classification of this technique can be made. If the gradient is mixed at atmospheric pressure, the technique is called low pressure gradient method. On the other hand, if the solvents are pumped by individual pumps and subsequently mixed, the method is called high pressure gradient [6, 7].

4.2.4 Detectors

The most commonly used detector in HPLC analyses is the photometric detector. Its application accounts more than 70% of analyses. The laws of photometry (Lambert-Beer etc.) are valid. The Z-shaped flow cell is considered as a cuvette. A filter photometer is the simplest version of a UV-detector. Here, the absorbance of the compounds is measured at one or several wavelength. The standard wavelength of detection is 254 nm, which is the emission maximum of the mercury vapor lamp. In particular, many organic and organic compounds absorb at this spectral range. A further development of this technique is the diode array detector (DAD), which records the total UV/VIS-spectrum (from 190 to 950 nm) of the eluted compounds [2].

Additional detectors in HPLC analyses are fluorescence detectors, mass spectrometers (MS), refractive index (RI) detectors, conductivity detectors, electrochemical detectors, and evaporative light scattering detectors (ELSD) [2, 3, 7-9]. The choice of the detector is always dependent on the analyte to be examined.

4.3 Gas chromatography (GC)

Gas chromatography (GC) is a separation method where solid particles or liquid immobilized films are used as stationary phases and gases as mobile phase. To this purpose, the analysis sample needs to be vaporized.

In order to analyze a sample by GC, it has to be assured that the substance to be analyzed is volatile and thermally stable at high temperatures. The evaporation temperature is usually between 50 and 300 °C. Furthermore, it is possible to convert nonvolatile or thermal degradable compounds into volatile stabile derivatives, which are suitable for GC analysis. Common chemical derivatization techniques are silylation, alkylation, and acylation [3, 10, 11].

4.3.1 Procedure

A simplified scheme of a typical GC system with the most important unit parts is shown in Figure 4.4. The separation process is described in the following. First of all, a gas cylinder equipped with a pressure regulator and a precise flow controller provides a constant flow of the carrier gas as mobile phase. An injector is used to introduce the sample by a syringe or

Autosampler in the GC system. The sample is evaporated and transported to the column. After the separation of the compounds in the column, the single compounds can be examined by a suitable detector. By means of the detector, an electrical signal is generated and the final chromatogram is obtained. In addition, the temperature of the injector, column oven and detector can be adjusted to increase the selectivity of the separation process. In general, the temperature values of the inlet and outlet are kept constant, whereas, the temperature of the oven or rather the column is often varied. This is a consequence of the faster elution of compounds with increasing temperature. Thus, the analysis time of a sample can be decreased [4].

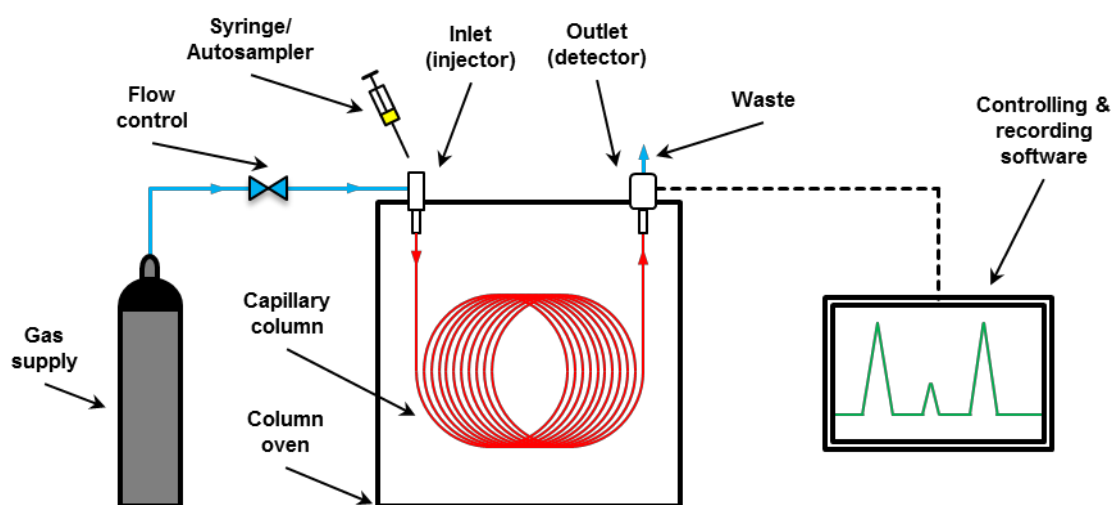


Figure 4.4: Simplified scheme of a gas chromatography (GC) system.

4.3.2 Injector

There are several techniques to introduce the sample to be analyzed in the GC system. The most common method is the split/splitless injector. By means of this technique, the sample is immediately evaporated and only a part of the volatilized mixture is guided to the column in split mode. This method is especially used for highly concentrated samples. In the splitless mode the whole evaporated sample is guided to the column, which is particularly performed in trace analysis. An additional technique is the on-column injection. Here, the sample is directly injected on the column in its liquid form. Subsequently, the column is heated and the sample evaporates. This “cold injection” technique is suitable for thermal labile compounds [4].

4.3.3 Stationary phase

In general, two different types of stationary phases are feasible in GC analysis, which can be divided in packed and capillary columns. The former are glass or metal columns filled with fine solid particles consisting for example of silica gel, aluminum oxide, activated carbon or different organic polymers. The separation process is based on the different adsorption properties of the substances. In addition, the solid particles can be coated with a liquid film. The packed columns are typically 0.5-4.0 m long with an inner diameter of 2-4 mm. They are especially used for the determination and separation of gases or small organic compounds [4]. The utilization of packed columns in GC analyses is steadily decreasing due to the lower separation efficiency compared to capillary columns [3].

The latter are fused silica columns with a thin immobilized liquid film as stationary phase on the inside. These columns have an inner diameter of 0.10-0.32 mm and a length between 10 and 60 m, which enhances the separation efficiency significantly. The most common used stationary phases consist of polysiloxane with different side groups. The polarity of the stationary phase is a central characteristic. Nonpolar phases include 95-100% of dimethylsiloxane groups. The polarity of the phase can be slightly enhanced by increasing the content of phenyl groups on the polysiloxane structure. Highly polar stationary phases can be obtained by cyano (propyl) polysiloxane or polyethylene glycol. However, the latter is very sensitive to oxygen and high temperatures [3]. In addition, alkylated and acylated cyclodextrin films can be used to separate enantiomers of a substance [7].

The separation process is based on the dissimilar distribution of the analyte in the liquid stationary phase and the gaseous mobile phase. In general, thicker stationary films enhance the capacity of the column, however, the separation efficiency get worse. The selection of a column depends on the polarity of the analytes, which should be closely match the polarity of the stationary phase to increase the resolution and separation efficiency [4]. In detail, phenyl methyl siloxane columns are applied to separate medium to nonpolar analytes, whereas polar compounds are best separated on polyethylene glycol columns [7].

4.3.4 Mobile phase

The most common carrier gases in GC are nitrogen, helium and hydrogen. The mobile phase should be of high purity, thus it should not contain oxygen, water and other organic compounds. The extraction efficiency can be adjusted by the flow and selection of the gas, which can be explained by the Van Deemter equation (see Chapter 4.1.2). Nitrogen exhibits the highest viscosity of the given gases, thus the diffusion coefficient is very low. This results in a low height of the theoretical plate H , which enhances the resolution. However, this is only valid in a small range of the linear velocity u . If the velocity is increased, the height of the theoretical plate raises, which deteriorates the resolution of the separation significantly. In

contrast, the separation efficiency stays nearly constant in a wide range of the velocity for hydrogen. Helium is an intermediate of both gases [3].

4.3.5 Detectors

The most common detector in GC analyses is the flame ionization detector (FID). There, the eluted compounds are burned in a flame, created by a mixture of oxygen and air (oxyhydrogen). An anode is placed at the nozzle head of the detector where the flame is produced, whereas the collector cathode is positioned above the flame. The two electrodes provide a potential difference. During the combustion, the generated radicals break down to ions. Consequently, a current flow between the two electrodes is initiated, which results in a signal. However, the detection method is destructive and water, carbon dioxide, nitrogen and similar compounds cannot be detected. The major advantages of the FID are its high sensitivity and large range of linearity. This means that organic compounds can be detected at very low and very high concentration with a linear response. In addition, the signal of the detector is directly proportional to the amount of substance [3, 7, 12]

Additional detectors in GC analyses are thermal conductivity detectors (TCD), mass selective detectors (MSD), electron capture detectors (ECD), flame photometric detectors (FPD), nitrogen-phosphorous detector (NPD), and atomic emission detectors (AED) [3, 12]. However, a very simple and efficient detector in GC analysis is the human nose. By means of GC-sniffing, the scent of the separated compounds can be identified and classified. This technique is of major interest in the analysis of fragrances [7, 13]. The choice of the detector is always dependent on the properties of the analyte to be examined.

4.4 Determination of antioxidant activity

In particular, there are several procedures to determine the total antioxidant activity of compounds, like spectrophotometric methods such as DPPH assays [14], Folin-Ciocalteu assays [15], and many others. Also (bio-)amperometry and cyclic voltammetry can be used [16].

A fast and easy method to investigate the total antioxidant scavenging activity of a compound is the 2,2-diphenyl-1-picrylhydrazyl (DPPH) assay. The experimental procedure can be easily and fast adjusted and customized to the analysis experiments. It was first developed by Blois to determine the total antioxidant activity of compounds [17]. DPPH is a dark colored powder of stable free-radical molecules, which is soluble in methanol or ethanol. It has a strong absorption maximum at a wavelength around 515 nm due to the presence of an unpaired electron. As this electron becomes paired off in the presence of an antioxidant compounds (hydrogen donor), the absorption strength decreases. A color change from violet to yellow can be observed (see Figure 4.5). The change of color and more precisely the change of the

absorbance maximum can be used to determine the antioxidant activity of compounds [18, 19].

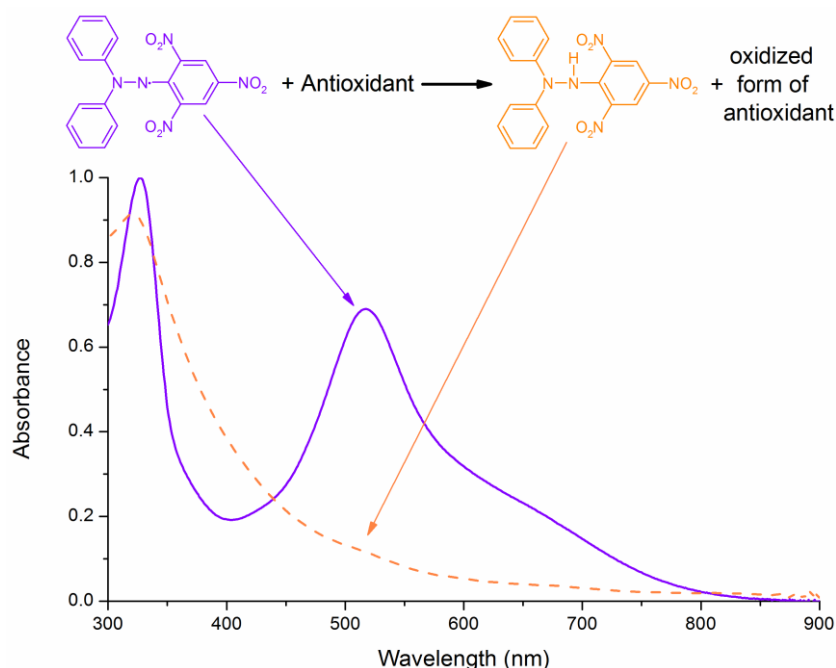


Figure 4.5: Reaction between the DPPH radical (violet) and an antioxidant yielding the neutralized DPPH molecule (orange). The corresponding UV/VIS spectra are also shown. A significant decrease of the absorbance at 518 nm appears during the reaction and can be used to follow the reaction.

However, the investigation of the reaction kinetics of DPPH on the antioxidant compound is important to obtain reproducible results. The time until the reaction reaches a steady state is depending on the antioxidant compound [14].

4.5 References

- [1] M. Tswett, *Berichte der Deutschen Botanischen Gesellschaft*, **1906**, 24, 384.
- [2] M. Otto, *Analytische Chemie*, 4. ed, **2011**, Weinheim: Wiley-VCH.
- [3] G. Schwedt and C. Vogt, *Analytische Trennmethode*, **2010**, Weinheim: Wiley-VCH-Verlag.
- [4] A. Dominik, D. Steinhilber, and M. Wurglics, *Instrumentelle Analytik kompakt: Mit kommentierten Originalfragen für Pharmazeuten*, **2013**, Stuttgart: Wiss. Verlag-Ges.
- [5] J.J. van Deemter, F.J. Zuiderweg, and A. Klinkenberg, *Chem. Eng. Sci.*, **1956**, 5, 271-289.
- [6] K. Cammann, *Instrumentelle Analytische Chemie: Verfahren, Anwendungen, Qualitätssicherung*, **2010**, Heidelberg: Spektrum Akademischer Verlag.
- [7] M. Neugebauer, G.K.E. Scriba, and M.A. Hubert, *Instrumentelle pharmazeutische Analytik*, **2013**, Stuttgart: Wissenschaftliche Verlagsgesellschaft

- [8] W.J. Lough and I.W. Wainer, *High Performance Liquid Chromatography: Fundamental Principles and Practice*, **1995**, Glasgow: Blackie Academic & Professional.
- [9] R.P.W. Scott, *Liquid Chromatography Detectors*, **1986**, Amsterdam: Elsevier Science.
- [10] D.R. Knapp, *Handbook of Analytical Derivatization Reactions*, **1979**, New York: John Wiley & Sons.
- [11] K. Blau and J.M. Halket, *Handbook of derivatives for chromatography*, 2. ed, **1993**, New York: John Wiley & Sons.
- [12] W. Engewald, P.J. Baugh, A. Steinborn, C. Struppe, and H.G. Struppe, *Gaschromatographie: Eine anwenderorientierte Darstellung*, **2012**, Berlin, Heidelberg: Springer
- [13] A. Galfré, P. Martin, and M. Petrzilka, *J. Essent. Oil Res.*, **1993**, 5, 265-277.
- [14] W. Brand-Williams, M.E. Cuvelier, and C. Berset, *LWT-Food Sci. Technol.*, **1995**, 28, 25-30.
- [15] R.L. Prior, X. Wu, and K. Schaich, *J. Agric. Food Chem.*, **2005**, 53, 4290-302.
- [16] A.M. Pisoschi and G.P. Negulescu, *Biochem. Anal. Biochem.*, **2012**, 01.
- [17] M.S. Blois, *Nature*, **1958**, 181, 1199-1200.
- [18] S.B. Kedare and R.P. Singh, *J. Food Sci. Technol.*, **2011**, 48, 412-422.
- [19] O.P. Sharma and T.K. Bhat, *Food Chem.*, **2009**, 113, 1202-1205.

5 Supercritical fluid extraction unit „LAB SFE 100mL – 4368“

5.1 General information

In 2012, a new research topic dealing with “plant extractions” was introduced at the “Institute of Physical and Theoretical Chemistry” of the University Regensburg. For this reason, a supercritical fluid extraction unit was purchased. The unit, with the designation "LAB SFE 100 mL – 4368", was constructed by Separex in Champigneulle/France. This device enables extractions with supercritical carbon dioxide up to 1,000 bar and 150 °C. Also pressurized solvent extraction with water, ethanol, and other solvents up to 400 bar and 250 °C is feasible. In addition, a combination of both techniques can be performed. The structure and the different instrumentation components of the extraction unit are described in this chapter. In addition, some modifications during the design of the unit will be presented. A general procedure to run the extraction unit is also described. This section is considered to be a handbook and instruction manual for the handling of the unit, especially for future PhD students. Besides, some problems with the unit and the corresponding troubleshooting will be described. The commissioning of the SFE-unit took place in November 2013. Figure 5.1 presents a sketch of the extraction unit.

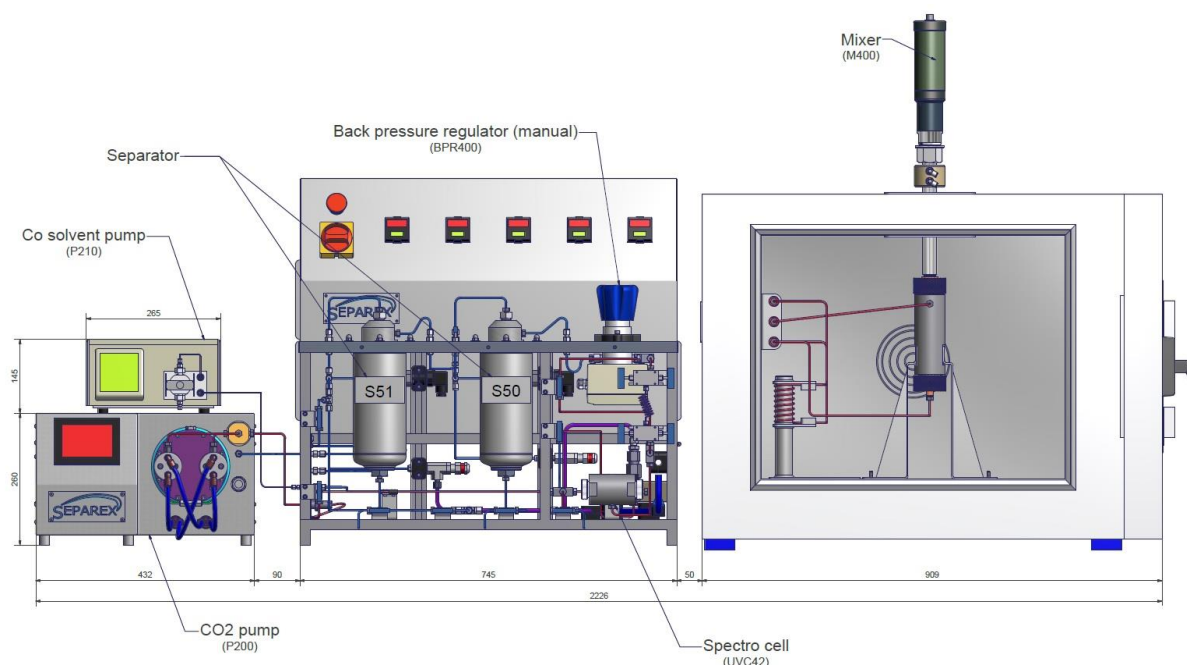


Figure 5.1: Sketch of the supercritical fluid extraction unit "LAB SFE 100 mL – 4368".

5.2 Engineering plan

Figure 5.2 presents the engineering line diagram of the supercritical fluid extraction unit "LAB SFE 100 mL – 4368", which consists of different sections. A short explanation of the important parts and their corresponding labeling in the engineering drawing will be given in the following. First of all, liquid carbon dioxide is supplied by a gas bottle (CO₂) with a dip tube. The carbon dioxide is transported through a one-way-valve (CV100) and pressurized by the CO₂ pump (P200) equipped with a flow meter (FT200). A second pump (P210) enables the addition of a cosolvent to the carbon dioxide in the extraction unit. The extraction vessels (A40, A41) are brought to a constant temperature in an oven (H3000). A mixer (M400) can be used to homogenize viscous liquid extraction samples in the extraction vessel. An UV-cell (UVC42) with sapphire windows can be used to perform online spectroscopy. Furthermore, online sample collection can be performed by a sampling loop. The extract is collected in two separators (S50, S51). Furthermore, a chiller (C1000) is used to ensure a constant temperature of 0 °C in the CO₂ pump, the mixer, and the pipe section after the extraction vessel (CE400). However, this pipe section needs only to be cooled if extractions are carried out with water at high temperatures.

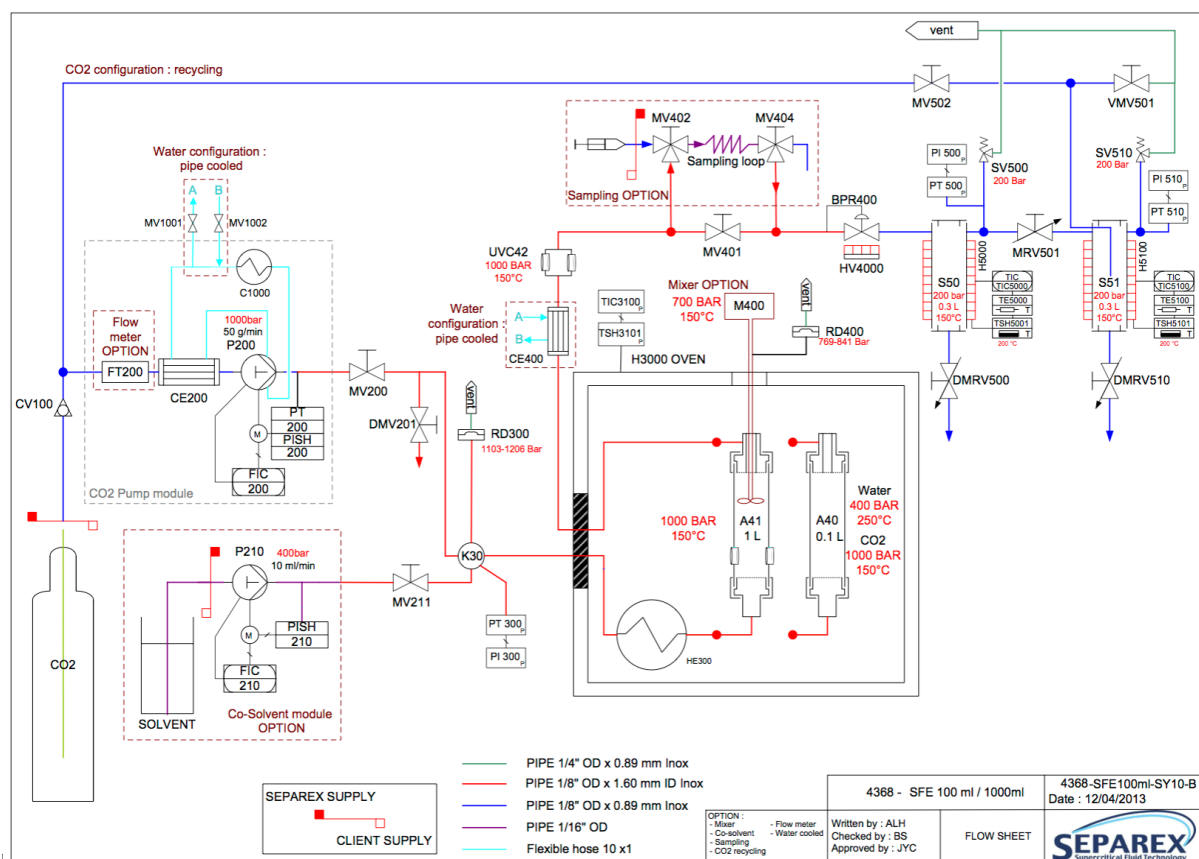


Figure 5.2: Engineering plan of the supercritical fluid extraction unit "LAB SFE 100 mL – 4368".

In addition, the system is connected to a computer with the control software Labview™ “Application 4368”. It is used to set the values of CO₂ and solvent flow, as well as the temperatures in the extraction vessel and separators. Moreover, it can also be used to record the extraction parameters (temperature, pressure, flow of solvent).

The pressure in the single sections of the unit is regulated manually by different valves. The most important valve is the back pressure regulation valve (BPR400), which is used to control the pressure in the extraction vessel very precisely. Moreover, some smaller valves with different uses are installed. A manual valve (MVxxx) is used to ensure or stop the flow of the solvent through the pipes. These valves are either closed or fully opened. A manual regulating valve (MRVxxx) is supposed to regulate the pressure in different sections of the extraction unit, for example in the separators. Draining manual valves (DMVxxx) should only be opened at the end of an extraction process or if any plugging of a pipe occurs. The venting manual valve (VMV501) is installed at the end of the unit to allow the gaseous carbon dioxide to exhaust to the vent line.

The pressures in the extraction vessel and separators are measured by pressure transducers (PT xxx). Temperature sensors (TSH xxxx) are used to measure and regulate the temperature in the oven and separators.

Moreover, rupture discs (RDxxx) and relief valves are installed as safety equipment and should protect the extraction unit from damages by over-pressuring. These discs burst or the valves open at a given pressure range.

5.3 Instrumentation

The next section presents the different parts of the extraction unit in detail. Furthermore, the correct handling of the instrumentation will be described. In addition, modifications of some parts during the design of the extraction unit will be presented.

5.3.1 Cabinet and pressure cylinder

First of all, liquid carbon dioxide is supplied by a pressure cylinder equipped with a dip tube. The gas bottle is placed in a cabinet and connected to a pipe adapter. The adapter should only be screwed hand-tight on the thread of the pressure cylinder. Also, no additional sealing (e.g. coating with Teflon) is necessary. Two different valves are installed in the cabinet. One is used for depressurization of the pipes, whereas the second valve enables the transport of liquid carbon dioxide through the pipe towards the extraction unit. Furthermore, the pressure in the CO₂ cylinder is measured by a manometer. The value must not fall below 55 bar, as only liquid carbon dioxide can be transported by the CO₂ pump. Rupture discs are also installed as safety equipment.

5.3.2 Chiller

The chiller (C1000) is used to ensure a constant temperature of 0 °C in the CO₂ pump, the mixer, and the pipe section after the extraction vessel (CE400). The device is filled with a mixture of ethylene glycol and water. The fluid level has to be in the right range before starting an experiment. The fluid level gauge is on the backside of the chiller. If the filling level is too low, water can be added. However, the content of ethylene glycol (technical grade is sufficient) must be always in the range of 5-10%. The chiller should be turned on approximately 20 min before starting an experiment. A temperature of 0 °C in the CO₂ pump ensures the precise flow and the liquid state of carbon dioxide.

5.3.3 CO₂ pump

The CO₂ pump (P200) is a double piston pump with the designation LGP 50 designed by Separex. It is used to transport and pressurize carbon dioxide in the extraction unit. The switcher to start the pump is on the backside. The pump heads are constantly cooled to 0 °C by the chiller. The density of liquid CO₂ is 0.93 g/mL at this temperature. Consequently, the liquid can be pumped with a defined mass. The flow rate can be varied from 5 to 50 g/min and extraction pressures up to 1,000 bar can be reached. The minimum pressure after filling the pump with carbon dioxide must not fall below 50 bar. It is also possible to carry other solvents (e.g. water) with this pump.

The display of the pump is equipped with a touch screen allowing the management of the pump. It can either be operated with the finger, but it is recommended to make use of a stylus for a better accuracy. The home screen after starting the pump is shown in Figure 5.3.



Figure 5.3: Home screen of the CO₂ pump (P200) with configuration options and actual values.

The CO₂ pump can be started or stopped manually by pressing the ON/OFF-buttons. The display also shows the actual value of pressure (PRESSURE VALUE in bar) in the pump and the flow rate of the solvent (FLOWRATE VALUE in g/min). It is also possible to adjust the PRESSURE SET POINT (pressure control mode) or the FLOW SET POINT (Flow Control mode), which will be explained later on. If there is any problem with the pump, a flashing circle will appear on the home screen (see Figure 5.3). It is possible to reset the alarm on the screen. Three other sub-screens (ALARM, CONTROL, and PARAMETER) are accessible by pushing the respective tab at the bottom of the display.

In the case of an occurring alarm, the type of problem can be seen in the ALARM-screen. There are four different types of alarm:

- **PRESSURE SENSOR BREAKING:** It occurs if the pressure sensor is disconnected or out of service. Separex should be contacted in order to fix this problem.
- **HIGH PRESSURE ALARM:** This alarm appears if the maximal pressure value of 1,000 bar is exceeded. The pump stops automatically and the extraction unit should be depressurized slowly. Furthermore, it should be verified if any plugging of pipes caused this problem. If everything is alright, the alarm can be reset by pressing RESET ALARM.
- **LEXIUM ALARM:** This is a serious error of the pump and Separex should be contacted. Lexium is the designation of the motor pump adjuster.
- **USER PRESSURE ALARM:** The pump stops also automatically if this type of alarm occurs. It appears if the maximal value of the adjusted user pressure is reached. In this case, the extraction unit must be depressurized and the alarm can be reset by pressing the button RESET ALARM.

The next sub-screen is called CONTROL. Here, the value of the maximal user pressure is defined. It can be changed by pushing over the value and entering a new one. It is recommended to set the value at approximately 50 bar above the pressure of the chosen extraction pressure. The other parameters displayed on this screen should not be changed. These values must only be changed if another fluid than CO₂ has to be pumped, as these parameters are different with for example ethanol or CO₂. In this case, it is recommended to contact Separex.

The operating mode of the pump can be selected in the PARAMETER-screen. The choice of the operating mode is dependent on the experiment to be carried out. The configured mode is highlighted by a filled square next to the designation. In particular, three different modes are available:

- **Mode FLOW CONTROL:** The pump takes into account the value of the “FLOWRATE SET POINT” from the home screen. It can be changed by pushing over the value and entering a new one. The pump keeps the flow rate constant at the desired value.

- Mode PRESSURE CONTROL: The pump takes into account the value of the “PRESSURE SET POINT” from the home screen. This can also be changed by pushing over the value and entering a new one. The pump runs with a maximal solvent flow (FLOWRATE SET POINT) until the desired pressure is reached. The deviation of the pressure can be adjusted by tapping on the value on the right side of the designation (+/- x bar). The flow rate will be adjusted by the pump in order to keep the pressure constant in the given range.
- Mode REMOTE SET POINT FLOW: This is the most often used mode for the pump. This mode enables the control of the pump by the computer software. The flow rate set point and starting/stopping the pump is managed remotely by the control software.

Before starting the pump the extraction vessel has to be correctly closed. In addition, at least one valve (MV200) after the pump has to be opened to ensure that pumping pressurizes the vessel and not only a short pipe. If the valve is closed, the pressure switch stops the pump.

5.3.4 Cosolvent pump

An additional pump for organic solvents (P210) is also part of the extraction unit. This is a customary HPLC pump with a flow rate value of 0.1 to 10 mL/min and a maximal working pressure of 400 bar. The pump needs to be primed at atmospheric pressure before starting the control software of the extraction unit. Therefore, a syringe is connected to the prime/purge valve, which is subsequently opened counterclockwise (1 to 2 turns). The pump is purged by pulling approximately 20 mL of solvent through the system into the syringe. Priming can be started by pressing the “Prime”-button on the pump. In addition, the pump can be controlled by the software Labview™ “Application 4368”. The desired flow rate value can be entered in the software and applied by tapping the “On”-button. However, at least one valve (MV211) after the pump has to be opened to avoid over-pressuring and damaging of the pump. This pump is also used to purge the extraction unit after every experiment in order to remove residual compounds. To this purpose, isopropanol is pumped with a flow rate of 5 mL/min through the unit for approximately 10 min. If the solvent pump is only used to clean the pipes after an extraction process it is not obligatory to preliminary prime the pump.

5.3.5 Extraction vessel and oven

The oven (H3000) is used to keep the temperature of the extraction vessel at a constant value. In addition, a heat exchanger (HE300) is placed in the oven to preheat the solvents before entering the vessel. Moreover, two different extraction vessels are available for the extraction procedure. A picture of both is shown in Figure 5.4

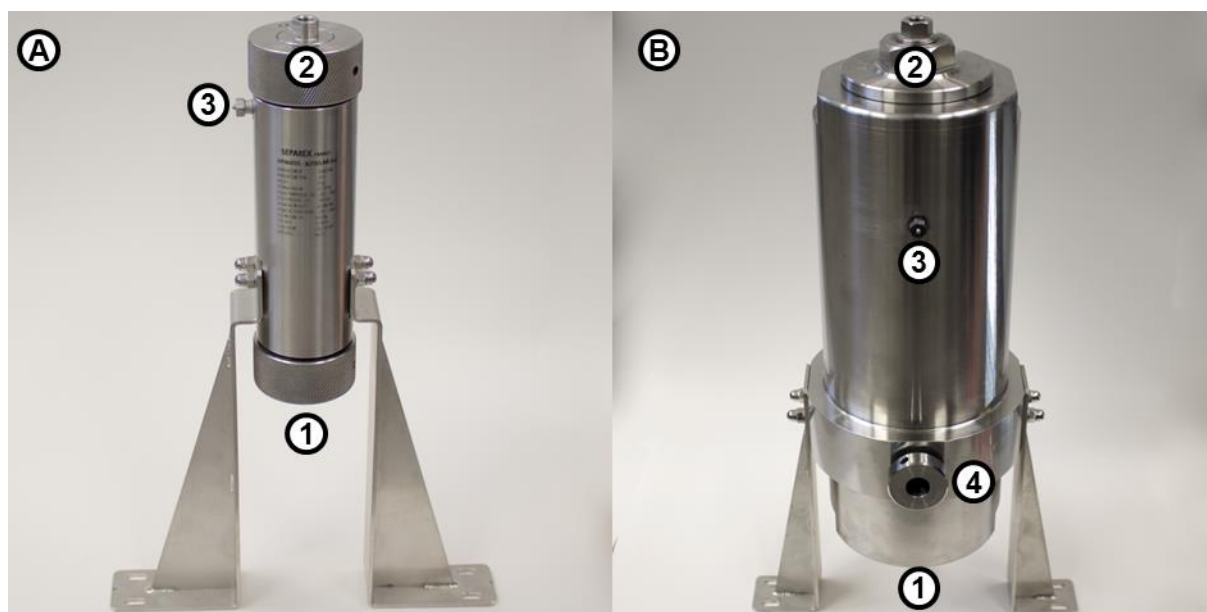


Figure 5.4: Picture of the (A) 0.1 L (A40) and (B) 1 L (A41) extraction vessel with different connection options for the pipes. Normally, (1) is used as inlet at the bottom and (2) as outlet of the vessel. The lateral outlet (3) is used if the mixer is used during extraction. Also the sapphire windows (4) of the A41-vessel can be seen.

The A40-vessel has a feeding volume of 0.1 L. It is designed for high pressures up to 1,100 bar and a maximal temperature of 250 °C. It is sufficient to close the lid by screwing it hand tight. The vessel is equipped with two black lip seals in order to prevent leakages. The intactness of these seals should be proofed at the beginning of every experiment.

The second vessel is called A41 and has a feeding volume of 1 L. The design pressure of this vessel is also 1,100 bar. However, the temperature of the vessel must not exceed 150 °C. The handling of this vessel is challenging as it weighs 31 kg. In addition, the A41-vessel is equipped with two sapphire windows which placed opposite to each other. The position of the windows was planned to be at the lower side of the vessel. This position should assure the visual observation of extraction processes. Moreover, the lids need to be screwed completely with a wrench, a further tightening is not necessary. The tightness of the vessel is assured by two white lip seals, which should also be checked before every experiment.

Normally, the flow direction of the solvents through the vessels is from bottom (1) to top (2) (see Figure 5.4). However, outlet has to be laterally (3) when the mixer is used. The corresponding pipes for each configuration are marked with a label, like “A40 inlet”. The pipes have to be connected firmly to the extraction vessel and to the adapters in the oven.

Besides, both vessels can be also equipped with two sintered metal discs (porosity of 30 µm) in the lids. These discs prevent small particles to be transported in the high pressure pipes. In addition, a paper filter can be placed directly on the sintered discs to withhold very small

particles. The A40-vessel should be placed in the oven at least one hour before the scheduled experiment. This assures the right temperature of the vessel during the extraction process. It is recommended to put the A41-vessel already the previous day in the oven. The extraction material is put only a few minutes before the experiment in the preheated vessel. However, the vessels must not be filled completely, as foaming or swelling of the plant material can occur. This can lead to plugging of the sintered discs or pipes.

After every experiment, it is mandatory to wait a few minutes before dismantling the pipes and opening the lids of the vessels. A plug placed between the pressure sensor and the vessel may occur and carbon dioxide may still be in the vessel. Subsequently, all parts of the extraction vessel should be cleaned with an appropriate organic solvent (e.g. isopropanol). The sintered discs and lip seals are separately cleaned with isopropanol in an ultrasonic bath.

5.3.6 Pressure regulators

The pressures in the extraction unit are manually controlled by different valves (see Figure 5.5). The most important valve is the back pressure regulator valve (BPR400). This valve is supposed to control the pressure in the extraction vessel very precisely. In addition, the valve is automatically heated. This should prevent plugging of the valve due to the formation of dry ice by expanding CO₂.

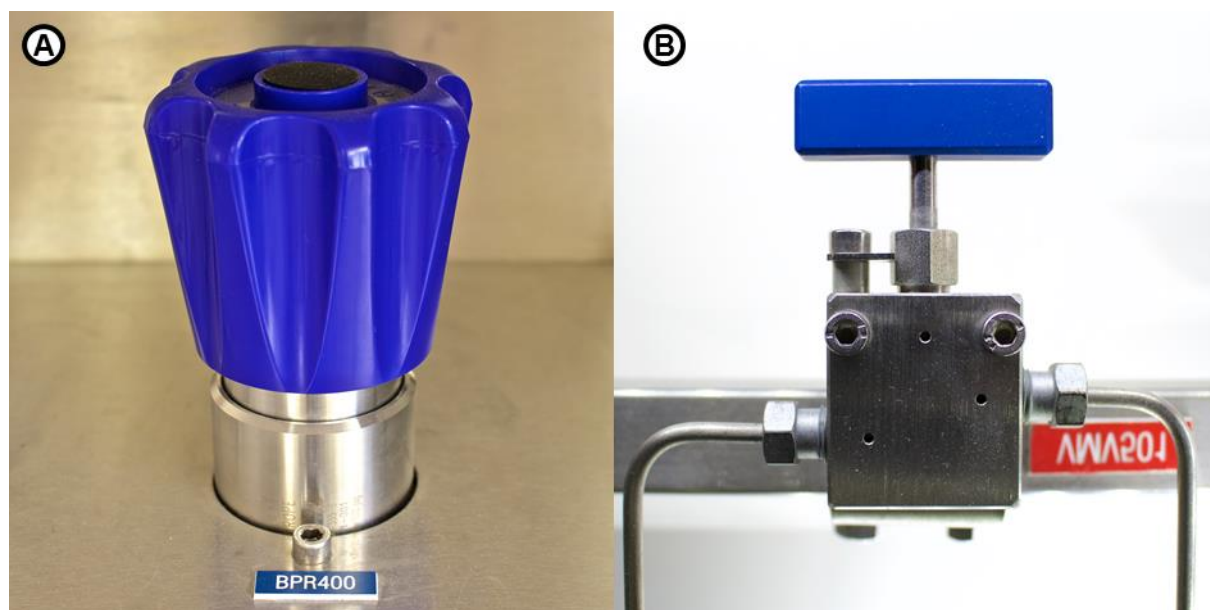


Figure 5.5: (A) Back pressure regulator valve (BPR400) and (B) normal valve to control manually the pressure in the extraction unit.

The pressures in the separators can be controlled manually by simpler valves. The pressure can be increased by tightening the valve (turn clockwise) and decreased by turning it counterclockwise. In detail, the pressure in the first separator (S50) is regulated by the

manual regulating valve MRV501. Moreover, the pressure in the second separator (S51) is manually controlled by the valve MV502 or VMV501, depending on the experiment. If the pressure is high enough in the second separator and the residual carbon dioxide should be recycled, the valve MV502 should be opened and VMV501 closed. If the pressure is too low and the carbon dioxide should be carried to the vent line, the valve VMV501 is used to control the pressure in the second separator.

A minor disadvantage of these valves is that they are not heated. If the pressure difference is too high, the valves and adjacent pipes are cooled down due to the Joule-Thomson effect [1]. This can result in a blockage of the pipe or of the valve due to the formation of dry ice, frozen water or precipitated extract. For this reason, it is recommended to put a heating mantle around these valves during the experiment. This approach also provides a more constant pressure value without any readjustment of the valve.

5.3.7 Separators

Two separators are installed in the extraction unit in order to collect the extract. In addition, a fractionation of the extract can be achieved by applying different conditions in the separators. A picture of the first (S50) and second (S51) separator is presented in Figure 5.6. They have an inner volume of 300 mL and are designed for pressure values up to 200 bar and a maximum temperature of 150 °C.

The temperature of the separators can be applied by tipping the desired value in the control software Labview™ and press the “ON”-button. This should be done approximately 30 min before the scheduled experiment in order to obtain a constant temperature value.

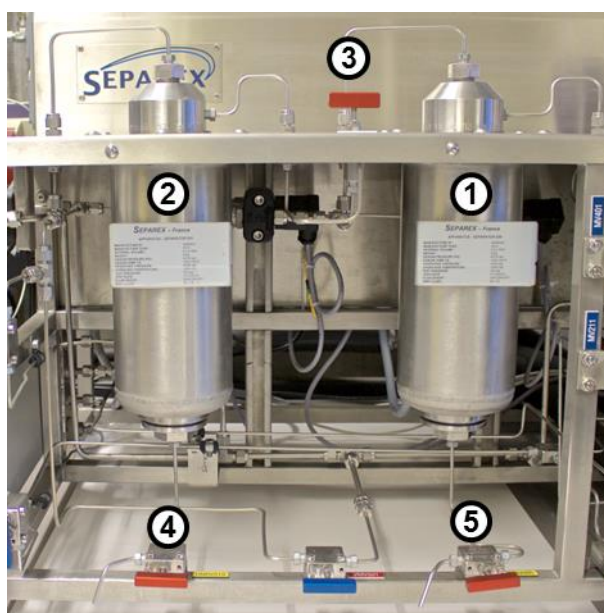


Figure 5.6: Picture of the (1) first and (2) second separator and (3) the regulating valve MRV501. Additionally, the draining valves of both separators (4, 5) are shown.

After the experiment and depressurizing, the extracts need to be recovered from the separators. Most extractions yield only a small amount of extract. Thus, it is important to recover the whole extract. For this reason, the connection pipes and dip tubes of the separators have to be dismantled. Subsequently, the separators are washed with a suitable solvent, in which the extract is soluble. For example, diethyl ether was used to recover the extract from iris rhizomes (see Chapter 6.3.3.4). Afterwards, the extract solutions can be recovered via the draining manual valves DMRV500 and DMRV510. The recovery of the solutions can be enhanced by applying a low pressure of nitrogen on the top of the separator. This washing step is repeated two times in order to guarantee a complete recovery of the extracts. In addition, the adjacent pipes to the separators are also purged with the same solvent. The pure extracts are obtained by evaporating the solvent.

A minor drawback of the separators is that they can only be heated and not cooled down. Normally, lower temperatures in the separators would be more preferable for a better precipitation of the extract [2]. Nonetheless, a minimum temperature value of 30 °C is recommended for the separators. As a result, it is possible to perform the experiments over the whole year under the same conditions.

5.3.8 Computer and control software

The whole equipment is connected to a computer with the control software Labview™ named "Application 4368". After starting the software, the starting window appears (see Figure 5.7). Before using the software, it is necessary to refresh it by clicking on the button containing two circular arrows ("wiederholt ausführen", see (1) in Figure 5.7). The software shows the complete flow sheet of the extraction unit. In addition, an alarm panel of different parts of the unit is given at the bottom. In detail, the green boxes of the alarm panel indicate no disorder, whereas red boxes implicate a malfunction of the corresponding part. These alarms can be deleted by clicking the "RESET ALARM"-button. This is obligatory before every experiment.

The software enables also the recording of every parameter value during an extraction experiment. The following parameters are recorded: time, flow of CO₂, and pressures and temperatures in the extraction vessel and both separators. In order to save the values of these parameters, the "SELECT FILE"-button needs to be clicked (see (3) in Figure 5.7). Afterwards, a new Open-Document-Spreadsheet (.ods-file) has to be created and selected. The "LOGG DATA"-button has to be activated in order to henceforth record the parameters.

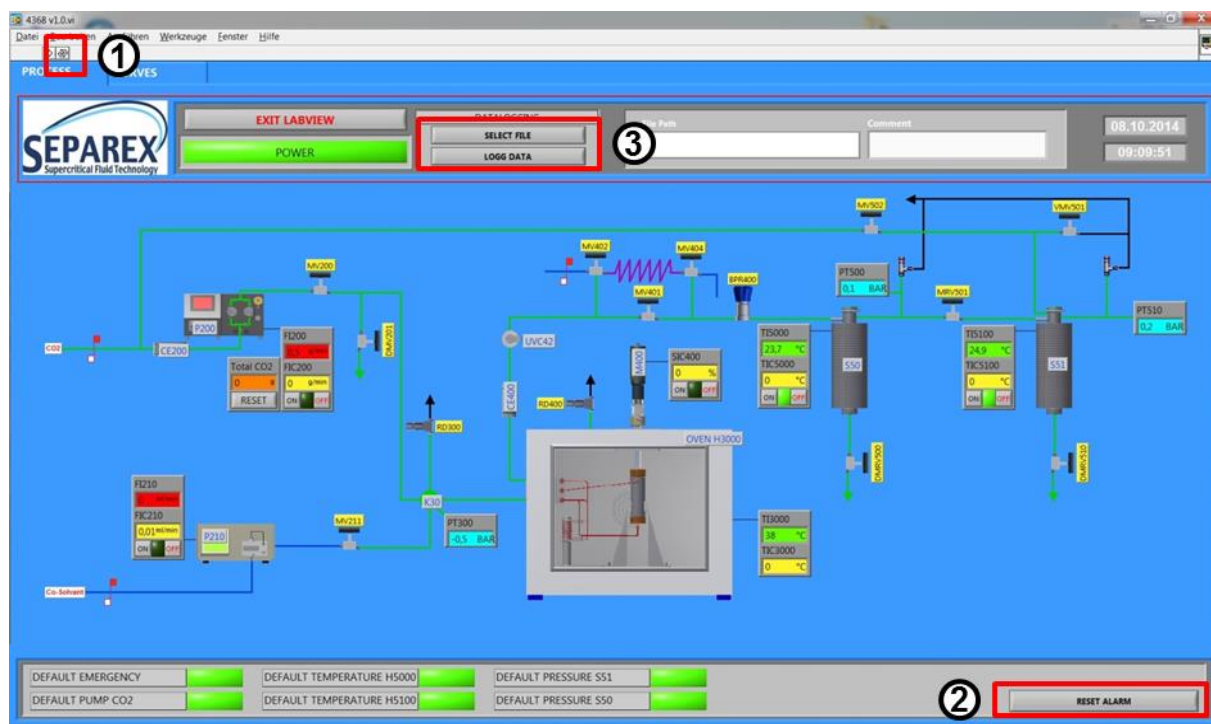


Figure 5.7: Starting window of the software Labview™ with the different steps that should be performed before starting an experiment.

As already mentioned, the program can also be used to control the extraction unit. The flow of CO₂ and the cosolvent, the velocity of the mixer, and the temperature of the oven and separators can be adjusted. In detail, yellow boxes in the software window indicate the possibility to enter a desired value of the corresponding part. Furthermore, green boxes display the actual temperature and turquoise boxes the associated pressure of the section. Moreover, red boxes are used to present the actual value of the solvent flow, whereas the orange box displays the total amount of consumed carbon dioxide during the experiment. In addition, the “CURVES”-tab can be used to see a diagram exhibiting the development of the different parameters during the current experiment.

5.3.9 Other components

The extraction unit includes some additional parts, which can be used for special experiments. The application and purpose of these parts are described shortly in this section.

First of all, a view cell (UVC42) is installed in the pipes after the extraction vessel. The design pressure of this cell is also 1,100 bar with a maximum temperature of 150 °C. The inner volume is 5 mL. The cell is equipped with two sapphire windows which are placed opposite to each other. The distance between the windows was planned to be exactly 1 cm. The cell is intended to perform online UV spectroscopy during the SFE experiment. In detail, two optical fibers can be connected on both sides of the cell. Unfortunately, this project could not

be realized due to the lack of a UV source and detector. Nonetheless, this cell can be used to follow the reaction visually.

Furthermore, a recycling line is connected to the second separator (S51). If the pressure is high enough in the second separator, the carbon dioxide can be recycled by condensation in the CO₂ pump. Therefore, the valve MV502 has to be opened. However, the carbon dioxide must not contain any residual extract as this would cause damage or blockage of the pump.

In addition, a pipe cooler (CE400) can be installed in the pipes after the extraction vessel. However, this cooler is only required for subcritical water extractions with extraction temperatures above 200 °C. Therefore, the device must be connected to the chiller. The cooling of the effluent is necessary to avoid damaging of the UV-cell and back pressure regulator valve. Furthermore, its utilization during supercritical carbon dioxide extraction is prohibited. The low temperature can cause plugging of the pipe due to the precipitation of extract.

Finally, a dynamic magnet drive mixer (M400) with rotating shaft and marine propellers can be screwed on the top lid of an extraction vessel. It can be used to stir the extraction medium in order to improve the extraction. In this case, the pipe is connected on the lateral outlet of the vessel. Furthermore, it is important to connect the mixer to the cooling system of the chiller, as demagnetization of the mixer can occur if the temperature exceeds 100 °C. Moreover, the mixer is designed for a maximal extraction pressure of 700 bar. The speed (0-2000 rpm) of the mixer can be adjusted with the software Labview™. The use of the mixer is not recommended for solid powdery extraction materials. The small particles cannot be withheld in the extraction vessel, as the lateral outlet does not contain any filter medium. Thus the transport of small particles in the pipes is very probable, which causes plugging of the pipes. Actually, this event happened one time during the extraction of sunflower seed by supercritical carbon dioxide assisted with the mixer. For this reason, the mixer is more suitable to stir liquid viscous extraction materials to enhance the mass transfer rate of a compound into the supercritical fluid [3].

5.4 Operation manual

The following section describes each step of a supercritical fluid extraction with the unit “LAB SFE 100mL – 4368”.

5.4.1 Preparations

First of all, before starting a SFE experiment with a new plant material, the possible reactions and the behavior of the products in CO₂ have to be checked. In addition, potential damage of the stainless steel pipes and PTFE seals by the used solvents and extracted compounds should be excluded. Particularly, it has to be noted that chlorine ions may cause severe

damage of the unit. It is also recommended to wear safety glasses during the whole experiment. Furthermore, it should be ensured that the complete unit is clean and no residual extract remained in the pipes or fittings. When all these questions have been considered, it is possible to perform experiments with the extraction unit. A detailed description of the process will be explained in the next chapter.

5.4.2 General procedure of SFE

In general, supercritical fluid extraction can be divided in five different main steps: equilibration, pressurization, extraction, depressurization, cleaning.

The first step is the equilibration of the extraction unit. Therefore, the general power switch (red control knob) of the control cabinet is turned to the position “ON”. In the case that the emergency stop switch is activated, it can be unlocked by a special key. Afterwards, all other electrical parts (pumps, oven, chiller, and computer) of the unit should be powered on. The cosolvent pump can be primed with a suitable solvent.

Furthermore, the software Labview™ “Application 4368” has to be opened and refreshed. After resetting the alarms, the temperature values of the oven and separators can be entered in the software (see (1) and (2) in Figure 5.8. The “ON”-button has to be activated to initiate the heating.

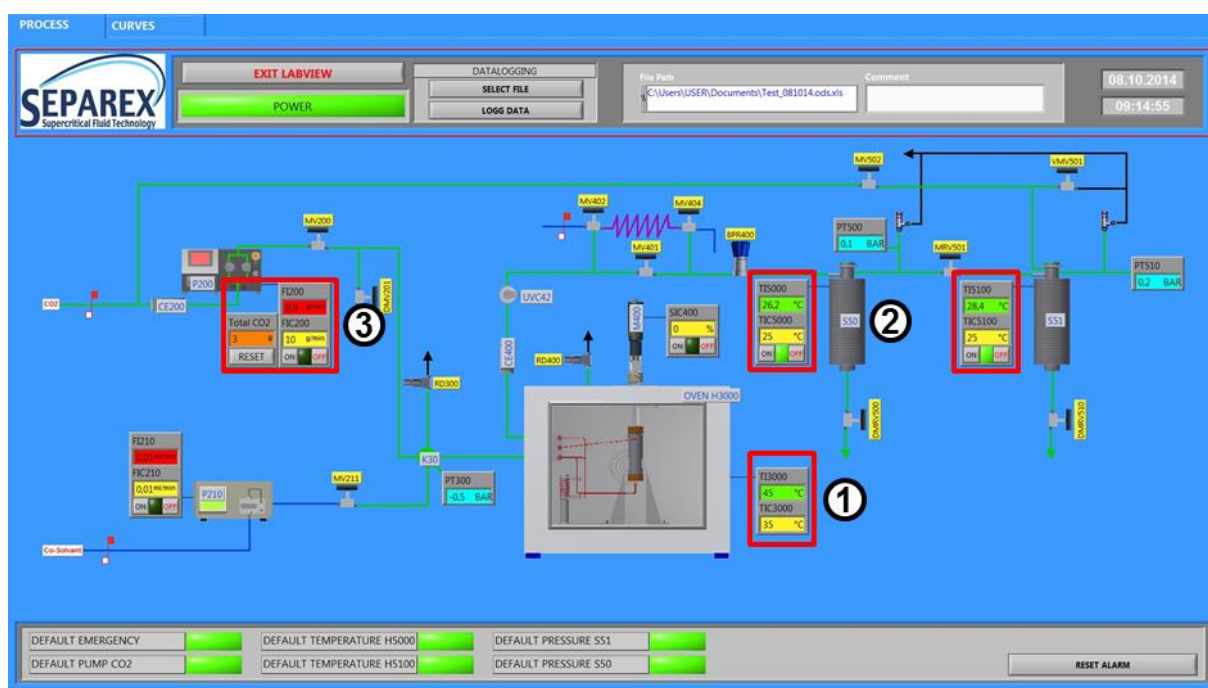


Figure 5.8: Window of software to adjust the value of the temperature in the oven (1) and the separators (2). The flow value of CO₂ can be entered in (3).

Afterwards, the extraction vessel and connection pipes should be put in the oven in order to warm the parts up. It is recommended to wait at least one hour of equilibration before starting

the extraction process. The duration can be shortened by preheating the extraction vessel overnight. This procedure is strongly recommended for the large A40-vessel to ensure a consistent temperature of the vessel.

At this point, all valves of the unit and the CO₂ supply equipment should be closed. It can be continued with the experiment when the temperature values of the separators and oven are constant and a temperature of 0 °C is displayed on the chiller. The preparation of the extraction vessel lids can be seen in Figure 5.9.

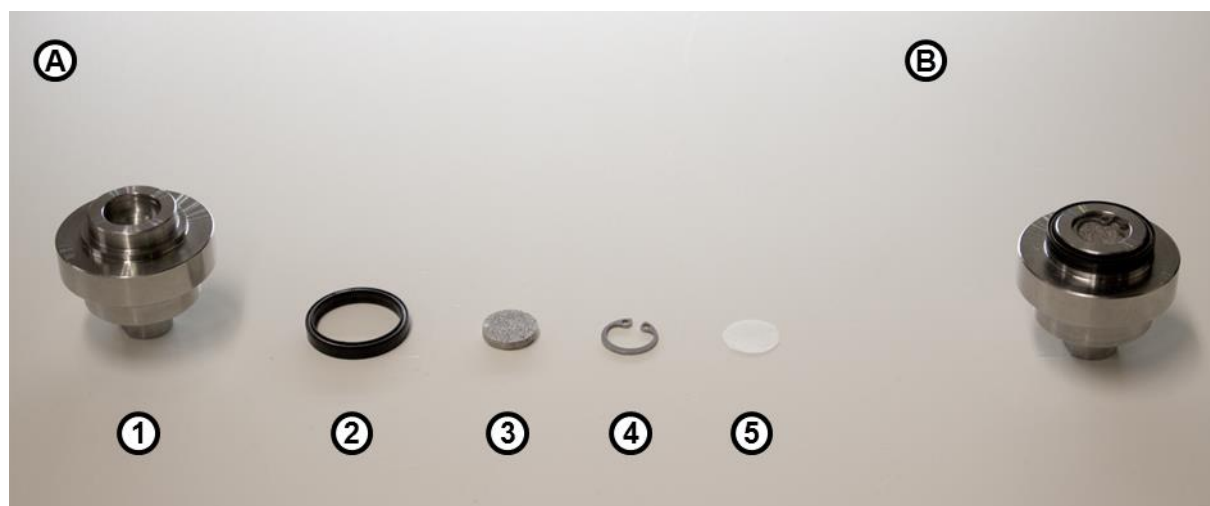


Figure 5.9: (A) Installation of the vessel lid (1) with a lip seal (2), sintered disc (3), snap ring (4), and filter paper (5). (B) Mounted lid of the extraction vessel A40.

First of all, the clean lip seal needs to be mounted carefully. Afterwards, the sintered disc and filter paper are placed in the designated opening of the lid and fixed with a snap ring. Subsequently, the extraction material is filled into the extraction vessel. The latter can be closed carefully. The extraction material must not be filled to the top of the vessel, as swelling of the material can occur during the extraction process. A filling volume of 80% is recommended. Then, the extraction vessel can be placed and fasten in the oven. In addition, the pipes can be connected properly to the vessel. After that, it is recommended to wait 10 min for the temperature equilibration of the extraction material.

Afterwards, the value of “TOTAL CO₂” is reset by the software in order to determine the exact consumption of carbon dioxide during the experiment. Moreover, a heating mantle is placed below the valve MRV501 (between separators) to heat it. This approach avoids plugging of the valve and ensures a constant pressure value of the first separator.

The second step of SFE is the pressurization of the extraction unit. Therefore, the main valve of the CO₂-bottle is opened. The indicated pressure of the manometer in the cabinet should exceed 55 bar. In the case of a lower value, the CO₂ cylinder needs to be replaced by a new one equipped with a dip tube. Then, the valve (“Kohlenstoffdioxid”) in the cabinet has to be opened to transport liquid carbon dioxide towards the extraction unit. There is an additional

valve ahead of the CO₂ pump, which has to be opened. The increase of pressure can also be detected on the display of the CO₂ pump. The pressure should not fall below a value of 50 bar.

The use of the engineering plan (see Figure 5.2) of the extraction unit is suggested for the next steps in order to know the order in which the valves are opened. Afterwards, the valve MV200 is gently opened. The pressure in the extraction vessel increases. The valve should be closed again in order to determine any decrease of the pressure, which would indicate some leakage of the pipes or vessel. In the case of any leakage, see Chapter 5.5.2. If the pressure is constant or slowly increasing, the unit is tight and the valve MV200 can be fully opened.

The next step is to tighten the back pressure regulating valve (BPR400) slightly by turning it counterclockwise. Subsequently, the valve MV401 is opened and the pressure in the first separator increases slowly, and the valve MRV501 is opened to pre-pressurize the second separator. The pressure value of the separators should be 10 bar below the desired final pressure. Afterwards, a value of the CO₂ flow can be entered in the software and the CO₂ pump can be started by activating the “ON”-button (see (3) in Figure 5.8). As a result, the pressure in the extraction vessel increases. The exact value can be achieved by tighten (turn clockwise) or loosen (turn counterclockwise) the BPR400. If the desired pressure is reached and stays constant, the pressure in the first separator can be adjusted by the valve MRV501. The pressure in the second separator is regulated by VMV501 (vent valve) or MV502 (recycling valve). Whenever SFE is performed with the addition of a modifier, the flow rate of the solvent can be adjusted by the software. Subsequently, the cosolvent pump can be started and the valve MV211 needs to be fully opened.

The third main step of SFE is the extraction process by itself, which starts when the pressure values in the extraction vessel and in both separators are constant. Here, the extraction parameters have to stay constant. Eventually, a readjustment of the valves is necessary to keep the pressure values constant. If any unexpected event occurs like plugging of the pipes, leakage or others (see Chapter 5.5) it is mandatory to stop the experiment.

The fourth step of the extraction process is the depressurization of the unit. After the desired extraction time is reached, the CO₂ pump (and cosolvent pump) can be stopped and the valve (ahead of the CO₂ pump) for additional CO₂ supply is closed. Moreover, the BPR400 has to be slowly and stepwise fastened (turn counterclockwise) in order to depressurize the extraction vessel. When the pressure is equal to the one in the first separator, the valve MRV501 is carefully opened. The same approach is used to depressurize the second separator with the valve VMV501. In general, depressurization of the high pressure parts have to be performed slowly by opening smoothly the venting valves. The flow in the valves has to be controlled and limited in order to prevent dry ice formation and plugging in the lines. When an atmospheric pressure is reached in the vessels, it is mandatory to wait a few

minutes before dismantling the pipes and opening the lids of the vessels. A plug placed between the pressure sensor and the vessel may appear and carbon dioxide may still be present in the vessel.

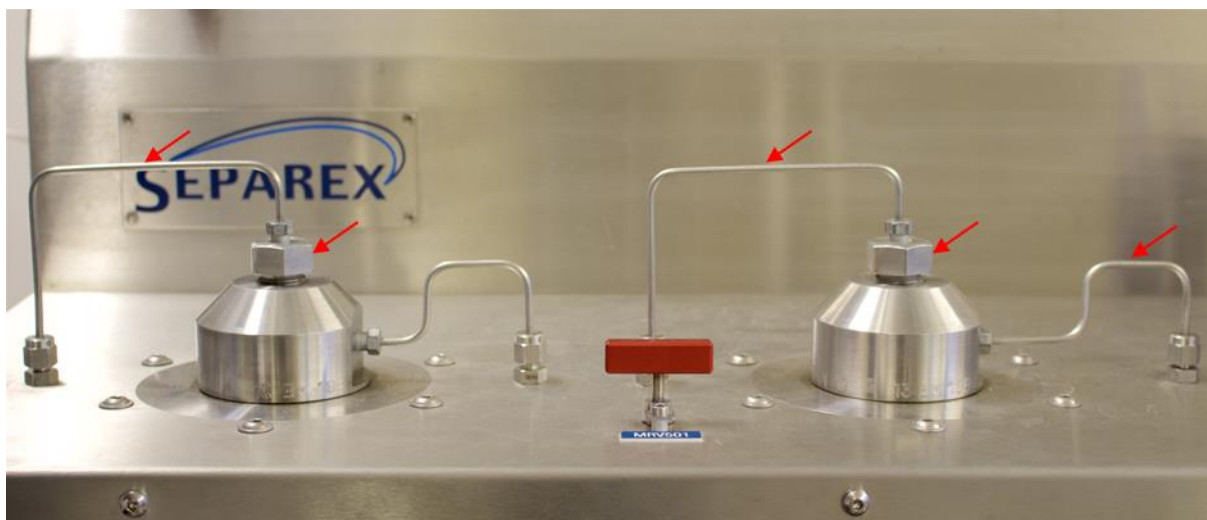


Figure 5.10: (A) Pipes and dip tube of the separator to be removed for recovery of the extract. (B) Connection pipe in oven.

The fifth and last step of SFE is the recovering of the extract and cleaning of the extraction unit. In order to recover the extract from the separators, the connection pipes and dip tubes of the separators have to be dismantled. The pipes to be removed are shown in Figure 5.10 (A). Subsequently, the separators are purged with a suitable solvent, in which the extract is soluble. For example, diethyl ether was used to recover the extract from iris rhizomes (see Chapter 6.3.3.4). Afterwards, the extract solutions can be recovered via the draining manual valves DMRV500 and DMRV510. The collection of the solutions can be enhanced by applying a low pressure of nitrogen on the top of the separator. This washing step is repeated two times in order to guarantee a complete recovery of the extracts. In addition, the adjacent pipes to the separators are also purged with the same solvent. Afterwards, the pipes and dip tubes are re-installed in the separators.

In addition, the extraction vessel is removed from the oven. After the disposal of the extraction material, the vessel and adjacent pipes are cleaned with a suitable solvent. Furthermore, a connection pipe is placed from the heat exchanger directly to the outlet of the oven. The configuration is presented in Figure 5.10 (B). After that, the cosolvent pump is started with a flow of 5 mL/min to purge the pipes after the extraction process for 10 min. This proceeding removes the residual compounds in the pipes and valves. The transport of the solvent can be enhanced by flushing liquid carbon dioxide through the unit. The purge solution can be recovered from the separators. Finally, the residual carbon dioxide in the supply pipe can be used to dry the pipes by applying a slow flow.

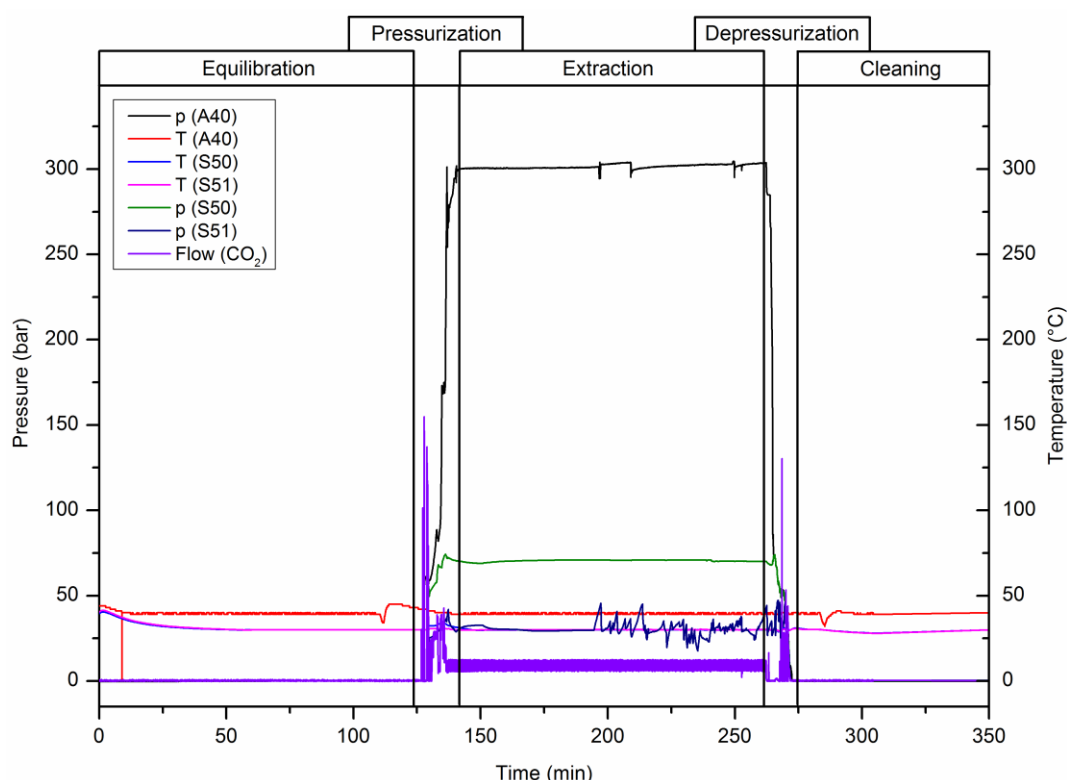


Figure 5.11: Development of pressure and temperature in the extraction vessel (A40), first separator (S50), and second separator (S51). In addition, the flow of CO₂ in g/min is plotted.

The development of pressure and temperature in the extraction vessel, first separator, and second separator, as well as the CO₂ flow (in g/min), can be seen in Figure 5.11. In addition, the corresponding main steps of supercritical fluid extraction are presented.

5.5 Troubleshooting

Nonetheless, problems may occur due to unexpected events during the extraction procedure. Several problems with their corresponding troubleshooting are described in this chapter. In the case of a serious problem or the failure of fixing the problem it is recommended to contact the manufacturing company of the extraction unit Separex.

The troubleshooting for pipe plugging, leakage of adapters and the back pressure regulation valve (BPR400) will be explained in the following.

5.5.1 Plugging in pipe

A blockage in the pipes is indicated by an uncontrolled and steady increase of the pressure in a section of the unit. In the case of this event, the pumps must be immediately turned off and the CO₂ supply closed. First of all, it is important to find the source of plugging. Mainly, the blockage is located in one of the valves. The blockage may be released by loosening and tightening the corresponding valve until the pressure decreases. Afterwards, the unit should

be completely depressurized. If the plugging of the pipe cannot be eliminated with this procedure, the unit should be depressurized by the draining manual valves (DMVxxx). Finally, it is necessary to clean the complete unit by purging the pipes with an organic solvent.

5.5.2 Leakage of pipe adapters

The leakage of pipe adapters is a relatively frequent event during SFE. It can be seen by a low temperature or the formation of ice on the pipe connectors. Furthermore, a hiss is often perceptible. In addition, the uncontrolled decrease of pressure in a part of the unit can refer to a leakage. In the case of leakage, it is mandatory to stop the pumps and close the CO₂ supply. Afterwards, it is important to find the position of the leakage. The finding of an untighten adapter can be facilitated by the use of a leak detection spray. In most of the cases, it is sufficient to tighten up the pipe connector with a wrench. Usually, the extraction procedure can be carried on after the repair of the leakage. If the problem persists, a new pipe ferrule or seal should be installed.

5.5.3 Leakage of back pressure regulation valve

The leakage of the back pressure regulation valve (BPR400) is observable at the beginning of the extraction procedure during pressurization of the unit. The leakage can be spotted by a hiss and the formation of small dry ice particles in the BPR400. Here again, the unit should be completely depressurized. Subsequently, the valve needs to be dismantled. The procedure is presented in Figure 5.12. This process should also be carried out in the case of an unreleased blockage of the valve.

First of all, the blue knob needs to be removed, followed by the loosening of the metal top (A). In addition, the fitting (B) at the bottom of the valve is removed and the PTFE seal (red arrow) is examined for potential damage. The cover of this fitting can be unscrewed, obtaining the valve piston (C). All three seals (red arrow) should be checked for their intactness. Moreover, a screw (D) at the bottom of the valve should also be detached. In the case of any damage, the seals should be exchanged. Apart from that, all parts should be intensively cleaned.

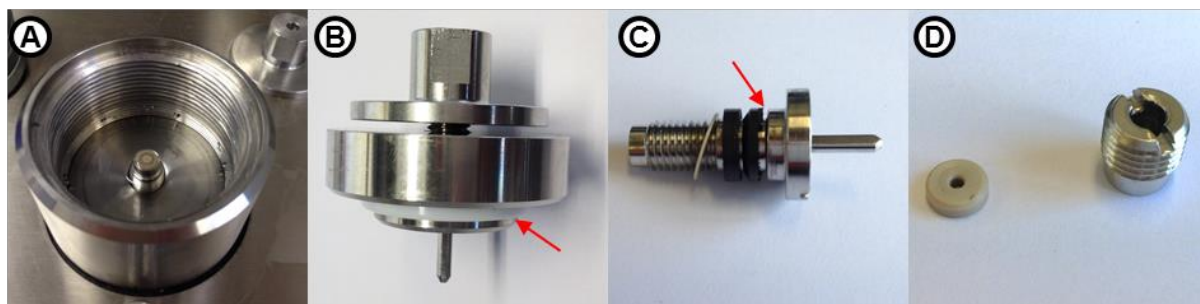


Figure 5.12: Dismounting procedure of the back pressure regulation valve (BPR400).

Finally, all parts should be reassembled in the reverse order of disassembly. However, the lid of the fitting (B) must be strongly tightened, as the loosening of this lid often implicates the leakage of the BPR400.

5.6 Summary of maximum operating conditions

The maximum pressure and temperature values for the different parts of the unit are summarized in Table 5.1.

Table 5.1: Maximum operating conditions (pressure, temperature) of different process parts.

Process Part	Operating conditions	
	Max. Pressure	Max. Temperature
CO₂ pump (P200)	1,000 bar	Ambient
Cosolvent pump (P210)	400 bar	Ambient
Extraction vessel (A40)	1,000 bar	250 °C
Extraction vessel (A41)	1,000 bar	150 °C
Magnetic mixer (M400)	700 bar	250 °C ¹
View cell (UVC42)	1,000 bar	150 °C
Separators (S50, S51)	200 bar	150 °C

5.7 References

- [1] P.W. Atkins and J. de Paula, *Physikalische Chemie*, 4. ed, **2006**, Weinheim: Wiley-VCH.
- [2] E. Reverchon, *J. Supercrit. Fluids*, **1997**, 10, 1-37.
- [3] P.G. Jessop and W. Leitner, *Chemical Synthesis Using Supercritical Fluids*, **2008**, Weinheim: Wiley-VCH.

¹ Cooling of the mixer is necessary if the temperature in the oven exceeds 100 °C.

6 Extraction of *Iris germanica* L.

6.1 Introduction

Iris germanica L. is a species of the genus *iris* and belongs to the family of Iridaceae. The essential oil from iris rhizomes, called iris butter, is one of the most valuable raw materials for the perfume and cosmetic industries. The typical violet-like smell is due to the irones. These compounds are not present in the rhizomes directly after the harvest. The fragrances are generated by oxidative degradation of iridals during the aging and the storage of rhizomes for at least 3 years [1-3]. Commonly, iris butter is obtained by steam distillation with an extraction yield of 0.1-0.25% [4]. The price of iris butter containing about 15% of irones is estimated around 20,000 €/kg [5]. The irone content can be increased up to 85% by the production of an iris absolute. The price of this absolute may exceed 100,000 €/kg [5-7].

An alternative fast, selective and environmentally friendly extraction method of irones from *Iris germanica* L. rhizomes is investigated in this thesis chapter. Therefore, supercritical fluid extractions (SFE) with carbon dioxide were carried out.

First of all, analytical methods were established in order to examine the quality and irone content of the extracts. For this purpose, HPLC/UV, GC/FID and TLC were used. It was also important to characterize the used iris rhizomes, which were rhizomes of the species *Iris germanica* L. with different storage periods. Three different methods were investigated in order to determine the residual moisture of the rhizomes. In addition, an appropriate solvent was searched in order to examine the actual irone content using Soxhlet extractions. The surveyed solvents were methanol, ethanol, ethyl acetate, ethanol/ethyl acetate (30/70 v/v), acetone, and methyl *tert*-butyl ether. An artificial oxidation method of iris rhizomes was also performed to determine the maximum irone content.

Steam distillation is not only a long-lasting and high energy-consuming process, but the high temperature can also induce thermal degradation of the fragrance compounds. Therefore, an alternative method, supercritical fluid extraction with CO₂, was investigated. Carbon dioxide is used in SFE because of its comparatively low critical pressure (73.7 bar) and temperature (31.1 °C). Above the critical pressure and temperature, the liquid-gaseous phase boundary vanishes and CO₂ adopts the properties of both states. Advantages of SFE are the high availability of carbon dioxide at low cost and its high purity, nontoxicity, and nonflammability. Also, critical conditions are easily obtained and are suitable for mild extractions [8-12]. The extraction unit "LAB SFE 100 mL" from Separex was used for all experiments.

Preliminary SFE experiments showed that the extraction of irones from iris rhizomes is a very complex process. The first experiments were performed with the „trial & error“-method, at which only one parameter was varied per experiment. As the examination and the

assessment of all extraction parameters would have been too time consuming, a method was searched to investigate the influence of several parameters on the extraction yield with a small effort. To this purpose, a design of experiments (DoE), with an experiment plan of Plackett and Burman, was used [13]. In detail, seven different parameters of SFE and their significance on the extraction yield were investigated: extraction time, flow of CO₂, and both the temperature and pressure in the extraction vessel, first separator, and second separator. However, the results of DoE showed that the extraction of irones by SFE is not exhaustive, as only one third of the actual irone content in the rhizomes could be extracted. For this reason, the parameters obtained by DoE formed the basis of further experiments in order to improve the extraction method.

A method was established to obtain a higher amount of irones in the extract by SFE compared to conventional extraction techniques. The obtained result demonstrates that a more selective extraction of irones can be achieved by supercritical carbon dioxide in comparison to steam distillation. Nonetheless, the extraction of irones from iris rhizome by SFE was still not exhaustive. For this reason, the influence of a cosolvent, additives and pretreatment of iris rhizomes during SFE was further investigated.

The investigation of an alternative extraction method for iris rhizomes presented in this section is part of a superior project. The intention is to improve the entire process, starting from the planting to the extraction of iris plants. For instance, methods were investigated in order to increase the irone content in iris rhizomes or accelerate the formation of irones during storage. In addition, some new environmentally friendly and sustainable extraction methods were established.

6.2 Fundamentals: *Iris germanica* L.

Iris germanica L. or German iris is a species of the genus iris and belongs to the family of the Iridacea. The plant can be especially found on the Mediterranean area and in south-west Asia and was introduced in Germany as a popular garden or park plant. It is an enduring and erect plant, with a creeping and branched rootstock. It can grow up to a height of 100 cm. The sword-shaped leafs are double-spaced, upright with a sea green color. The blossoms are usually blue or violet, but also other color variations are known. The color may vary depending on the family plant. The blossoms are up to 10 cm tall and consist of six petals, three of which are directed up and three down. The latter are carrying a strip of yellow hair (beard) [14-16]. Figure 6.1 presents a full picture of an *Iris germanica* L. plant with blossoms, leafs, roots and the rhizome. *Iris pallida* Lam. and *iris florentina* L. are two other well-known iris species. They differ only slightly in the appearance, especially the color of the blossoms, from *iris germanica* L. plants.

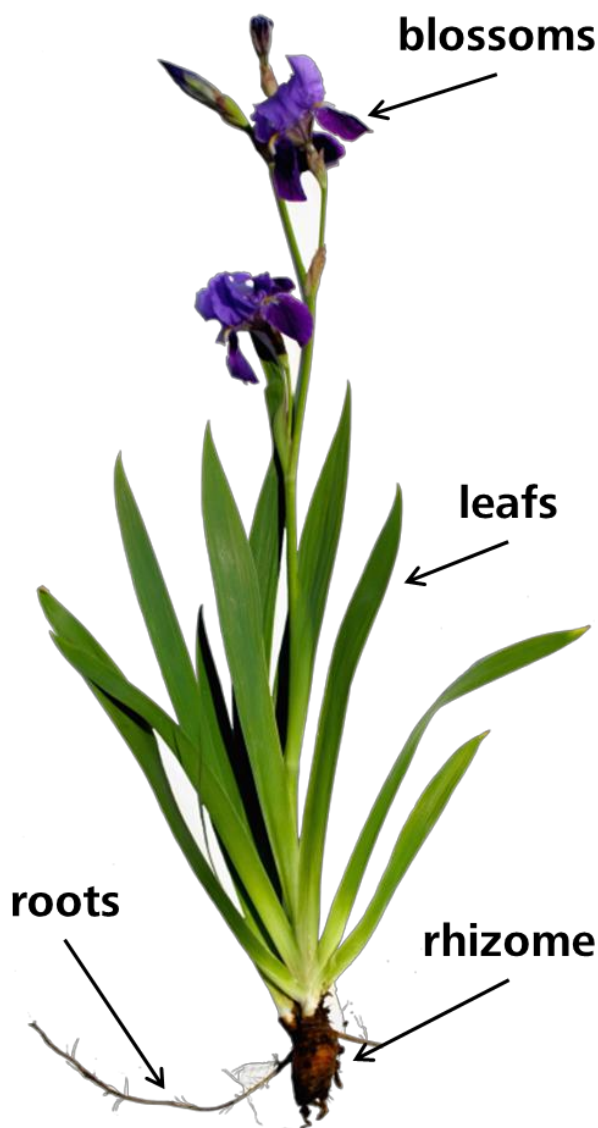


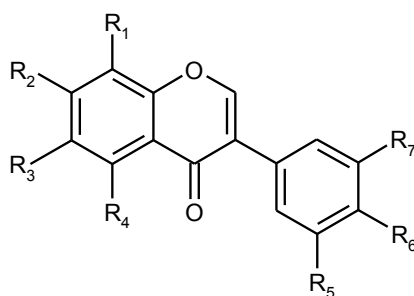
Figure 6.1: Full picture of an *Iris germanica* L. plant with blossoms, leaves, roots and the rhizome.

Iris germanica L. is flowering from May until July. The plant needs only little maintenance and prefers stony, calcareous, loam rich, well-drained soil in sunny mountain slopes. The crop is mainly cultivated in Italy, South-France, Morocco, China and India for the recovery of the rootstock. It is a hardy plant, so the cultivation is also possible in Germany. The divided rhizomes are planted in fields in September at a distance of about 25 cm and 10 cm deep with the cut surfaces facing up. Harvesting is done in July or August after two or three years of growing. A part of the harvest is again cultivated, while the other part is further processed. Also in vitro propagation and plant regeneration via embryogenesis from leaves of iris plants is possible [17-19]. The harvested rhizomes are extensively washed, peeled, and dried in the sun. Fresh rhizomes contain approximately 70% of water. Artificial drying of the rhizomes should be avoided. The dried rhizomes are subsequently stored in containers, where they are protected from light, dust, moisture, and insects [14, 16, 20, 21].

6.2.1 Ingredients of rhizomes

The rhizome, also called orris root, is the key organ of the iris plant and assures the propagation and persistence of the species. It consists largely of reserve carbohydrates with 20 to 50% of starch and sucrose. Other ingredients are mucilage, resin, tanning agents, wax, and ascorbic acid [16, 22].

Another class of substances which is present in iris rhizomes are isoflavones. The most important isoflavones are irigenin, nigricin, iristectorigenin A, nigricanin, irisflorentin, irilone, iriflogenin and irisolidone [1, 22-25]. The chemical structures of these compounds are shown in Figure 6.2. It has been shown that irigenin, irilone and iriflogenin are potent inhibitors of the cytochrome P450 1A-isoenzyme which is involved in the metabolic conversion of procarcinogens into carcinogens [26]. In addition, some other isoflavones show cytotoxic and anti-inflammatory activities [27-29]. Irogenin is the most common isoflavone in *Iris germanica* rhizomes with a concentration of 78 mg/g. The amount of other isoflavones is lower and varies according to the iris species [1].



	R ₁	R ₂	R ₃	R ₄	R ₅	R ₆	R ₇
Irogenin:	H	OH	OCH ₃	OH	OCH ₃	OCH ₃	OH
Iristectorigenin A:	H	OH	OCH ₃	OH	H	OCH ₃	OH
Nigricin:	H	-O-CH ₂ -O-		OCH ₃	H	OH	H
Irisflorentin:	H	-O-CH ₂ -O-		OCH ₃	H	OH	OCH ₃
Nigricanin:	H	-O-CH ₂ -O-		OCH ₃	OCH ₃	OCH ₃	OCH ₃
Iriskumaonin methyl ether:	H	-O-CH ₂ -O-		OCH ₃	OCH ₃	OCH ₃	H
Irilone:	H	-O-CH ₂ -O-		OH	H	OH	H
Iriflogenin:	H	-O-CH ₂ -O-		OH	OCH ₃	OH	H
Irisolidone:	H	OH	OCH ₃	OH	H	OCH ₃	H
8-hydroxyirigenin:	OH	OH	OCH ₃	OH	OCH ₃	OCH ₃	OH

Figure 6.2: Chemical structures of isoflavones present in *Iris germanica* and *Iris pallida* rhizomes [1].

Other ingredients are phenolic compounds like acetovanillone, protocatechuic acid and sinapinic acid. However, acetovanillone, also called apocynin, is the most important phenolic

compound in iris rhizomes [16]. It is structurally related to vanillin and has a slight vanilla odor. In addition, the compound shows anti-inflammatory properties and might be an effective and safe drug in bronchial asthma [30].

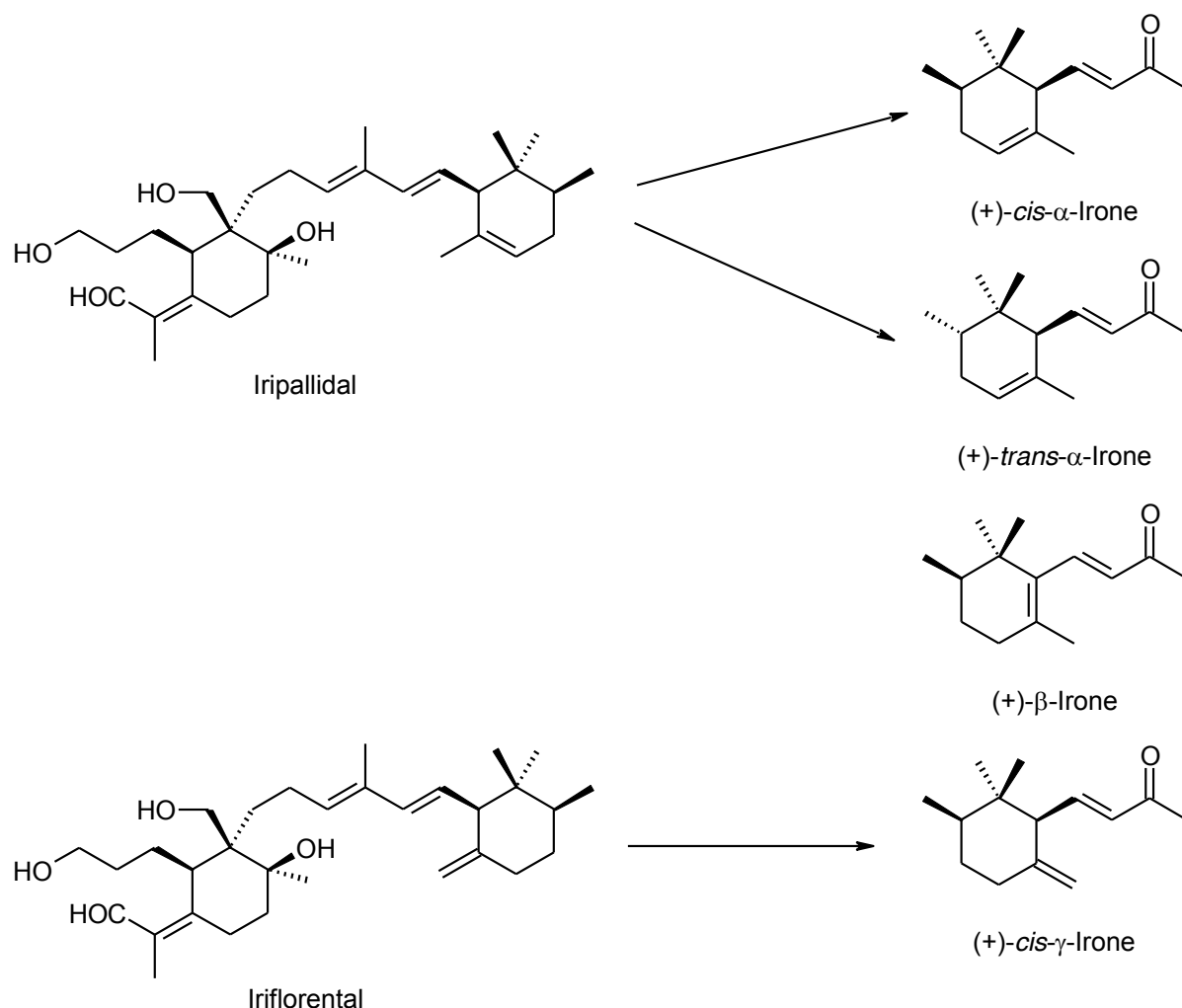


Figure 6.3: Formation of different irone isomers (*cis*-α-irone, *trans*-α-irone, β-irone, *cis*-γ-irone) due to oxidation of their precursors iridals (iripallidal, iriflorental).

Nonetheless, the most important and valuable ingredient in iris rhizomes is the essential oil. Orris roots contain only 0.1-0.25% of essential oil than can be commonly recovered by steam distillation of peeled, dried, and ground iris rhizomes. Due to its buttery consistency, the extract is called iris butter or orris oil. It is a pale yellow compound with a melting point of 38-40 °C. Iris butter contains a large amount of myristic acid and other fatty acids. The main odorants in the essential oil are irones, which have a violet-like scent [4, 14, 16]. These cyclic ketone terpenes ($C_{14}H_{22}O$) are not initially contained in fresh iris rhizomes. They are formed by oxidative degradation of C_{31} -triterpenes, the iridals, during storage. That is the reason why rhizomes are stored for at least 3 years (up to 6 years) after harvest [2, 3]. The four natural isomers, which can be found in iris rhizomes, are *trans*-α-irone, *cis*-α-irone, β-irone and

cis- γ -irone [31]. Figure 6.3 presents the chemical structures of these odorants and their corresponding precursors.

Iridals can be divided into three classes: cycloiridals, bicycloiridals and spiroiridals [32]. *Iris germanica* L. and *iris pallida* Lam. rhizomes contain up to 1% of iridals related to the fresh weight [3, 16]. 70% are present as free iridals and the remaining amount as iridal esters of fatty acids [33]. The bicyclic iridals, iripallidal and iriflorental are the precursors for α -irone and for the γ -isomer. A precursor for β -irone was not found in any iris species. Therefore, it is assumed that β -irone derives from the isomerization of the α - or γ -isomer [3, 34]. Other iridals in fresh iris rhizomes are α -irigermanal and γ -irigermanal, which form *cis*-hydroirones by oxidative degradation [35]. Up to now, more than 30 different iridal structures have been elucidated. Consistently, various new iridals and iridal-type triterpenoids in different iris species are reported [32, 36-39]. The ecological relevance of iridals in iris rhizomes is still not fully clarified. It was suggested that iridals are constituents in cell membranes comparable to sterols [40]. Dehydration experiments with rhizome slices indicated that iridals are involved in drought resistance and/or healing of rhizome in order to maintain the cell function and membrane integrity [21]. Due to the very bitter taste of iridals, also the function as deterrent is conceivable. The mechanism of iridal formation is still not clarified. However, monocyclic iridals are formed in a hitherto unknown metabolism of squalene, followed by a methylation reaction. A further cyclization of the compound, leads to the bicyclic iridals (iripallidal and iriflorental) [41]. It was discovered that young rhizomes contain mainly monocycloiridals. As their amount decreases with the growth of the rhizome, the iridals iriflorental and iripallidal become predominant. Iridals are the major products in one and two years old iris rhizomes. In addition, the iridals are not uniformly distributed in rhizomes. The total amount of iridals is the highest in young rhizome parts, whereas the amount decreases slightly with age [42]. Also seasonal variations of the total iridal content in iris rhizomes are reported. Apparently, the content of triterpenoids reaches a maximum value in spring and fall [33]. Iridals possess a broad range of biological activities like antitumor, antiplasmodial, membrane reinforcing, and protein kinase C activation [43, 44].

Nonetheless, the main application of iridals is the formation of irones by oxidative degradation. For that reason, iris rhizomes are stored for at least 3 years (up to 6 years) until the oxidation is almost complete [2, 3]. But the activator of the oxidation process from iridals to irones is still unknown. Possibly, the formation of irones is due to a chemical reaction by oxidation with oxygen or a biological reaction by microorganism or the plant cells themselves [45]. The four natural isomers found in iris rhizomes are *trans*- α -irone, *cis*- α -irone, β -irone and *cis*- γ -irone [31]. The distribution of the different irone isomers depends on the iris species [46]. The total content of irones after 3 years of storage is on average 300 mg per kg in *Iris germanica* L. rhizomes [2]. Maximum values up to 595 mg/kg are reported. However, *Iris pallida* Lam. rhizomes contain a higher amount of irones with a maximum content up to 1400 mg/g [46].

In the last decades, different methods were invented to accelerate the oxidative degradation of iridals and increase the irone yield in young iris rhizomes. However, regulatory specialists are still questioning the naturalness and thus debating the legal status of these artificial oxidation processes [7]. The first established method was the oxidation of extracts from fresh iris rhizomes with potassium permanganate, which leads to the typical violet-like scent of irones [47]. Furthermore, different methods to treat iris rhizomes were patented. Artificial oxidation was performed using bacteria [45, 48], ionizing radiation [49], enzymes [50], fungus [51], or nitrite salts [52]. Recently, a method was patented by Dr. Flemming *et al.* (SKH GmbH) for the treatment of fresh iris rhizomes with pure oxygen. The formation of irones can be accelerated with these methods within few days or weeks.

Furthermore, irones can also be synthesized. The most valuable method is the cyclization of methyl-3-pseudo ionone catalyzed by sulfuric or phosphoric acid. The product contains mainly *trans*- α -irone and *cis*- α -irone, but only a minor amount of β -irone [53]. Also enantioselective synthesis of different irone isomers are reported in literature [54-56]. However, from an organoleptic point of view, commercial racemic irone mixtures do not meet the requirements of iris fragrance in modern perfumery [57].

Iris rhizomes are used in different applications. In folk medicine and pharmacy they were used against diseases of the respiratory system as expectorants and against inflammation of the alimentary tract. However, the effectiveness of this drug is currently not proven for these applications. In addition milled iris rhizomes were used as additive in tooth powders, smelling pillows, loose powders and as a fumigant. Dried and peeled rhizomes were formerly used for teething children as chewing medium. But this is not recommended for hygienic reasons, as intensive bacterial growth can occur in saliva moistened pieces. Over time, the pharmacological applications of the iris rhizomes have become less important. An important field of application is the food industry, where iris rhizomes are used to flavor fine liqueurs as Benediktiner, Danziger Goldwasser, Cordial Medoc or for seasoning Chianti wine [14, 16]. For example, fine ground iris rhizomes are added in the production process of Bombay Sapphire Gin™ to release the full floral flavors of iris during distillation [58]. However, the rhizomes are mainly used for the extraction by steam distillation to gain the essential oil, called iris butter.

6.2.2 Extraction methods

The extraction of iris rhizomes is a complex and long-lasting process. Figure 6.4 presents an overview of the complete extraction process. The process starts by harvesting the iris rhizomes in July or August after two or three years of growing. Afterwards, the rhizomes are extensively washed, peeled, and dried in the sun for several months. Subsequently, the dry rhizomes are stored in containers, where they are protected from light, dust, moisture, and insects. This storage period lasts about 3 years, but can also be extended up to 6 years.

During this time, irones are formed by oxidative degradation of iridals. These odorants are responsible for the typical violet-like scent. Finally, the rhizomes are milled to a coarse powder and subsequently extracted. The most common way is the extraction by steam distillation for 48 h to obtain the iris butter. Alternative methods can be used to extract iris rhizomes, but the extraction method influences the quality and price of the extract, which will be presented in the following.

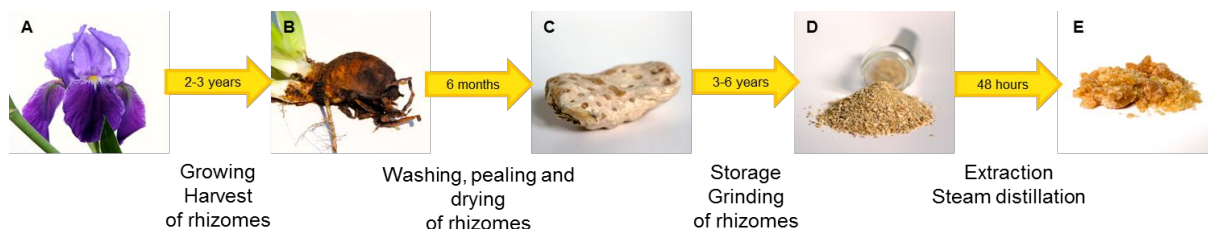


Figure 6.4: Overview of the current procedure to extract iris rhizomes and obtain iris butter. (A) iris plant; (B) fresh iris rhizome; (C) peeled and dried iris rhizome; (D) milled iris rhizomes; (E) iris butter;

An easy method to recover compounds from plant materials is solvent extraction. Therefore, pure hexane or a combination with other volatile solvents (e.g. ethyl acetate) is used to extract dried and matured iris rhizomes. To this purpose, the iris powder is extracted through several warm washes, followed by filtration and concentration. With this method an extract, called resinoid, is obtained, which contains approximately 1-3% irones. The total extraction yield related to the mass of dry rhizomes is in average 5%. Resinoids have a pasty consistency at room temperature and are orange/brown. They are much less expensive than iris butter. Also the odor is quite different. It is described as chocolate, woody, leathery, and hay scent. The chemical composition of this solvent extract is very complex as it contains both volatile and non-volatile compounds. The main compounds are flavonoids, polyphenols, fatty acids and their esters, iridals, iridal esters and irones [1, 2, 7]. In addition, aqueous and ethanol extracts of iris rhizomes show strong antioxidant and radical scavenging activities [59]. In another study the therapeutic properties of ethanol extracts were investigated in rats. It was established that the extract helps decreasing the serum level of cholesterol, triglycerides and total lipids. Moreover, the toxicity of the extract was determined to be minimal at low doses [60].

Another method is the extraction of iris rhizomes with supercritical carbon dioxide. But only one scientific article is available on this topic. It has been shown that supercritical CO₂ is able to extract only 44% of the total irone content in iris rhizomes, probably because of the inappropriate polarity of CO₂. The extraction yield can be increased by using methanol as a modifier. Nevertheless, sc-CO₂ is a suitable solvent to extract iridals from iris rhizomes. Actually, a higher yield in iridals can be achieved compared to conventional solvent extraction. An advantage is that SFE is a very selective extraction method and very low amounts of flavonoids were detected in the extract [61]. These results are in contrast to the

industrial extraction of iris rhizomes by supercritical fluid extraction with natural carbon dioxide. The company Flavex/Germany commercially sells a sc-CO₂ extract of *Iris germanica* L. rhizomes. The extract can be purchased in different quality grades depending on the irone content with a maximum content of 10%. It has a sweet balsamic, weak woody, and violet-like smell. The CO₂-extract contains a high amount of myristic acid, irones (mainly *cis*- α -irone and *cis*- γ -irone, traces of *trans*- α -irone and β -irone), aldehydes, terpenes, and other steam volatile ingredients. It is mainly used in perfumery and in soap industry, as well as in the liqueur industry for flavoring [62, 63].

In addition, a method was recently patented by Höß *et al.* (Institute of Physical and Theoretical Chemistry II, University of Regensburg) for the extraction of iris rhizomes with aqueous micellar soap solutions.

Nevertheless, the most common way to extract iris rhizomes is steam distillation. Therefore, dried and matured iris rhizomes are primarily soaked in an aqueous acetic solution for 12 h. The subsequent steam distillation for 48 h provides the iris butter [4]. The composition and applications of iris butter are described in chapter 6.2.3. A major disadvantage of steam distillation is the time-consuming and energy-consuming process. Also thermal degradation of sample components can occur due to the high temperature during distillation [64]. For this reason, alternative extraction methods gain more and more importance.

6.2.3 Iris butter

Iris butter is the essential oil from iris rhizomes extracted by steam distillation. The total extraction yield of distillation is very low, around 0.1-0.25% [4, 16]. The extract is also called orris oil, orris concrete, orris butter or beurre d'iris. It is a pale yellow buttery compound with a melting point of 38-40 °C [6, 65]. Due to its complex production, it is one of the most valuable natural product [66]. The price of iris butter containing about 15% of irones is estimated around 20,000 €/kg [1, 5].

The main odorant in the essential oil are irones. Conventional iris butter contains about 5-20% of these odorants. Four natural isomers can be found in iris butter: *trans*- α -irone, *cis*- α -irone, β -irone and *cis*- γ -irone [6, 31]. The isomer *trans*- γ -irone was also identified in iris butter, but only traces were detected [31]. The isomeric distribution of the different irones depends on the iris species. An overview is presented in Table 6.1. It can be seen that *cis*- α -irone is the predominant isomer in *Iris germanica*, whereas *cis*- γ -irone predominates in *Iris pallida* [1, 6]. This results in a slight difference in the scent of iris butter from *Iris germanica* and *iris pallida*. *Iris pallida* gives an essential oil which is generally more popular and has a more powerful, woody, floral, and powdery odor. Whereas the iris butter of *Iris germanica* is fruity with notes of red fruits and offers a more diverse range of flavors [7]. This is due to the different odors of the single irone isomers, which were investigated by GC sniffing [67].

Table 6.1: Isomeric distribution of irones in iris butter of *Iris germanica* L. and *Iris pallida* Lam. from literature, with the corresponding odor [1, 6, 67].

	Proportion of each isomer (% of total irone content)			
	<i>trans</i> - α	<i>cis</i> - α	β	<i>cis</i> - γ
<i>Iris germanica</i> L.	1	61	1	37
<i>Iris pallida</i> Lam.	5	34	0	61
Odor (dextrorotatory (+)-isomers)	floral, fresh, fruity, honey, sweet chamomile, low violet odor	Iris, sweet irone, ionone woody, floral, fruity	iris, sweet, woody, ionone, dry and floral	iris family, anise, licorice, green

Furthermore, iris butter contains approximately 71-95% of free or partially esterified fatty acids, mainly myristic acid. Other fatty acids are palmitic acid, caprylic acid, lauric acid and pelargonic acid [6, 65]. In addition, 20 irone related compounds containing from 10 to 16 C-atoms have been identified in commercial iris oil of Moroccan origin [68]. Also other ketones like acetophenone, acetovanillone and acetoveratrone were detected. Benzaldehyde, furfural, naphthalene, terpene and sesquiterpene alcohols, aldehydes, and esters can also be found in small quantities [6, 16, 22].

Orris absolute can be obtained by dissolving iris butter in ethanol and performing a subsequent precipitation of insoluble compounds by cooling the solution at -20 °C. The precipitated compounds are mainly fatty acids and waxes. Also distillation or vacuum rectification of the iris butter can be done to obtain orris absolute. The yield is very low with a value of 0.03-0.04% related to the initial mass of dry rhizomes. However, this absolute contains up to 85% of irones. This is the most valuable product that can be recovered from iris rhizomes [6, 7]. The price of iris absolute may exceed 100,000 €/kg [5].

Iris butter is mainly used for odorant and flavoring applications in perfume and cosmetic industry. It is especially contained in luxury perfumes like Chanel No. 19™ (Chanel), Chanel No. 5™ (Chanel), Dior Homme™ (Dior), No. 1 Iris™ (Prada) and many more [69]. The company Weleda, which is specialized on natural cosmetics, distributes a special beauty care series with iris butter as ingredient in face lotions [70].

6.3 Experimental section

6.3.1 Plant material and iris butter

Iris rhizomes (*Iris germanica* L. and *Iris pallida* Lam.) were obtained from Phytotagante/France. The plants were cultivated in Morocco. The rhizomes were harvested after approximately 3 years of growth. Afterwards, they were washed, peeled and dried for 6 months. The following storage time varied from 1 to 9 years for the used rhizomes. Rhizomes of *Iris germanica* L. were milled into a coarse powder, whereas rhizomes of *Iris pallida* Lam. were delivered in cut small pieces. The rhizomes were milled into a fine powder with a commercially available coffee mill for some experiments. Some samples of the rhizomes were infested with flour beetles. Table 6.2 gives an overview of the different used rhizomes.

Table 6.2: Overview of the different used iris rhizomes. The storage time refers to the value which was current at the delivery date. The name of the samples includes the year of delivery.

Name	Species	Storage time	Appearance	Bug infestation
Iris 2011	<i>Iris germanica</i> L.	3 years	milled	no
Iris2015.2	<i>Iris germanica</i> L.	2 years	milled	yes
Iris2015.1	<i>Iris germanica</i> L.	1 year	milled	no
Iris 2013	<i>Iris pallida</i> Lam.	9 years	cut rhizome pieces	yes

Iris butter was also obtained from Phytotagante/France as a reference substance. The beige colored extract was gained by steam distillation of *Iris germanica* L. rhizomes. The exact irone content was determined by HPLC/UV and was equal to 4.5%. A commercial available CO₂ extract of *Iris germanica* L. rhizomes was obtained from Flavex/Germany. The orange extract contained 9.8% of irones (mainly *cis*- α - and *cis*- γ -irones). Other ingredients were myristic acid, aldehydes, terpenes and other steam-volatile compounds. Both substances were used as reference compounds and for the identification of the different irone isomers in the HPLC and GC chromatograms. For this purpose, also a technical mixture of *cis*- and *trans*- α -irone (90%, Sigma-Aldrich) was used.

6.3.2 Residual moisture

The residual moisture of iris rhizomes was determined with three different methods. High temperatures during the drying processes must be avoided to prevent the loss of flavor through volatilization of essential oil [71].

The first method was to dry the rhizomes in a compartment drier at 45 °C. To this purpose, the mass loss of five samples (each 1 g) with finely ground iris rhizomes was determined every hour until a constant weight was reached. A constant value was achieved after approximately 48 h. The second method, was the determination of the residual moisture according to the Pharmacopoea Europaea (Ph. Eur.) [72]. To this purpose, five samples (each 1 g) with finely ground iris rhizomes were dried at 105 °C in a compartment drier for 2 h. The mass loss was subsequently determined.

The third method to determine the residual moisture was freeze drying. Here, about 10 g of grinded iris rhizomes were weighed in a small Schott bottle and then frozen with liquid nitrogen. Altogether, five samples were prepared. Afterwards, the samples were put into a lyophilization unit and a vacuum was generated. The experiment was stopped after 17 h and the mass loss of the samples was recorded.

6.3.3 Extraction methods

6.3.3.1 Macerations

Macerations of iris rhizomes were carried out with different solvents. To this purpose, 0.5 g of finely ground rhizomes was mixed with 2.5 mL of solvent. The samples were stirred for approximately 18 h at room temperature. Investigated solvents were: methanol (HPLC-grade, Merck), ethanol (99.9%, Sigma-Aldrich), ethanol (96%, technical grade), ethyl acetate (99.9%, Acros Organics), a mixture of ethyl acetate and ethanol (70/30 v/v), acetone (99.9%, Merck), methyl *tert*-butyl ether (99.0%, Merck), diethyl ether (99.8%, Sigma-Aldrich), hexane (95.0%, Merck) water (Millipore), dichloromethane (99.9%, Acros Organics), isopropanol (99.9%, VWR), toluene (99.9%, Merck), 1 M sodium hydroxide (TitriPUR®, Merck), and 1 wt% formic acid solution. The extracts were subsequently analyzed by TLC.

6.3.3.2 Ultrasound-assisted extraction

Ultrasound-assisted extractions of iris rhizomes were carried out in order to investigate the extraction efficiency of irones with different solvents. To this purpose, 30 mL of solvent were added to 5 g of finely ground iris rhizomes. Surveyed solvents were methyl-tetrahydrofuran (Me-THF, 99.0%, Sigma-Aldrich), *n*-hexane (95.0%, Merck), and methanol (HPLC-grade, Merck). After 20 min of maceration, the samples were put in an ultrasonic bath for 20 min. Subsequently, the solutions were filtrated and the solvent was evaporated under a nitrogen stream. The mass of the dry extract was determined. The extracts were dissolved in 5 mL of methanol. 11 mg (1 drop) of the pure internal standard α -ionone was pipetted in a 50 mL volumetric flask. The extract solution was quantitatively transferred into the flask and the volume was readjusted at room temperature. The solutions were filtrated through 0.2 μ m PTFE-syringe filters and then analyzed by HPLC/UV.

6.3.3.3 Soxhlet extractions

In order to determine the actual irone content in the different iris rhizomes, various Soxhlet extractions were carried out. To this purpose, about 7 g of fine ground rhizomes ($m(\text{rhizomes})$) were extracted for 6 h with approximately 50 mL of solvent. Different solvents were investigated: methanol (HPLC-grade, Merck), ethanol (99.9%, Sigma-Aldrich), ethanol (96%, technical grade), a mixture of ethyl acetate and ethanol (70/30 v/v), acetone (99.9%, Merck), ethyl acetate (99.9%, Acros Organics), and methyl *tert*-butyl ether (99.0%, Merck). The total weight of the extraction thimble with the rhizomes ($m(\text{thimble})_{\text{before}}$) was weighed before the extraction. After the extraction process, the thimble was put in the compartment drier at 45 °C overnight and weighed again ($m(\text{thimble})_{\text{after}}$). The percentage extraction yield was calculated with equation (6.1).

$$\text{Yield (\%)} = \frac{m(\text{thimble})_{\text{before}} - m(\text{thimble})_{\text{after}}}{m(\text{rhizomes})} - \text{residual moisture (\%)} \quad (6.1)$$

After extraction, 11 mg (1 drop) of the pure internal standard α -ionone was pipetted in a 50 mL volumetric flask. The Soxhlet extract solution was transferred into this flask and the volume was readjusted at room temperature with the corresponding solvent. In the case of methyl *tert*-butyl ether, the ether was primarily evaporated under a nitrogen stream. The pure extract was then dissolved in methanol and prepared in the same way as it is described above. The solutions were filtrated through 0.2 μm PTFE-syringe filters and then analyzed by HPLC/UV. All extractions and analyses were carried out three times.

6.3.3.4 Supercritical carbon dioxide extraction

Extractions with sc- CO_2 were carried out on the “Lab SFE 100 mL – 4368” extraction unit. The detailed procedure to control the extraction unit is described in Section 5.4. A short description of the most relevant steps during SFE is given in the following. At first, the temperature of the extraction vessel and the two separators were adjusted. The exact values are always given in the corresponding “results & discussion” part. After approximately 30 min of equilibration, about 25 g of grinded iris rhizomes were put in the extraction vessel and all pipes were connected. After another 10 min of equilibration, the unit was filled with liquid carbon dioxide. The CO_2 flow of the pump was set at the desired value and the pressure in the extraction vessel was regulated with the back pressure regulator. For some experiments, ethanol was used as a cosolvent, which was added to the CO_2 stream with a second pump. The solvent passed through the extraction vessel from the bottom to the top. The flow of carbon dioxide/cosolvent and the pressure in the extraction vessel and separators were kept constant during the experiment. The extraction time was started when all values were

constant. After the desired extraction duration the CO₂ pump was stopped and the unit carefully and slowly depressurized. The extraction vessel and the separators were opened 10 min after the complete depressurization of the unit.

The residual iris rhizomes were weighed in order to calculate the total mass extraction yield. The extracts in the separators and pipes were recovered with approximately 40 mL of diethyl ether. The sample name *S50* refers to the first separator and *S51* to the second separator. The unit was purged with isopropanol in order to recover deposited extract in the pipes (sample *Purge*). The solvents were evaporated under a nitrogen stream and the mass of the extract was determined.

Furthermore, the CO₂ extract was dissolved in 5 mL of methanol. The solubilization of the extract was enhanced in an ultrasonic bath. 11 mg (1 drop) of the pure internal standard α -ionone was pipetted in a 10 mL volumetric flask. The extract solution was quantitatively transferred into the flask and the volume was readjusted at room temperature. The solutions were filtrated through 0.2 μ m PTFE-syringe filters and then analyzed by GC/FID. To analyze the samples by HPLC/UV, the solutions were diluted to a factor of 1/5.

6.3.4 Oxidation process

The artificial oxidation procedure of iris rhizomes was performed using the method of Ehret *et al.* [52]. This method is employed to investigate the maximum possible iron content in the rhizomes. To this purpose, 0.5 g of fine ground *Iris germanica* L. rhizomes (storage time: 1, 2 and 3 years) were mixed with 10 mL of a 2 g/L aqueous NaNO₂ (97.0%, Sigma Aldrich) solution. A control sample was prepared only with pure water. One drop of phosphoric acid (85%, Merck) was added to every sample to decrease the pH value. The samples were stirred for 48 h at 30 °C in an oil bath. Afterwards 50 μ L of a 10 mg/mL α -ionone solution in methanol was added to every sample. The solutions were neutralized with 10 drops of a 1M sodium hydroxide solution. Subsequently, 4 mL of diethyl ether were added to the samples. After centrifugation the supernatant was taken and the solvent was evaporated under a soft nitrogen stream. The residue was dissolved in 5 mL of methanol. Solubility was enhanced in an ultrasonic bath. The solutions were filtrated through 0.2 μ m PTFE-syringe filters and then analyzed by HPLC/UV.

6.3.5 Analysis methods

6.3.5.1 Gas chromatography (GC)

Gas chromatography was carried out on a Hewlett Packard HP 6890 Series GC system equipped with a flame ionization detector (FID). A nonpolar HP-5 (5% phenyl- and 95% methyl-siloxane) capillary column (30 m x 0.32 mm i.d., 0.25 μ m film thickness) was used for separation. Analyses were performed with a constant helium flow of 1.0 mL/min. The GC

was equipped with a split/splitless injector at a temperature of 275 °C. A HP 6890 Autosampler was used to inject 1 µL of the sample in split mode using a split ratio of 1:10. The FID was maintained at a temperature of 275 °C. The temperature of the oven was initially set at 50 °C for 3 min and then increased to 300 °C at 10 °C/min. This temperature was maintained for 10 min. Analysis of each sample was carried out three times.

The irone content in the extracts was determined quantitatively by internal standard (IS) calibration with α -ionone. To this purpose, two independent stock solutions (4 mg/mL, 2 mg/mL) of a technical mixture of *trans*- and *cis*- α -irone ($\leq 90\%$, Sigma-Aldrich) in methanol were prepared. These primary stock solutions were diluted to concentrations of 2, 1, 0.5, and 0.25 mg/mL. 2 mL of a 2 mg/mL solution of the internal standard α -ionone ($\leq 90\%$, Sigma-Aldrich) were added to 2 mL of each irone solution. The solutions were filtrated through 0.2 µm PTFE-syringe filters and then measured by GC/FID. All samples were analyzed three times. Afterwards the response factor K was calculated and was equal to $K(\text{irones}) = 0.94$ for the irones. For the analysis of the extracts, an α -ionone solution was added to reach a concentration of 1 mg/mL of α -ionone in every sample to be analyzed. The amount of irones was estimated with the response factor and according to equation (6.2).

$$m_{\text{irones}} = K_{\text{irones}} \frac{a_{\text{irones}}}{a_{\alpha\text{-ionone}}} m_{\alpha\text{-ionone}} \quad (6.2)$$

where m_{irones} = mass [mg] of irone isomer, K_{irones} = response factor of irones and α -ionone, a_{irones} = peak area of all irone isomer, $a_{\alpha\text{-ionone}}$ = peak area of internal standard, $m_{\alpha\text{-ionone}}$ = mass [mg] of internal standard.

6.3.5.2 High-performance liquid chromatography (HPLC)

Another method to analyze the extracts and determine the content of irones was HPLC/UV. The analyses were performed on a "Waters HPLC System" with two Waters 515 HPLC Pumps, Waters 717plus Autosampler and Waters 2487 UV/VIS-Detector. Separation was achieved on Knauer Eurosphere C18-column (100 Å, 250 x 4.6 mm). The injection volume was 10 µL. The compounds were eluted at a flow rate of 0.7 mL/min and at a temperature of 40 °C. The solvents for gradient HPLC consisted of a 0.1% formic acid solution (A) and methanol (B) (HPLC-grade, Merck). The composition of the mobile phase started at 30% B, it was increased to 100% B within 35 min and hold then for 15 min. The detection wavelength was 230 nm. Analysis of each sample was carried out three times.

The irone content in the extracts was determined quantitatively by internal standard (IS) calibration. Again, α -ionone was used as internal standard. To this purpose, two independent stock solutions (4 mg/mL, 2 mg/mL) of a technical mixture of *trans*- and *cis*- α -irone ($\leq 90\%$, Sigma-Aldrich) in methanol were prepared. These primary stock solutions were diluted to concentrations of 2, 1, 0.5, and 0.25 mg/mL. 2 mL of a 2 mg/mL solution of the internal

standard α -ionone ($\leq 90\%$, Sigma-Aldrich) were added to 2 mL of each irone solution. Afterwards, 0.75 mL of each concentration was diluted with 3 mL methanol. The solutions were filtrated through 0.2 μm PTFE-syringe filters and then measured by HPLC/UV. All samples were analyzed three times. Afterwards, the response factor K was calculated, which is $K(\text{irones}) = 1.08$ for the irones. For the analysis of the extracts, an α -ionone solution was added to reach an end concentration of 0.25 mg/mL α -ionone in every analyzed sample. The amount of irones was estimated with the response factor and according to equation (6.2).

6.3.5.3 Thin-layer chromatography (TLC)

Thin-layer chromatography (TLC) was used as a fast screening method to determine the presence of irones in the extracts. This method was only used for making first predictions of the irone content. To this purpose, a solution of toluene and ethyl acetate (97/3, v/v) is used as mobile phase and silica gel (Merck) as stationary phase. A defined volume (usually 1 μL) of the sample to be analyzed was spotted with a capillary on the TLC sheet. A solution of iris butter (1 mg/mL) or the technical mixture of *trans*- and *cis*- α -irone (0.1 mg/mL) in methanol were used as references. The residual mobile phase on the TLC sheet was evaporated after the development of the chromatogram.

For colorization of the irone spots, two different staining agents were used. The first method was the sprinkling of the TLC plate primarily with a 1 wt% vanillin (99.0%, Merck) solution in ethanol followed by a 20 wt% sulfuric acid solution in ethanol. Afterwards, the plate was heated to 110 $^{\circ}\text{C}$ for 10 min. The corresponding irone spot became visible and showed a violet color. The second method was staining with an anisaldehyde/sulfuric acid solution. The agent consisted of 0.25 mL anisaldehyde (98.0%, Merck), 5 mL acetic acid (96.0%, Merck), 43.5 mL methanol, and 2.5 mL sulfuric acid (98.0%, Merck). After sprinkling the TLC plate with this solution, it was heated slowly to 110 $^{\circ}\text{C}$ and developed for 7 min. The irone spot showed a dark violet color.

6.4 Results & discussion

6.4.1 Analytical method development

Before starting the extraction, it was necessary to establish suitable and efficient analysis methods. Due to the fact that irones are volatile and UV/VIS light absorbent compounds, they can be analyzed by GC/FID or HPLC/UV. In order to investigate the content of irones in the extracts both methods can be employed. Also, the identification of irones by TLC and subsequent staining is possible. The development of these methods is described in the following.

6.4.1.1 HPLC

In order to investigate the selectivity of solvent extractions, analysis by HPLC/UV were carried out. HPLC/UV is recommended for solvent extracts, as they contain volatile and non-volatile compounds. The applied HPLC system consisted of two Waters 515 HPLC pumps, Waters 717plus Autosampler and Waters 2487 UV/VIS-detector. The software "Empower 3[®]" was used for the recording and evaluation of the chromatograms. Separation of the compounds was achieved on a Knauer Eurosphere C18-column (100 Å, 250 x 4.6 mm).

6.4.1.1.1 Improvement of compound separation

Different methods for the separation of compounds of iris extracts by HPLC are available in literature. The most common method is a gradient elution with methanol and acidified water at a detection wavelength of 254 nm or 230 nm [21, 39, 42, 61, 73]. For this reason, gradient elution with methanol and acidified water was selected for separation. Furthermore, the detection wavelength was set at 230 nm. The temperature of the column was kept constant at 40 °C. The injection volume was set at a value of 10 µL. The first method was developed by analyzing an ethanol Soxhlet extract of iris rhizomes. Therefore only the composition of the solvents during gradient HPLC was changed. The total flow of the eluent was set at 0.7 mL/min. The separation was started with a solvent composition of 50% acidified water (0.1% formic acid) and 50% methanol. The ratio of methanol was linearly increased up to 100% in 35 min and hold for 10 min. The starting ratio of the solvents was reinstated within 3 min and held for 7 min in order to equilibrate the column. But the separation of the compound, especially the ones with short retention times, was not sufficient enough.

Thus, the ratio of acidified water was increased for the start conditions in order to elongate the elution of the more polar substances. For this reason, the separation was started with an eluent composition of 30% acidified water (0.1% formic acid) and 70% methanol to elute the very polar compounds at higher retention times. The ratio of methanol was linearly increased up to 100% in 35 min and hold for 15 min to remove potential residues from the column. The starting ratio of the solvents was reinstated within 5 min and held for 10 min in order to equilibrate the column. This gradient elution improved not only the separation of the hydrophilic compounds, but also the one of the more hydrophobic compounds. The run time for one analysis is thus 65 min. The next step was to assign the peaks to the compounds present in iris extracts.

6.4.1.1.2 Identification of compounds

Resinoids obtained by Soxhlet extraction of iris rhizomes contain a lot of different compounds like isoflavones, phenolic compounds, irones, and iridals. The identification of these different compounds was carried out in two ways. On the one hand, samples with the pure substance

were analyzed with the previous investigated method. By comparing the retention times of the pure substance with the chromatogram of the extract, a classification of the peaks was done. The procedure was carried out for acetovanillone, irones and myristic acid each with a concentration of 0.4 mg/mL. The assignment of the other peaks was carried out by comparing the chromatograms with literature data [73]. The chromatogram of a Soxhlet extract obtained from iris rhizomes is presented in Figure 6.5.

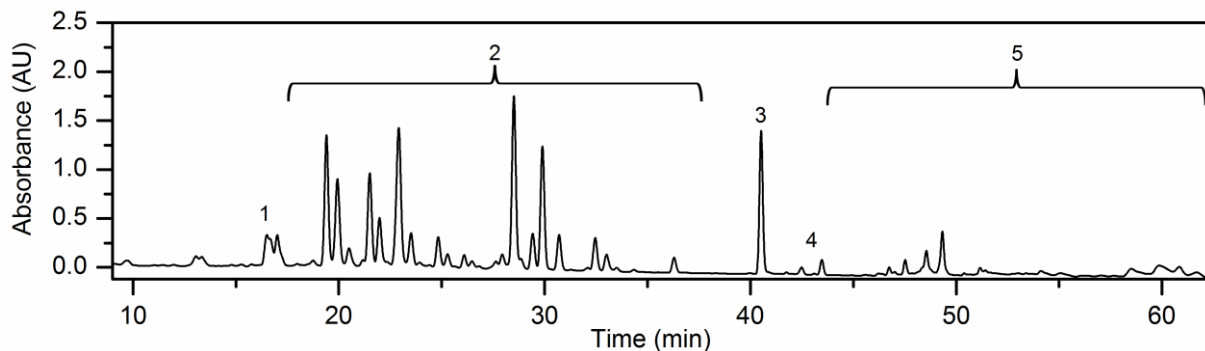


Figure 6.5: HPLC chromatogram of a Soxhlet extract obtained from iris rhizomes. Peak identification: (1) acetovanillone; (2) isoflavones and irone related compounds; (3) α -ionone (IS); (4) irones; (5) iridals and iridal esters;

It can be seen that the resinoid contains a large number of compounds. The retention time of acetovanillone was determined to be 16.5 min. Isoflavones and irone related compounds are eluted at higher retention times, followed by α -ionone and the isomers of irones after 42.5 min. The compound α -ionone cannot be preliminary found in the extract. It was added before analyses as internal standard (IS) (see chapter 6.4.1.1.3). Finally, the iridals and iridal esters are eluted. Myristic acid and other fatty acids cannot be detected with this method, as these compounds show no absorbance at a wavelength of 230 nm.

The assignment of the irone peaks to the different isomers was more complicated. For the identification, solutions of iris butter (10 mg/mL) and a technical irone standard (1 mg/mL) in methanol were analyzed by HPLC/UV. A section of the chromatograms is presented in Figure 6.6. In fact, iris butter contains mainly *cis*- α - and *cis*- γ -irone, whereas the technical irone standard purchased from Sigma-Aldrich contains mainly *cis*- α - and *trans*- α -irone. By comparing both chromatograms, it is possible to identify the different irone isomers.

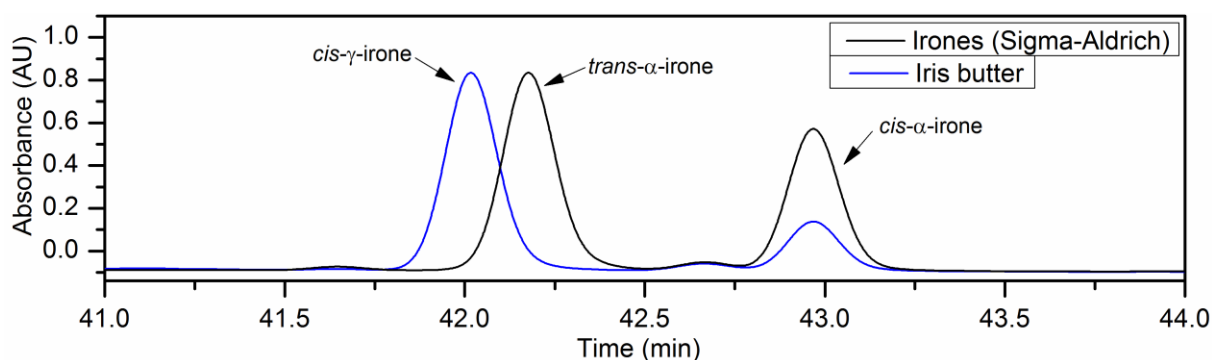


Figure 6.6: Section of HPLC chromatograms of a technical irone mixture (Sigma-Aldrich) and iris butter (Phytogante) with the assignment of the different irone isomers.

As it can be seen, one peak of both samples is exactly overlapping in both chromatograms. This peak can be related to *cis-α-irone*, which is present in iris butter and the irone standard. The retention time of *cis-α-irone* was determined to be 42.98 min. The compound *trans-α-irone*, which is only present in the technical irone sample, has a retention times of 42.20 min, whereas *cis-γ-irone*, which is only contained in iris butter, is eluted at 42.02 min. The other isomers (β -irone and *trans-γ-irone*) present in iris extracts could not be detected. For this reason, only *cis-α-* and *cis-γ-irone* are examined in this thesis.

6.4.1.1.3 Internal standard calibration

Initially, external calibration was used to determine the irone content in the extracts. The standard deviation of the measurements was eventually too high and the results were not consistent enough for an efficient interpretation. For this reason, a new method with internal standard calibration was established. Many articles in literature can be found where irones are quantified by internal standard calibration.

A compound has to fulfill different requirements for its use as internal standard. The substance may not be present in the test sample at the beginning. It should be chemically stable and inert to the solvent and other compounds in the test sample. A suitable internal standard should also be a pure, clearly defined compound with similar properties with respect to the analyte. Another important requirement for an appropriate substance is that the peak should not overlap other peaks in the chromatogram [74, 75]. The response factor between the analyte and internal standard compound can be used to estimate the suitability of a certain compound for internal standard calibration. The response factor K can be calculated by transformation of equation (6.2). The value of the response factor should be ideally 1.

The most common compound reported in literature is *trans-anethole* [45, 76]. However, this compound is normally used as internal standard in GC analyses. Nevertheless, the suitability for HPLC analyses was also investigated. To this purpose, a sample with 0.9 mg/mL irones

and 0.8 mg/mL *trans*-anethole was analyzed by HPLC/UV. Most of the requirements are fulfilled for *trans*-anethole. The retention time of *trans*-anethole was determined to be 39.71 min and no overlap with other peaks was observed. But the determined response factor is only 0.36, which makes *trans*-anethole not suitable for internal standard calibration of irones [77]. This can be a consequence of the large structural differences of *trans*-anethole and irones (see Figure 6.7).

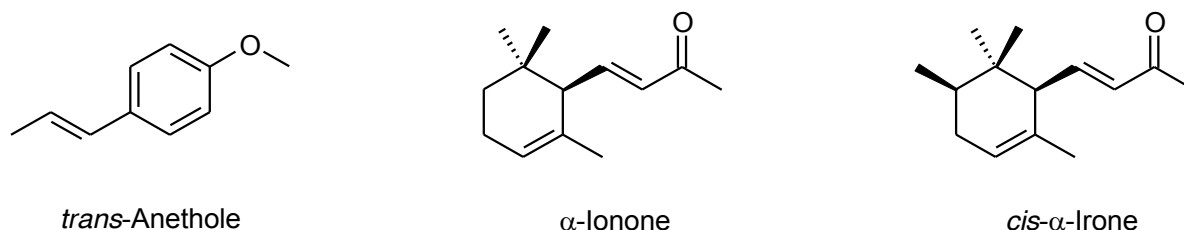


Figure 6.7: Chemical structures of *cis*- α -irone and the potential internal standard compounds *trans*-anethole and α -ionone.

The compound α -ionone can be an alternative for internal standard calibration of irones [2]. The chemical structures of *cis*- α -irone and α -ionone are very similar to each other. Irones possess one methyl group more than ionones, which can be seen in Figure 6.7. However, in literature it is reported that is present in iris rhizomes in small amounts [16]. For this reason, a Soxhlet extract of iris rhizomes was analyzed, but α -ionone was not detected. By adding α -ionone to the sample, the retention time of α -ionone was determined to be 39.73 min and no overlap with other peaks was observed. Thus, all requirements for internal standard calibration are fulfilled for α -ionone. Nevertheless, the response factor has to be determined preliminary.

First measurements with a one-point-calibration showed that the response factor of irones and α -ionone is around one. But a meaningful determination of the response factor is necessary. To this purpose, two stock solutions of irones (Sigma-Aldrich) in methanol were prepared. These primary stock solutions were diluted to concentrations between 0.25 and 4.0 mg/mL. To 2 mL of each sample, 2 mL of a 2 mg/mL solution of the internal standard α -ionone in methanol were added. These solutions were furthermore diluted by the factor 1/5 and subsequently measured by HPLC/UV. The final concentrations of irones varied between 0.025 and 0.4 mg/mL. The concentration of α -ionone was in all samples constant at 0.2 mg/mL.

The response factor of α -ionone to irones is determined by plotting the ratio of the irone peak area (sum of *trans*- α - and *cis*- α -irone peak area) and α -ionone area against the ratio of irone concentration and α -ionone concentration. Figure 6.8 shows that a linear trend can be observed. In this case, the slope of the linear function represents the response factor, which is $K = 1.07$.

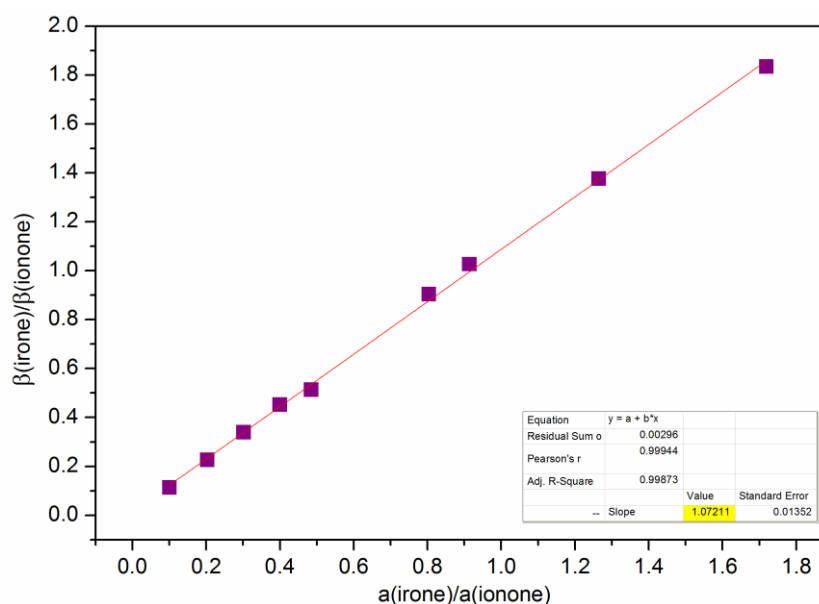


Figure 6.8: Determination of the response factor of irones with α -ionone for internal standard calibration by HPLC/UV. The slope of the graph indicates the response factor (yellow block). β correlates to the mass concentration of irones and α -ionone and a is the determined peak area of the compounds.

For the analysis of further extracts, α -ionone was added to every sample to reach a concentration of 0.2 mg/mL in the analysis sample. Finally, it is possible to determine the concentration of irones in the extracts with α -ionone and the corresponding response factor by internal standard calibration using HPLC/UV.

6.4.1.2 GC

Analyses of iris rhizome extracts were also carried out on a Hewlett Packard HP 6890 Series GC system equipped with a flame ionization detector (GC/FID). Due to the fact that irones are volatile, an alternative method to quantify irones by GC/FID was investigated. This method is also suitable to determine and identify fatty acids, which could not be detected by HPLC/UV.

6.4.1.2.1 Improvement of compound separation

Different methods for compound separation of iris extracts by capillary gas chromatography are available in literature. Polar capillaries (carbowax polyethylene glycol) are the most common columns used for the analysis of essential oils [78, 79]. Also columns with a cyclic oligosaccharide (mainly cyclodextrins) film can be used for enantioselective analyses [1]. Contrary to these approaches, a nonpolar capillary column was used for separation in this case.

In detail, the nonpolar HP-5 (5% phenyl- and 95% methyl-siloxane) capillary column (30 m x 0.32 mm i.d., 0.25 μ m film thickness) was used for separation. Analyses were performed with a constant helium flow of 1.0 mL/min. The first investigated method was based on a procedure reported in literature, where iris extracts are analyzed by GC/FID with a nonpolar column [2]. For this reason, the split/splitless injector was held at 275 °C and the temperature of the FID was 250 °C. A HP 6890 Autosampler was used to inject 1 μ L respectively 5 μ L of the sample in split mode using a split ratio of 1:10. The temperature of the oven was initially held at 70 °C for 3.2 min and then increased to 220 °C at 8 °C/min, followed by a further increase to 295 °C at 16 °C/min. This temperature was held for 10 min. Analyses were carried out with iris butter (10 mg/mL) dissolved in ethanol.

It was observed that the separation of the compounds, especially of the irone isomers, was not satisfactory with this method. Another problem of the described procedure was the large deviation of peak areas between the single measurements. This was a result of the injection volume of 5 μ L, which was too high for the used liner (inlet). This led to the contamination of some parts of the GC equipment. "GC calculators" of the company Agilent Technologies is a helpful tool to calculate the maximum injection volume of a sample dissolved in a certain solvent for a given liner (inlet) [80]. The previously described problem can be avoided with this program. It was found out that the maximum injection volume for samples which are dissolved in ethanol or methanol must not exceed 1 μ L.

Following these results, a second method was established. The injection volume was always 1 μ L with a split ratio of 1:10. The temperatures of the injector and detector were held at 275 °C. The initial temperature of the oven was decreased to 50 °C, as this temperature should be 20 °C lower than the boiling point of the sample solvent. The initial temperature of the oven was kept constant for 3 min, then increased to 300 °C at 10 °C/min and held for 10 min. This procedure improved the separation of the compounds. The next step was to assign the peaks to the compounds present in iris extracts.

6.4.1.2.2 Identification of compounds

Resinoids obtained by Soxhlet extraction of iris rhizomes contain a lot of different volatile compounds like fatty acids, phenolic compounds, and irones. The identification of these different compounds was carried out on the analogy of the HPLC method (Chapter 6.4.1.1.2). The retention times of the pure substances (acetovanillone, irones and myristic acid) with a concentration of 2 mg/mL were compared with the chromatogram of the extract. The assignment of other peaks was carried out by comparing the GC chromatograms with literature data [73]. The chromatogram of a Soxhlet extract obtained from iris rhizomes is presented in Figure 6.9.

It can be seen that the resinoid contains a large number of volatile compounds. The first eluted compound is α -ionone, which is not contained preliminary in the extract. It was added

before analyses as internal standard (IS). Irones are eluted at retention times around 15 min, followed by myristic acid at 17.23 min. Finally, other fatty acids and compounds are eluted. Acetovanillone could not be detected, probably due to its low concentration.

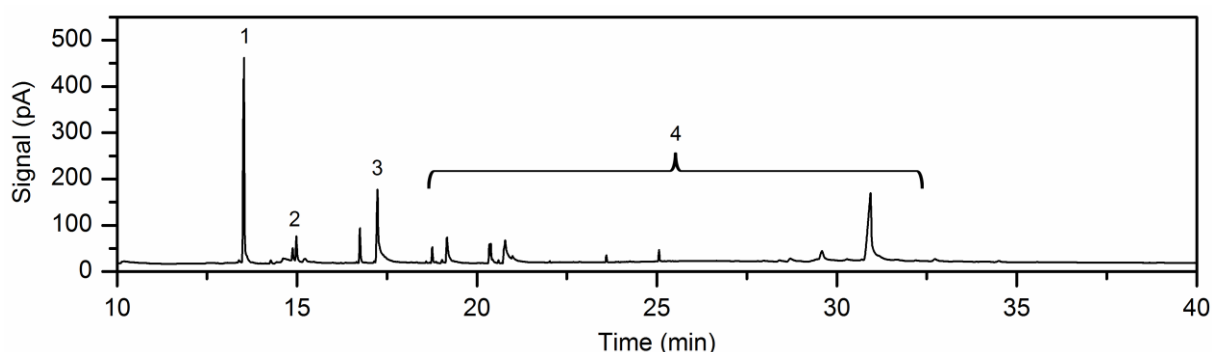


Figure 6.9: GC chromatogram of a Soxhlet extract obtained from iris rhizomes. Peak identification: (1) α -ionone (IS); (2) irones; (3) myristic acid (IS); (4) other fatty acids and compounds;

The assignment of the irone peaks was carried out on the analogy of the procedure of HPLC analyses. For identification, solutions of iris butter (10 mg/mL) and a technical irone standard (2 mg/mL) in methanol were analyzed by GC/FID. A section of the chromatograms is presented in Figure 6.10. In fact, iris butter contains mainly *cis*- α - and *cis*- γ -irone, whereas the technical irone standard purchased from Sigma-Aldrich contains mainly *cis*- α - and *trans*- α -irone. By comparing both chromatograms, it is possible to identify the different irone isomers.

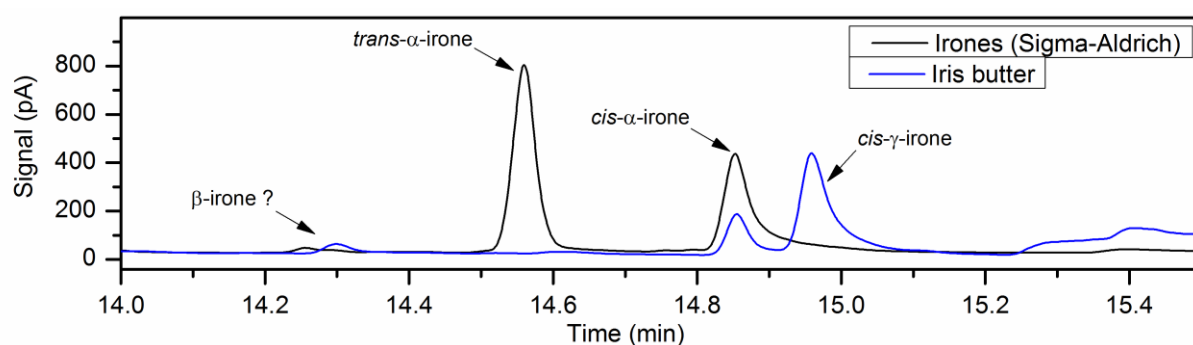


Figure 6.10: Section of GC chromatograms of a technical irone mixture and iris butter with the assignment of different irone isomers.

As it can be seen, one peak of both samples is exactly overlapping in both chromatograms. This peak can be related to *cis*- α -irone, which is present in iris butter and the irone standard. The retention time of *cis*- α -irone was determined to be 14.86 min. The compound *trans*- α -irone, which is only present in the technical irone sample, has a retention time of 14.56 min. However, *cis*- γ -irone, which is only contained in iris butter, is eluted at 14.97 min. The isomer β -irone is probably present at a retention time of 14.25 min, whereas *trans*- γ -irone is not detectable. In this thesis only *cis*- α - and *cis*- γ -irone are examined.

6.4.1.2.3 Internal standard calibration

The determination of the irone content was executed with internal standard calibration from the beginning. As α -ionone was proved to be a suitable internal standard in HPLC analyses, this compound was also investigated for GC analyses. First of all, α -ionone was added to a Soxhlet extract of iris rhizomes and subsequently analyzed by GC/FID. The retention time of α -ionone was determined to be 13.49 min and no overlap with other peaks was observed. All requirements for internal standard calibration are fulfilled for α -ionone.

The next step was to determine the response factor of irones and α -ionone. To this purpose, two stock solutions of irones (Sigma-Aldrich) in methanol were prepared. These primary stock solutions were diluted to concentrations between 1.0 and 4.0 mg/mL. 2 mL of a 2 mg/mL solution of the internal standard α -ionone in methanol were added to 2 mL of each irone sample. The final concentrations of irones varied between 0.5 and 2.0 mg/mL. The concentration of α -ionone was in all samples constant at 1.0 mg/mL.

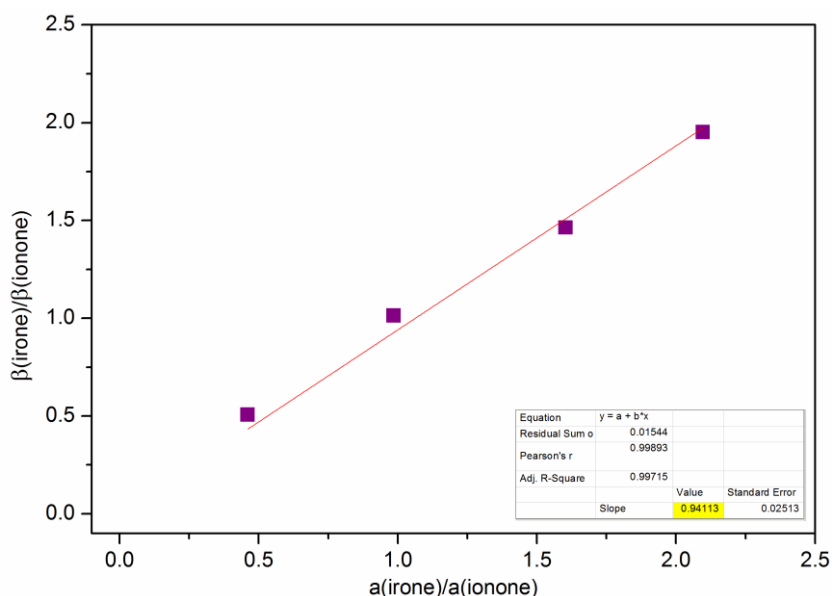


Figure 6.11: Determination of the response factor of irones with α -ionone for internal standard calibration by GC/FID. The slope of the graph indicates the response factor (yellow block). β correlates to the mass concentration of irones and α -ionone and a is the determined peak area of the compounds.

The response factor of α -ionone to irones is determined by plotting the ratio of the irone peak area (sum of *trans*- α - and *cis*- α -irone peak area) and α -ionone area against the ratio of irone concentration and α -ionone concentration. Figure 6.11 shows that a linear trend can be observed. In this case, the slope of the linear function represents the response factor, which is $K = 0.94$. For the analysis of further extracts, α -ionone was added to every sample to reach a concentration of 1.0 mg/mL in the analysis sample. Finally, it is possible to determine the concentration of irones in extracts with α -ionone and the corresponding response factor

by internal standard calibration using GC/FID. Furthermore, the same sample can be diluted to a factor of 1/5 and subsequently analyzed by HPLC/UV. For this reason, no separate preparation of HPLC samples is necessary.

6.4.1.2.4 Problems

During the analyses of the extract samples a problem occurred. In detail, the 5 μ L-syringe of the GC-Autosampler was damaged several times during the analyses of Soxhlet extracts from iris rhizomes. The thin plunger of the syringe got stuck during the injection and was bent over. This problem was further investigated and it was found out that some sticky compounds in the iris extract deposit at the inner side of the syringe. The sticky film could not be removed by purging the syringe several times with ethanol or methanol. For this reason, Soxhlet extracts were not further analyzed by GC/FID in order to avoid damaging additional syringes.

6.4.1.3 TLC

Thin-layer chromatography (TLC) and subsequent staining was used as a fast screening method to examine the presence of irones in the extract. This method is very easy to carry out and was in particular used to determine rapidly the presence of irones in the extracts. Furthermore, first predictions of the irone content could be made. The method is already described in literature [15, 16].

First of all, 1 μ L of a reference substance was spotted with a capillary on the TLC sheet. It was determined that a technical mixture of *trans*- and *cis*- α -irone in methanol with a concentration of 0.1 mg/mL is the most suitable reference. Afterwards, 2 μ L of the sample to be analyze, are spotted next to the reference spot. This spotted volume is suitable for extract solutions which were obtained by extraction of 1 g of iris rhizome with 5 mL of solvent. The TLC sheet was developed in a chromatography chamber with a solution of toluene and ethyl acetate (97/3, v/v) as mobile phase. The separation was stopped when the solvent front climbed approximately 5 cm. The residual mobile phase on the TLC sheet was evaporated after the development of the chromatogram.

Furthermore, two different staining agents were examined the coloring of the irone spot. The first method was the sprinkling of the TLC plate primarily with a 1 wt% vanillin solution in ethanol, followed by a 20 wt% sulfuric acid solution in ethanol. In the second method an anisaldehyde/sulfuric acid solution was used for staining. The plates were always heated to 110 °C for 10 min revealing violet irone spots for both staining agents. The anisaldehyde/sulfuric acid solution was preferred the coloring, as the irone spot has a darker violet color compared to the one with the vanillin reagent.

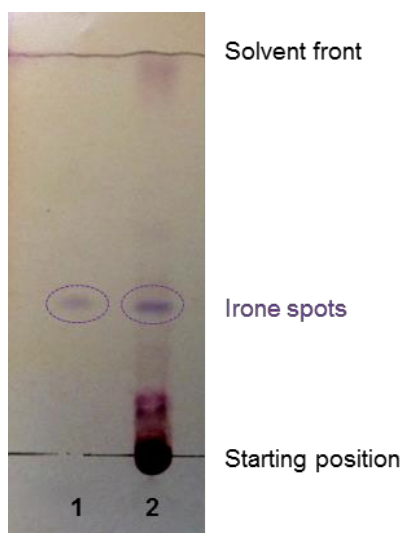


Figure 6.12: TLC-sheet of a technical irone mixture (1) and methanol extract of iris rhizomes (2) stained with an anisaldehyde/ sulfuric acid solution. The violet spot corresponds to irones.

Figure 6.12 presents a TLC-sheet, where a technical irone mixture (1) and methanol extract of iris rhizomes (2) was separated and subsequently stained with an anisaldehyde/sulfuric acid solution. The violet spot corresponds to irones. To summarize, this method can be used on the one hand to determine the presence of irones in the extract. On the other hand, a rough quantitative prediction can be made if defined volumes of the extract and reference solutions are applied on the TLC-sheet. The intensity of the spot is correlated to the irone concentration. As a result, a first assessment of the extraction efficiency can be made.

6.4.2 Characterization of iris rhizomes

Iris rhizomes are a natural product and the composition is subjected to large variations. For this reason a characterization of the used rhizomes is important, because. The deviations can be due to seasonal variations, environmental influences, species, and growing origin. Also large fluctuations in the individuals of the same population have been reported [33, 46]. Investigated parameters of the rhizomes are the residual moisture, the actual and the maximum irone content.

6.4.2.1 Residual moisture

Three different methods were compared for the determination of the residual moisture of the ground iris rhizomes. The investigated methods are i) drying in a compartment drier at 45 °C, ii) at 105 °C, and iii) lyophilization. The experiments showed that there is a large deviation between the different methods. Actually, some of the experiments influence the irone content in the rhizomes. All experiments were carried out with 3-year-old ground iris germanica rhizomes (Iris 2011).

The first investigated method was lyophilization, also called freeze drying. The functional principle is based on the sublimation of crystalline water at reduced pressure. To this purpose, frozen iris rhizome powder was dried under vacuum for 17 h. After the experiment, the smell of irones was present in the lyophilization unit. This observation indicates the volatilization of irones during the drying procedure. For this reason, the method was not further investigated.

The second method was the investigation of the residual moisture of a drug according to the Pharmacopoea Europaea (Ph. Eur.) [72]. To this purpose, iris rhizome powder was put in a compartment drier at 105 °C for 2 h. Subsequently, the mass loss was monitored and was calculated to be approximately 8% of the initial mass. Furthermore, the rhizomes were analyzed after this drying method. It was found out that 55% of the total irone content gets lost during this drying procedure. Thus, this method is also not suitable to determine the residual moisture.

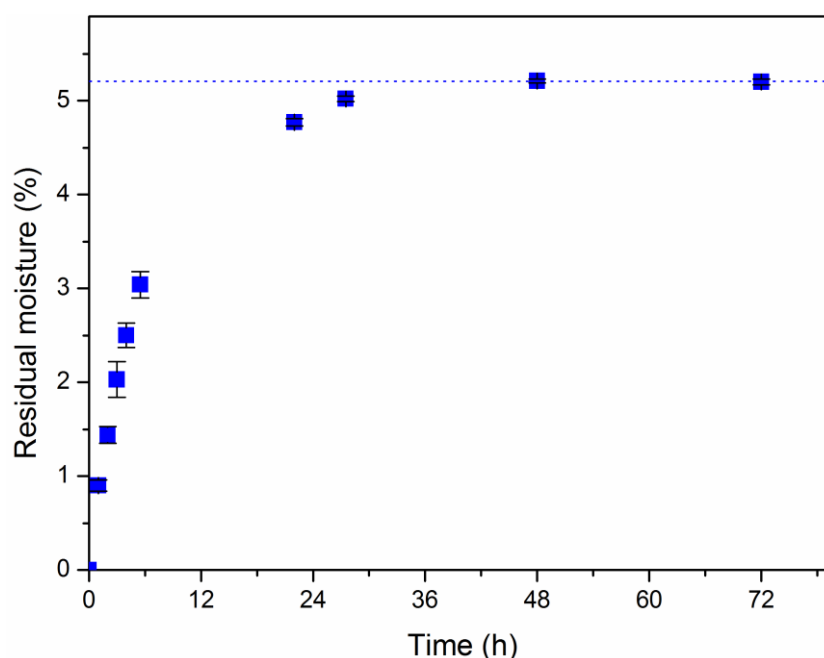


Figure 6.13: Investigation of the residual moisture of *Iris* 2011 rhizomes. The values were determined by the mass loss of grinded rhizomes in a compartment drier at 45 °C. A maximum value of 5.20% is reached after 48 h.

For this reason, another procedure with mild drying conditions had to be found. The third investigated method was to dry the iris rhizome powder in a compartment drier at 45 °C and monitor the weight loss of the samples over time. The mass of the rhizomes decreases significantly in the first six hours of drying. After approximately 48 h a maximum value is reached (Figure 6.13). This mass loss related to the initial mass is considered to be the residual moisture of the rhizomes. It is calculated to be $5.20 \pm 0.03\%$ for *Iris* 2011 rhizomes. In addition, the rhizome powder was analyzed after this drying method and it was proved that

the irone content in the rhizomes is not influenced significantly. Thus, this is the best method to investigate the residual moisture of iris rhizomes. The experiments were also conducted for the other iris rhizome samples. The corresponding storage times are presented in brackets. The residual moisture was determined to be $6.63 \pm 0.03\%$ for Iris 2015.2 (2 years), $6.45 \pm 0.08\%$ for Iris 2015.1 (1 year) and $4.19 \pm 0.02\%$ for Iris 2013 (9 year). It can be noticed that the residual moisture decreases with increasing storage time.

Apart from that, the volatilization of irones (technical mixture of *cis*- and *trans*- α -irone from Sigma-Aldrich) was investigated in the compartment drier at $45\text{ }^{\circ}\text{C}$. For the sake of comparison, samples with the same mass of water (millipore) were put in the compartment drier. Figure 6.14 presents the time-dependent mass loss of water and irones at $45\text{ }^{\circ}\text{C}$.

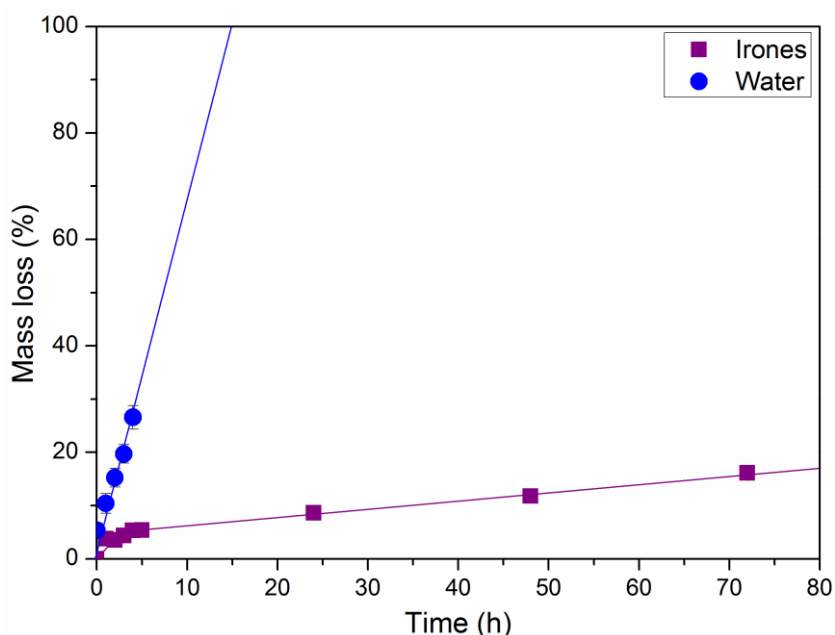


Figure 6.14: Time-dependent mass loss of water (millipore) and irones (technical mixture of *cis*- and *trans*- α -irone from Sigma-Aldrich) in the compartment drier at $45\text{ }^{\circ}\text{C}$.

It can be determined that water evaporates much faster than irones. In detail, water is completely volatilized after approximately 14 h, whereas only 16.7% of irones are evaporated after 72 h at $45\text{ }^{\circ}\text{C}$ in the compartment drier. Besides, the stability of irones was investigated. To this purpose, the samples were analyzed before and after this experiment by GC/FID. The total ratio of the irone peaks areas in the chromatogram decreases from 97% before drying to 67% after 72 h of drying at $45\text{ }^{\circ}\text{C}$. This is correlated to a decomposition of irones, which is also in accordance with the appearance of several other peaks in the GC chromatogram. Solely the decomposition of pure irones is observed, this does not imply the same behavior in the rhizome, as no matrix effect is taken into account with these measurements.

Nevertheless, the determination of the residual moisture or the drying of iris rhizomes can be carried out in a compartment drier at 45 °C for several hours. This is a soft method which does not influence the content or the stability of irones in the rhizomes.

6.4.2.2 Actual irone content

In literature, different methods are described to investigate the actual irone content of iris rhizomes. The official method after ISO 18054:2004 prescribes the extraction of iris rhizomes by specific hydro distillation and subsequent quantification of irones in the iris butter by GC [76]. The drawback of this method is that 0.9 g of iris butter is necessary for analysis. This correlates to an approximate amount of 500 g iris rhizomes. It is also a very time consuming method, which includes a 36 h lasting hydro distillation step. An alternative method is the quantification of irones in rhizomes by headspace solid-phase micro-extraction (HS-SPME-GC) [2]. However, these methods were not feasible. For this reason, solid-liquid extractions with subsequent quantification of irones by HPLC or GC were carried out. This method is already known in literature, where Soxhlet extraction with ethanol for 6 h is applied [2]. Solid-liquid extractions of iris rhizomes with an appropriate solvent are further investigated in this section.

First of all, preliminary experiments were carried out in order to find an appropriate solvent for the extraction of irones. To this purpose, simple macerations of iris rhizomes with different solvents were performed. The extract solutions were subsequently analyzed by TLC. Consequently, the extraction efficiency of different solvents is screened. The investigated solvents were: methanol, ethanol (99.9%), ethanol (technical grade, 96%), ethyl acetate, a mixture of ethyl acetate and ethanol (70/30 v/v), acetone, methyl *tert*-butyl ether, diethyl ether, hexane, water, dichloromethane, isopropanol, toluene, 1 M sodium hydroxide and 1 wt% formic acid solution. After 18 h, a defined volume of each extract solution was spotted on a TLC sheet. Separation of the extract was achieved in a chromatography chamber with toluene/ethyl acetate (97/3 v/v) as mobile phase. The separated compound spots were stained with an anisaldehyde/sulfuric acid solution. The irone spot was colored violet. As a defined volume of each extract solution was used, the color intensity of the irone spot is correlated to the irone concentration. The darker the spot, the higher is the extracted irone concentration. Generally it is observed that strong polar or strong nonpolar solvents like water or hexane are not able to extract high amounts of irones. The most suitable solvents for irone extraction were evaluated to be methanol, ethanol, ethyl acetate, a mixture of ethyl acetate and ethanol (70/30 v/v), acetone, and methyl *tert*-butyl ether.

In order to investigate the best solvent for the extraction of irones, Soxhlet extractions of fine ground iris rhizomes were carried out for 6 h. Therefore, the most promising solvents of the maceration experiments were used. For all experiments, Iris 2011 rhizomes were used. After extraction, the extract solutions were analyzed by HPLC in order to determine the irone

concentration. Analyses of Soxhlet extracts by GC were stopped, as the samples induced damage of the Autosampler syringe (see Chapter 6.4.1.2.4). The concentration of irones in iris rhizomes is given in mg/kg, which is correlated to the mass of irones in mg per 1 kg of dry rhizomes. In addition, the total mass extraction yield was also investigated by weighing the rhizomes before and after the extraction.

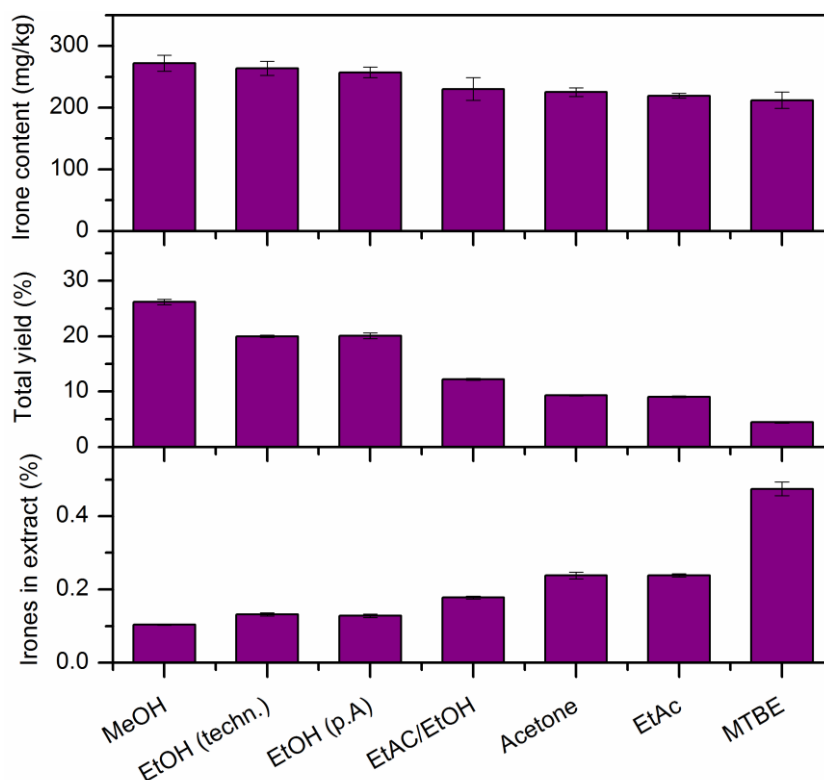


Figure 6.15: Soxhlet extractions of *Iris germanica* L. rhizomes with different solvents. Comparison of the iron content in the rhizomes, total mass extraction yield and the content of irones in the extract for methanol (MeOH), ethanol (EtOH), acetone, ethyl acetate (EtAc), a mixture of EtAc/EtOH (70/30 v/v), and methyl *tert*-butyl ether (MTBE).

The investigated iron content in the rhizomes, the total mass extraction yield and the content of irones in the extract are presented in Figure 6.15 for methanol, ethanol, acetone, ethyl acetate, a mixture of EtAc/EtOH (70/30 v/v) and methyl *tert*-butyl ether. The given iron concentration is the sum of the isomers *cis*- α - and *cis*- γ -irone. Other isomers are not considered, as they were not detectable.

It can be noticed that protic solvents with a medium polarity like methanol and ethanol are the most suitable for the exhaustive extraction of irones. Whereby, aprotic solvents with high (ethyl acetate, acetone) or low (methyl *tert*-butyl ether) polarity are not suitable. The highest amount of irones can be extracted with methanol, which makes it suitable to determine the actual total iron content in iris rhizomes. This is in contrast to the method described in the literature, where ethanol (96%) is used for this purpose [2]. Anyway, the maximum iron (*cis*- α - & *cis*- γ -irone) content in Iris 2011 rhizomes was determined by Soxhlet extraction with

methanol as solvent and was equal to 272 ± 13 mg irones /kg of dry mass. The highest mass extraction yield of 26.2% can also be obtained with methanol. The high mass extraction yield is due to the extraction of other compounds like isoflavones, phenolic compounds, and probably resins, tanning agents, and waxes. The iron content of a methanol extract is very low, with a value of 0.1%. A higher amount of irones in the extract can be obtained with MTBE. Thus, the extraction of by-products is lower with MTBE compared to the other solvents. In comparison, the amount of irones in conventional iris butter is approximately 10%. Nevertheless, these extractions were only carried out in order to estimate the maximum iron content in iris rhizomes.

Soxhlet extractions of the other iris rhizome samples were also performed with methanol in order to determine the actual iron content. Table 6.1 summarizes the determined values of the actual iron content and the isomer distribution in iris rhizomes of different species and varying storage period.

Table 6.3: Overview of the actual iron content and isomer distribution in iris rhizomes of different species and varying storage times.

Name	Species	Storage time	Actual iron content / (mg/kg)	Distribution of isomers / %	
				cis- α -irone	cis- γ -irone
Iris 2011	<i>Iris germanica</i>	3 years ¹	272 ± 13	69.2	30.8
Iris2015.2	<i>Iris germanica</i>	2 years	381 ± 10	66.8	33.2
Iris2015.1	<i>Iris germanica</i>	1 year	374 ± 12	65.5	34.5
Iris 2013 [77]	<i>Iris pallida</i>	9 years	639 ± 40	37.2	62.8

It can be noticed that the iron content in *Iris germanica* rhizomes depends on the storage time. The amount of irones slightly increases from 374 mg/kg (1 year) to 381 mg/kg (2 years). Whereby, the content decreases again with a longer storage period. The rhizome parts (3 years) were analyzed after an approximate storage time of 6 years. The iron content decreases further to 253 mg/kg after 7 years of storage, which indicates a natural decomposition of irones during storage after several years. These values are in accordance to literature data, where iron contents around 300 mg/kg are reported [2]. The concentration of irones in *Iris pallida* rhizomes is 639 mg/kg and thus significantly higher than in *Iris germanica*. The distribution of the iron isomers also differs in the various iris species. *Iris pallida* rhizomes contain 37.2% cis- α -irone and 62.8% cis- γ -irone [77]. The isomer

¹ Storage time is related to the value which was current at the delivery date. The real storage time at the date of analysis was approximately 6 years.

distribution is reversed for *Iris germanica*, a fact already known [1]. It can also be noticed that this contribution in *Iris germanica* slightly changes with increasing storage time. After several years the formation of *cis*- α -irone is predominant.

Apart from that, the variation of the irone content in single iris rhizomes was investigated. To this purpose, five different *Iris pallida* rhizome pieces were partly ground into a fine powder and subsequently extracted. Afterwards, the extracts were analyzed by GC/FID. Figure 6.16 shows the external appearance of different single iris rhizomes and the corresponding total irone peak area determined by GC/FID.

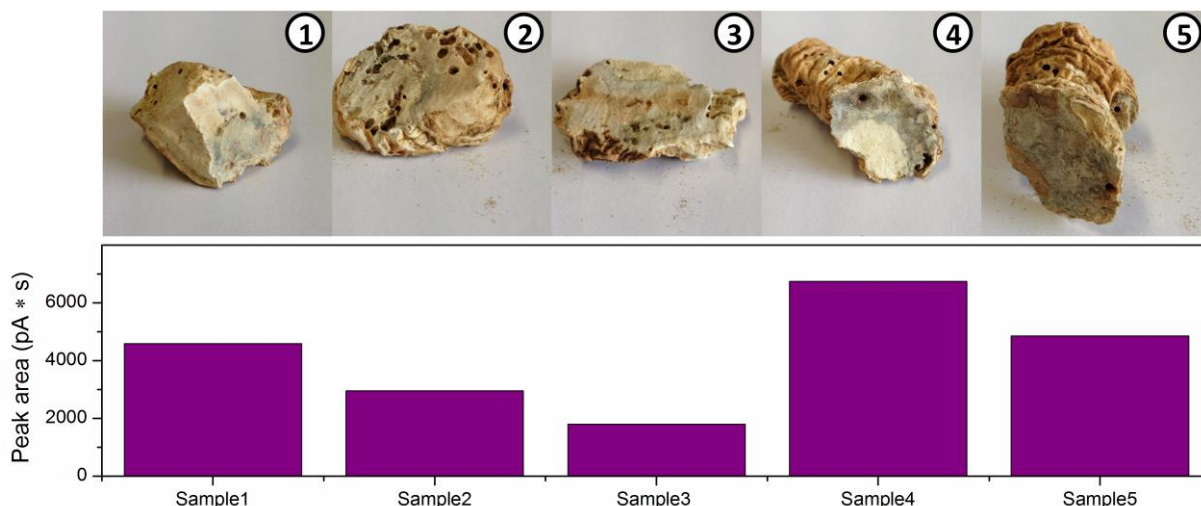


Figure 6.16: External appearance of different single iris rhizomes and the corresponding total irone peak area determined by GC/FID.

It was observed that the irone content varies in a large range in the different rhizome pieces with a standard deviation of 31%. The pictures of the single rhizomes show that they are of minor quality. Flour beetles are responsible for the small holes that can be seen in the rhizomes. Also dark colored parts are visible, which indicate the presence of a mold fungus in the rhizomes. Nevertheless, by comparing the external appearance with the corresponding irone content of the rhizomes it can be seen that rhizomes with a larger dark area possess a higher content of irones. For this reason, it can be assumed that the scruffy parts enhance the formation of irones during storage. This may be the reason why artificial oxidation processes with fungus [51], bacteria [45, 48] or enzymes [50] are suitable to enhance the formation of irones in iris rhizomes. For this reason, it is always important to produce a big composite sample of iris rhizomes in order to compare the results.

6.4.2.3 Maximum irone content

In order to investigate the maximum possible irone content, artificial oxidation of the iris rhizomes was carried out using the method of Ehret *et al.* [52]. To this purpose, iris rhizomes were oxidized by aqueous sodium nitrite solutions (NaNO_2) at 30 °C for 48 h. Figure 6.17

presents the irone content of 1, 2 and 3 years stored *Iris germanica* rhizomes before and after the artificial oxidation by sodium nitrite.

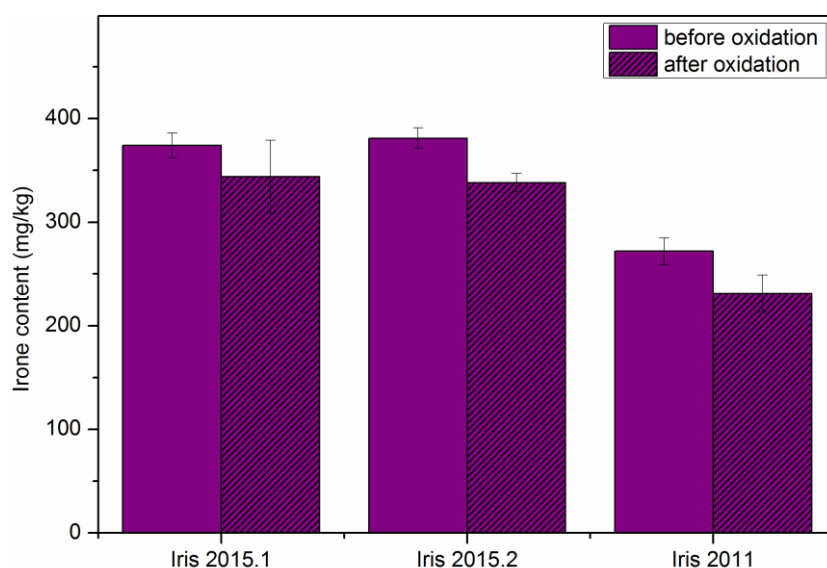


Figure 6.17: Irone content of 1 year (Iris 2015.1), 2 years (Iris 2015.2) and 3 years (Iris 2011) stored *Iris germanica* rhizomes before and after the artificial oxidation by sodium nitrite.

It can be noticed that the irone content in the rhizomes decreases after the oxidation process for every sample. This indicates an oxidative degradation of irones during the experiments. This behavior is very probable as the irone content is already very high before the artificial oxidation process. For that reason, the oxidation of aged iris rhizomes by sodium nitrite is too powerful and not applicable to determine the maximum irone content. Presumably, this method is only suitable for the oxidation of fresh iris rhizomes

6.4.2.4 Summary

Different characteristic parameters of iris rhizomes were determined in the previous chapters. The results are summarized in Table 6.4. It was found that the drying of iris rhizomes in a compartment drier at 45 °C for several hours is a suitable method to determine the residual moisture. Other methods led to a decomposition and volatilization of irones. The residual moisture was determined to be 6.63% for rhizomes stored 1 year. The moisture decreases with increasing storage time. In addition, Soxhlet extractions were carried out for 6 h with different solvents in order to investigate the total irone content in the rhizomes. Methanol was identified to be a suitable solvent to extract exhaustively irones. It was noticed that the irone content increases with increasing storage time. However, after several years, a natural decomposition of irones occurs. The concentration of irones in *Iris pallida* rhizomes is significantly higher than in *Iris germanica*.

Table 6.4: Summary of the examined characteristic parameters of iris rhizomes from different species and varying storage time.

Name	Species	Storage time	Residual moisture / %	Actual irone content / (mg/kg)	Maximum irone content / (mg/kg)
Iris 2011	<i>Iris germanica</i>	3 years ²	5.20	272 ± 13	-
Iris2015.2	<i>Iris germanica</i>	2 years	6.45	381 ± 10	-
Iris2015.1	<i>Iris germanica</i>	1 year	6.63	374 ± 12	-
Iris 2013	<i>Iris pallida</i>	9 years	4.19	639 ± 40	-

In addition, it was attempted to investigate the maximum possible irone content by artificial oxidation of iris rhizomes with aqueous sodium nitrite solutions. However, it was found that the irone content in the rhizomes decreases during the oxidation process. This indicates an oxidative degradation of irones during the experiment. This behavior is very probable as the irone content is already very high before the artificial oxidation process. For this reason, the oxidation of aged iris rhizomes by sodium nitrite was not applicable to determine the maximum irone content.

6.4.3 Ultrasound-assisted extraction

An alternative method to extract irones from iris rhizomes is ultrasound-assisted extraction. This procedure can enhance the extraction efficiency and also reduce extraction time by breaking the plant cells [81]. To this purpose, extractions of iris rhizomes were carried out with methanol, hexane, and 2-methyltetrahydrofuran (MeTHF) in an ultrasonic bath. These solvents were selected as methanol was proven to be the best solvent for exhaustive irone extraction and hexane is used in literature to obtain the iris concrete [5]. MeTHF was chosen as it was recently considered to be a green alternative for the petroleum-based *n*-hexane in extraction processes. MeTHF is a biodegradable and plant derived solvent. It is produced by hydrogenation of products obtained from carbohydrate fraction of hemicellulose from various feedstocks. This solvent fulfills the requirements of several principles of green chemistry and of sustainable and green extraction. For this reason, the extraction efficiency and selectivity of MeTHF for ultrasound-assisted extraction is determined.

Figure 6.18 shows the HPLC chromatograms and corresponding irone yields of the ultrasound-assisted solvent extraction of iris rhizomes with hexane, MeTHF, and methanol. It

² Storage time is related to the value which was current at the delivery date. The real storage time at the date of analysis was approximately 6 years.

can be noticed that methanol extracts the highest amount of irones with 168.8 mg/kg. But the extraction is not exhaustive, as 272 mg/kg of irones are present in the rhizomes. This corresponds to an extraction efficiency of 62%. For exhaustive extraction it may be necessary to replace several times the extract solution with fresh solvent to regulate the equilibrium between irones and solvent. For example, in Soxhlet extractions, the rhizomes are extracted about 100 times with fresh solvent. The chromatogram of the methanol extract also shows that a lot of by-products, like isoflavones or acetovanillone, are also extracted. The irone content in the extract is very low, with a value of 0.13%. Thus, ultrasound-assisted extraction is not suitable to recover exhaustively irones from iris rhizomes.

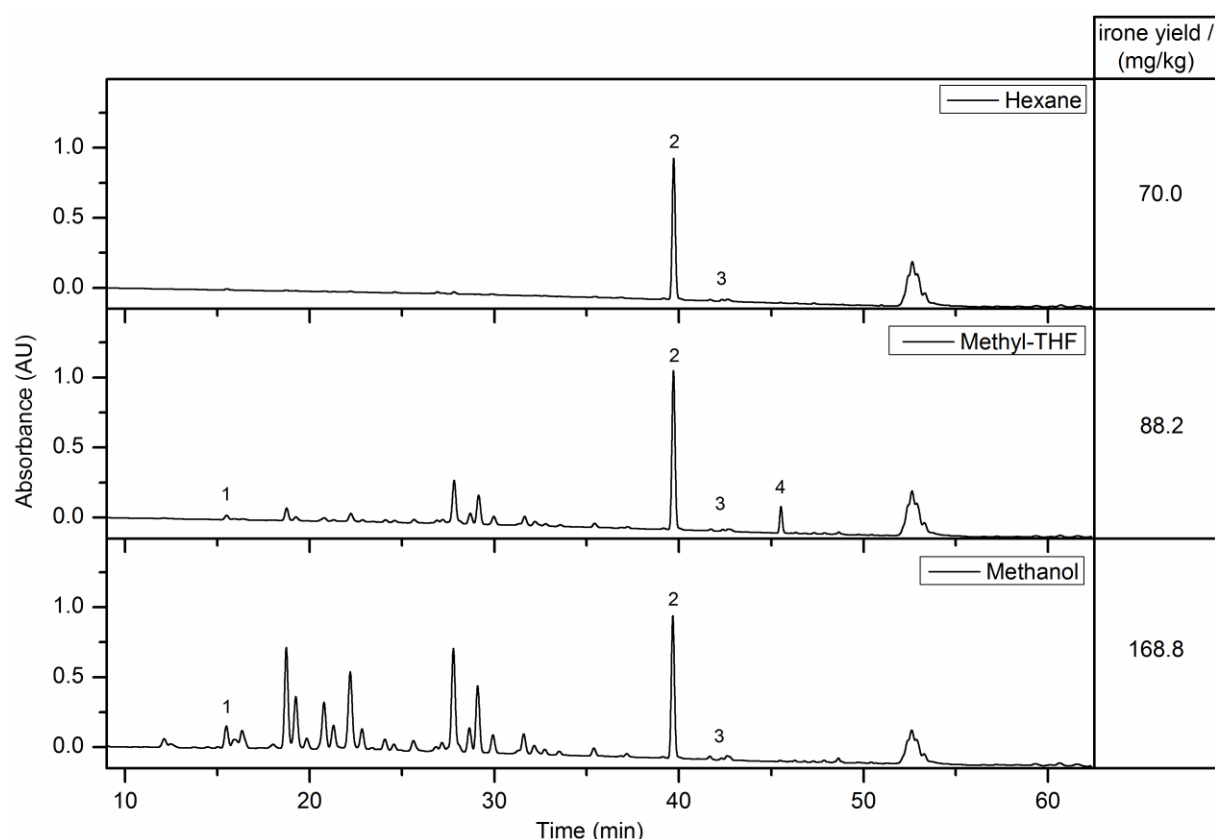


Figure 6.18: HPLC chromatograms and corresponding irone yields of the ultrasound-assisted solvent extraction of iris rhizomes with hexane, methyl-THF, and methanol. Peak identification: (1) acetovanillone; (2) α -ionone (IS); (3) irones (*cis*- α - and *cis*- γ -irone); (4) butylated hydroxytoluene (BHT);

Nevertheless, a comparison between the investigated solvent can be made. In detail, hexane and MeTHF only extract about half the amount of irones compared to methanol. In addition, hexane is a nonpolar solvent, hence no isoflavones or other polar substances are extracted. Probably, fatty acids and waxes are the main compounds in the extract, but they cannot be detected by HPLC/UV. The irone content in the extract using hexane is slightly higher with 0.88% compared to methanol. Otherwise, MeTHF is a slightly more polar solvent than hexane, which results in a negligible higher extraction yield of irones, but also polar by-

products. The irone content in the extract is also low, with a value of 0.36%. In addition, a peak corresponding to the artificial antioxidant butylated hydroxytoluene (BHT) can be observed in the chromatogram. MeTHF contains BHT as inhibitor to prevent the oxidation and the formation of explosive peroxides [82]. Summing up, the extraction efficiency and selectivity of MeTHF is in general comparable to *n*-hexane.

6.4.4 Extraction with sc-CO₂

In the following chapter, an alternative extraction method for irones from iris rhizomes is investigated. Therefore, supercritical fluid extraction (SFE) with carbon dioxide is carried out. The common method to obtain iris butter is steam distillation. However, this is a long-lasting and high energy-consuming process. In addition, the high temperature can induce thermal degradation of the fragrance compounds. Therefore, SFE is investigated as alternative method. Carbon dioxide is used in SFE because of its comparatively low critical pressure (73.7 bar) and temperature (31.1 °C). Above the critical pressure and temperature, the liquid-gaseous phase boundary vanishes and CO₂ adopts the properties of both states. Advantages of SFE with CO₂ are the high availability of carbon dioxide at low cost and its high purity, nontoxicity, and nonflammability. Also, critical conditions are easily obtained and are suitable for mild extractions [8-12]. The extraction unit "LAB SFE 100 mL" from Separex described in Chapter 5 was used for all experiments.

Only one scientific paper dealing with extraction of iris rhizomes by supercritical carbon dioxide is available in the literature. It has been shown that supercritical CO₂ with methanol as modifier is able to extract only 44% of the total irone content in iris rhizomes. The extraction yield of pure carbon dioxide is even worse. This is probably a consequence of the inappropriate polarity of CO₂. However, sc-CO₂ is reported to be a suitable solvent to extract iridals from iris rhizomes. Actually, a higher yield for iridals can be achieved compared to conventional solvent extraction. An advantage is that SFE is a very selective extraction method and very low amounts of flavonoids were detected in the extract [61]. These results are in contrast to the industrial extraction of iris rhizomes by supercritical fluid extraction with natural carbon dioxide. The company Flavex/Germany commercially sells a sc-CO₂ extract of *Iris germanica* L. rhizomes. For this reason, it is worth to investigate the extraction process of iris rhizomes with sc-CO₂ more precisely.

6.4.4.1 Comparison of iris butter and CO₂ extract

Before starting SFE, commercial available extracts from iris rhizomes were analyzed. On the one hand, iris butter was obtained from Phytotagante/France. This beige colored extract was obtained by steam distillation of *Iris germanica* L. rhizomes. On the other hand, a CO₂ extract of *Iris germanica* L. rhizomes with an orange color was obtained from Flavex/Germany. The extract was purchased with an irone content of 10%. It has a sweet balsamic, weak woody

and violet-like smell. According to the specification data sheet, the CO₂-extract contains a high amount of myristic acid, irones (mainly *cis*- α -irone and *cis*- γ -irone, traces of *trans*- α -irone and β -irone), aldehydes, terpenes, and other steam-volatile ingredients. The extraction yield of SFE, with a value of 0.2–0.3%, is comparable to steam distillation [63].

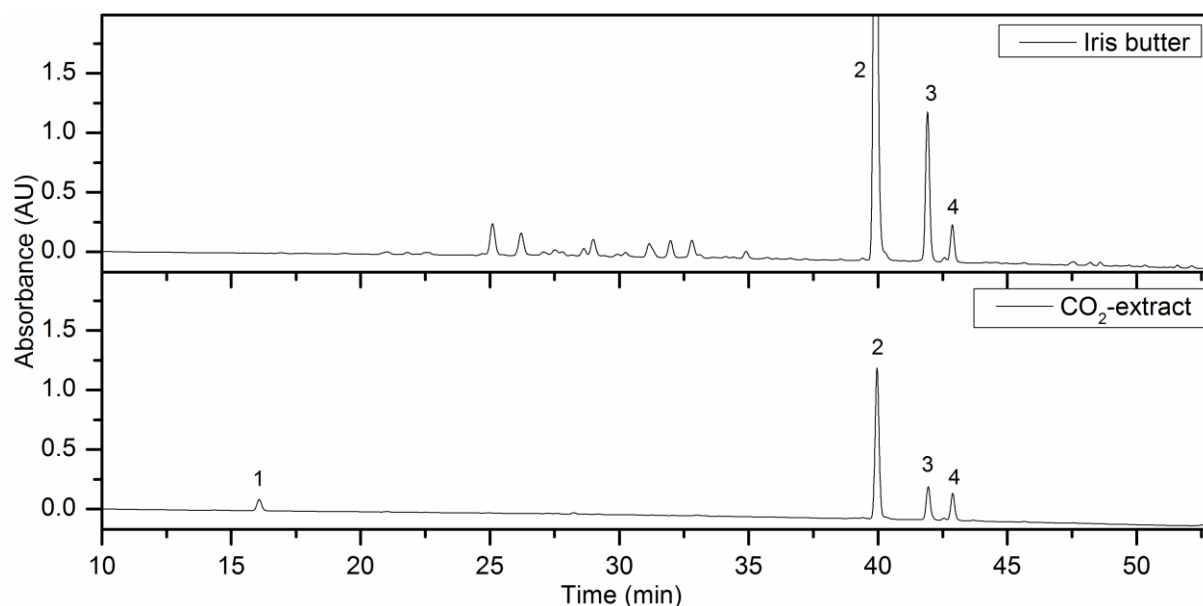


Figure 6.19: HPLC chromatograms of a common iris butter obtained by steam distillation and a commercial CO₂-extract (Flavex). Peak identification: (1) acetovanillone; (2) α -ionone (IS); (3) *cis*- γ -irone; (4) *cis*- α -irone;

Figure 6.19 presents HPLC chromatograms of a common iris butter obtained by steam distillation and a commercial CO₂ extract. It has to be mentioned that the peak heights of the compounds are not comparable as different mass concentrations were used. Nevertheless, it can be noticed that there are differences in the composition of both extracts detectable by HPLC/UV. Iris butter contains mainly *cis*- α - and *cis*- γ -irones, but also a large number of other compounds, which are probably degradation products of irones. The CO₂ extract contains more or less only both irone isomers and acetovanillone. In addition, GC analyses with the same samples were carried out in order to further investigate the composition of the extracts. Analyses showed that the amount of myristic acid is significantly higher in iris butter than in the CO₂ extract. However, a larger number of hydrophobic compounds are present in the CO₂ extract.

In addition, the exact irone content of both extracts was determined and was equal to 4.5% in the iris butter and 9.8% in the CO₂ extract. The amount of irones in the iris butter is significantly lower than in conventional iris butter (approximately 10%) obtained by steam distillation, which indicates the progressive degradation of irones during storage of the extract.

The goal of further investigations is to obtain an iris extract by SFE comparable or even better than those analyzed ones. This means that the extract should contain a high amount of irones and only have low concentrations of other compounds.

6.4.4.2 Preliminary experiments

Before starting the experiments, it had to be considered which parameters of supercritical fluid extraction are important for the extraction efficiency. A schematic drawing of the extraction unit and the corresponding variable parameters during SFE can be seen in Figure 6.20. For preliminary experiments, some of the parameters were chosen according to Bicchi *et al.* [61], who investigated the extraction of irones by SFE. However, an apparatus with a different technical structure was used for their experiments. For this reason, some parameters had to be chosen independently. Subsequently, experiments were carried out with the „trial & error“-method. This means that only one parameter was changed per experiment, whereby the values of the other parameters were kept constant. The disadvantage of this procedure is that many variable parameters have to be investigated, which makes it very time consuming.

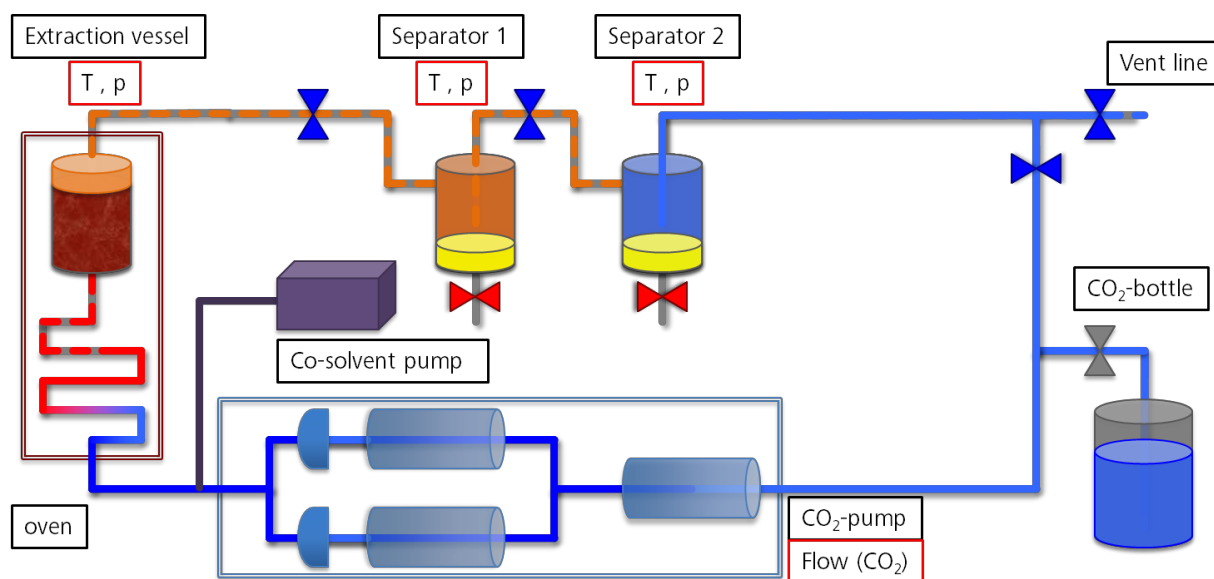


Figure 6.20: Schematic drawing of the supercritical fluid extraction unit with different components of the unit (black boxes) and corresponding variable parameters (red boxes).

Nevertheless, the first experiments were carried out by varying the pressure in the extraction vessel and keeping all other parameters constant. It was considered that the pressure in the extraction vessel is the most important parameter during SFE of iris rhizomes. The temperature of the extraction vessel was set at 60 °C. Experiments were performed for 2 h with a flow of CO₂ of 10 g/min. The temperature of both separators was set at 30 °C. The problem is that the separators can only be heated and not cooled down. However, as a result, it was possible to carry out the experiments under the same conditions over the whole

year. Normally, lower temperature would be more preferable for a better precipitation of the extract [9]. The pressure was kept constant at 70 bar in the first separator and 30 bar in the second one. Carbon dioxide was gaseous in both separators. All parameters for each performed experiment are summarized in Table 6.5.

Table 6.5: Overview of performed experiments for this sub-chapter. Parameters of the experiments were extraction time, flow of CO₂, temperature and pressure in the extraction vessel (A40), first (S50), and second (S51) separator.

Exp. No.	Time / h	Flow (CO ₂) / (g/min)	A40		S50		S51	
			T / °C	p / bar	T / °C	p / bar	T / °C	p / bar
1	2.0	10	60	100	30	70	30	30
2	2.0	10	60	300	30	70	30	30
3	2.0	10	60	500	30	70	30	30
4	2.0	10	60	700	30	70	30	30
5	2.0	10	40	100	30	70	30	30
6	4.0	10	60	300	30	70	30	30

In addition, extractions were carried out with about 40 g of coarse ground *Iris* 2011 rhizomes. This corresponds to a filling capacity of 80% in the A40-extraction vessel. After each experiment, the total mass yield in the separators was determined. Furthermore, the extracted amount of irones per one kilogram of rhizomes was calculated.

Figure 6.21 presents the mass extraction yield in the first (S50) and second (S51) separator obtained by SFE with CO₂ at 60 °C in dependence of the pressure in the extraction vessel. It can be noticed that the total mass extraction yield increases with raising pressure in the extraction vessel. An elevation of the pressure at 60 °C results in an increase of the CO₂-density, which means an enhanced solubility of the compounds. However, high pressures are not always recommended as the extraction of unwanted compounds also increases [8]. Above 300 bar the extraction yield is about 2.5%, which is 10 times higher than the average yield of steam distillation of *iris* rhizomes. Furthermore, the extractions were also carried out at 40 °C and 100 bar. This experiment delivers a slightly larger mass yield compared to the one at 60 °C and 100 bar. This behavior is also correlated to the higher density of CO₂ at lower temperatures and the subsequent enhanced solubility of compounds.

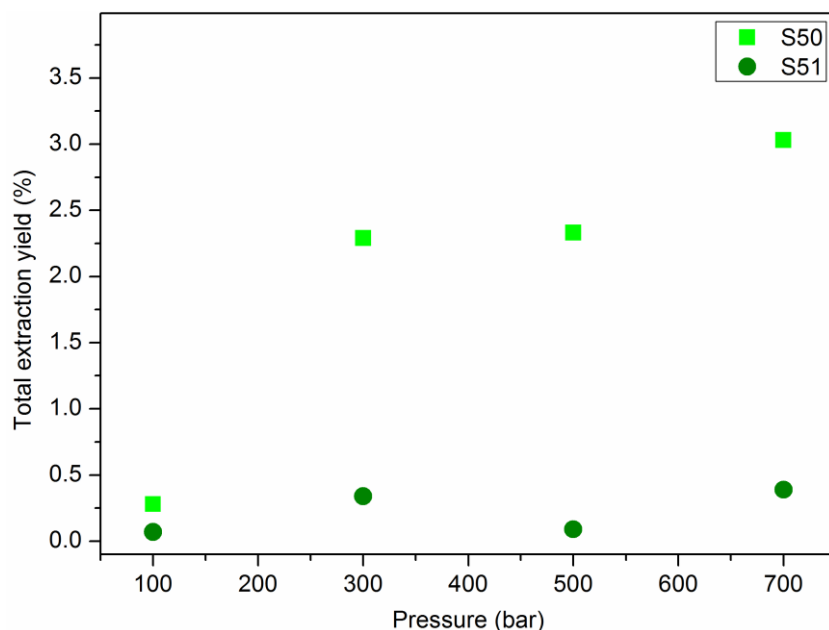


Figure 6.21: Mass extraction yield in the first (S50) and second (S51) separator obtained by SFE with CO_2 at 60 °C in dependence of the pressure in the extraction vessel.

Nevertheless, the extraction efficiency and selectivity of irones is more important than the total mass extraction yield. For this reason, the extracts were analyzed by HPLC/UV and the extraction yield of irones was calculated. Figure 6.22 shows the total extraction yield of irones obtained by SFE depending on the CO_2 -density in the extraction vessel.

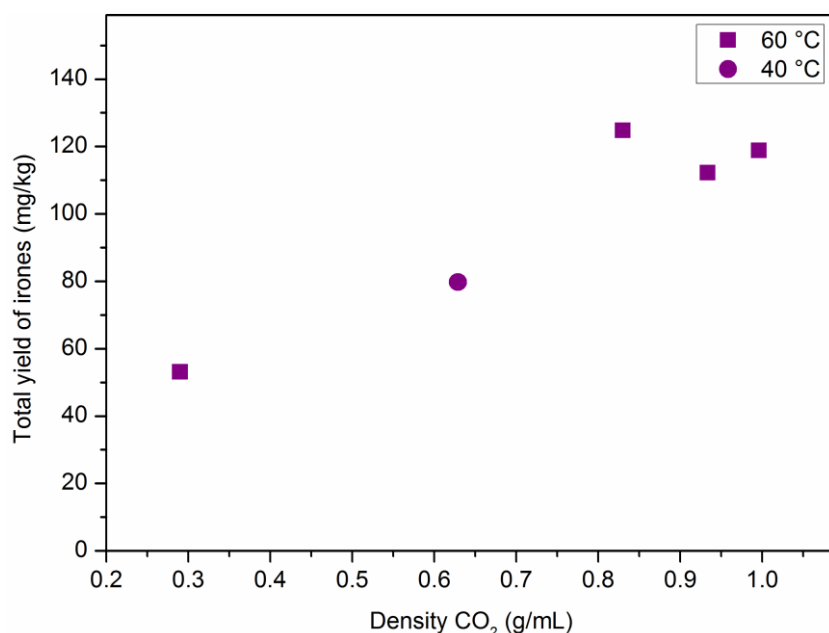


Figure 6.22: Total extraction yield of irones obtained by SFE in dependence of the CO_2 density in the extraction vessel. Extractions were carried out for 2 h with CO_2 at 60 °C and 40 °C at different pressure values.

The given yield was calculated as the sum of the irone contents in both separators. The extracted amount of irones in the second separator was always approximately 20 mg/kg. It can be noticed that the extraction yield of irones rises with increasing CO₂-density. The best yield of 124.8 mg/kg of irones can be obtained at 60 °C and 300 bar in the extraction vessel, which is correlated to a CO₂-density of 0.83 g/mL. Then, the yield reaches a plateau at higher densities.

Figure 6.23 shows the HPLC chromatograms and corresponding irone yields of the first (S50) and second (S51) separator obtained by SFE with CO₂. The experiment (No. 2) was carried out for 2 h at 60 °C and 300 bar in the extraction vessel, where the highest total irone yield was achieved. It can be seen that the extract of the first separator contains a large number of by-products, mostly flavonoids, irone related compounds, and acetovanillone. The extract in the second separator seems to be more pure, as only irones and acetovanillone were detected. However, the amount of irones in both extracts is very low with a value of 0.48%. GC analyses of the samples showed that there is a large amount of myristic acid and other fatty acids in both extracts. A positive observation of these experiments is that the extract can be selectively separated, but further investigations are necessary.

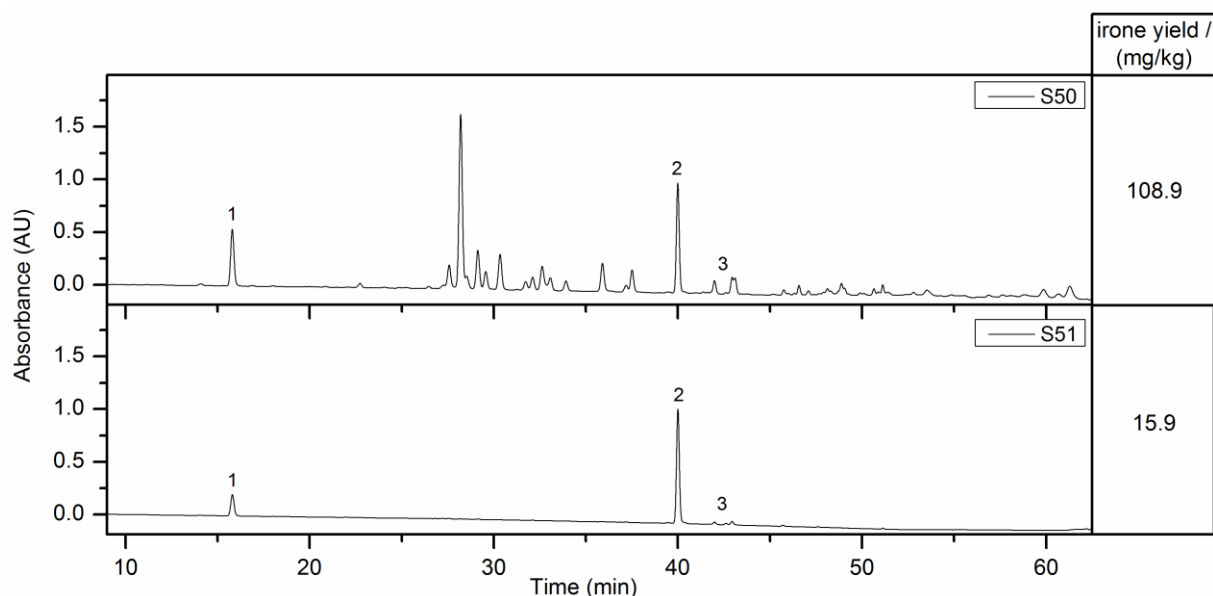


Figure 6.23: HPLC chromatograms and corresponding irone yields of the first (S50) and second (S51) separator obtained by SFE with CO₂. The experiment was carried out for 2 h at 60 °C and 300 bar in the extraction vessel. Peak identification: (1) acetovanillone; (2) α -ionone (IS); (3) irones (*cis*- α - and *cis*- γ -irone);

Furthermore, a drawback of this extraction method is that only 124.8 mg/kg of irones can be extracted by SFE. The actual content of irones in Iris 2011 rhizomes is 272 mg/kg. Thus, only one half of the total irones can be extracted with sc-CO₂.

For this reason, another experiment (No. 6) with a longer extraction time of 4 h was carried out. All other parameters were the same as in the previous experiment (No. 2). The intention was that a longer extraction time will increase the irone yield [8]. However, the results show an opposite behavior. Indeed, the extraction yield of irones decreases to 93.6 mg/kg for a 4 h-lasting experiment. Probably, irones get lost by volatilization during SFE.

Concluding, the extraction of irones from iris rhizomes is a very complex process by SFE. The „trial & error“-method was stopped to this point, as it would have taken too long to investigate every single parameter of the extraction. For this reason, another examination method had to be applied.

6.4.4.3 Design of experiments (DoE)

The preliminary experiments showed that it is a very time consuming method to investigate every single parameter of the extraction with sc-CO₂. Only one parameter could be investigated per experiment. However, the extraction of irones from iris rhizomes depends on many parameters like the flow of CO₂, extraction time and the temperature and pressure in the extraction vessel and separators. Also the particle size of iris rhizomes, the filling height of the extraction vessel, pretreatment of the rhizomes and the addition of a cosolvent can influence the extraction yield. For this reason, a method was searched to investigate the influence of as many parameters as possible on the extraction yield with a small effort. To this purpose, a design of experiments (DoE) was used. In detail, the screening experiment plan of Plackett and Burman was selected in order to estimate the main effects on the extraction of irones from iris rhizomes with sc-CO₂. This method is used to evaluate quantitatively the influence of a large number of independent parameters. The parameters can assume two values (maximum and minimum value). Eight different experiments have to be carried out and the total irone yield is investigated. With these results the significance and best value of each parameter can be calculated. The procedure will be shortly explained. The used literature is recommended for further explanations [13, 83-86].

First of all, it had to be decided which parameters during SFE should be investigated. It was assumed that the extraction time, flow of CO₂, and both the temperature and pressure in the extraction vessel, first separator, and the second separator have a major influence on the extraction yield. Furthermore, a maximum (+1) and minimum (-1) value for each factor of the parameter (X_i) have to be considered. Table 6.6 summarizes the chosen parameters and the corresponding values of the factors. In detail, seven ($n = 7$) different parameters were investigated. The temperature in the second separator was kept constant at 30 °C and is not included in the DoE. It was presumed that a lower temperature enhances the precipitation of the extract in the separator. Another reason is that eight experiments have to be carried out to determine the influence of seven parameters on the extraction. If eight parameters have to be investigated, eleven experiments have to be carried out. In addition, it should be noted

that the DoE supposes that the parameters do not influence each other and that there is a linear relation between the maximum and minimum value. X_i represents the factor of the investigated parameter, which can take a value of +1 (maximum) or -1 (minimum), whereas i is the number of the parameter.

Table 6.6: Overview of investigated factors (X_i) of the parameters and their corresponding maximum (+1) and minimum (-1) values.

	Parameter	-1	+1	Factor
	<i>Time</i>	0.5 h	2.0 h	X_1
	<i>Flow (CO₂)</i>	5 g/min	20 g/min	X_2
Extraction vessel (A40)	<i>Temperature</i>	40 °C	60 °C	X_3
	<i>Pressure</i>	100 bar	700 bar	X_4
	<i>Temperature</i>	30 °C	50 °C	X_5
Separator 1 (S50)	<i>Pressure</i>	40 bar	70 bar	X_6
	<i>Temperature</i>	30 °C	50 °C	
Separator 2 (S51)	<i>Pressure</i>	0 bar	40 bar	X_7

The next step is to generate an order for the screening experiments by Plackett and Burman. The principle is based on the orthogonal Hadamard matrices. These matrices exist only for a number of lines with a multiple of 4 ($m = 4 \mathbb{N}^*$), where m is the number of experiments and \mathbb{N}^* a natural positive number. This allows to study a number of parameters $n \leq m - 1$, each taking two levels (a maximum (+) and minimum (-) value). This means that eight experiments ($m = 8$) have to be performed to determine the influence of maximum seven parameters ($n = 7$). The first lines of the Hadamard matrix are given in Table 6.7.

Table 6.7: First line to establish the Hadamard matrix for the design of experiments with the number of maximum investigable parameters (n) and number of experiments (m). (+) indicates the maximum value and (-) the minimum value of a parameter.

n	m	First line of Hadamard matrix
$n \leq 3$	4	+ + -
$4 \leq n \leq 7$	8	+ + + - + - -
$8 \leq n \leq 11$	12	+ + - + + + - - + -

With the help of the first line of the Hadamard matrix, the total matrix can be established by circular permutation of the levels from the left to the right side and adding a last line composed solely of (-)-signs. Although, a column of (+) is added on the left side (X_0), which represents the model parameter of the experiments. The complete matrix of experiments and effects is given in Table 6.8.

Table 6.8: Matrix of experiments and effects obtained by circular permutation of the first line of the Hadamard matrix by Plackett and Burman. (+) indicates the maximum value and (-) the minimum value of the factor (X_i) of the parameter.

Matrix of effects								
Matrix of experiments								
Exp. No.	X_0	X_1	X_2	X_3	X_4	X_5	X_6	X_7
1	+	+	+	+	-	+	-	-
2	+	-	+	+	+	-	+	-
3	+	-	-	+	+	+	-	+
4	+	+	-	-	+	+	+	-
5	+	-	+	-	-	+	+	+
6	+	-	-	+	-	-	+	+
7	+	+	-	-	+	-	-	+
8	+	-	-	-	-	-	-	-

The order of the experiments is obtained by completing the chosen maximum (+1) and minimum (-1) values of each factor (X_i) of the parameter to the matrix of experiments. The complete plan of experiments is shown in Table 6.9. Subsequently, the experiments were carried out with the given parameters. For example experiment No. 1 ($j = 1$) was performed for 2 h with a CO_2 -flow of 20 g/min. The pressure in the extraction vessel was kept constant at 100 bar with a temperature of 60 °C. Furthermore, the temperature and the pressure of the first separator were constant at respectively 50 °C and 40 bar. No pressure was applied in the second separator, but the temperature was set at 30 °C. 25 g of ground iris rhizomes (Iris 2011) were used for every experiment. It is also important to carry out the experiments in a random order and not in the given one. Thereby, systematical errors can be avoided.

Table 6.9: Schedule of experiments which have to be carried out based on the Hadamard matrix (matrix of experiments). Y_j represents the response of each experiment, thus the extraction yield.

Exp. No.	Time / h	Flow (CO ₂) / (g/min)	A40		S50		S51	Y_j
			T / °C	p / bar	T / °C	p / bar	p / bar	
1	2.0	20	60	100	50	40	0	Y_1
2	0.5	20	60	700	30	70	0	Y_2
3	0.5	5	60	700	50	40	40	Y_3
4	2.0	5	40	700	50	70	0	Y_4
5	0.5	20	40	100	50	70	40	Y_5
6	2.0	5	60	100	30	70	40	Y_6
7	2.0	20	40	700	30	40	40	Y_7
8	0.5	5	40	100	30	40	0	Y_8

Table 6.10: Overview of the extraction yields (mass extraction yield and irone yield: total, separator 1 [S50] and separator 2 [S51]) obtained for every experiment.

	Exp. No. 2		Exp. No. 5		Exp. No. 6		Exp. No. 7	
	Yield / %	Irone / (mg/kg)	Yield / %	Irone / (mg/kg)	Yield / %	Irone / (mg/kg)	Yield / %	Irone / (mg/kg)
S50	0.86	48.1	0.61	20.9	0.29	10.7	1.40	58.2
S51	0.32	45.8	0.14	7.4	0.07	30.8	0.52	19.9
total	1.18	93.9	0.75	28.3	0.36	41.5	1.92	78.1

	Exp. No. 1		Exp. No. 3		Exp. No. 8		Exp. No. 4	
	Yield / %	Irone / (mg/kg)	Yield / %	Irone / (mg/kg)	Yield / %	Irone / (mg/kg)	Yield / %	Irone / (mg/kg)
S50	0.95	39.2	1.16	89.6	0.63	54.9	1.34	42.4
S51	0.03	2.2	0.17	1.7	0.01	3.6	0.21	11.4
total	0.98	41.1	1.33	91.3	0.64	58.5	1.55	53.8

The total mass extraction yield was determined for every experiment, as well as for the first and second separator. Furthermore, the irone extraction yield was calculated for both

separators and the whole experiment. These yields represent the response Y_n of every experiment. The results and extraction yields of each experiment are shown in Table 6.10. It can be noticed that there are large deviations of the extraction yields between the experiments. Also the color of the extracts varied from colorless to dark orange. However, the most important result is the total extraction yield of irones. The maximum obtainable total extraction yield of irones is only 93.9 mg/kg with these experiments. This is approximately one third of the extractable amount of irones, as the used rhizomes contain 272 mg/kg of irones. All further calculations with the design of experiments will be discussed in matters of the total irone extraction yield (yellow marked in Table 6.10). Notwithstanding, the calculations were also carried out for the other extraction yields. The results will be presented later.

In the case of a screening study, meaning a study to estimate the "weight" of each of the studied parameters, it is assumed in principle that the effects are totally additive. This implies a relationship between the measured responses (Y_j) and the factors of parameters (X_i , value of -1 or +1) in the form of a polynomial function of the first degree. All interactions between the factors are neglected. The value b_i reflects the importance or the "weight" of a single factor X_i . The mathematical function for 7 parameters is given in equation (6.3).

$$Y = b_0 + b_1X_1 + b_1X_1 + b_2X_2 + b_3X_3 + b_4X_4 + b_5X_5 + b_6X_6 + b_7X_{7n} \quad (6.3)$$

where Y = determined response, $X_i = ([+1]$ or $[-1]$), b_0 = constant of the equation or average of Y , b_i = effect or "weight" of the factor X_i .

Subsequently, the values of b_i can be calculated by transformation of equation (6.3). b_0 is calculated as mean average of the determined Y_j -values, whereas the other b -values can be calculated with equation (6.4).

$$b_i = \left(\frac{1}{m}\right) [X_{i,1}Y_1 + X_{i,2}Y_2 + X_{i,3}Y_3 + X_{i,4}Y_4 + X_{i,5}Y_5 + X_{i,6}Y_6 + X_{i,7}Y_7 + X_{i,8}Y_8] \quad (6.4)$$

where b_i = effect or "weight" of the factor X_i , m = total number of experiments, $X_{i,j}$ = corresponding factor of the parameter i of the experiment j with a value of (+1) or (-1), Y_j = response of the experiment j .

The process to calculate for example the value of b_i is presented in equation (6.5). For this purpose, the values of the factors of $X_{i,j}$ are taken according to the column X_i in Table 6.8 to the corresponding experiment j . The responses Y_j of each experiment are taken from Table 6.10. The total irone extraction yield was taken for the calculations.

$$b_1 = \left(\frac{1}{8}\right)(+41.4 - 93.9 - 91.3 + 53.8 - 28.3 + 41.5 + 78.1 - 58.5) \quad (6.5)$$

$$b_1 = -7.15$$

Furthermore, the calculations were carried out for all other b -values in the same way. The results of the calculated b -values and responses (total irone yield) are summarized in Table 6.11. The algebraic sign of the b -value indicates which value is the best for the extraction. In detail, if the b -value is negative, the minimum value of the investigated parameter is the best value for a maximum yield in the experiment. Otherwise, the maximum value of the parameter is important if the b -value is positive. For example, the value of b_1 is -7.15. This means that an extraction time (parameter 1) of 0.5 h (minimum value) is more suitable for the extraction of irones by SFE than 2.0 h (maximum value). It can also be noticed that the average irone yield (b_0) of all experiments during the DoE is very low with a value of 60.85 mg/mg. This means that only 20% of the maximum irone yield can be extracted in average by SFE with the given extraction conditions.

Table 6.11: Summary of the performed experiments according to the Hadamard matrix (matrix of experiments) with the corresponding total irone yield (response Y_j) and calculated b -values (b_i) of the investigated parameters.

A40										S50		S51	
Exp. No.		Time / h	Flow (CO ₂) / (g/min)	T / °C	p / bar	T / °C	p / bar	p / bar	Irone / (mg/kg)				
	X ₀	X ₁	X ₂	X ₃	X ₄	X ₅	X ₆	X ₇	Y _j				
1	+	2.0	20	60	100	50	40	0	41.4				
2	+	0.5	20	60	700	30	70	0	93.9				
3	+	0.5	5	60	700	50	40	40	91.3				
4	+	2.0	5	40	700	50	70	0	53.8				
5	+	0.5	20	40	100	50	70	40	28.3				
6	+	2.0	5	60	100	30	70	40	41.5				
7	+	2.0	20	40	700	30	40	40	78.1				
8	+	0.5	5	40	100	30	40	0	58.5				
	b ₀	b ₁	b ₂	b ₃	b ₄	b ₅	b ₆	b ₇					
	60.85	-7.15	-0.42	6.18	18.43	-7.15	-6.48	-1.05					

Summing up, it can be noted that the b -values give information about which value of a parameter is the best for a maximum irone yield. But it cannot be concluded whether a single

parameter has a strong or weak influence on the extraction yield. Therefore, further experiments have to be performed in order to estimate the significance of each parameter

For this purpose, one experiment with a mean extraction yield of irones had to be carried out three more times to estimate the variance of the experiments. The experiment No. 8 with an extraction yield of 58.5 mg/kg of irones was chosen for this purpose. The extraction yields of the experiments are presented in Table 6.12.

Table 6.12: Overview of the extraction yields (mass extraction yield and irone yield: total, separator 1 [S50] and separator 2 [S51]) obtained for the experiment No. 8 from the matrix of experiments.

	Exp. No. 8.1		Exp. No. 8.2		Exp. No. 8.3		Exp. No. 8.4	
	Yield / %	Irone / (mg/kg)	Yield / %	Irone / (mg/kg)	Yield / %	Irone / (mg/kg)	Yield / %	Irone / (mg/kg)
S50	0.63	54.9	0.48	55.5	0.50	48.7	0.28	53.7
S51	0.01	3.6	0.06	4.7	0.21	5.2	0.00	4.4
total	0.64	58.5	0.54	60.2	0.71	53.9	0.28	57.8

It can be noticed that the obtained results and extraction yields are quite equal. These results show that experiments with the SFE-unit can be carried out to obtain reproducible results. The irone content in the extract was always approximately 1%. Besides, these results can be used to calculate the variance of the experiments. The variance of the response Y is calculated according to equation (6.6).

$$var(Y) = \frac{\left[\sum (Y_i - Y_{average})^2 \right]}{(k - 1)} \quad (6.6)$$

where $var(Y)$ = variance of the repeated experiments, Y_i = response of each repeated experiment, $Y_{average}$ = mean average of repeated experiments, k = number of repeated experiments.

The variance describes the squared deviation of the variables (Y_i) from the mean average ($Y_{average}$) of the repeated experiments. It is a dimension for the spreading of the determined values of the response. A high variance value indicates that the determined data points are very spread out around the mean average and from each other. The variance of the repeated experiments was calculated to be 7.12 (mg/kg)^2 . The square root of the variance is called the standard deviation of the response Y and was calculated according to equation (6.7). It has the same dimension as the data, and hence is comparable to deviations from the mean average.

$$\sigma(Y) = \sqrt{\text{var}(Y)} \quad (6.7)$$

where $\sigma(Y)$ = standard deviation of response, $\text{var}(Y)$ = variance of the repeated experiments.

The standard deviation of the repeated experiments for the irone yield was calculated to be 2.67 mg/kg. This correlates to a relative standard deviation of 4.7%.

The next step was to calculate the variance and standard deviation of the b -value. The variance of b_i can be calculated by the variance of the response Y and the total number of experiments $m = 8$ according to equation (6.8). It is assumed that the variance of all experiments during the DoE is equal to the previously determined variance of the repeated experiment No.8.

$$\text{var}(b_i) = \frac{[\text{var}(Y)]}{m} \quad (6.8)$$

where $\text{var}(b_i)$ = variance of b -value during DoE, $\text{var}(Y)$ = variance of the repeated experiment No. 8, m = number of experiments during DoE.

The variance of the b -value for all experiments was calculated to be 0.89, whereas the standard deviation (square root of variance) of the b -value was determined to be $\sigma(b_i) = 0.94$.

The last step of the DoE was to calculate the $b_{i,exp}$ -value of the experiments. This value is important to estimate the significance of a parameter on the extraction yield. It was calculated according to equation (6.9). The basis of this calculation is the student's t -distribution, which is a probability distribution for a small number of experiments. The t -distribution is a symmetric and bell-shaped curve, like the normal (Gaussian) distribution, but has heavier tails. A t -value of 3.182 was used for calculation. This value includes a probability of 95% that the estimated value of $\sigma(b_i)$ is in the interval of distribution with three degrees of freedom (dof). The degree of freedom is the number of repeated experiments minus one. The t -values are listed in literature [86].

$$|b_{i,exp}| > t_{0.05,dof} \sigma(b_i) \quad (6.9)$$

Where $|b_{i,exp}|$ = absolute value of the level of significance of b_i , $t_{0.05,dof}$ = value for students t -distribution with 3 degrees of freedoms (dof) and a probability of 5% that the given value exceeds the probability distribution of the parameter, $\sigma(b_i)$ = standard deviation of b -value.

The $b_{i,exp}$ -value was calculated to be 3.0. This means that a parameter is significant for the extraction if the absolute value of b_i is higher than 3.0. A graphical overview of the investigated parameters and corresponding calculated b -values is shown in Figure 6.24. The dotted line represents the level of significance. A parameter is significant for the extraction of irones during SFE if the corresponding column exceeds the dotted line. It can be noticed that all parameters are significant, except the flow of CO_2 and pressure in the second separator.

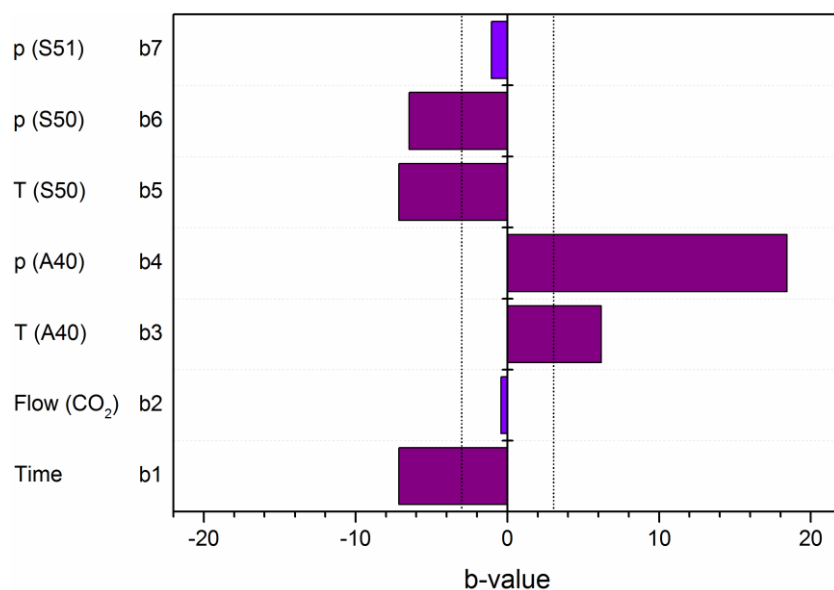


Figure 6.24: Overview of the investigated parameters during DoE and corresponding calculated b -values for the total iron yield. The dotted line represents the level of significance.

Summing up, the influence of the extraction time, flow of CO₂, and both the temperature and pressure in the extraction vessel, first separator, and second separator on the total extraction yield was examined by DoE. The parameters with the investigated minimum and maximum value are summarized in Table 6.13. The best values of the parameters are marked green. If a single value is not significant for the extraction the color is stripped.

Table 6.13: Overview of investigated factors (X_i) of the parameters and their corresponding maximum (+1) and minimum (-1) values. The best values are marked green if they are significant for the extraction and stripped green if they are not significant.

Parameter		-1	+1	No.
Extraction vessel (A40)	Time	0.5 h	2.0 h	X_1
	Flow (CO ₂)	5 g/min	20 g/min	X_2
	Temperature	40 °C	60 °C	X_3
	Pressure	100 bar	700 bar	X_4
Separator 1 (S50)	Temperature	30 °C	50 °C	X_5
	Pressure	40 bar	70 bar	X_6
Separator 2 (S51)	Temperature	30 °C	50 °C	
	Pressure	0 bar	40 bar	X_7

The reported calculations for the total irone yield were performed in the same way for the total mass extraction yield of iris rhizomes by SFE. Thereby, the maximal possible information from the DoE can be obtained.

In general, it can be noticed that a higher extraction pressure of 700 bar increases significantly the total mass and irone yield. This can be explained by the increased solubility power of CO₂ with increasing pressure at a given temperature [8]. A minor disadvantage of high pressures in the extraction vessel is that the extraction of unwanted compounds also increases. Thus, the irone content in the final extract is very low. The highest *b*-value in DoE showed that the pressure in the extraction vessel has a major influence on the irone extraction yield.

Furthermore, the temperature of the extraction vessel influences the irone yield and composition of the extract. The highest irone yield is obtained at 60 °C and 700 bar, which corresponds to a CO₂-density of 0.996 g/mL. However, the extracts contain a large number of by-products. The amount of these unwanted compounds also increases by extraction at a lower temperature of 40 °C with a CO₂-density of 1.04 g/mL. The yield of irones also decreases at a lower extraction temperature. This can probably be explained by the fact that the solubility of irones in CO₂ decreases with increasing temperature or lowering the CO₂-density. The increase of volatility of irones with increasing temperature does not affect the irone yield [8].

In addition, DoE showed that the extraction time has also a strong influence on the extraction yield. In detail, a short dynamic extraction time of 0.5 h enhances the irone yield, whereas longer times increase the total extraction yield. Extractions were only carried out in a dynamic way and no additional static extraction step was performed. It is reported that an increased dynamic extraction time enhances the extraction of most of the compounds [8]. However, the extraction yield of irones decreases with increasing dynamic extraction. Presumably, this behavior can be due to volatilization of irones during longer extraction experiments. Probably, the extraction efficiency of irones can be increased by the addition of a static extraction step to maximize the contact of sc-CO₂ with the sample material.

Besides, the best conditions for the precipitation of the extract in the first separator were determined to be 40 bar and 30 °C. Presumably, higher temperatures in the separator enhance the volatilization of irones during the extraction process. Furthermore, a high pressure or pressure gradient can enhance the exhaust of irones due to the larger extent of CO₂ during pressurizing. The state of CO₂ is always gaseous in the separator. In general, the efficient collection of the extract is, apart from the extraction process, the most important process in SFE.

However, the conditions in the second separator do not significantly affect the extraction yield. The total mass and irone yield were very low as most of the extract was already

precipitated in the first separator. For this reason, an atmospheric pressure in the second separator is recommended.

Finally, the flow of CO₂ has, against expectations, no significant effect on the irone yield. However, a low flow rate of 5 g/min favors the yield of irones, as a slow velocity of the supercritical fluid enhances the penetration of the plant matrix. In contrast, a high flow rate enhances the total mass yield, thus the extraction of by-products.

To sum up, DoE is a suitable method to get a first overview of the importance of different parameters during the extraction of iris rhizomes by SFE. Nevertheless, some assumptions of DoE can lead to an incorrect evaluation of the real significant parameters. On the one hand, a linear correlation is assumed between the minimum and maximum value of a parameter. But the optimal value of a parameter is probably in-between. This is for example the case of the pressure in the extraction vessel. DoE provides a value of 700 bar, which is the most suitable for the extraction of irones, whereas, preliminary results (see Chapter 6.4.4.2) showed that the extraction efficiency of irones is the best at a pressure of 300 bar. However, DoE confirms the result that a higher irone yield is obtained by extractions at 700 bar than at 100 bar. This behavior was already investigated in Chapter 6.4.4.2. On the other hand, interactions between the investigated parameters are not considered in DoE. Nevertheless, the design of experiments provides the best values of some parameters, which will be used in further investigations.

6.4.4.4 Static pressure during SFE with the best parameters of DoE

The design of experiment provided the best values of some parameters for the highest yield of irones from iris rhizomes. For this reason, an experiment was carried out which combines all these values. To this purpose, SFE of 25 g of iris rhizomes was performed at 700 bar and 60 °C in the extraction vessel for 0.5 h. This correlates to a CO₂-density of 0.996 g/mL. A CO₂-flow rate of 5 g/min was used. The temperatures in the separators were kept constant at 30 °C during the experiment. A pressure of 40 bar was supplied in the first separator and an atmospheric pressure in the second separator.

The experiment was carried out under static pressure. This means that the pressure in the extraction was increased to the desired value of 700 bar and kept constant for 0.5 h. After this period, the pressure was slowly decreased to the atmospheric value. The flow rate of CO₂ was kept constant during the whole experiment. The pressure values in the extraction vessel, in the first separator, and in the second separator of the SFE-unit were monitored and are presented in Figure 6.25.

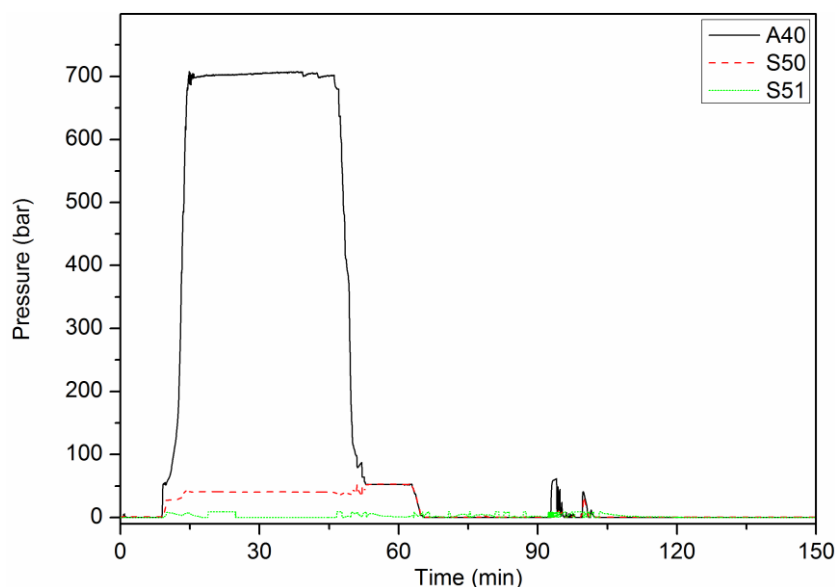


Figure 6.25: Variation of pressure during static pressure extraction of iris rhizomes in the extraction vessel (A40), the first separator (S50), and the second separator (S51) of the SFE-unit.

The extracts in both separators were analyzed to determine the irone yield. In addition, the SFE-unit was purged with isopropanol in order to remove the residual extract in the pipes. The obtained “Purge”-extract was also analyzed after the evaporation of the solvent. Furthermore, Soxhlet extractions of the residual rhizomes with methanol were carried out in order to investigate the quantity of irones content left in the rhizomes after SFE.

Figure 6.26 presents the HPLC chromatograms and corresponding irone yields of the first and second separator, as well as the purge solution and the Soxhlet extract of the residual rhizomes after SFE. It can be noticed that the irone yield of the yellow extract in the first separator is 93.5 mg/kg. This is about 34% of the total irone content in the iris rhizomes. The percentage of irones in the extract is low with an approximate value of 0.7%. The HPLC chromatogram shows that a large number of unwanted compounds like acetovanillone, flavonoids, and iridals/iridal esters are also contained in the extract. GC analyses of the sample indicate that there is a high amount of fatty acids, mostly myristic acid, in the extract. The extract in the second separator does not contain irones, but only a small amount of acetovanillone and other compounds. Furthermore, the chromatogram of the purge solution shows that some compounds remain in the pipes of the SFE unit after the extraction process. In detail, this residue contains a small amount of 6.3 of mg/kg irones related to the initial mass of rhizomes. The analysis of the Soxhlet extract of the residual rhizomes reveals that there is still a large amount of 127.6 mg/kg of irones left in the rhizomes after SFE. These results demonstrate that the extraction of iris rhizomes by sc-CO₂ is not exhaustive at the investigated conditions.

These experiments show that 227.4 mg/kg of irones can be extracted by SFE with a static pressure and subsequent Soxhlet extraction of iris rhizomes. The total irone content in the

used Iris 2011 rhizome is by contrast 272 mg/kg. This result indicates that 44.6 mg/kg of irones get lost during SFE, which is 16% of the total irones content. Presumably, this effect can be explained by the volatilization or the insufficient precipitation of irones in the separators. The irones odor of the exhaust gas also supports this hypothesis. As already mentioned, the efficient collection of the extract is, apart from the extraction process, the most important process in SFE. It is obvious that quantitative extraction conditions cannot be developed and evaluated unless the collection step is efficient.

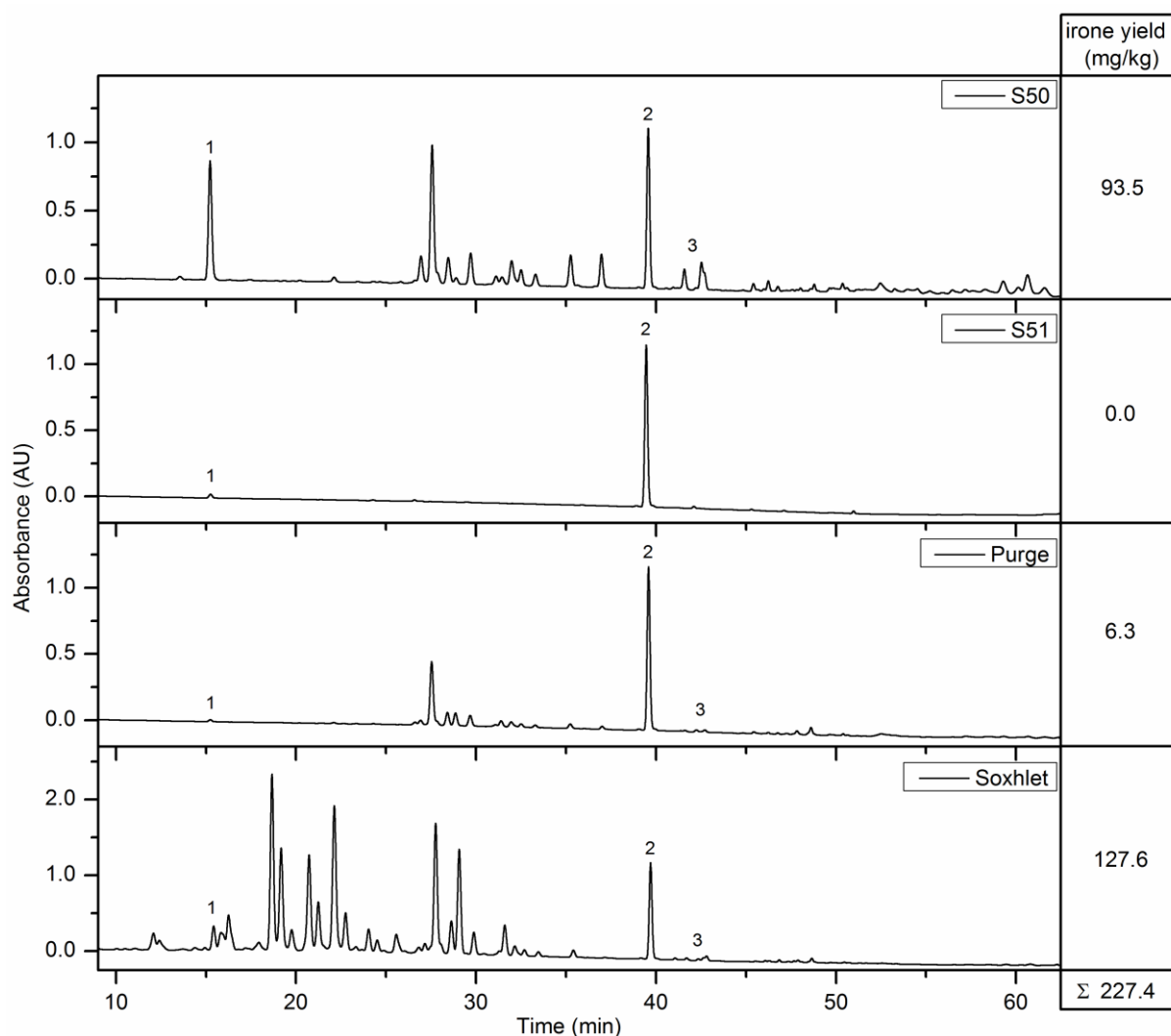


Figure 6.26: HPLC chromatograms and corresponding irones yields of the first (S50), and the second (S51) separator, as well as the purge solution (Purge) after the experiment and the Soxhlet extract (Soxhlet) of the residual rhizomes after SFE. Extractions were carried at a static pressure. Peak identification: (1) acetovanillone; (2) α -ionone (IS); (3) irones (*cis*- α - and *cis*- γ -irones);

6.4.4.5 Dynamic pressure during SFE with the best parameters of DoE

However, another approach to increase the irones yield in SFE was attempted. To this purpose, SFE with a dynamic variation of the extraction pressure was performed. This

means that the pressure in the extraction vessel is increased to the intended value of 700 bar and kept constant for 5 min. After this period, the pressure was slowly decreased to a value of 60 bar and kept constant for approximately 10 min. This procedure was repeated two more times. Finally, the extraction unit was depressurized to an atmospheric pressure. This leads to an increase of extraction time to a value of 2 h. The flow rate of CO₂ was constant at 5 g/min during the whole experiment. The course of pressure during the dynamic pressure extraction in the extraction vessel, the first separator, and the second separator of the SFE-unit is presented in Figure 6.27.

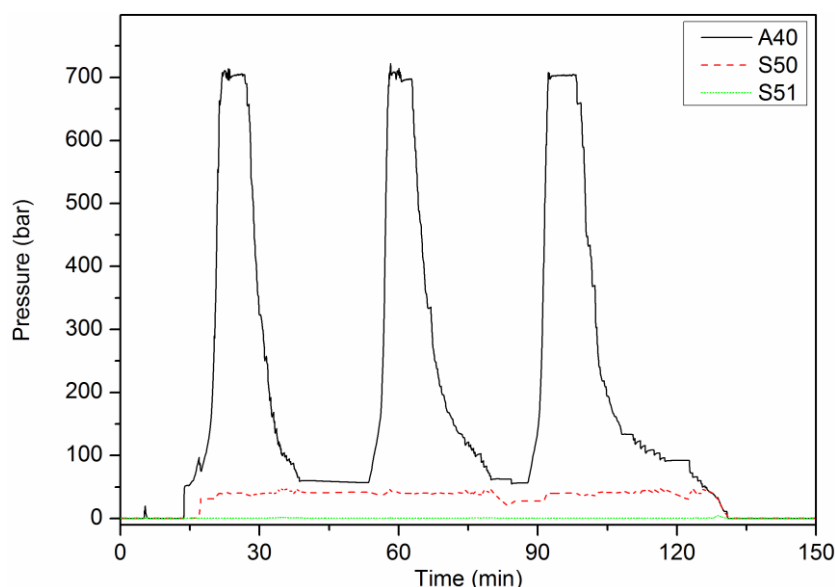


Figure 6.27: Variation of pressure during dynamic pressure extraction of iris rhizomes in the extraction vessel (A40), the first separator (S50), and the second separator (S51) of the SFE-unit.

The intention of this modified extraction procedure was that depressurizing during the extraction process might help the diffusion of CO₂ in the plant matrix and also increase the breakage of the plant structures in which the irones are contained. A further advantage of this method may be that the extraction equilibrium is emerged for three times. This procedure can enhance the extraction efficiency, if the extraction is limited by the solubility of irones in CO₂.

Figure 6.28 shows the HPLC chromatograms and corresponding ironie yields of the different extracts obtained by dynamic pressure variation. The extraction yields are not significantly distinguished from the values of static pressure extraction. In detail, the ironie yield in the first separator slightly increases to 100.8 mg/kg, which is about 37% of the total ironie content in the rhizomes. The composition of the extract is more or less the same, except the ironie content in the extract is somewhat higher with a value of 0.8%. The extract in the second separator does not contain irones, but only a very small amount of acetovanillone and other compounds. The purge solution contains smaller amounts of ingredients compared to the

static pressure experiment. However, Soxhlet extractions of the residual rhizomes show that there is still a large amount of 129.0 mg/kg of irones left in the rhizomes after SFE.

These experiments show that 234.8 mg/kg of irones can be extracted by SFE with dynamic pressure variation and subsequent Soxhlet extraction of iris rhizomes. This result indicates that 33.2 mg/kg of irones get lost during SFE, which is 13% of the total iron content. The loss of irones is slightly decreased in SFE with dynamic pressure variation compared to the static pressure experiment.

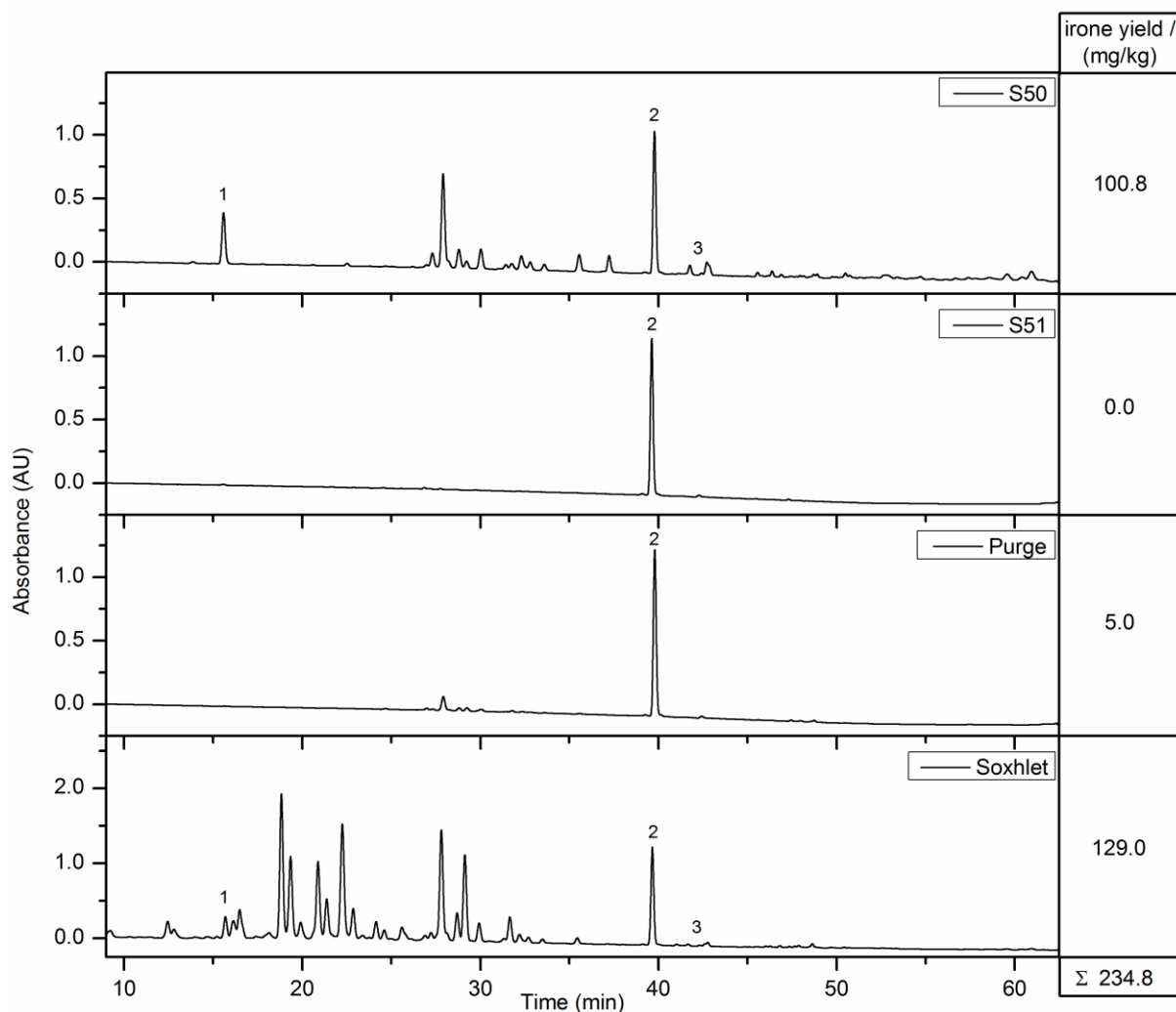


Figure 6.28: HPLC chromatograms and corresponding iron yields of the first (S50), and the second (S51) separator, as well as the purge solution (Purge) after the experiment and the Soxhlet extract (Soxhlet) of the residual rhizomes after SFE. Extractions were carried at with a dynamic pressure. Peak identification: (1) acetovanillone; (2) α -ionone (IS); (3) irones (*cis*- α - and *cis*- γ -irones);

It can be concluded that depressurizing during the experiment respectively dynamic pressure variation has no significant effect on the extraction yield of irones. Presumably, the plant structure is already destroyed before SFE due to the very dry nature of the used iris rhizomes. It can also be noticed that an increase of extraction time, which was in total 2 h for

this experiment, does not influence the irone yield. Probably, the extraction efficiency is limited by the poor solubilization of irones in sc-CO₂. Another reason for the insufficient extraction could be the poor accessibility of irones in the rhizomes by sc-CO₂. Concluding, it can be said that dynamic pressure variation during SFE has no significant effect on the extraction yield of irones compared to a static pressure.

6.4.4.6 Influence of filling capacity, particle size, and flow direction

In addition, the effect of particle size of iris rhizomes, packing density in the extraction vessel, and flow direction of CO₂ was investigated. The experimental conditions of the extraction process were the same as for SFE with a static pressure of 700 bar.

First of all, the double amount of iris rhizomes was extracted by SFE. To this purpose, 50 g of rhizomes were put in the extraction vessel. This corresponds to a filling capacity of 90% in the A40-extraction vessel. It was determined that the filling capacity of the extraction vessel does not at all influence the extraction efficiency of irones from iris rhizomes. The extracted amount of irones was almost identical to the previous reported yields by SFE with static pressure.

Furthermore, the influence of the rhizome particle size on the extraction yield was investigated. To this purpose, the rhizomes were ground to a fine powder in order to enhance the accessibility of irones in the rhizomes. Extractions by SFE with static pressure were carried out with the same conditions as previously described. In general, a smaller particle size creates more surface area and benefits extraction by sc-CO₂. But, it also may hinder the extraction, if the analyte re-adsorb on matrix surfaces [87]. It was found that the irone extraction yield can be slightly increased to 115.5 mg/kg in the first separator by decreasing the particle size of iris rhizomes. The irone content in the extract was equal to previous experiments with a value of 0.70%. Also the composition of the extract was comparable. The higher irone yield can be explained by the shorter diffusion path in the solid plant matrix resulting in smaller intra-particle resistance to solute diffusion [87]. However, small channels could be recognized in the packed iris rhizomes in the extraction vessel after the experiment. This formation of fluid channels in the plant bed can be a limiting effect for an exhaustive extraction of irones. These channels can result in an uneven extraction of the plant material.

Besides, it was investigated if the flow direction of CO₂ through the extraction vessel influences the extraction yield. Normally, the supercritical fluid enters the extraction vessel at the bottom and the extraction/solvent mixture is evacuated at the top. The flow direction was vice versa for one experiment. It was determined that exactly the same amount of irones and total extraction yield is obtained by a solvent flow from the top to bottom. Thus, the flow direction of the solvent in the extraction vessel does not influence the extraction yield.

The filling capacity of the extraction vessel does also not at all influence the extraction efficiency. However, the irone extraction yield can be increased by decreasing the particle size of the iris rhizomes. The smaller particle size enhances the accessibility of irones in the rhizomes. Probably, the extraction efficiency is limited by the poor solubilization of irones in sc-CO₂. For this reason, the polarity of carbon dioxide should be changed by the addition of a cosolvent during SFE.

6.4.4.7 Extractions with ethanol as cosolvent

An organic solvent, called modifier or entrainer, can be added to the supercritical carbon dioxide in order to enhance the solvating properties. Volatile polar solvents such as ethanol, methanol, acetone or acetonitrile are preferred as cosolvent [11]. At least, 17 different modifiers in SFE of natural products have been studied [88]. Previous results indicated that the extraction efficiency with the nonpolar solvent carbon dioxide is limited by the poor solubilization of the weak polar irones. Another proof that nonpolar solvents are not suitable for the extraction of iris rhizomes is the insufficient extraction of irones by hexane (see Chapter 6.4.3). Among all the modifiers, methanol is the most commonly used cosolvent for SFE because of its polar properties and good miscibility with CO₂ [10]. SFE of iris rhizomes also showed that the addition of methanol increases the yield of irones and iridals [61]. However, ethanol would be a better choice for SFE of iris rhizome because of its lower toxicity. For this reason, ethanol will be added to the SFE process in order to increase the polarity of the extraction solvent.

The previously used extraction parameters had to be adjusted for this experiment, as extractions with a cosolvent can only be carried out with a pressure up to 400 bar. For this reason, SFE with ethanol as modifier were carried out at 60 °C in the extraction vessel and a pressure of 300 bar. The flow of ethanol was set at a value of 1 mL/min. All adjusted parameters are summarized in Table 6.14.

Table 6.14: Overview of parameters of the experiment with ethanol as modifier: extraction time, flow of CO₂, flow of ethanol (EtOH), temperature and pressure in the extraction vessel (A40), first (S50), and second (S50) separator.

Time / h	Flow (CO ₂) / (g/min)	Flow (EtOH) / (mL/min)	A40		S50		S51	
			T / °C	p / bar	T / °C	p / bar	T / °C	p / bar
0.5	5	1	60	300	30	40	30	0

After the extraction process, a viscous yellow extract was obtained in the first separator. A white solid was recovered in the second separator. The total mass extraction yield was significantly higher with a value of 4.02% compared to the conventional SFE experiments.

Figure 6.29 presents the HPLC chromatograms and corresponding irone yields of the different extracts obtained by SFE with ethanol as modifier. It can be determined that a greater amount of irones can be extracted by the addition of a cosolvent, compared to conventional SFE. In detail, 149.6 mg/kg of irones can be extracted, which corresponds to 55% of the total irone content in the rhizomes. The extraction yield is slightly higher, compared to the extraction of iris rhizomes with sc-CO₂ and methanol as modifier reported in literature. There a yield of 44% irones was obtained [61]. However, a drawback of the addition of ethanol is that the irone content in the extract is significantly lower with a value of 0.37%, compared to pure sc-CO₂. This is a consequence of the larger variety and amount of by-products in the extract, as it can be seen in the chromatogram. The composition is comparable to a resinoid obtained by Soxhlet extraction of iris rhizomes. However, it can be noticed that the most polar compounds present in iris rhizomes with small retention times in the chromatogram are not extracted by SFE assisted with ethanol.

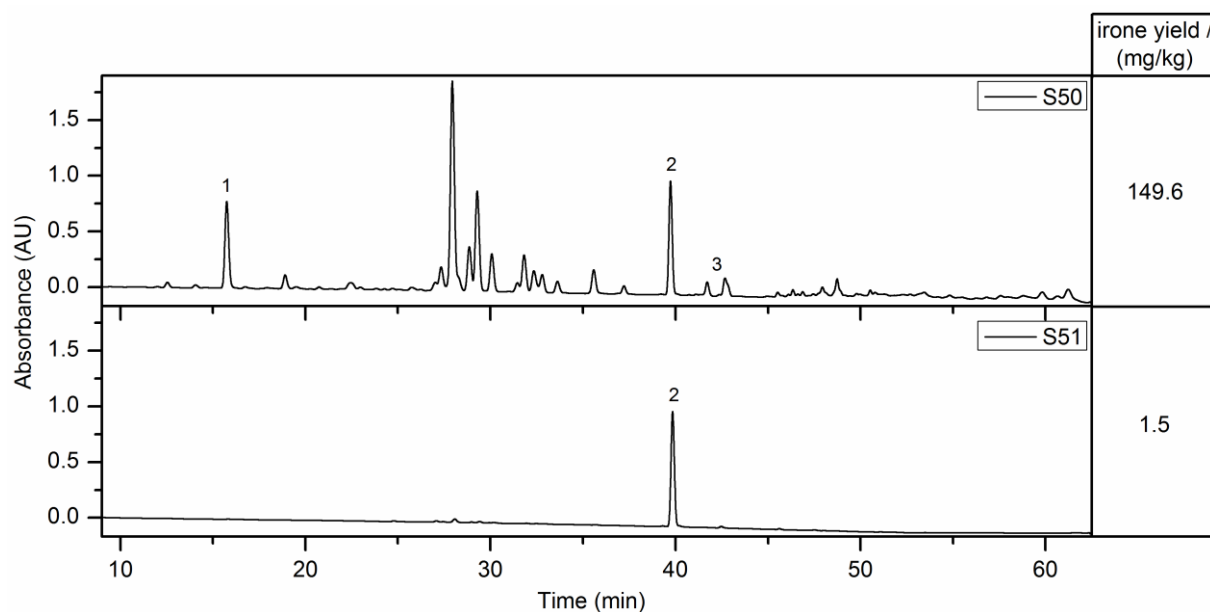


Figure 6.29: HPLC chromatograms and corresponding irone yields of the first (S50), and the second (S51) separator obtained by SFE with ethanol as cosolvent. Peak identification: (1) acetovanillone; (2) α -ionone (IS); (3) irones (*cis*- α - and *cis*- γ -irone);

It can be summarized that the addition of ethanol during SFE increases the extraction yield of irones, but also of other compounds. An exhaustive extraction of irones could have been probably achieved by a longer extraction time or higher amount of added ethanol. Furthermore, the extraction of by-products was too high, which makes the extract comparable to a resinoid of iris rhizomes. Another drawback of this method is that the

cosolvent is recovered together with the extract. Thus a further process step will be required to evaporate the solvent. Nonetheless, this procedure was not further investigated as the irone content in the extract was too low.

6.4.4.8 Enhancement of selective extraction of irones

Further investigations were focused on the selective extraction of irones by pure carbon dioxide. Previous results showed that extractions at high pressures or the addition of ethanol as cosolvent is not suitable to extract selectively irones from iris rhizomes. A drawback of these methods was the extraction of undesired compounds in a high amount. Another problem was the insufficient extraction efficiency of irones by SFE.

In literature, it is reported that a selective extraction of essential oils is achieved, when SFE is performed at a low pressure around 100 bar. Whereby the extraction of non-volatile and high molecular-weight compounds increases significantly with extraction pressure [9]. For this reason, further extractions are carried out with an extraction pressure of 100 bar. It is also reported that the density of CO₂ has a strong influence on the composition of the SFE-extract. On the one hand, low densities are preferred for the extraction of essential oils, terpenes and oxygenated terpenes. On the other hand, paraffin, waxes, triglycerides, and fatty acids are recovered at high CO₂-densities, as the solubility of these compounds increases at these operating conditions [8-10]. For this reason, the influence of CO₂-density on the extraction yield during SFE was observed by varying the temperature of the extraction vessel at a constant pressure of 100 bar. The other parameters were assumed from previous results respectively DoE and are summarized in Table 6.15.

Table 6.15: Overview of realized experiments for this sub-chapter. Parameters of the experiments were extraction time, flow of CO₂, temperature and pressure in the extraction vessel (A40), first (S50), and second (S50) separator.

Time / h	Flow (CO ₂) / (g/min)	A40		S50		S51	
		T / °C	p / bar	T / °C	p / bar	T / °C	p / bar
0.5	5	25-100 °C	100	30	40	30	0

Overall, five different extraction temperatures respectively densities of CO₂ were investigated. One of the experiments was performed with liquid CO₂ at 25 °C and 100 bar. The irone yields of the first and second separator in dependence of the density and the state of aggregation of CO₂ are shown in Figure 6.30.

It can be noticed that the total extraction yield of irones rises with increasing CO₂-density up to an extraction temperature of 32 °C. This corresponds to a density of CO₂ of 0.74 g/mL and carbon dioxide is in the supercritical state. A maximum extraction yield of 100.0 mg/kg of irones can be achieved. This is 37% of the maximum iron content in the rhizomes and comparable to previous SFE experiments. If the extraction is performed below the critical temperature (31.1 °C) and CO₂ is liquid, the iron yield declines slightly. It can also be determined that most of the irones are present in the first separator, whereas the extracted amount of irones in the second separator was always approximately 10 mg/kg. Soxhlet extractions of the residual rhizomes after SFE show again that there is large amount of irones left in the rhizomes. Furthermore, it is once more observed that approximately 15% of the irones get lost during SFE.

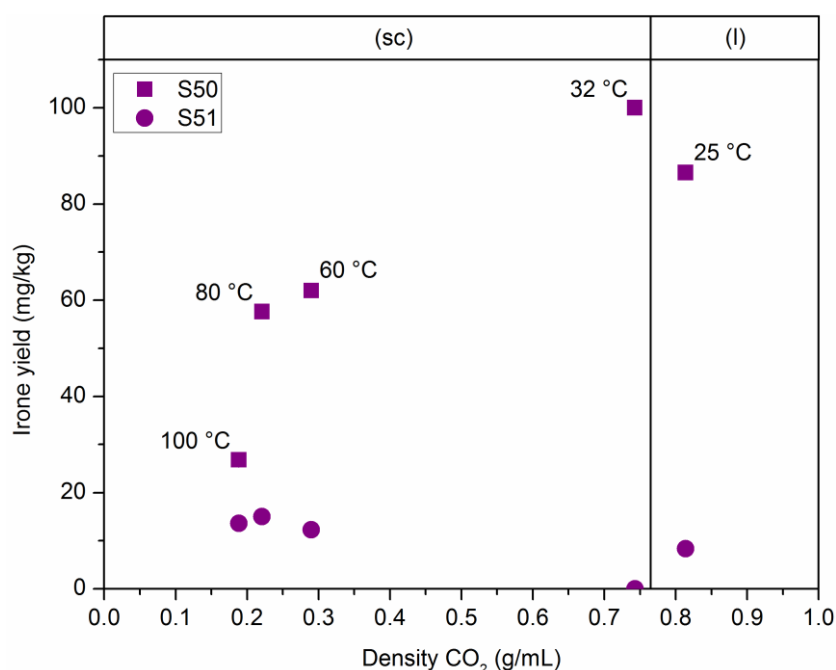


Figure 6.30: Iron yields of the first (S50) and second (S51) separator obtained by SFE with CO₂ at 100 bar in dependence of the CO₂-density in the extraction vessel. The corresponding temperatures and the supercritical (sc) or liquid (l) state of CO₂ are also given.

In addition, it was determined that the total mass extraction yield increases with the CO₂-density from 0.07% at 100 °C up to 0.41% at 32 °C. This indicates the superior extraction of other compounds at higher CO₂-densities, respectively lower extraction temperatures. However, the mass yield is somewhat lower compared to previous SFE experiments.

Nonetheless, most important improvement to previous investigated methods is that irones can be extracted in a more selective way. In detail, all extracts contain more than 2% of irones. For comparison, previous extracts solely contained up to 0.7% of irones. Actually, the iron content in the extract can be increased up to 20.4% respectively 30%, when SFE is

performed at 100 bar and 60 °C in the extraction vessel. This is a significant increase in selectivity of irone extraction by supercritical carbon dioxide. Extractions with liquid carbon dioxide are less sufficient. The extraction yield of irones is slightly lower compared to sc-CO₂. In addition, the content of irones in the extract is only 2.6%. This result can be a consequence of the high solvent power of liquid carbon dioxide towards lipophilic compounds. It has a lower selectivity than sc-CO₂ and enhances the extraction of high molecular weight compounds [9].

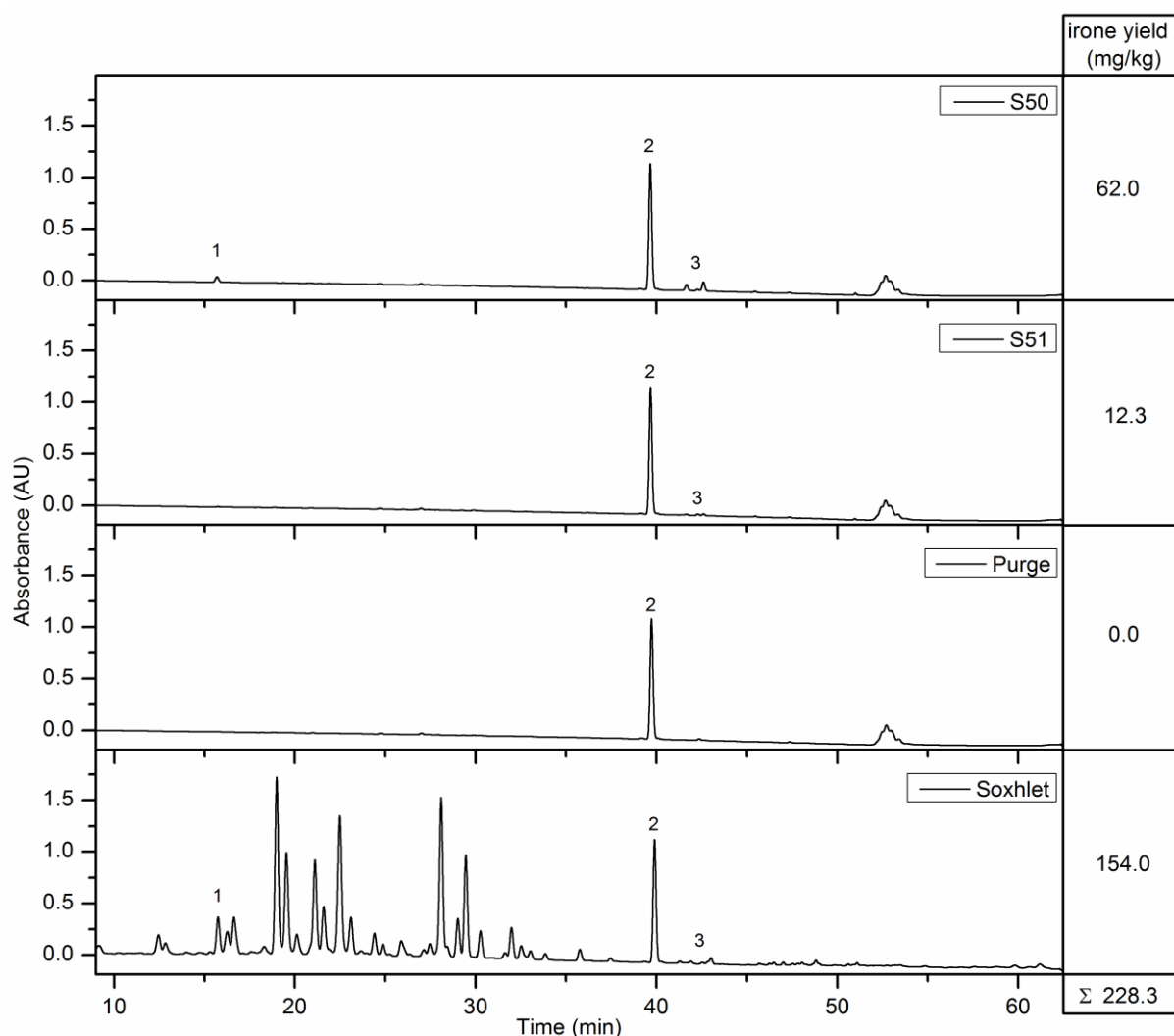


Figure 6.31: Chromatograms and corresponding irone yields of the first (S50) and second (S51) separator, as well as the purge solution (Purge) after the experiment and the Soxhlet extract (Soxhlet) of the residual rhizomes after SFE. Extractions were carried out at a temperature of 60 °C and pressure of 100 bar in the extraction vessel. Peak identification: (1) acetovanillone; (2) α-ionone (IS); (3) irones (*cis*-α- and *cis*-γ-irone);

Figure 6.31 presents the HPLC chromatograms and corresponding irone yields of the first and second separator obtained by SFE with CO₂ at 100 bar and 60 °C in the extraction vessel. It can be seen that the extract of the first separator contains 20.4% of irones and a

small amount of acetovanillone. The white extract contains likely a high amount of myristic acid and other fatty acids, which cannot be detected by HPLC/UV. Furthermore, the composition of the obtained extract is comparable to common iris butter respectively commercial CO₂-extract of iris rhizomes (see Figure 6.19, page 103).

However, the irone content is higher compared to commercial extracts, which contain averagely 10% of irones. Also the scent of the extract (sweet, woody, violet) differs slightly from conventional iris butter. The extract in the second separator seems to be comparable to the first separator, as only irones and acetovanillone were detected. But the irone content is higher with a value of 30.0%. In addition, analyses of the purge solution indicate that no irones or other compounds are remaining in the pipes of the extraction unit, as the solution does not contain any irones. A drawback of this procedure is that the extraction of irones is still not exhaustive. The residual irone content was determined to be 154.0 mg/kg. Furthermore, it is once more observed that approximately 15% of the irones get lost during SFE.

Summing up, a decrease of the extraction pressure to a value of 100 bar increases significantly the selectivity of irone extraction from iris rhizomes by SFE. The irone content in the obtained SFE-extract is higher compared to the conventional iris butter obtained by steam distillation. However, the extraction efficiency is still probably limited by the diffusion of the irones out of the plant matrix. Therefore, a pretreatment of iris rhizomes is investigated in order to enhance the accessibility of irones by SFE.

6.4.4.9 Extractions with pretreatment of rhizomes

The intention of the following investigations was that water can enhance the irone extraction yield during SFE by swelling the plant matrix and open pores. This can lead to a better access of the analyte and support the flow through the matrix. Although, water is only weak soluble in supercritical carbon dioxide (0.3%), it could play an important role in SFE. If excess water is remaining in the extraction vessel, highly water soluble analytes would prefer to partition into the aqueous phase. Thus, the recovery of these compounds will be very low in SFE. Semi-polar analytes, like irones, will dissolve into the aqueous phase, but readily partition into the supercritical carbon dioxide yielding high recoveries [8, 89]. This method was for example successfully applied to the extraction of essential oil from oregano (*Origanum vulgare* L.) using supercritical carbon dioxide in the presence of water. The extraction of the essential oil could be increased by the discontinuous addition of water [90].

For this reason, 20 mL of an aqueous solution were added to 25 g of iris rhizomes extraction vessel before SFE. First of all, pure water was added to the rhizomes. In a second experiment a 1% solution of acetic acid was used to wet the rhizomes. Commonly, an organic acid is used for the pretreatment of iris rhizomes before steam distillation in order to enhance the extraction yield. A third experiment was performed with a sodium myristate

solution (0.1 M). This aqueous soap solution turned out to be a suitable solvent for the extraction of irones within 30 min at 45 °C. After the addition of the aqueous solution to the iris rhizomes, the mixture was equilibrated for 30 min at 45 °C. Subsequently, supercritical fluid extraction was performed with the previous conditions.

After the extraction, it was observed that the rhizomes became brown. This observation indicates a reaction during the extraction process. Nonetheless, white extracts with a violet-like smell were obtained for all experiments. The extracts were subsequently analyzed by HPLC/UV. It was observed that the extracts of the first separator contain mostly irones and acetovanillone. Only small amounts of other compounds were detected. The content of irones is between 2% and 4%, which is comparable to the previous results obtained by SFE with pure carbon dioxide. The main compounds in the extracts are probably myristic acid and other fatty acids. The extract in the second separator and purge solution contain only negligible concentrations of different compounds. However, the most important outcome is that the extraction yield of irones could not be increased by SFE in the presence of aqueous solutions.

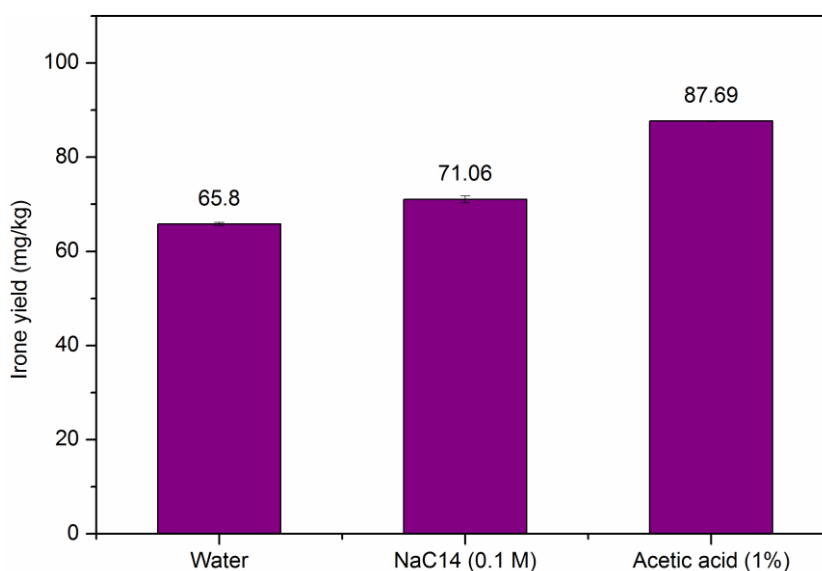


Figure 6.32: Irone yield of SFE in depending on different pretreatment aqueous solutions (water, sodium myristate, acetic acid).

The determined iron yields are summarized in Figure 6.32. It can be noticed that the type of pretreatment solution does not significantly change the extraction yield of irones. Water seems to be the most unfavorable solvent for the pretreatment of iris rhizomes as only 65.8 mg/kg of irones were extracted. Furthermore, acetic acid (1%) provides a slightly better yield with 87.69 mg/kg. The extraction efficiency of a 0.1 M sodium myristate solution is in between. But the iron yield is smaller compared to SFE with pure CO₂, where a maximum value of 100.0 mg/kg of irones could be extracted.

Nonetheless, an additional experiment was performed, in which the ratio of rhizomes to aqueous solution was varied. Here, 60 mL of a 0.1 M aqueous sodium myristate solution was added to 6 g of iris rhizomes. The suspension was extracted by SFE after 30 min of pretreatment. However, excessive foaming occurred when CO₂ was added to the suspension. This behavior resulted in a carryover of the extraction solution into the first separator. Subsequently, SFE was carried out for 0.5 h. A brown colored extract solution was recovered from the first separator. HPLC analyses confirmed that a large number of unwanted compounds, especially water soluble substances, were extracted. In addition, the irone yield is very poor with a value of 11.0 mg/kg. Consequently, the extraction yield of irones could not be increased by SFE in the presence of aqueous solutions. This method was not further investigated as it generates a low extraction yield and also favors the contamination of the extraction unit.

6.4.4.10 Extractions with myristic acid as “cosolvent”

Further investigations were concentrated on water free extractions with supercritical carbon dioxide. Pure myristic acid was added to the rhizomes in the extraction vessel. This is one of the main compounds contained in iris rhizomes. The intention of the addition of a fatty acid is that the molecules can form aggregates in sc-CO₂. Probably, these aggregates are able to enhance the solubility or rather extraction efficiency of irones during SFE. In literature the formation of aggregates by stearic acid above a Krafft-pressure of 90 bar in supercritical carbon dioxide was observed. This is comparable to the formation of inverse-micelles of surfactants in organic solvent [91].

To this purpose, 5 g of myristic acid were added to 25 g of iris rhizomes and thoroughly mixed in the extraction vessel. SFE was performed at an extraction pressure of 100 bar, whereas the other parameters were set at the values of the previous experiments. Only the temperature of the extraction was varied. The melting point of myristic acid is 54.1 °C [92]. Therefore, extractions with supercritical carbon dioxide were performed at 60 °C, where myristic acid is in a liquid state, and 32 °C, where the fatty acid is solid. Thereby, the influence of the state of aggregation of myristic acid on the irone extraction yield is investigated. Preferably, myristic acid only enhances the extraction of irones and is not extracted itself.

The results of these experiments show a large deviation between the obtained extracts. It can be noticed that the irone yield decreases significantly by adding myristic acid and an extraction temperature of 60 °C. Myristic acid is liquid at this temperature and only 27.4 mg/kg of irones can be extracted. It seems that the addition of myristic acid interfere the extractions of irones by sc-CO₂. For comparison, the irone yield of extractions without myristic acid at the same conditions was 74.3 mg/kg. Furthermore, the extract in the second separator and the purge solution did not contain any irones.

The results of SFE at 32 °C and 100 bar with the addition of myristic acid show a different behavior. Under these conditions, myristic acid is solid. The irone extraction yield is 80.4 mg/kg in the first separator and thus higher compared to the previous experiment with myristic acid at 60 °C. However, a relatively large amount of irones (13.8 mg/kg) is remaining in the purge solution. For comparison, the total irone extraction yield of SFE without myristic acid was 100.0 mg/kg at the same conditions. During the experiment, it could be observed that the extract respectively myristic acid precipitated in the pipes of the extraction unit. Actually, this led to plunging of the pipes during one experiment. After the extraction crystalline myristic acid was observed above the plant feed in the extraction vessel. The extract contains only a small amount of irones (0.4%), which is most likely due the higher amount of extracted myristic acid.

The obtained results are somewhat in contrast to literature data. In fact, the solubility of most solvents in sc-CO₂ is better when they are in their liquid state [8]. This is not the case for myristic acid. Actually, there is always a competition between the solubility of a compound, which decreases with increasing temperature, and desorption of the compound from the plant matrix. Probably, the interactions between the plant matrix and myristic acid are higher if the fatty acid is liquid. Thus, the solvent power of CO₂ at 60 °C and 100 bar is too small to solubilize myristic acid. Furthermore, this adsorption of myristic acid hinders the extraction of irones.

It can be concluded that the addition of myristic does not enhance the extraction efficiency of irones during SFE. On the contrary, the irone yield and the irone content in the extracts are decreased. Hence, the extraction of iris rhizomes with pure supercritical carbon dioxide is more suitable.

6.5 Conclusion

The main aim of this work was to investigate an alternative fast, selective, and environmentally friendly extraction method of irones from *Iris germanica* L. rhizomes. Therefore, supercritical fluid extraction (SFE) with carbon dioxide was applied.

The first step was to establish suitable and efficient analyses methods (Chapter 6.4.1) in order to examine the quality and irone content of the extracts. Therefore, HPLC/UV, GC/FID and TLC were used for analyses. It was examined that α -ionone is a suitable compound for internal standard calibration of irones in HPLC/UV and GC/FID.

Subsequently, the characterization of different iris rhizomes (Chapter 6.4.2) was performed. For this purpose, the residual moisture, actual and maximum irone content of iris rhizomes with different storage periods were investigated. It was examined that the drying of iris rhizomes in a compartment drier at 45 °C for several hours is a suitable method to determine the residual moisture. Other method led to the decomposition and volatilization of irones. The

residual moisture was determined to be 6.63% for 1 year stored rhizomes. Furthermore, the moisture decreases with an increasing storage period. Soxhlet extractions were carried out with different solvents in order to investigate the total irone content of the rhizomes. Methanol was identified to be a suitable solvent to extract exhaustively irones. It was noticed that the irone content increases with an increasing storage time. However, during storage of several years a natural decomposition of irones occurs. The irone content of the most often used iris rhizomes (*Iris* 2011) was determined to be 272 mg/kg after a storage time of approximately 5 years. The concentration of irones in *Iris pallida* rhizomes was significantly higher than in *Iris germanica*. It was also attempted to investigate the maximum possible irone content by artificial oxidation of iris rhizomes with aqueous sodium nitrite solutions. However, it was found out that the irone content in the rhizomes decreases during the oxidation process. This indicates an oxidative degradation of irones during the experiment. This behavior is very probable as the irone content is already very high before the artificial oxidation process.

Ultrasound-assisted extractions of iris rhizomes (Chapter 6.4.3) with methanol, *n*-hexane, and 2-methyltetrahydrofuran (MeTHF) were also carried out. MeTHF was chosen as it was recently considered to be an alternative solvent for the petroleum-based *n*-hexane in extraction processes. It can be noticed that methanol recovers the highest amount of irones. However, the extraction selectivity is small, as a large number of by-products, like isoflavones or acetovanillone, were also extracted. Hexane and MeTHF are more nonpolar solvents, thus no or only low concentrations of isoflavones or other polar substances are present in the extract. From this follows that a more selective extraction of irones is possible. The extracted irone content of both solvents was significantly lower in comparison to methanol. Consequently, ultrasound-assisted extraction with MeTHF and hexane is not suitable for the exhaustive extraction of irones from iris rhizomes. However, the extraction efficiency and selectivity of MeTHF is in general comparable to *n*-hexane.

The main part of this chapter dealt with the extraction of iris rhizomes by supercritical carbon dioxide (Chapter 6.4.4) as an alternative to conventional extraction methods. Supercritical fluid extraction (SFE) is a simple, inexpensive, fast, and selective method for the extraction of organic compounds from herbs and other plants. The goal of the investigations was to establish a more selective, faster and lower energy consuming extraction method of irones compared to steam distillation. The extraction unit "LAB SFE 100 mL" from Separex was used for all experiments.

Preliminary experiments by SFE showed that the extraction of irones from iris rhizomes is a very complex process. Preliminary, it was considered that the pressure in the extraction is the most important parameter during SFE of iris rhizomes. The pressure was varied for each experiment from 100 to 700 bar at a constant temperature of 60 °C in the extraction vessel. The other parameters of SFE were kept constant. It was noticed that the extraction yield of irones increases with ascending CO₂-density. The best yield of 124.8 mg/kg of irones was

obtained at 60 °C and 300 bar in the extraction vessel. However, this is only one half of the possible yield. A further drawback of these conditions was the extraction of a large number of by-products, mostly flavonoids, irone related compounds, and acetovanillone. The amount of irones in the extract was very low with a value of 0.48%, which is 20 times lower in comparison to conventional iris butter. A further improvement of the extraction parameters was necessary. But, the examination respectively assessment of all parameters would have been too time consuming by varying only one parameter per experiment.

For this reason, a design of experiments (DoE) was used in order to investigate the influence and significance of several parameters on the irone extraction yield. In detail, the following parameters of SFE were examined: extraction time, flow of CO₂, and each the temperature and pressure in the extraction vessel, first separator, and second separator. The results of DoE showed that all parameters, except the flow of CO₂ and the pressure in the second separator, influenced significantly the irone yield. In detail, the highest amount of irones could be obtained at a high pressure (700 bar) and temperature (60 °C) in the extraction vessel. It was also shown that extractions should only be performed for 0.5 h, as an extended extraction period decreases the irone yield. This behavior could be due to volatilization of irones during long-lasting SFE. The best conditions for the precipitation of the extract in first separator were determined to be 40 bar and 30 °C. Finally, a low CO₂-flow rate of 5 g/min favored the yield of irones, but had no significant influence on the yield. Thus, a slow velocity of the supercritical fluid enhances the penetration of the plant matrix. However, the extraction of irones by SFE was not exhaustive and selective enough. Only one third of the actual irone content in the rhizomes could be extracted with the best parameters of DoE. For this reason, the parameters obtained by DoE formed the basis of further experiments in order to improve the extraction efficiency and selectivity.

Additional parameters, which could affect the extraction by SFE, were investigated. The first approach was the dynamic variation of pressure during SFE. The intention was that depressurizing during the extraction process might help the diffusion of CO₂ in the plant matrix and also might lead to the breakage of the plant structures. But this procedure had no significant effect on the extraction yield of irones compared to the normal static pressure during SFE. The filling capacity of the extraction vessel and flow direction of CO₂ did also not at all influence the extraction efficiency. The only successful attempt to increase slightly the irone extraction yield was to decrease the particle size of iris rhizomes. The smaller particle size enhanced the accessibility of irones in the rhizomes. Nonetheless, the extraction efficiency is probably limited by the poor solubilization or diffusion of irones in sc-CO₂.

For this reason, the polarity of carbon dioxide was increased by the addition of ethanol during SFE. Indeed, the extraction yield of irones, but also the extraction of other compounds, could be significantly increased. The composition of the extract was comparable to a resinoid of iris

rhizomes. This procedure was not further investigated as the extraction selectivity was strongly impaired and the irone content in the extract was very low.

Further investigations were focused on the selective extraction of irones by pure carbon dioxide. It was found that a decrease of the extraction pressure to a value of 100 bar increased significantly the selectivity of irone extraction from iris rhizomes. SFE-extracts were obtained which contained up to 30% of irones. This is three times the amount compared to conventional iris butter, which is obtained by steam distillation and usually contains only 10% of irones. Other compounds of the extract were acetovanillone and fatty acids (mainly myristic acid). The extraction efficiency is probably still limited by the diffusion of the irones out of the plant matrix.

Furthermore, it was attempted to enhance the extraction efficiency of irones by swelling the plant matrix and open pores with the addition of aqueous solutions before SFE. It was assumed that this could lead to a better access of irones and support the flow through the matrix. However, the irone yield was even deteriorated by the addition of water in comparison to pure carbon dioxide. A last approach to enhance the extraction of irones by SFE was the prior addition of myristic acid to the iris rhizomes in the extraction vessel. The intention was that fatty acid molecules can form aggregates in sc-CO₂ and probably increase the recovery of irones. But also this attempt was not successful, as the irone yield and the irone content in the extracts decreased. Hence, the extraction of iris rhizomes with pure supercritical carbon dioxide is more suitable.

Generally, it can be concluded that supercritical fluid extraction with carbon dioxide is suitable to produce higher-quality iris butter from iris rhizomes in comparison to steam distillation. A further advantage is the fast extraction time of 0.5 h, which results in a lower energy consumption. Moreover, no further purification steps are necessary, as the final extract is already gathered in the separators. Furthermore, no residual solvents, which are sometimes toxic, are contained in the extract as CO₂ evaporates cleanly at ambient conditions. The only disadvantage of this procedure so far is the non-exhaustive extraction efficiency of irones. Probably this can be compensated by the higher price of the obtained SFE-extract. In particular, the residual rhizomes can subsequently be re-used to extract the remaining irones with an alternative method. In future, it would be preferable to refine the extraction parameters in order to increase the irone yield.

Another approach could be the selective extraction of iridals with supercritical carbon dioxide from fresh iris rhizomes. SFE should be more suitable to extract the precursors of irones as they are more nonpolar compounds. Subsequently, the degradation of iridals to irones can either be performed by a natural degradation or artificial oxidation process. This would result in lower storage costs, as the long-lasting storage period of a large amount of iris rhizomes becomes no longer necessary.

6.6 References

- [1] B. Roger, V. Jeannot, X. Fernandez, S. Cerantola, and J. Chahboun, *Phytochem. Anal.*, **2012**, 23, 450-5.
- [2] B. Roger, X. Fernandez, V. Jeannot, and J. Chahboun, *Phytochem. Anal.*, **2010**, 21, 483-8.
- [3] W. Krick, F.-J. Marner, and L. Janicke, *Z. Naturforsch. C*, **1983**, 38, 179-184.
- [4] J. Garnero and D. Joulain, *Riv. Ital. EPPOS*, **1978**, 60, 568-590.
- [5] CBI Market Information Database, *CBI Product Factsheet: Iris extracts in Europe*, Cited: 13.01.2016, Available from: <https://www.cbi.eu/sites/default/files/study/product-factsheet-iris-extracts-natural-flavours-europe-natural-colours-flavours-thickeners-2014.pdf>.
- [6] C.o. Europe, *Natural Sources of Flavourings*, Vol. 2, **2007**, Strasbourg: Council of Europe Pub.
- [7] P.-J. Hellivan, *Orris: A Star of Inspiration*, in *Perfumer & Flavorist* **2009**.
- [8] S.M. Pourmortazavi and S.S. Hajimirsadeghi, *J. Chromatogr. A*, **2007**, 1163, 2-24.
- [9] E. Reverchon, *J. Supercrit. Fluids*, **1997**, 10, 1-37.
- [10] Q. Lang and C.M. Wai, *Talanta*, **2001**, 53, 771-782.
- [11] O. Sticher, *Nat. Prod. Rep.*, **2008**, 25, 517-554.
- [12] J.L. Martinez, *Supercritical Fluid Extraction of Nutraceuticals and Bioactive Compounds*, **2007**, Boca Raton, London, New York: CRC Press.
- [13] R.L. Plackett and J.P. Burman, *Biometrika*, **1946**, 33, 305-325.
- [14] L. Roth and K. Kormann, *Duftpflanzen Pflanzendüfte - Ätherische Öle und Riechstoffe*, **1997**, ecomed verlagsgesellschaft AG & Co. KG: Landsberg.
- [15] M. Wichtl, *Teedrogen und Phytopharmaka - ein Handbuch für die Praxis auf wissenschaftlicher Grundlage* 5. ed, **2009**, Stuttgart: Wiss. Verl.-Ges.
- [16] W. Blaschek, R. Hänsel, K. Keller, J. Reichling, H. Rimpler, and G. Schneider, *Hagers Handbuch der Pharmazeutischen Praxis: Folgeband 2: Drogen A-K*, Vol. 5, **2013**, Berlin, Heidelberg: Springer.
- [17] Y. Gozu, M. Yokoyama, M. Nakamura, R. Namba, K. Yomogida, M. Yanagi, and S. Nakamura, *Plant Cell Rep.*, **1993**, 13, 12-6.
- [18] K. Shimizu, H. Nagaike, T. Yabuya, and T. Adachi, *Plant Cell Tissue Organ. Cult.*, **1997**, 50, 27-31.
- [19] H. Jehan, D. Courtois, C. Ehret, K. Lerch, and V. Petiard, *Plant Cell Rep.*, **1994**, 13, 671-5.
- [20] H. Ellenberg and C. Leuschner, *Vegetation Mitteleuropas mit den Alpen*, 6. ed, **2010**, Stuttgart: Ulmer UTB.
- [21] J.-P. Bonfils, Y. Sauvaire, Y. Baissac, and F.-J. Marner, *Phytochemistry*, **1994**, 37, 701-705.
- [22] M. Pailer and F. Franke, *Monatsh. Chem.*, **1973**, 1394-1408.
- [23] A. Ali, N. Elemery, M. Elmoghazi, F. Darwish, and A. Frahm, *Phytochemistry*, **1983**, 22, 2061-2063.
- [24] K.L. Dhar and A.K. Kalla, *Phytochemistry*, **1973**, 12, 734-735.

- [25] S. Al-Khalil, D. Al-Eisawi, M. Kato, and M. Iinuma, *J. Nat. Prod.*, **1994**, 57, 201-205.
- [26] E. Wollenweber, J.F. Stevens, K. Klimo, J. Knauff, N. Frank, and C. Gerhauser, *Planta Med.*, **2003**, 69, 15-20.
- [27] A.-u. Rahman, S. Nasim, I. Baig, S. Jalil, I. Orhan, B. Sener, and M.I. Choudhary, *J. Ethnopharmacol.*, **2003**, 86, 177-180.
- [28] G.Y. Xie, X.Y. Qin, R. Liu, Q. Wang, B.B. Lin, G.K. Wang, G.K. Xu, R. Wen, and M.J. Qin, *Natural product research*, **2013**, 27, 2173-7.
- [29] S.R. Ibrahim, G.A. Mohamed, and N.M. Al-Musayeib, *Molecules*, **2012**, 17, 2587-98.
- [30] J. Stefanska, A. Sarniak, A. Wlodarczyk, M. Sokolowska, E. Pniewska, Z. Doniec, D. Nowak, and R. Pawliczak, *Exp. Lung Res.*, **2012**, 38, 90-9.
- [31] V. Rautenstrauch, B. Willhalm, W. Thommen, and G.t. Ohloff, *Helv. Chim. Acta*, **1984**, 67, 325-331.
- [32] F.-J. Marner, *Curr. Org. Chem.*, **1997**, 1, 153-186.
- [33] F.-J. Marner and B. Kerp, *Z. Naturforsch. C*, **1991**, 47, 21-25.
- [34] F.-J. Marner and L. Jaenicke, *Helv. Chim. Acta*, **1989**, 72, 287-294.
- [35] W. Krick, F.-J. Marner, and L. Janicke, *Helv. Chim. Acta*, **1984**, 67, 318-324.
- [36] L. Taillet, J.P. Bonfils, F.-J. Marner, and Y. Sauvaire, *Phytochemistry*, **1999**, 52, 1597-1600.
- [37] R. Fang, P.J. Houghton, C. Luo, and P.J. Hylands, *Phytochemistry*, **2007**, 68, 1242-1247.
- [38] A. Littek and F.-J. Marner, *Helv. Chim. Acta*, **1991**, 74, 2035-2042.
- [39] C. Bicchi and P. Rubiolo, *Phytochem. Anal.*, **1993**, 4, 171-177.
- [40] J.-P. Bonfils, C. Bonfils, C. Larroque, A. Surjus, D. Gleize, and Y. Sauvaire, *Phytochemistry*, **1995**, 38, 585-587.
- [41] L. Jaenicke and F.J. Marner, *Pure & Appl. Chem.*, **1990**, 62.
- [42] J.-P. Bonfils and Y. Sauvaire, *Phytochemistry*, **1996**, 41, 1281-1285.
- [43] A. Corbu, M. Aquino, T.V. Pratap, P. Retailleau, and S. Arseniyadis, *Org. Lett.*, **2008**, 10, 1787-90.
- [44] F. Benoit-Vical, C. Imbert, J.-P. Bonfils, and Y. Sauvaire, *Phytochemistry*, **2003**, 62, 747-751.
- [45] B. Belcour, D. Courtois, V. Petiard, and C. Ehret, *Phytochemistry*, **1993**, 34, 1313-1315.
- [46] L. Firmin, D. Courtois, V. Pétiard, C. Ehret, and K. Lerch, *HortScience*, **1998**, 33, 1046-1047.
- [47] F.J. Marner, W. Krick, B. Gellrich, L. Jaenicke, and W. Winter, *J. Org. Chem.*, **1982**, 47, 2531-2536.
- [48] B. Belcour, D. Courtois, and C. Ehret, *Process for the preparation of gamma-irone*, **1990**, Google Patents, US 4963480 A.
- [49] J.C. Baccou, J.M. Bessiere, P. Boisseau, P. Faugeras, N. Jouy, E. Peyrot, and Y. Sauvaire, *Process for the accelerated ageing and treatment of iris rhizomes*, **1992**, Google Patents, US 5085994 A.
- [50] G. Gil, J.L. Petit, and J.L. Seris, *Process for obtaining irone by enzymatic route*, **1992**, Google Patents, US 5100790 A.

- [51] G. Gil and J.L. Petit, *Process for obtaining irone by microbiological route*, **1992**, Google Patents, US 5106737 A.
- [52] C. Ehret, L.M.M. Firmin, and D. Courtois, *Process for the production of irones*, **2001**, Google Patents, US 6224874 B1.
- [53] N. Yves-Rene, *Process for preparing alpha-irone isomers by cyclization of pseudoirones*, **1950**, Google Patents, US 2517800 A.
- [54] P. Gosselin, A. Perrotin, and S. Mille, *Tetrahedron*, **2001**, 57, 733-738.
- [55] T. Inoue, H. Kiyota, and T. Oritani, *Tetrahedron: Asymmetry*, **2000**, 11, 3807-3818.
- [56] E. Brenna, C. Fuganti, and S. Serra, *Chem. Soc. Rev.*, **2008**, 37, 2443.
- [57] E. Brenna, C. Fuganti, and S. Serra, *C. R. Chimie*, **2003**, 6, 529-546.
- [58] *Bombay Sapphire: Our Gin*, Cited: 08.01.2016 Available from: <https://www.bombaysapphire.com/en-GB/ourgin.aspx>.
- [59] H. Nadaroğlu, Y. Demir, and N. Demir, *Pharm. Chem. J.*, **2007**, 41, 409-415.
- [60] M.I. Choudhary, S. Naheed, S. Jalil, J.M. Alam, and R. Atta ur, *J. Ethnopharmacol.*, **2005**, 98, 217-220.
- [61] C. Bicchi, P. Rubiolo, and C. Rovida, *Flavour Fragr. J.*, **1993**, 8, 261-267.
- [62] Safety Data Sheet: Orris Root CO₂-se Extract, 3% Irone (Typ Nr. 008.003), Flavex, Version: 06.11.2013
- [63] General Specification Sheet: Orris Root CO₂-se Extract, 10% Irone (Typ Nr. 008.004), Flavex, Date accessed: 22.11.2013
- [64] D.J. Rowe, *Chemistry and Technology of Flavors and Fragrances*, **2005**, Oxford: Blackwell Publishing Ltd.
- [65] K. Bauer, D. Garbe, and H. Surburg, *Common Fragrance and Flavor Materials: Preparation, Properties and Uses*, 3. ed, **1997**, Weinheim: Wiley VCH Verlag GmbH.
- [66] G. Ohloff, *Irdische Düfte — Himmlische Lust: Eine Kulturgeschichte der Duftstoffe*, **1992**, Basel: Birkhäuser Verlag.
- [67] A. Galfré, P. Martin, and M. Petrzilka, *J. Essent. Oil Res.*, **1993**, 5, 265-277.
- [68] B. Maurer, A. Hauser, and J.-C. Froidevaux, *Helv. Chim. Acta*, **1989**, 72, 1400-1415.
- [69] Olga Ikebanova, *Perfumes and Colognes With Iris*, Cited: 13.01.2016, Available from: <http://www.fragrantica.com/notes/Iris-11.html>.
- [70] Weleda, *Pflegeserie: Iris*, Cited: 13.01.2016, Available from: <http://www.weleda.de/produkte/gesicht/pflegeserie/iris>.
- [71] M.C.S.G. Blanco, L.C. Ming, M.O.M. Marques, and O.A. Bovi, *Acta Hort.*, **2002**, 569, 99-103.
- [72] *Europäisches Arzneibuch*, 7. ed, **2011**, Stuttgart: Deutscher Apotheker Verlag.
- [73] B. Roger, *Contribution à l'étude des rhizomes, huiles essentielles et extraits d'Iris germanica L. et d'Iris pallida Lam. du Maroc*, Ph.D. Thesis, **2010**, Ecole Doctorale Sciences Fondamentales et Appliquées: LABORATOIRE DE CHIMIE DES MOLECULES BIOACTIVES ET DES AROMES at Université de Nice-Sophia Antipolis
- [74] V.R. Meyer, *Practical High-Performance Liquid Chromatography*, 5. ed, **2013**: Wiley.
- [75] J.K. Swadesh, *HPLC: Practical and Industrial Applications*, 2. ed, **2000**: CRC Press.

- [76] T.C.I.T. 54, *Oils of orris rhizome (Iris pallida Lam. or Iris germanica L.) — Determination of irone content — Method using gas chromatography on a capillary column*, **2004**, ISO copyright office Geneva.
- [77] T. Höß, *Extraction of Iris pallida Lam. with cholinebased ionic liquids*, Master Thesis, **2014**, Institute of Physical and Theoretical Chemistry at University of Regensburg
- [78] E.R. Chamorro, S.N. Zambón, W.G. Morales, A.F. Sequeira, and G.A. Velasco, *Study of the Chemical Composition of Essential Oils by Gas Chromatography*, in *Gas Chromatography in Plant Science, Wine Technology, Toxicology and Some Specific Applications*, D.B. Salih, Editor. **2012**, InTech: Rijeka, Shanghai.
- [79] D. Frohne and U. Jensen, *Systematik des Pflanzenreichs: unter besonderer Berücksichtigung chemischer Merkmale und pflanzlicher Drogen*, 5. ed, **1998**, Stuttgart: Wissenschaftliche Verlagsgesellschaft.
- [80] Agilent Technologies, *GC Calculators* Cited: 19.01.2016, Available from: <http://www.agilent.com/en-us/support/gas-chromatography/qccalculators>.
- [81] L. Petigny, M.Z. Özel, S. Périno, J. Wajsman, and F. Chemat, *Water as Green Solvent for Extraction of Natural Products*, in *Green Extraction of Natural Products*. **2015**, Wiley-VCH Verlag GmbH & Co. KGaA. 237-264.
- [82] Safety Data Sheet: 2-Methyltetrahydrofuran, Sigma-Aldrich, Version: 27.02.2015
- [83] A. Hedayat and W.D. Wallis, *The Annals of Statistics*, **1978**, 6, 1184-1238.
- [84] F. Rais, A. Kamoun, M. Chaabouni, M. Claves-Bruno, R.P.T. Luu, and M. Sergen, *Journal de la Société Chimique de Tunisie*, **2011**, 13, 191-202.
- [85] D. Montgomery, *Design and analysis of experiments*, 8. ed, **2013**, Hoboken, NJ: John Wiley & Sons, Inc. .
- [86] S.D. Brown, R. Tauler, and B. Walczak, *Comprehensive Chemometrics: Chemical and Biochemical Data Analysis*, 1. ed, Vol. 1, **2009**, Amsterdam: Elsevier Science.
- [87] V. Louli, G. Folas, E. Voutsas, and K. Magoulas, *J. Supercrit. Fluids*, **2004**, 30, 163-174.
- [88] W.K. Modey, D.A. Mulholland, and M.W. Raynor, *Phytochem. Anal.*, **1996**, 7, 1-15.
- [89] S.J. Lehotay, *J. Chrom. A*, **1997**, 785, 289-312.
- [90] G. Leeke, F. Gaspar, and R. Santos, *Ind. Eng. Chem. Res.*, **2002**, 41, 2033-2039.
- [91] D.A. Miller, D.S. Clark, H.W. Blanch, and J.M. Prausnitz, *J. Supercrit. Fluids*, **1991**, 4, 124-126.
- [92] Safety Data Sheet: Myristic acid, C.R.G.C. KG, Version: 05.05.2011

7 Extraction of *Rosmarinus officinalis* L.

7.1 Introduction

Rosemary (*Rosmarinus officinalis* L.) is a perennial herb with an intensive aromatic flavor. Its most important chemical constituents are essential oils (e.g. 1,8-cineole, camphor) and antioxidants (e.g. carnosic acid, rosmarinic acid) [1]. In future, natural sources of antioxidants get more and more important. They can be an alternative for artificial antioxidants, which have been partially restricted for food additive [2]. Synthetic antioxidants like butylated hydroxyanisole (BHA; E320) and butylated hydroxytoluene (BHT; E321) are harmful and potential carcinogen [3-5].

Steam or hydro distillations are the common methods to extract the essential oil from rosemary leaves. The influence of hydro and steam distillation was investigated in the first part of this chapter. On the one hand, the residual antioxidants in the leaves after hydro distillation were investigated. On the other hand, the hydro distillation water residues were analyzed by HPLC/UV to determine the content especially of rosmarinic acid and carnosic acid. Moreover, the influence of the extraction duration on the concentration of the antioxidants was investigated. The total antioxidant activity of the extracts and of the pure compounds was determined by DPPH assays. It is shown that after 2.5 h of hydro distillation the amount of rosmarinic acid and the antioxidant activity in the water residue reaches a maximum value. The concentration of carnosic acid and rosmarinic acid in the rosemary leaves decreases during hydro distillation. The longer the duration of hydro distillation the more antioxidants get lost due to solubilization or degradation. In addition, the yield and the quality of the essential oil were investigated to draw a comparison between steam and hydro distillation of Moroccan rosemary leaves.

The second goal of this section was to investigate the antioxidant activity of the hydro distillation water residue of rosemary leaves in different microemulsions. To this purpose, the water residue was mixed with SDS, 1-pentanol, and *n*-dodecane. Phase diagrams were established and microstructures in the microemulsion were roughly identified by conductivity measurements. Furthermore, a method was developed to carry out DPPH-assays in microemulsions. It was found out that the use of the hydro distillation water residue does not influence neither the shape of the phase diagram or the structure of the microemulsion. Moreover, the structures in different regions of the microemulsion do not influence the antioxidant activity. Finally, this residue was introduced to a drinkable microemulsion in order to enhance the antioxidant activity. This antioxidant water residue can be an alternative to conventional antioxidants, like ascorbic acid, in beverages. Currently this water residue is a waste product of hydro distillation. Here, a possible application of this compound was found.

In the last part of this chapter an alternative green method for the extraction of antioxidants from rosemary leaves will be described. The goal was to extract simultaneously the water-soluble rosmarinic acid and the water insoluble carnosic acid with aqueous micellar solutions and avoid toxic or hazardous solvents. Aqueous solutions of the soap sodium myristate, the salt of the saturated fatty acid myristic acid, were used for the extractions. Different parameters like extraction time, soap concentration, pH-value, particle size of rosemary leaves, and ultrasound-assisted extraction on the yield were investigated. Alternative soap compounds were also examined. It is shown that almost the total amount of rosmarinic acid and three-quarter of the water insoluble carnosic acid can be extracted with a 4 wt% soap solution within 5 min. In addition, an alternative processing method to extract specific carnosic acid by micellar solutions was invented. This is the first process obtaining selectively carnosic acid by extraction with aqueous solutions. A method to increase the content of carnosic acid in the extract is also presented.

7.2 Fundamentals: *Rosmarinus officinalis* L.

Rosemary (*Rosmarinus officinalis* L.) is a perennial shrub, which is originated in the Mediterranean area. It belongs to the family of Lamiaceae, with over 200 genera and 3,500 species [6]. Leaves of rosemary have an intense aromatic flavor and a bitter, slightly spicy taste. The plant is mainly cultivated in Spain, Morocco, Tunisia, and the south-east of Europe [1].



Figure 7.1: Pictures of (A) fresh and (B) dried leaves of *Rosmarinus officinalis* L.

The thin-lineal, almost needle-like rosemary leaves (Figure 7.1) are 3 cm long and up to 4 mm broad. They are narrowly lanceolate, sessile, leathery, and very brittle. The leaves are colored green on the upper side and white below with dense, short, woolly hair. The

evergreen shrub can reach a height of approximately 1 m [1]. The plant prefers calcareous substrates with scant humus and high aridity. It blossoms from April until August [6].

Rosemary is widely used for seasoning and flavoring foods, as preservative agent and antioxidant. Also pharmaceutical applications are known for digestive disorders, flatulence, feeling of fullness, but also to quicken the appetite. External application in form of ointments or skin oils supports the therapy for rheumatism and circulatory problems. In folk medicine rosemary is used in compresses for poorly healing wounds and eczema. Also the use as insecticides is known. These applications are due to the ingredients in rosemary leaves [1].

7.2.1 Ingredients

The essential oil from rosemary with a maximum extraction yield of 1.0-2.5% is commonly gained by hydro (HD) or steam distillation (SD). The colorless or slightly yellow oil contains 1,8-cineole (15-30%), camphor (10-25%), α -pinene (10-25%), and borneol (3-20%). The chemical structures of these substances are presented in Figure 7.2. Other compounds are bornyl acetate (1-5%), camphene (5-10%), α -/ β -terpineol, myrcene, limonene, and caryophyllene. Essential oils from Spain or Tunisia can additionally contain a relatively high amount of verbenone. The ratio of these terpenes varies depending on the origin and chemo type of the rosemary plant [1, 7, 8]. The essential oil is located in glandular trichomes at the surface of the rosemary leaves [9]. Rosemary oil is used as antibacterial, antifungal, and anticancer agent [10]. Also applications in aromatherapy are reported. The fragrance of rosemary essential oil has positive effects on the mood and cognitive performance of humans [11].

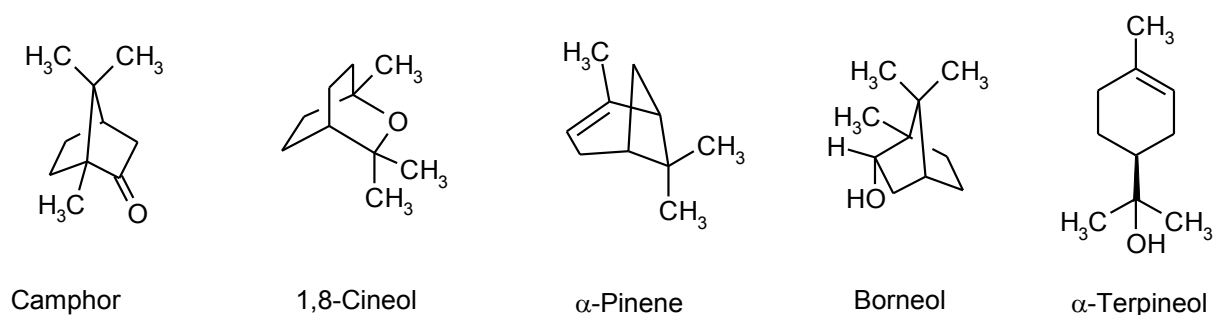


Figure 7.2: Chemical structures of the main essential oil compounds (camphor, 1,8-cineole, α -pinene, borneol, α -terpineol) present in rosemary leaves.

Antioxidants (AO) are compounds which can inhibit or retard the oxidation of lipids and other biomolecules. They prohibit the start of an oxidizing chain reaction by radicals or quench the propagation. These reactions can cause functional damage to the human body, like cancer or cardiovascular diseases. Antioxidants can prevent this process due to their redox properties like reductive behavior, the donation of hydrogen or quenching of singlet oxygen [12, 13]. Rosemary is one of the major resources for natural antioxidants. The most important

compounds are the phenolic diterpene carnosic acid (CAc) and the phenolic acid rosmarinic acid (RAc). Carnosol (CA) and rosmanol are formed by oxidative degradation of carnosic acid and are not contained initially in the leaves. Thus, these compounds are artifacts of the extraction process. The chemical structures of these antioxidants are presented in Figure 7.3 [8, 14].

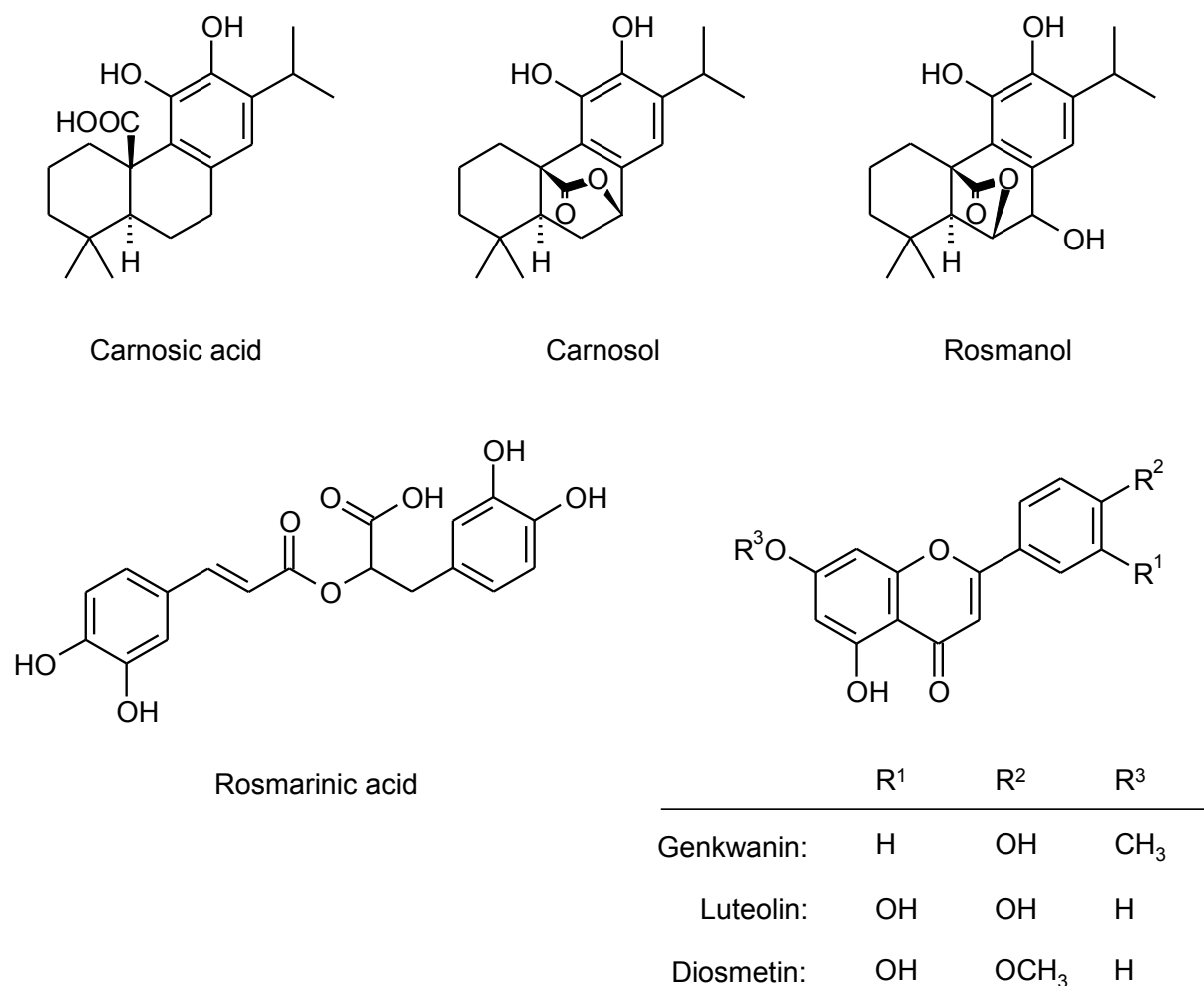


Figure 7.3: Chemical structures of the main antioxidants (carnosic acid, carnosol, rosmanol, rosmarinic acid) and flavones (genkwanin, luteolin, diosmetin) present in rosemary leaves.

The content of these antioxidants in the leaves varies in a large range due to seasonal variations, environmental influences, species and growing origin. Also large fluctuations in the individuals of the same population have been reported. In literature the content of carnosic acid varies from 4 to 30 mg per 1 g of rosemary leaves. The mass concentration of rosmarinic acid in the leaves is in a range between 2 and 25 mg/g [15-17]. However, these compounds do not only show antioxidant activity. Rosmarinic acid is also known for its antiviral, antibacterial, anti-inflammatory, and chemo-protective properties. Moreover, rosmarinic acid is a potent HIV-1 integrase inhibitor [18, 19]. Furthermore, carnosol and carnosic acid have anti-carcinogen and anti-inflammatory properties [20, 21].

Other ingredients in rosemary leaves are flavone glycosides and flavones, like genkwanin, luteolin, diosmetin [22]. Oleanolic acid and its structure isomer ursolic acid are also contained in the leaves with an amount of 10% respectively 5%. The compounds are triterpenoid saponins which are often present in the epicuticular waxes. They should prevent water loss of the plant and serve as a first defense barrier against pathogens. Oleanolic acid and ursolic acid have anti-inflammatory and anti-hyperlipidemic properties as well as antitumor-promotion effects. These saponins are relatively non-toxic and are used in cosmetics and health products [23-25]. Lipids are present as 97% *n*-alkanes and 2.3% aliphatic and cyclic alkenes in the wax of the leaves. In addition, 15 different hydroxy carbon acids were verified in the plant cuticle of the leaves. Carbohydrates are present with 5.8% acid-labile polysaccharides and 0.4% free monosaccharides [22]. In addition, small amounts of free unsaturated fatty acids (e. g. α -linolenic acid, linoleic acid, palmitic acid, myristic acid) were determined in rosemary leaves [26]. In order to recover these compounds, different extraction methods are used.

7.2.2 Extraction methods

Hydro and steam distillation are easy methods to extract the essential oil from rosemary leaves. For hydro distillation, rosemary leaves and water are put together into a flask. The suspension is heated until boiling. This procedure is in contrast to steam distillation, where the steam is generated in a separate flask and guided through the plant material. The steam takes the essential oil along and the water/oil mixture is condensed. A two phase system with water and the essential oil is produced, where the oil can be decanted and recovered [27]. The distilled and condensed water phase is called hydrosol. If this hydrosol is recycled and taken to carry out another steam or hydro distillation the process is called cohobation [28]. Hydro and steam distillation merely work because of the coexistence of two immiscible liquids (water and essential oil). The vapor pressure of the system is equal to the sum of the vapor pressures of the pure compounds. The boiling point of the mixture is lower than the boiling points of water and the essential oil. Thus, the essential oil can be extracted without reaching the boiling point of the single compounds. A limitation of this method is that low volatile substances can only be recovered in small quantities [7, 29]. Alternative methods to extract the essential oil from rosemary are supercritical carbon dioxide extraction [10, 30], subcritical water extraction [31] or microwave assisted extraction [6, 32]. Depending on the extraction also the composition of the essential oil differs.

Common methods to extract antioxidants from rosemary leaves are solvent extraction (methanol, acetone, hexane, etc.) sometimes assisted by sonication [33, 34], supercritical carbon dioxide extraction [35, 36], and subcritical water extraction [37]. Since 2010, rosemary extracts are classified as food additives by the European Commission and assigned the number E392. "Antioxidant: extracts of rosemary" has to be produced either by

solvent extraction (ethanol, acetone or ethanol followed by hexane) or supercritical carbon dioxide extraction. According to the regulation, only deodorized extracts with carnosic acid and carnosol are accredited. The content of antioxidants (carnosic acid and carnosol) has to be 15 times higher than the amount of volatile compounds [38]. This extract can be an alternative for artificial antioxidants, which have been partially restricted for food additive [2]. Synthetic antioxidants like butylated hydroxyanisole (BHA; E320) and butylated hydroxytoluene (BHT; E321) are harmful and potential carcinogen [3-5]. For this reason, the application of natural plant extracts respectively natural antioxidants in food industry gain more and more interest and importance.

7.3 Experimental section

7.3.1 Plant material

Dried rosemary (*Rosmarinus officinalis* L.) leaves were obtained from Phytotagante/France. The plants were cultivated in the region of Oujda, in the north of Morocco and dried there in the sun after harvest. "Defatted rosemary" leaves were used for some experiments. Therefore, steam distillation was previously performed by Phytotagante with these leaves to extract the essential oil. The residual leaves were dried after distillation.

For some experiments, the leaves were ground with a mortar and pestle into a coarse powder. To get a fine powder, the leaves were first frozen with liquid nitrogen in a mortar. Afterwards the leaves were grounded in the liquid nitrogen with a pestle until the nitrogen evaporated. The powder was put for 10 min in the compartment drier at 40 °C to remove the condensed water.

7.3.2 Residual moisture

The residual moisture of the rosemary leaves was determined with three different methods. High temperatures during the drying processes must be avoided to prevent the loss of flavor through volatilization of essential oil and the decomposition of antioxidants [39-43].

The first realized method was to dry rosemary in a compartment drier at 40 °C. To this purpose, the mass loss of five samples (each 1 g) with finely ground rosemary leaves was determined every hour until a constant weight was reached. A constant value was achieved after approximately 48 h.

The second method to determine the residual moisture was freeze drying. Here, about 10 g of grinded rosemary leaves were weighed in a small Schott bottle and then frozen with liquid nitrogen. Altogether, five samples were prepared. Afterwards the samples were put into a freeze drying unit and vacuum was generated. The experiment was stopped after 17 h and the mass loss of the samples was recorded.

The rotary evaporator was used in the third method. Here, about 5 g of grinded rosemary were put into a 50 mL-round bottom flask and plugged to the rotary evaporator [44]. The sample was heated to 35 °C under rotation. A vacuum of 80 mbar was generated for 4 h. The mass loss of the sample was determined afterwards.

7.3.3 Extraction methods

7.3.3.1 Soxhlet extractions

To determine the total content of rosmarinic acid and carnosic acid in the leaves, various Soxhlet extractions were carried out. To this purpose, about 6 g of ground rosemary leaves were extracted for 4 h with approximately 50 mL of solvent. Three different solvents were investigated: water (millipore), methanol (99.8%, HPLC-grade, Merck) and acetone (99.8%, Merck). After extraction, the volume of the extract was readjusted at room temperature to 50 mL with the corresponding solvent. Then, 0.5 mL of the extract solution was mixed with 0.5 mL of methanol (90%). Afterwards, 1 mL of the internal standard solution (see 7.3.4.2) was added. The solution was filtrated through a 0.2 µm PTFE syringe filter and then analyzed by HPLC/UV. All extractions were carried out three times.

7.3.3.2 Hydro distillation

Hydro distillations of rosemary leaves were performed in lab scale. To this purpose, 25 g of dried non-grinded rosemary leaves were put in a 500 mL round bottom flask and 400 mL of water (Millipore) were added. A condenser was put on top of the flask. The temperature of the steam was observed with a thermometer. The mixture was heated with a heating mantle until boiling. Extraction time was started when the first drop of the distillate was collected. The essential oil/water mixture was collected in a 100 mL graduated cylinder filled with 10 mL methyl *tert*-butyl ether (≥ 99%, Merck) as receiver for the essential oil. The suspension was heated with a heating mantle while stirring. Extractions were carried out for 0.5, 1.5, 2.5 and 4 h each three times.

The hot rosemary/water mixture was filtrated immediately after the experiment in a 500 mL volumetric flask through a filter paper. The brown solution, called “tea”, was filled up to the end volume at room temperature and stored at -20 °C until analyses. For HPLC analyses, 1 mL of the aqueous solution was mixed with 1 mL of the internal standard solution, filtrated through a 0.2 µm PTFE syringe filter and then analyzed by HPLC/UV (see 7.3.4.2). For DPPH assays the crude product or dilutions were directly used (see 7.3.4.3).

For the preparation of the distillate, the ether phase containing the essential oil was collected in a vial. The volatile solvent was evaporated under a nitrogen stream and the mass of the pure essential oil was examined. For GC analyses a 10 mg/mL solution of the essential oil in

ethanol ($\geq 99.8\%$, Sigma-Aldrich) was prepared, filtrated through a $0.2\ \mu\text{m}$ PTFE syringe filter and then analyzed by GC/FID (see 7.3.4.1).

The residual leaves were dried in a compartment drier over night at $40\ ^\circ\text{C}$. To determine the remaining amount of antioxidants, Soxhlet extractions with methanol (see 7.3.3.1) were carried out.

7.3.3.3 Steam distillation

Steam distillations of rosemary leaves were performed in an industrial scale by the company Phytotagante. To this purpose, 800 kg of dried non-grinded rosemary leaves were loaded on a perforated grid on the bottom of a stainless-steel preheated alembic and compacted to ensure the spreading of steam over the entire load. The alembic top lid was closed and the water at the bottom was heated until boiling. The pressure regulation valve was fully opened until the first drops of the distillate appeared. The valve was then slightly closed so that the distillate could be rightly cooled in the condenser which prevented the oil from being evaporated. The essential oil and the hydrosol were simultaneously collected in essence containers. The effect of cohobation was investigated during some experiments. In this method, the water phase from the distillate is poured back in the alembic to avoid the loss of essential oil in the hydrosol. Every 30 min the yield of the essential oil was examined and a sample was taken for GC analysis.

7.3.3.4 Infusion and percolation

A combination of infusion and percolation with water was used to remove rosmarinic acid and other water soluble compounds from the rosemary leaves. To this purpose, about 40 g of dried non-grinded rosemary leaves were filled in a slim and long glass column. Afterwards, 300 mL of $40\ ^\circ\text{C}$ warm water (millipore) were added. After 20 min of infusion, the water was slowly removed obtaining a yellow/brown colored solution. This procedure was repeated one more time. Then, again 200 mL of water were added and infusion was carried out for 22 h. Finally, the water was removed and the column with the rosemary leaves was purged with 200 mL of water until an almost clear solution is obtained. The extracted rosemary leaves were dried in the compartment dried at $40\ ^\circ\text{C}$ overnight. The leaves got a brown/dark green color. The leaves were grinded for further extraction experiments.

7.3.3.5 Micellar extraction

For micellar extraction of rosemary leaves, different concentrations (1, 2, 3, 4, 5 wt%) of aqueous sodium myristate solutions were prepared. To this purpose, sodium myristate (99%, Sigma-Aldrich) was weighed in a snap cap vial and the appropriate amount of water was added to obtain a total weight of 5 g. The mixture was stirred at $45\ ^\circ\text{C}$ in an oil bath to dissolve sodium myristate. After a clear solution was obtained, about 0.25 g of ground

rosemary leaves was added and the mixture was put in the oil bath at 45 °C again. A control sample was prepared in the same way, but only with water (millipore) as extraction solvent. Extractions were carried out for 5, 30 and 60 min. For some experiments the solid/liquid ratio was varied to 1/40 instead of 1/20.

The influence of the pH value on the extraction yield of antioxidants was also investigated. To this purpose, solutions with pH values of 9, 11, 13, and 14 were prepared. Therefore, a 1 M sodium hydroxide solution (TitriPUR®, Merck) was diluted with water until the desired pH value was reached. The measurements of the pH value were performed using a pHenomenal PC 5000 L multi-parameter meter from VWR International. In addition, a choline hydroxide solution (45 wt%, Taminco) was used without further treatment for some experiments. The pH value of this solution was 13.4. All extractions were carried for 5 min. The further extraction procedure was carried analogous to the micellar extraction method described before.

Furthermore, the effect of ultrasound-assisted extraction on the extraction yield was studied. At first, a 3 wt% sodium myristate solution was prepared. After the addition of grinded rosemary leaves the samples were put in ultrasonic bath at 45 °C. The frequency of the Bransonic ultrasound bath was 50 kHz. The extraction was stopped after 5 min.

After extraction, the suspensions were centrifuged for 10 min at 4000 rpm. Then 500 µL of the supernatant were taken, acidified with 100 µL formic acid, and 500 µL of the internal standard solution (0.98 mg/mL) were added (see 7.3.4.2). The solution was filtrated through a 0.2 µm cellulose acetate syringe filter and then analyzed by HPLC/UV. All extractions were carried out three times.

In addition, the extraction efficiency of alternative surfactants was investigated. Researched surfactants were: potassium myristate (97.5%, Stéarinerie Dubois), Ligastar KA M (90%, Peter Greven) and a self-prepared sodium myristate solution. The last one was prepared by dissolving 1.6 g (7 mmol) of myristic acid (98%, Carl Roth) and the exact amount of substance of sodium hydroxide pellets (99%, Merck) (7 mmol = 0.28 g) in 40 mL of water at 60 °C. After 30 min a clear solution was obtained. All extractions were carried out in the same way. Therefore, 0.25 g of grinded rosemary leaves were extracted with 5 mL of a 4 wt% surfactant solution at 45 °C in the ultrasonic bath within 5 min. After centrifugation of the suspension, 500 µL of the supernatant were taken, acidified with 100 µL formic acid, and 500 µL of the internal standard solution (0.98 mg/mL) was added. The solution was filtrated through a 0.2 µm cellulose acetate syringe filter and then analyzed by HPLC/UV. All extractions were carried out three times.

7.3.3.6 Alternative processing of the extract

An alternative processing of the micellar extract solutions was investigated. First, 0.5 g of normal grinded rosemary were extracted with 10 mL of a 4 wt% sodium myristate solution at 45 °C in the ultrasonic bath for 5 min. 5 mL of the supernatant were taken after centrifugation of the suspension. Afterwards 1 mL of formic acid was added to the solution to precipitate the myristic acid. The solution was filtrated through a tared filter paper and subsequently washed with water. On the one hand, the filter paper containing the precipitate was put in the compartment drier at 40 °C until the weight was constant. The total extraction yield was calculated by weighing the filter paper with the extract. On the other hand, the remaining filtrate was filled up to an end volume of 10 mL with water. Furthermore, extractions were carried out with acetone to classify the selectivity of the extraction method. All extraction parameters were equal to the micellar extraction. The solution was filtrated through a filter paper after extraction and washed with fresh acetone. The solvent was evaporated under a soft nitrogen stream and shortly dried in the compartment drier at 40 °C. In order to determine the total extraction yield, the snap cap vial with the extract was weighed.

In order to analyze the filtrate, 500 µL of the aqueous solution were mixed with 100 µL of methanol and 500 µL of the internal standard solution (see 7.3.4.2) were added. To analyze the content of antioxidants of the precipitate from the micellar extraction, 40 mg of the solid were dissolved in 600 µL methanol and 500 µL of the internal standard solution were added. The acetone extracts were analyzed by taking 10 mg of the solid, which was dissolved in 600 µL methanol and 500 µL of the internal standard solution (0.98 mg/mL). Solubility of all samples was enhanced in an ultrasonic bath. All solutions were filtrated through a 0.2 µm PTFE syringe filter and then analyzed by HPLC/UV. To investigate the stability of the antioxidants, especially carnosic acid, the extracts were also analyzed after 1, 3 and 7 days. The samples were stored in the dark at room temperature during this time. All experiments were carried three times.

7.3.3.7 Removal of myristic acid from the extract

A method was developed to increase the content of carnosic acid and remove myristic acid from the extract. To this purpose, extractions with aqueous sodium myristate solutions using the best parameters were carried out. Therefore, 0.5 g of grinded rosemary leaves were extracted with 10 mL of a 4 wt% solution of sodium myristate at 45 °C in the ultrasonic bath within 5 min. After centrifugation of the suspension 5 mL of the supernatant were neutralized with 1 mL of formic acid. The precipitate was filtrated, washed with water and dried in the compartment drier at 45 °C. The extract was dissolved in approximately 3 mL of ethanol. The solution was filtrated through a 0.2 µm PTFE syringe filter and put in the fridge at -20 °C for 24 h. The cooled extract was again filtrated through a 0.2 µm PTFE syringe filter to remove the precipitated myristic acid. The solvent was evaporated under a nitrogen stream and the

mass of the extract was determined. The residue was dissolved in 600 μL methanol and 500 μL of the internal standard solution were added. The solutions were filtrated through a 0.2 μm PTFE syringe filter and then analyzed by HPLC/UV. All experiments were carried three times.

7.3.4 Analysis methods

7.3.4.1 Gas chromatography (GC)

GC analyses of the essential oil samples of hydro distillation were carried out on a Hewlett Packard HP 6890 Series GC system equipped with a flame ionization detector (FID). A nonpolar HP-5 (5% phenyl- and 95% methyl-siloxane) capillary column (30 m x 0.32 mm i.d., 0.25 μm film thickness) was used for separation. Helium was applied as carrier gas at a flow of 1 mL/min. The GC was equipped with a split/splitless injector which was held at 275 °C. A HP 6890 Autosampler was employed to inject 1 μL of the sample in split mode using a split ratio of 1:10. The FID was maintained at 275 °C. The temperature of the oven was initially held at 70 °C for 3 min and then increased to 220 °C at 6 °C/min. In a final step, the temperature was raised to 250 °C at 10 °C/min and was then remained at 250 °C for 10 min. Analysis of each sample was carried out three times.

The content of the camphor in the essential oil was determined quantitatively by external calibration. To this purpose, a stock solution (1 mg/mL) of camphor (96.5%, Alfa Aesar) in ethanol ($\geq 99.8\%$, Sigma-Aldrich) was prepared. This primary stock solution was diluted to concentrations of 5.0, 2.5 and 0.5 mg/mL. The solutions were filtrated through a 0.2 μm PTFE syringe filter and then measured by GC/FID.

GC analyses of the essential oil samples of steam distillation were carried out on a Hewlett Packard HP 6850 Series GC system equipped with a flame ionization detector (FID). A polar DB-WAX (polyethylene glycol) capillary column (20 m x 0.1 mm i.d., 0.2 μm film thickness) was used for separation. Hydrogen was applied as carrier gas at a flow of 0.7 mL/min. The temperature of the injector was held at 250 °C and 0.2 μL of the pure essential oil was injected. The FID was maintained at 275 °C. The temperature of the oven was initially held at 60 °C for 2 min, increased to 248 °C at 12 °C/min and remained for 5 min. Analysis of each sample was carried out three times. The quantification of camphor was also performed by external calibration.

7.3.4.2 High-performance liquid chromatography (HPLC)

The contents of rosmarinic acid (RAc) and carnosic acid (CAc) in the extracts were determined by HPLC/UV. The analyses were performed on a "Waters HPLC System" with two Waters 515 HPLC Pumps, Waters 717plus Autosampler and Waters 2487 UV/VIS-Detector. Separation was achieved on Knauer Eurosphere C18-column (100 Å, 250 x

4.6 mm). The injection volume was each 10 μ L. The compounds were eluted at a flow rate of 1.0 mL/min and a temperature of 30 °C. The solvents for gradient HPLC consisted of 0.1% formic acid (A) and acetonitrile (B) (99.8%, HPLC-grade, Merck). The composition of the mobile phase started at 10% B, it was increased to 40% B within 40 min, further increased to 100% B within 20 min and hold then for 20 min. The detection wavelength was 204 nm. Analysis of each sample was carried out three times.

The content of the antioxidants (AO) was determined quantitatively by internal standard (IS) calibration. To this purpose, stock solutions (1 mg/mL) of rosmarinic acid (99%, Sigma-Aldrich) and carnosic acid (99%, Phytolab) in methanol (90%) were prepared. These primary stock solutions were diluted to concentrations of 1.0, 0.8, 0.6, 0.4, 0.2 mg/mL. To 1 mL of each sample, 1 mL of a 1 mg/mL solution of the internal standard gemfibrozil (98%, Cayman) was added [45]. The solutions were filtrated through 0.2 μ m PTFE syringe filters and then measured by HPLC/UV. All samples were analyzed three times. Afterwards the response factor K was calculated, which is $K(CAc) = 1.36$ for carnosic acid and $K(RAc) = 0.84$ for rosmarinic acid. For the analysis of the extracts, a gemfibrozil solution (1 mg/mL) was added to every sample and the concentration of the antioxidants was estimated with the response factors and according to equation (7.1).

$$m_{AO} = K_{AO} \frac{a_{AO}}{a_{IS}} m_{IS} \quad (7.1)$$

where m_{AO} = mass [mg] of antioxidant, K_{AO} = response factor of antioxidant and internal standard, a_{AO} = peak area [AU·s] of antioxidant, a_{IS} = peak area [AU·s] of internal standard, m_{IS} = mass [mg] of internal standard.

In literature unequal compounds are reported to quantify carnosic acid and rosmarinic acid with HPLC by internal standard calibration. Most of these compounds were used to quantify either rosmarinic acid or carnosic acid. Here, one compound should be identified for internal standard calibration which is suitable for both antioxidants. The following four compounds were selected to make a rough estimation of the response factor: butylated hydroxyanisole (BHA) (96%, Acros organics), butylated hydroxytoluene (BHT) (99%, Merck), coumarin (99%, Sigma-Aldrich), and gemfibrozil (98%, Cayman Chemical). To this purpose, solutions (1 mg/mL) of rosmarinic acid, carnosic acid and each of the potential internal standard compounds in methanol (90%) were prepared. 0.5 mL of the antioxidant solution was mixed with 0.5 mL of an IS-solution. These eight solutions were filtrated through 0.2 μ m PTFE syringe filters and then measured by HPLC/UV. The chromatograms were recorded simultaneous at 204 nm and 285 nm in order to determine the best detection wavelength. Finally, the response factors of the antioxidants to the potential IS-compounds were calculated according to equation (7.1). A detailed discussion for the decision of gemfibrozil as simultaneous internal standard for rosmarinic acid and carnosic acid is explained in chapter 7.4.1.1.3 (page 159).

7.3.4.3 DPPH assay

The free radical scavenging activity was determined using the stable 2,2-diphenyl-1-picrylhydrazyl (DPPH) radical (Sigma-Aldrich). The experiments were performed according to methods proposed by Popovici *et al.* [46] and Roby *et al.* [47], which were modified for the present assays. For calibration, a stock solution (0.1 mg/mL) of DPPH in methanol (90%) was prepared. Solubilization of the compound was enhanced in an ultrasonic bath. The solution was diluted to concentrations of 0.075, 0.05, 0.025, and 0.0125 mg/mL. Due to photosensitivity the DPPH samples are protected from light until analyses. All samples were transferred in disposable polystyrene cuvettes (10x10x45 mm, Sarstedt). The UV/VIS spectra from 350 to 700 nm of the solutions were acquired using a Varian Cary 3E UV/VIS spectrometer.

The antioxidant activity was measured for different pure compounds. To this purpose, solutions of rosmarinic acid, carnosic acid, butylated hydroxyanisole (BHA) (96%, Acros organics), ascorbic acid (98%, Sigma-Aldrich), and α -tocopherol (95.5%, Sigma-Aldrich) with a concentration of 1 mg/mL in methanol (90%) were prepared. Each solution was diluted to concentrations of 0.75, 0.5, 0.25, and 0.125 mg/mL. Dilutions of the hydro distillation water residues were prepared with the following proportions: 1/2, 1/5, 1/10, 1/20. To classify the results of the antioxidant activity, DPPH assays were also carried out for the Soxhlet extracts. To this purpose, dilution of the Soxhlet extract solutions with proportions of 1/2, 1/5, 1/10, 1/20, and 1/40 were prepared.

0.05 mL of every sample was mixed with 3.95 mL of DPPH solution (0.1 mg/mL = 250 μ M) in a lockable glass envelope, transferred in a disposable polystyrene cuvette and the UV/VIS spectrum was measured after exactly 60 min of reaction time. A blank sample was prepared at the same way, but only with 0.05 mL methanol and 3.95 mL DPPH solution. Every sample was prepared and measured three times.

The Inhibition I of the DPPH radical was calculated with equation (7.2). Inhibition is the ratio between the decrease of the absorbance in the sample and the initial absorbance of the blank DPPH solution at 518 nm.

$$I_{\text{Sample}} = \frac{A_{\text{DPPH}} - A_{\text{Sample}}}{A_{\text{DPPH}}} \quad (7.2)$$

where I_{Sample} = Inhibition of the sample, A_{DPPH} = absorbance of DPPH blank solution at 518 nm after 1 h, A_{Sample} = absorbance of DPPH/sample solution at 518 nm after 1 h reaction time.

The antioxidant activity of some essential oils was investigated in a slight modified way. First a solution of DPPH (0.1 mg/mL) in methanol was prepared. Solutions of each essential oil in methanol were prepared with an approximate concentration of 15 mg/mL. 1 mL of the essential oil solution was mixed with 3 mL of DPPH solution. The samples were transferred

in disposable polystyrene cuvettes. The UV/VIS spectra were measured after exactly 60 min of reaction time. Investigated essential oil compounds were: *trans*-anethole (99%, Sigma-Aldrich), R-(+)-limonene (97%, Sigma-Aldrich), linalool (97%, Sigma-Aldrich), citronellol (97%, Merck), citral (mixture of *cis* and *trans*, 96%, Sigma-Aldrich), α -terpineol (96%, Sigma-Aldrich), 1,8-cineole (99%, Alfa Aesar), camphor (96.5%, Alfa Aesar), α -ionone (90%, Sigma-Aldrich), and nana mint oil (Phytotagante).

7.3.5 Microemulsions

7.3.5.1 Ternary phase diagram

For the determination of a (pseudo-) ternary phase diagram the transition points between the two phasic system and the microemulsion area have to be found. This method is described by Clausse *et al.* [48]. In order to investigate the phase behavior, samples with a given weight ratio of surfactant (+ cosurfactant) to water respectively oil were prepared in screwable tubes. The initial total mass of each sample was 3 g. The temperature of the samples was kept constant at 25 °C in a thermostatically controlled water bath. Water respectively oil was added dropwise to the samples with a Pasteur pipette until a phase transition occurred. The mixture was stirred thoroughly after every drop and it was observed if a phase transition occurred. These phase transitions were detected with the naked eye. Polarizing filters were used to recognize liquid crystalline phases. These phases appeared birefringent between the cross polarizers. The amount of added water respectively oil until a phase transition occurred was determined by weighing the total mass of the samples. Finally, the weight ratios of the compounds were calculated and the (pseudo-) ternary phase diagram was drawn.

Two different systems were investigated in this thesis. The first system consisted of sodium dodecyl sulfate (SDS) (99%, Applichem), 1-pentanol (99%, Sigma-Aldrich) as cosurfactant, *n*-dodecane (99%, Merck) as oil and the hydro distillation water residue. The water residue derived from a 2.5 h lasting hydro distillation of rosemary leaves. The ratio of surfactant to cosurfactant was kept constant with 1:2. The second system consisted of TWEEN® 60 (Sigma-Aldrich) as surfactant, ethanol as cosurfactant, limonene as oil and the hydro distillation water residue as water phase. The ratio of surfactant to cosurfactant was kept constant with 2:1.

7.3.5.2 Conductivity measurements

Conductivity measurements were carried out for the system SDS/1-pentanol (1:2)/*n*-dodecane/water. The influence of the hydro distillation water residue from rosemary leaves on the present structure distribution in the microemulsion is investigated with this method. At first, a microemulsion of 4.5 g SDS, 9 g 1-pentanol, 9 g *n*-dodecane, and 2.2 g water was

produced. 20 mL of this w/o-microemulsion were introduced in the measuring cell of the conductometer. The measurements were carried out with a WTW series inoLab® Cond 730 conductivity meter equipped with a TetraCon® 325 conductivity cell. The temperature was held constant at 25 °C during the experiment. Water was progressively added to the microemulsion with an Eppendorf pipette each time the conductivity reached a stable value. The added amount of water and the corresponding specific conductivity κ was recorded. A second experiment was carried out in the same way but the hydro distillation water residue from rosemary leaves was used instead of water.

7.3.5.3 DPPH assay

The establishment of a method to measure the antioxidant activity with DPPH in microemulsions described in chapter 7.4.6.1.3 (page 184). The final procedure is described in this chapter. The antioxidant activity was investigated for the systems SDS/1-pentanol (1:2)/*n*-dodecane/hydro distillation water residue and TWEEN® 60/ethanol (2:1)/limonene/hydro distillation water residue. The ratio between surfactant/cosurfactant and oil was always 3:2. The amount of water respectively hydro distillation water residue in the final microemulsions was varied.

First of all 30 g of a microemulsion with water (Millipore) was prepared. Then, 2.5 mg DPPH were dissolved in 25 mL of this microemulsion in a volumetric flask. The solubility of the dye was enhanced in an ultrasonic bath. The remaining microemulsion without DPPH was used as a zero sample for the UV/VIS measurements. Another microemulsion with the same composition was produced, but with hydro distillation water residue instead of millipore water. The total weight of this sample was always 3 g. 0.05 mL of the hydro distillation water residue microemulsion was mixed with 3.95 mL of DPPH microemulsion (0.1 mg/mL = 250 μ M) in a lockable glass envelope. The solution was transferred in a disposable polystyrene cuvette and the UV/VIS spectrum was measured after exactly 60 min of reaction time. A blank sample was prepared at the same way, but only with 0.05 mL water-microemulsion and 3.95 mL of the DPPH microemulsion. Every sample was prepared and measured three times. The UV/VIS spectra from 350 to 700 nm of the solutions were acquired using a Varian Cary 3E UV/VIS spectrometer. Finally, the Inhibition I of the DPPH radical was calculated with equation (7.2).

7.4 Results & discussion

7.4.1 Analytical method development

Before starting the extraction experiments, it was necessary to establish suitable and efficient analyses methods. The volatile essential oil of rosemary is analyzed by GC/FID, whereas the

solvent extracts containing antioxidants are investigated by HPLC/UV. A good working analysis method is the key to meaningful results and the following discussion.

7.4.1.1 HPLC

At the beginning the HPLC system only consisted of one Waters 515 HPLC pump, Waters 717plus Autosampler, Waters 2487 UV/VIS-detector, and Waters 410 RI-Detector (Differential Refractometer). The software "Millenium 32[®]" was used for the recording and evaluation of the chromatograms. Separation of the compounds was achieved on a Knauer Eurosphere C18-column (100 Å, 250 x 4.6 mm). Due to the presence of just one solvent pump, only isocratic elution of the compounds was possible. In literature only a few methods are described to separate rosemary extracts with isocratic elution on a C18-column. However, the composition of the eluents acetonitrile and acidified water varied between the citations [49, 50]. For this reason, acetonitrile/phosphoric acid (0.1%) solutions with different ratios were investigated for an efficient separation. A Soxhlet extract of rosemary served as test sample to compare the separation efficiency. But the appearance of the chromatograms was not satisfactory. The higher the content of water the better was the peak resolution. But adverse effects, like the extension of analysis time and the broadening of the peak shape especially at higher retention times occurred. In summary, it was difficult to separate the Soxhlet extract of rosemary leaves with isocratic elution. This is primarily due to the fact that in general plant extracts contain a lot of compounds with different properties. This characteristic made it impossible to separate the mixture properly. Detailed results will not be shown. To analyze and separate the complex composition of a plant extract it is inevitable to perform the separation with a gradient mobile phase. Fortunately the HPLC system was upgraded with a second Waters 515 HPLC pump and a PCM II module to control the pumps with the computer. In addition the recording and evaluation software was updated to "Empower 3[®]". Henceforth, it was possible to perform gradient elution and to run the HPLC overnight due to the integrated safety precautions. A small disadvantage was that the RI-detector cannot be used anymore with gradient elution.

7.4.1.1.1 Improvement of compound separation

A lot of different methods and solvents for the separation of compounds present in rosemary extracts are available in literature. But the most common method was gradient elution with acetonitrile and acidified water with a detection wavelength of 285 nm or 230 nm. For this reason, gradient elution with acetonitrile and acidified water was selected for separation. The detection wavelength was set at 285 nm. The temperature of the column was kept constant at 30 °C. The injection volume was set at a value of 10 µL. Again, a first method was developed by analyzing a Soxhlet extract of rosemary leaves. Therefore only the composition of the solvents for gradient HPLC was changed. The total flow of the eluent was 0.7 mL/min.

The separation was started with a solvent composition of 98% acidified water (0.1% formic acid) and 2% acetonitrile. The ratio of acetonitrile was linearly increased up to 100% in 50 min and hold for 10 min. The starting ratio of the solvents was reinstated within 3 min and held for 7 min in order to equilibrate the column. The chromatogram of a rosemary leave methanol Soxhlet extract is shown in Figure 7.4.

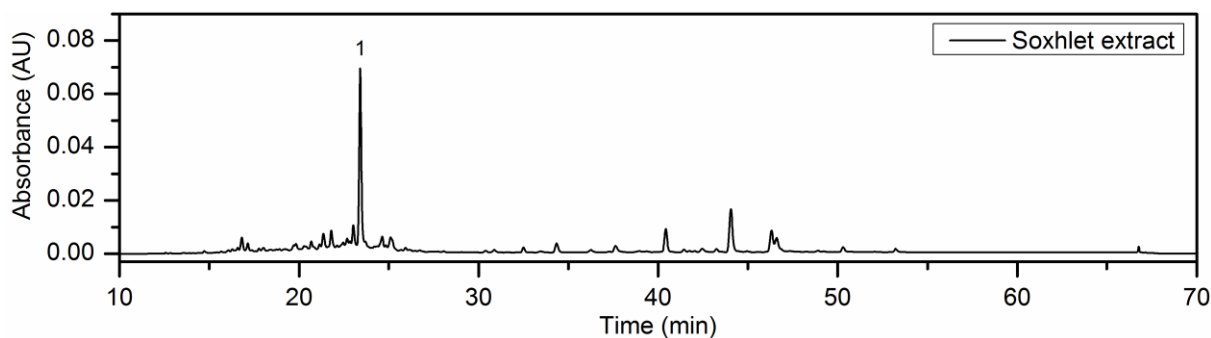


Figure 7.4: HPLC chromatogram of a methanol Soxhlet extract of rosemary leaves. Peak identification: (1) rosmarinic acid; Carnosic acid and carnosol are probably present at retention times between 40 and 50 min.

This method was mainly used for the analyses of the hydro distillation water residue of rosemary leaves. In comparison to the methanol Soxhlet extract, the chromatogram of the water residue shows only peaks with a small retention time. Consequently, the polar water-soluble compounds have small retention times and the polarity of the separated compounds decreases with rising retention time. This first method was good enough to determine rosmarinic acid at a retention time of 23.45 min. Qualitative and quantitative determination of rosmarinic acid was carried out by external standard calibration. A disadvantage of this analysis method was that carnosic acid could not be determined due to the lack of an appropriate standard. A further drawback of this method was that the separation of the polar compound could have been more sufficient.

Thus, the separation method was again changed to determine simultaneously rosmarinic acid and carnosic acid. Total flow was set at 1 mL/min. The separation was started with an eluent composition of 90% acidified water (0.1% formic acid) and 10% acetonitrile to elute the very polar compounds at lower retention times. A slower increase of the acetonitrile ratio led to a better separation of the polar compounds at smaller retention times. That is why the ratio of acetonitrile was linearly increased up to 40% in 40 min and further increased to 100% within 20 min. This composition was held for 20 min to remove potential residues from the column. The starting ratio of the solvents was reinstated within 3 min and held for 7 min in order to equilibrate the column. This gradient elution improved not only the separation of the hydrophilic, but also the more hydrophobic compounds like carnosic acid or carnosol. The retention times with this separation method are now 27.71 min for rosmarinic acid, 56.09 min

for carnosic acid and 54.04 min for carnosol. The only disadvantage of this improved method is that the total analyses time increases from 70 min to 90 min for one injection.

7.4.1.1.2 External calibration

As already mentioned, the amount of rosmarinic acid in an analysis sample was preliminary determined quantitatively by external standard calibration. To this purpose, the first investigated gradient with a total analyses time of 70 min was used for separation. Four different samples with concentrations of rosmarinic acid in methanol between 0.01 mg/mL and 0.15 mg/mL were analyzed under the same conditions with a detection wavelength of 285 nm. The concentrations of the calibration samples should be in the range of the investigated extract samples. The peak areas of rosmarinic acid at a retention time of 23.45 min were determined for the different calibration samples. The linear calibration function was obtained by plotting the concentration of rosmarinic acid against the corresponding peak areas.

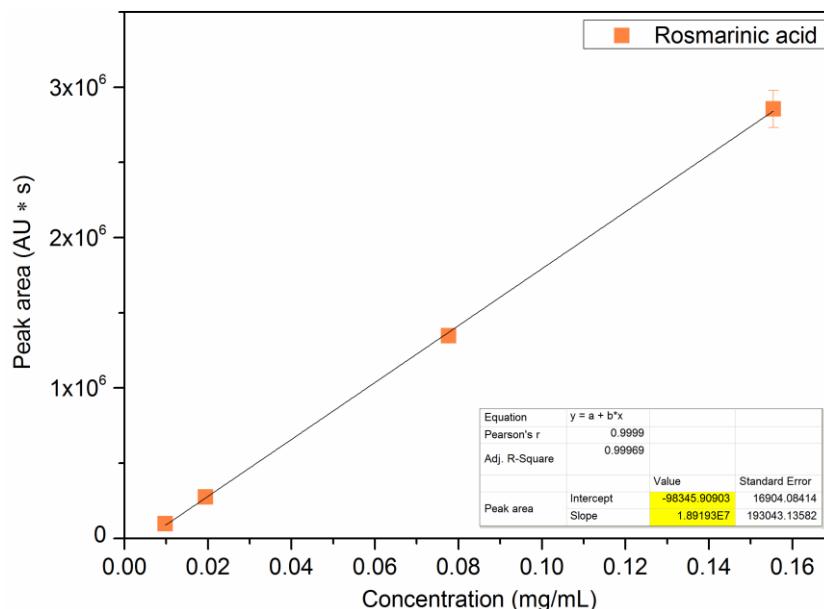


Figure 7.5: Determination of the linear function of rosmarinic acid for external calibration. The concentration of rosmarinic acid is plotted against the corresponding peak area. By means of the slopes and intercept of the graph, the rosmarinic acid concentration of an extract sample can be calculated.

The concentration of rosmarinic acid in an extract sample can be calculated by means of the slopes and intercept of the graph with equation (7.3).

$$\beta_{RAC}(sample) = \frac{a_{RAC}(sample) - intercept}{slope} = \frac{a_{RAC}(sample) + 98345 \text{ AU} \cdot s}{1.89 \cdot 10^7 \frac{\text{AU} \cdot s}{\text{mg/mL}}} \quad (7.3)$$

where $\beta_{RAC}(sample)$ = calculated mass concentration [mg/mL] of the analyzed sample, $a_{RAC}(sample)$ = peak area [AU·s] of rosmarinic acid in the analyzed sample, $intercept$ = intercept [AU·s] of the external calibration function, $slope$ = slope [(AU·s)/(mg/mL)] of the external calibration function.

Analysis with external calibration is a simple method to carry out, because the analyzed sample has not to be prepared in a special way. Only an inappropriate concentration respectively dilution of the sample need to be found. But systematic errors can occur and falsify the results. Possible errors can be the inaccuracy of Autosampler syringe, volatilization of solvent or dilution respectively pipetting errors. The standard deviation of the sample was sometimes getting too high and the results were not consistent enough for an efficient interpretation. For this reason, a new method with internal calibration had to be established, which should avoid dissimilar results of the analyses.

7.4.1.1.3 Internal standard calibration

In literature various compounds are reported to quantify carnosic acid and rosmarinic acid with HPLC by internal standard calibration. Most of these compounds were used to quantify either rosmarinic acid or carnosic acid. Here, a compound should be identified which is suitable for internal standard calibration of both antioxidants. The following four compounds were selected to make a rough estimation of the response factor: butylated hydroxyanisole (BHA) [22], butylated hydroxytoluene (BHT), coumarin [51], and gemfibrozil [45]. The chemical structures of these compounds are presented in Figure 7.6.

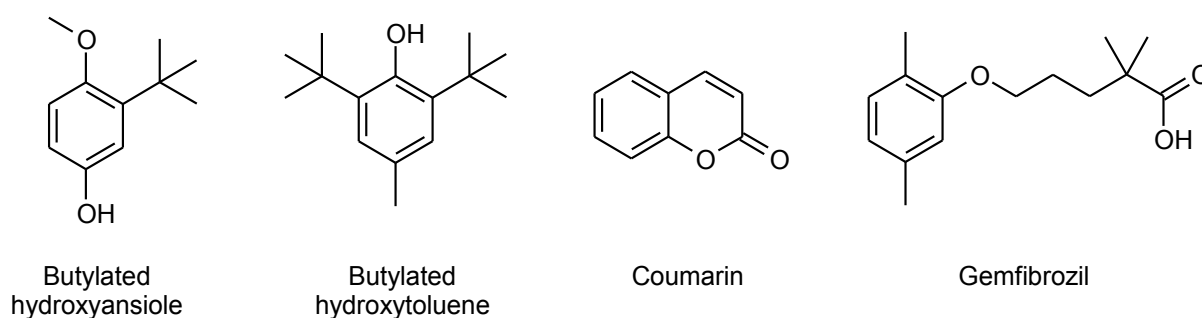


Figure 7.6: Chemical structures of potential internal standard molecules (butylated hydroxyanisole, butylated hydroxytoluene, coumarin, gemfibrozil).

These compounds have to fulfill different requirements for the application as internal standard. The substance may not be present in the test sample at the beginning. It should be chemical stable respectively inert to the solvent and other compounds in the test sample. A suitable internal standard should also be a pure, clearly defined compound with similar

properties with respect to the analyte. Another important requirement for an appropriate substance is that the peak is without any overlap to other peaks in the chromatogram [52, 53].

Solutions of rosmarinic acid and carnosic acid mixed with each of the potential internal standard compounds in methanol were prepared and then measured by HPLC/UV. Also measurements of the pure compounds were carried out to identify the peaks and determine the corresponding retention times. The second investigated gradient with an analyses time of 90 min was used for separation. The chromatograms were recorded simultaneous at 204 nm and 285 nm in order to determine the best detection wavelength. Figure 7.7 shows the HPLC chromatograms of different potential internal standards, rosmarinic acid, and carnosic acid at detection wavelengths of 204 nm and 285 nm.

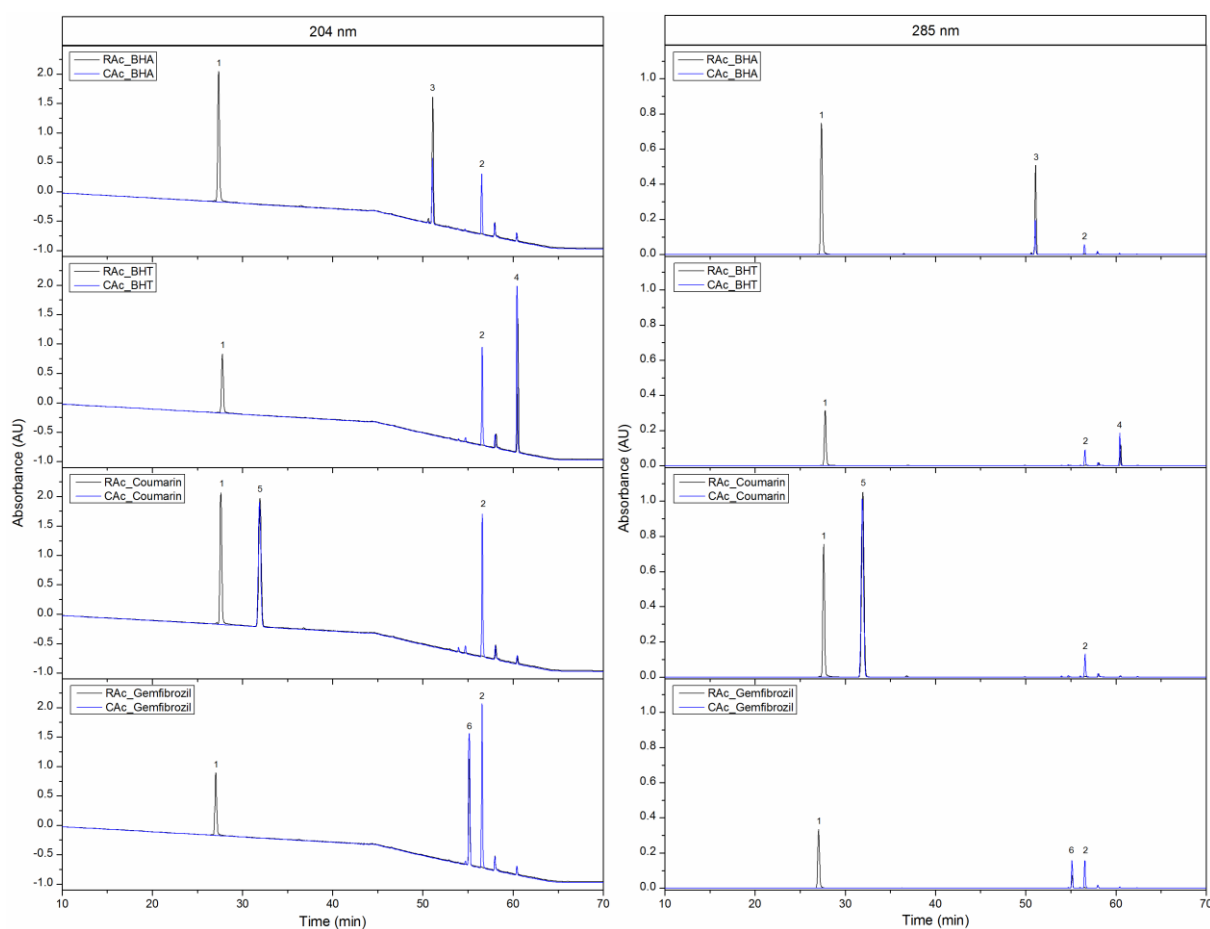


Figure 7.7: HPLC chromatograms of different potential internal standards, rosmarinic acid and carnosic acid at detection wavelengths of 204 nm and 285 nm. Peak identification: (1) rosmarinic acid; (2) carnosic acid; (3) BHA; (4) BHT; (5) coumarin; (6) gemfibrozil

First of all it can be seen that the absorbance of the compounds is higher at a detection wavelength of 204 nm compared to 285 nm. As a consequence, lower concentrations of the compounds are detectable at 204 nm. This results in a better limit of detection at 204 nm compared to 285 nm. The retention times of carnosic acid was determined to be 56.09 min

and 27.71 min for rosmarinic acid. The retention time of the potential internal standard compounds are 31.94 min for coumarin, 50.98 min for BHA, 55.06 min for gemfibrozil and 60.45 min for BHT. An additional knowledge of these measurements is that a low amount of BHT is present in every analyzed sample. This suggests a possible contamination of the HPLC system with BHT. Perhaps, this is due to sediments of other analyzed samples, which were prepared with diethyl ether. Because this ether contains BHT as inhibitor to prevent oxidation and formation of explosive peroxides [54]. Although purging the system with different solvents could not remove the butylated hydroxytoluene.

The chromatogram of a pure Soxhlet extract was compared with the chromatograms of the potential internal standard compounds. It is determined that no compound is present in the extract at the beginning. Only a small peak of BHT was certainly observed. Subsequently, the potential internal standards substances were added to the Soxhlet extract sample and analyzed. It was found out that the peaks of the potential internal standard compounds do not disturb the chromatogram. Also no overlap or interference of the peaks was determined.

Some requirements for internal standard calibration are conformed. But for a better evaluation of the suitability for internal standard calibration, the response factors K_{AO} for the antioxidants to the potential IS-compounds were calculated. This was only a simple determination of the response factor, as only one sample with a defined amount of the antioxidant and the IS-compound was analyzed and from this the K-value was calculated. Ideally the response factor should be 1. The determined values of K_{AO} for carnosic acid and rosmarinic acid for different internal standards in dependence on the detection wavelength are summarized in Table 7.1.

Table 7.1: Response factors K_{AO} of carnosic acid and rosmarinic acid for different internal standards (BHA, BHT, coumarin, gemfibrozil) in dependence on the detection wavelength. Suitable K-values are marked green, whereas inappropriate values are marked red.

Internal standard	$K_{\text{Rosmarinic acid}}$		$K_{\text{Carnosic acid}}$	
	204 nm	285 nm	204 nm	285 nm
BHA	0.756	0.466	1.217	3.720
BHT	1.052	0.219	1.652	1.587
Coumarin	1.365	1.912	1.947	16.317
Gemfibrozil	1.121	0.130	1.026	0.953

Table 7.1 shows that all compounds are suitable for internal standard calibration of rosmarinic acid at a detection wavelength of 204 nm, but only BHA and gemfibrozil for carnosic acid. Due to these results BHT and coumarin will not further be investigated for the

simultaneous internal standard calibration of carnosic acid and rosmarinic acid. Another argument against BHT is the presence of the compound in the chromatograms of all measurements. For this reason, only BHA and gemfibrozil are still potential internal standards. However, gemfibrozil will be further investigated because of the higher purity of the chemical product compared to BHA.

Subsequently, a meaningful determination of the response factor for rosmarinic acid and carnosic acid to gemfibrozil is necessary. To this purpose, stock solutions of rosmarinic acid and carnosic acid in methanol were prepared. These primary stock solutions were diluted to concentrations of 1.0, 0.8, 0.6, 0.4, 0.2 mg/mL. To 1 mL of each sample, 1 mL of a 1 mg/mL solution of the internal standard gemfibrozil in methanol was added and then measured by HPLC/UV. The detection wavelength in further measurements was set at 204 nm. The concentration of gemfibrozil in all samples was kept constant at 0.5 mg/mL.

The response factor of gemfibrozil and both antioxidants is determined by plotting the ratio of the antioxidant peak area and gemfibrozil area against the ratio of antioxidant concentration and gemfibrozil concentration. Figure 7.8 shows that a linear trend can be observed. In this case, the slope of the linear function represents the response factor, which is $K(CAc) = 1.36$ for carnosic acid and $K(RAc) = 0.84$ for rosmarinic acid. For the analysis of further extracts, a gemfibrozil solution (1 mg/mL) was added to every sample and the concentration of the antioxidants was estimated with these response factors

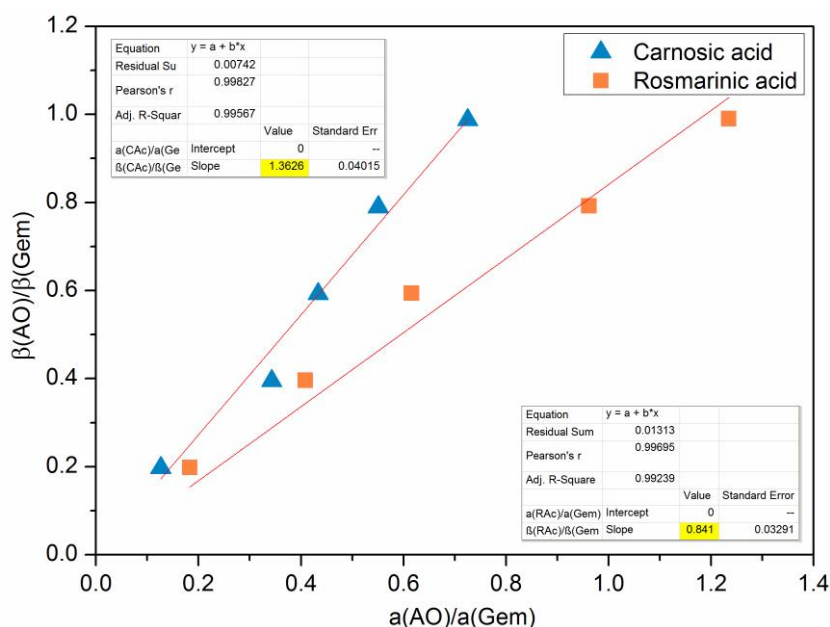


Figure 7.8: Determination of the response factors of rosmarinic acid (K_{CAc}) and rosmarinic acid (K_{RAc}) with gemfibrozil for internal standard calibration. The slopes of the graphs indicate the corresponding response factors of the antioxidants. β correlates to the mass concentration of the antioxidants and gemfibrozil, whereas, a is the determined peak area of the compounds.

To sum up, a new method for internal standard calibration of rosemary extracts was established. By means of the compound gemfibrozil and the corresponding response factors it is possible to determine simultaneously the content of rosmarinic acid and carnosic acid.

7.4.1.2 GC

The essential oil of rosemary leaves obtained by steam or hydro distillation only contains volatile compounds. For this reason, analyzes were carried out by capillary gas chromatography with a flame ionization detector (GC/FID). Analysis was focused on the two main compounds 1,8-cineole and camphor.

7.4.1.2.1 Improvement of compound separation

The requirements for the analysis of essential oil by gas chromatography are well resolved peaks and not distorted ones, a good signal to noise relation and a horizontal base line with the absence of drift. The essential oil contains compounds with different molecular weights, from the most volatile hydrocarbons of ten carbon atoms (monoterpenes), oxygenated compounds of 15 atoms of carbon (sesquiterpenes) and aromatic hydrocarbons. For this reason, it is necessary to start with low temperatures which allow the separation of the most volatile ones. Then the temperature is raised with 5 °C or 10 °C per minute to reach the temperature of 200 °C to achieve the elution of the heaviest. Preferably, polar capillaries (carbowax polyethylene glycol) are the most common columns used for the analysis of essential oils [55, 56]. Contrary to this approach, a nonpolar HP-5 (5% phenyl- and 95% methyl-siloxane) capillary column was used for separation in this case. For this reason only the temperature profile had to be adjusted.

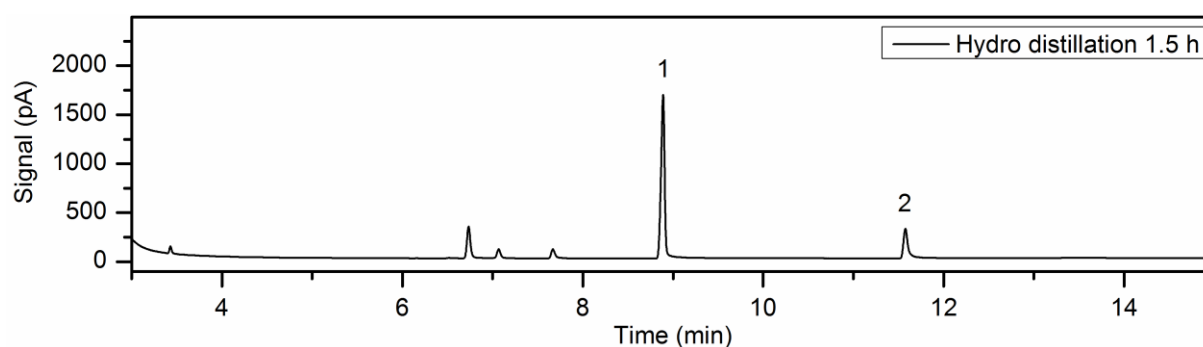


Figure 7.9: GC/FID chromatogram of rosemary essential oil obtained by hydro distillation. Separation was achieved on a nonpolar HP-5 column. Peak identification: (1) 1,8-cineole; (2) camphor;

Figure 7.9 shows a GC/FID chromatogram of rosemary essential oil obtained by hydro distillation. The sequence of separation of the compounds are eluted in ascending order of their boiling points (bp) [57]. The retention times of the main compounds were determined to be 8.90 min for 1,8-cineole (bp = 176-177 °C [58]) and 11.60 min for camphor

(bp = 204 °C [59]). Separation of the compounds of the extract was achieved by a temperature gradient of the column. First of all, the temperature of the oven was held at 70 °C for 3 min and then increased to 220 °C at 6 °C/min. At least the temperature was raised to 250 °C at 10 °C/min and was then remained at 250 °C for 10 min. Temperature was kept at higher values in order to remove some residual compounds from the column.

7.4.1.2.2 External calibration for camphor and 1,8-cineole

The quantitative analysis of the extracted samples was carried out by external calibration for camphor and 1,8-cineole, which are the main compounds in the essential oil of rosemary. Four different samples of each 1,8-cineole and camphor with concentrations between 0.25 mg/mL and 5.0 mg/mL in ethanol were analyzed under the same conditions by GC/FID. The linear calibration functions were obtained by plotting the concentrations of the compounds against the corresponding peak areas.

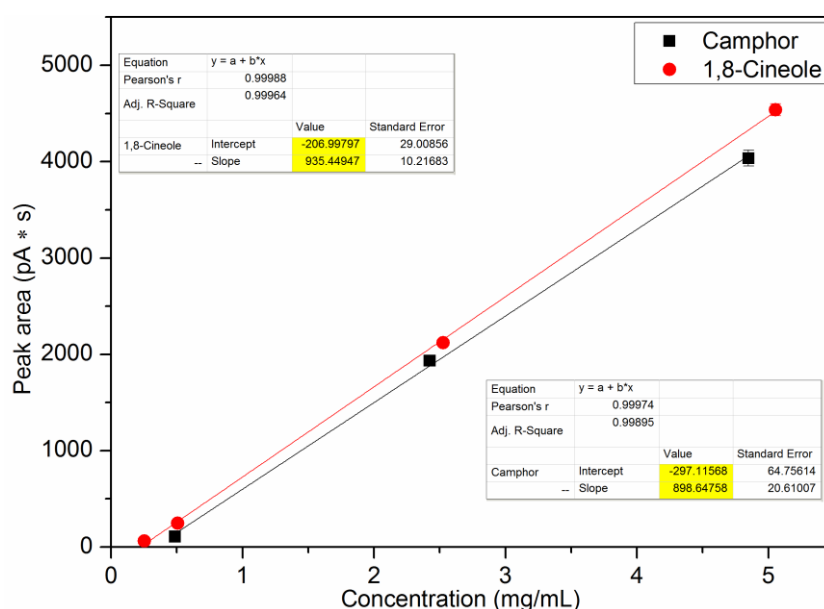


Figure 7.10: Determination of the linear functions of 1,8-cineole and camphor for external calibration. The concentrations of the essential oils are plotted against the corresponding peak areas. By means of the slopes and intercept of the graph, the concentrations of 1,8-cineole and camphor in an extract sample can be calculated.

The concentrations of 1,8-cineole and camphor in an extract sample can be calculated by means of the slopes and intercepts of the graphs with equation (7.4).

$$\beta_{EO}(\text{sample}) = \frac{a_{EO}(\text{sample}) - \text{intercept}}{\text{slope}} \quad (7.4)$$

where $\beta_{EO}(\text{sample})$ = calculated mass concentration [mg/mL] of the essential oil in the analyzed sample, $a_{EO}(\text{sample})$ = peak area [pA·s] of the essential oil compound in the

analyzed sample, *intercept* = intercept [pA·s] of the external calibration function, *slope* = slope [(pA·s)/(mg/mL)] of the external calibration function.

Analysis with external calibration is a simple method to carry out, because the analyzed sample has not to be prepared in a special way. An appropriate concentration of the sample to be analyzed is approximately 10 mg/mL of extract in ethanol. Summing up, external calibration was sufficient for the determination of the concentration of 1,8-cineole and camphor in the extracts.

7.4.2 Characterization of rosemary leaves

The characterization of the used rosemary leaves is important, because rosemary leaves are a natural product and the composition is subjected to large variations. These deviations can be due to seasonal variations, environmental influences, species and growing origin. Also large fluctuations in the individuals of the same population have been reported [15-17]. For this reason, the residual moisture, the content of antioxidants (rosmarinic acid, carnosic acid), and the fraction of essential oil of the used rosemary leaves are investigated.

7.4.2.1 Residual moisture

Three different methods were compared for the determination of the residual moisture of normal dry rosemary leaves. The investigated methods were drying in a compartment drier at 40 °C, in a rotary evaporator at 35 °C under reduced pressure and freeze drying. It is known that high temperatures during the drying processes must be avoided in order to prevent the loss of flavor compounds through volatilization of the essential oil and the decomposition of antioxidants [39-43]. Therefore, a drying method for 2 h at 105 °C after the Pharmacopoea Europaea (Ph. Eur.) was not realized [60].

The results of the experiments showed that there is a large deviation between the different methods to determine the residual moisture. The first investigated method was to dry rosemary leaves in a compartment drier at 40 °C and monitor the weight loss of the samples over time. The mass of the leaves decreases significantly in the first six hours of drying. After approximately 48 h a maximum value is reached (Figure 7.11). This mass loss related to the initial mass is considered to be the residual moisture of the leaves. It is calculated to be $3.48 \pm 0.04\%$ for the rosemary leaves.

Freeze drying is also a gentle method to remove water from plants. The functional principle is based on the sublimation of crystalline water at reduced pressure. The weight of the samples was weighed back after 17 h of freeze drying. The calculated residual moisture of the leaves is 3.03% and thus comparable to the value obtained by the compartment drier experiments. But this method was not further carried out because of the more elaborate procedure.

The third researched method to determine the residual moisture was by means of the rotary evaporator. Rosemary leaves were dried at 35 °C under a reduced pressure of 80 mbar for 4 h. After this time only a fraction of the water amount compared to the other methods was recovered from the leaves. For this reason, this method was not further investigated. Summing up, drying and the simultaneous weighing of rosemary samples in the compartment drier at 40 °C is an easy and not elaborate way to determine the residual moisture.

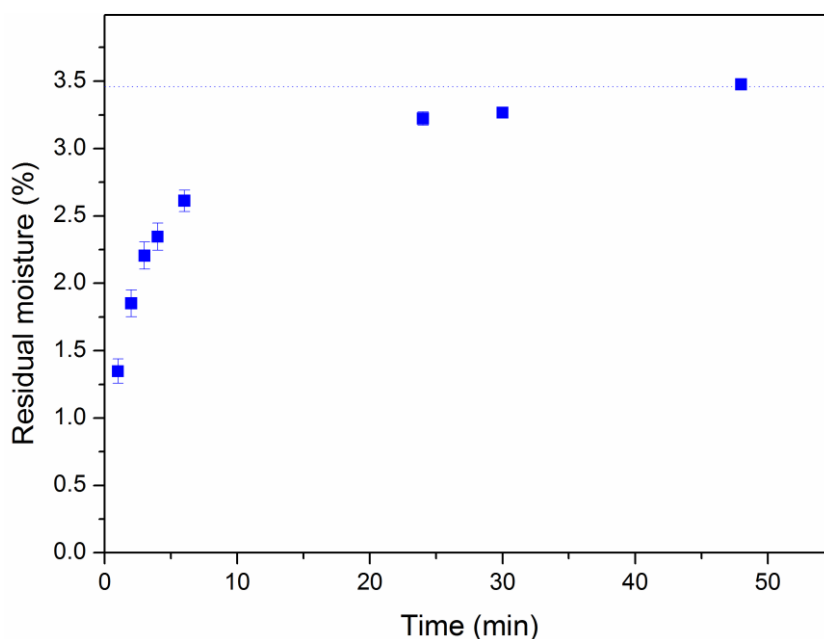


Figure 7.11: Investigation of the residual moisture of normal rosemary leaves. The values were determined by the mass loss of grinded leaves in a compartment drier at 40 °C. A maximum value of 3.48% is reached after 48 h.

The residual moisture of the defatted rosemary leaves was also determined in the compartment drier at 40 °C. The value of 2.55% is slightly smaller than the one of normal rosemary leaves.

7.4.2.2 Content of antioxidants

Soxhlet extractions were carried out in order to determine the total amount of rosmarinic acid and carnosic acid. The challenge to extract these compounds is that rosmarinic acid is soluble in water, whereas carnosic acid is not. Figure 7.12 shows the three different investigated solvents for Soxhlet extractions. As expected, water, a polar protic solvent, can extract the highest amount of rosmarinic acid with 8.90 mg per 1 g rosemary, but only a negligible amount of carnosic acid. The extraction behavior of the aprotic polar solvent acetone is opposite and the highest amount of carnosic acid with 23.62 mg/g can be extracted. Methanol is also a protic solvent, but less polar than water. It combines the extraction efficiency of both, water and acetone.

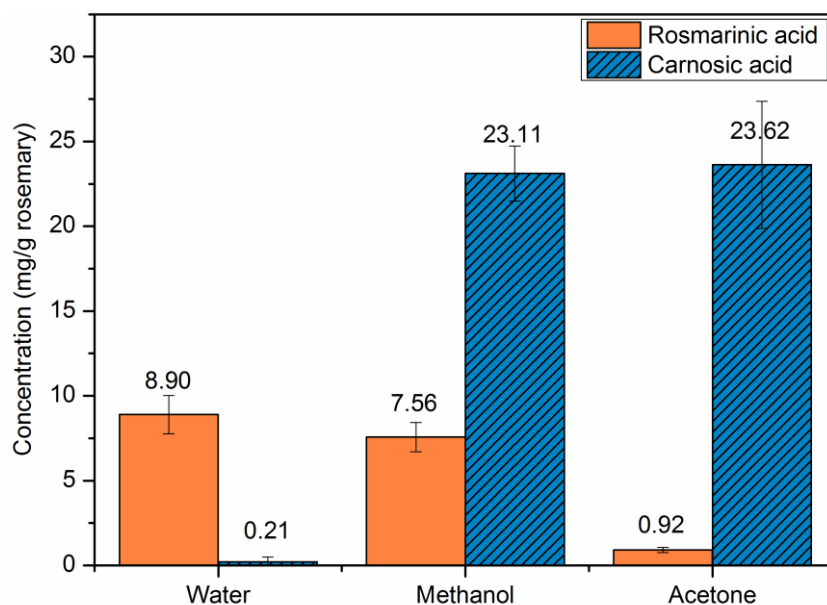


Figure 7.12: Mass concentration of rosmarinic acid and carnosic acid yields obtained by Soxhlet extraction lasting 4 h with different solvents: water, methanol and acetone. Concentrations are given in mg of antioxidant per 1 g of rosemary leaves.

The differences in extraction selectivity can also be seen in the chromatograms of the different solvent extracts (see Figure 7.13). Water extracts compounds with small retention times (r.t.), which are polar substances, whereas acetone extracts less polar substances with higher retention times. The chromatogram of the methanol extract is nearly a combination of both. Also the main degradation product of carnosic acid, which is carnosol, can be extracted with each solvent. Other antioxidants which are present in the extracts are rosmanol (r.t. = 28.2 min) and methyl carnosate (r.t. = 57.9 min). As a result, methanol is a suitable solvent for Soxhlet extraction to determine the total amount of the antioxidant compounds, rosmarinic acid and carnosic acid, from rosemary leaves.

The content of antioxidants in the defatted rosemary leaves was also investigated. It is determined that less antioxidant compounds are contained in the leaves after steam distillation. In detail, 3.94 mg/g of rosmarinic acid and 14.05 mg/g of carnosic acid are left in the rosemary leaves. This means that the amount of rosmarinic acid is lowered to 44.3% and 59.4% for carnosic acid related to the initial content. Consequently, steam distillation strongly influences the antioxidant content in rosemary leaves. Results from literature are in agreement with these findings, where the degradation of carnosic acid to carnosol and the loss of rosmarinic acid during steam distillation were described [61]. In this thesis the influence of hydro distillation on the antioxidant compounds in the rosemary leaves were investigated in detail. The results are presented and discussed in chapter 7.4.4.2.

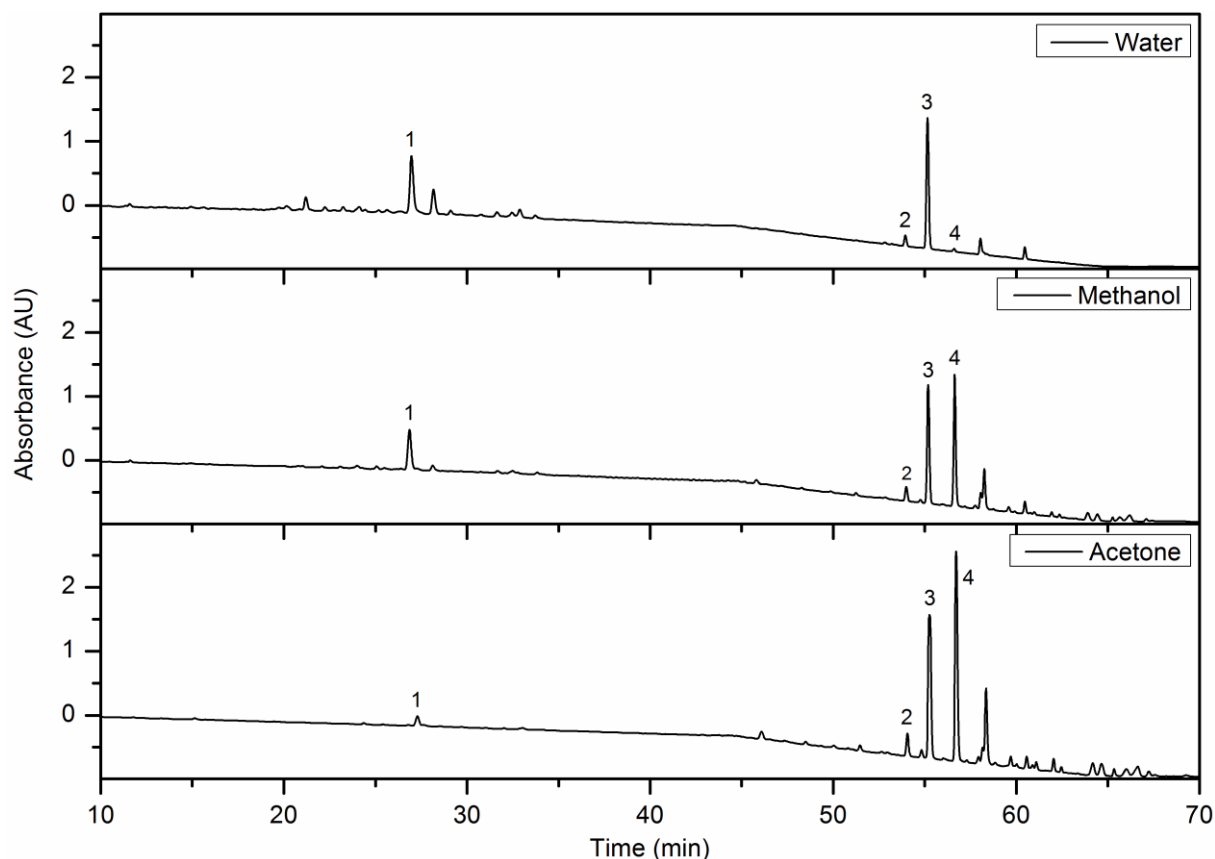


Figure 7.13: HPLC chromatograms of Soxhlet extracts from rosemary leaves obtained by different solvents: water, methanol and acetone. Peak identification: (1) rosmarinic acid; (2) carnosol; (3) gemfibrozil (IS); (4) carnosic acid;

7.4.2.3 Content of essential oil

The maximum content of essential oil in the dried rosemary leaves was investigated by exhaustive hydro distillation. It was determined to be 1.8% (w/w) of the initial mass of rosemary leaves. A detailed examination of the essential oil extraction and composition is presented in chapter 7.4.3. In contrast, the defatted rosemary leaves contain no more essential oil.

7.4.2.4 Summary

Different characteristic parameters of the normal and defatted Moroccan rosemary leaves were determined in the previous chapters. The results are summarized in Table 7.2. It was found out that the residual moisture is 3.48% for normal rosemary leaves and 2.55% for defatted leaves. An appropriate method to examine the residual moisture is the monitoring of the mass loss of grinded rosemary leaves in a compartment drier at 40 °C within 48 h. In addition, Soxhlet extractions were carried out in order to investigate the content of antioxidant compounds in the leaves. Methanol is a suitable solvent to extract and determine simultaneously the total amount of rosmarinic acid and carnosic acid. The amount of carnosic

acid is 23.62 mg/g in normal rosemary leaves and 8.90 mg/g for rosmarinic acid. The content of antioxidant compounds in defatted rosemary leaves is lower. In detail, the concentration of carnosic acid is 14.02 mg/g and 3.94 mg/g for rosmarinic acid. The maximum content of essential oil in the dried rosemary leaves was investigated by hydro distillation. It was determined to be 1.8% (w/w) related to the initial mass of rosemary leaves. In contrast, the defatted rosemary leaves contain no more essential oil.

Table 7.2: Summary of the examined characteristic parameters of normal and defatted rosemary leaves.

		Normal rosemary leaves	Defatted rosemary leaves
Residual moisture		3.48%	2.55%
Content of	Rosmarinic acid	8.90 mg/g	3.94 mg/g
	Carnosic acid	23.62 mg/g	14.02 mg/g
	Essential oil	1.80%	-

7.4.3 Extraction of essential oil

The essential oil from rosemary is commonly gained by hydro (HD) or steam distillation (SD) with a maximum extraction yield of 1.0-2.5%. The differences of these two methods on the extraction yield and the time-dependent content of camphor in the essential oil are compared.

The results of this section are part of a publication, submitted to the Journal *Comptes rendus Chimie*. The article with the title “Antioxidant activity of hydro distillation water residues from *Rosmarinus officinalis* L. determined by DPPH assays” will be published in the special issue “WAS2015 - Alternative solvents for extraction, purification and formulation” of the journal. The chapters 7.4.4 and 7.4.5 are also part of the publication.

7.4.3.1 Yield of essential oil

First, the differences between steam and hydro distillation for the recovery of the essential oil were examined. These processes have been already extensively studied for rosemary leaves from different origins [27, 62, 63]. In this study, the results refer to rosemary which was cultivated in Morocco. The maximum extraction yield of essential oil obtained by steam distillation is 2.5% (w/w), whereas hydro distillation only provides 1.8% (w/w) of the initial leave weight. These values are higher than the one of the Algerian and Tunisian rosemary, where the maximum yield of essential oil by steam distillation was approximately 1.2% and

0.44% by hydro distillation [27]. Figure 7.14 shows the differential and total extraction yields of essential oil as a function of distillation time. A similar behavior for hydro and steam distillation can be observed. At the beginning the yield increases quickly and then becomes slower with time until a plateau is reached. The trend of the curves is similar to the ones reported in literature [32]. After 4 h of extraction the complete amount of essential oil is recovered. Moreover, it is shown that after 30 min of distillation 67% of the essential oil are recovered by steam distillation, but only 22% by hydro distillation. The yield after 0.5 h of extraction is indeed 1.7% (w/w) for steam distillation and 0.54% (w/w) for hydro distillation.

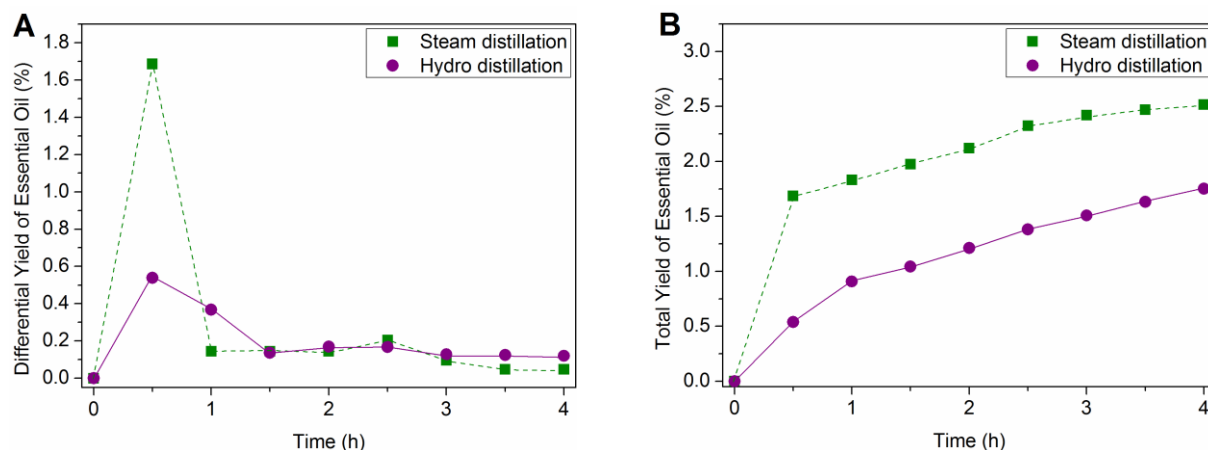


Figure 7.14: (A) Differential and (B) total extraction yield of essential oil gained by hydro distillation and steam distillation at different times. The yield is given in weight percent of the initial mass of rosemary leaves.

In addition, the influence of cohobation during steam distillation has been investigated. Normally, the rosemary hydrosol is cohobated separately in an empty alembic after reaching a certain volume. In this case, a fixed volume of hydrosol was added to the alembic filled with rosemary before the distillation. In view of the results, the addition of hydrosol negligibly decreases the extraction yield of rosemary oil from 2.5% to 2.3% by slowing down the distillation.

7.4.3.2 Content of camphor in essential oil

The appearance of crystallized camphor was once noticed during the steam distillation of rosemary after 1.5 h. The crystals generated significant attention with regard to the rosemary essential oil quality. Actually, a high dose of camphor is toxic when ingested and may cause convulsions and vomiting [64]. Therefore, the composition of rosemary essential oil for commercial use is regulated in the NF ISO 1342:2001 [65]. The content of camphor in the essential oil gained by hydro and steam distillation is thus investigated over time for the Moroccan rosemary.

Figure 7.15 presents the camphor content in the essential oil as a function of distillation time. Again, a similar behavior for hydro and steam distillation can be observed. At the beginning, the camphor content increases quickly and then decreases again. Only the distillation time with the maximum content differs between hydro and steam distillation. Hydro distillation reaches a maximum value of camphor after 1 h of distillation, whereas the maximum using steam distillation is reached only after 2 h. The differences can be explained by the varying order of compounds depending on the distillation method. In literature it is suggested that the volatile compounds are recovered in ascending order of their boiling points by steam distillation. By contrast, in case of hydro distillation the order of compound recovery depends on their polarity [27]. Due to the high boiling point (209 °C) of camphor and the slightly polar structure the extraction time is smaller in hydro than in steam distillation.

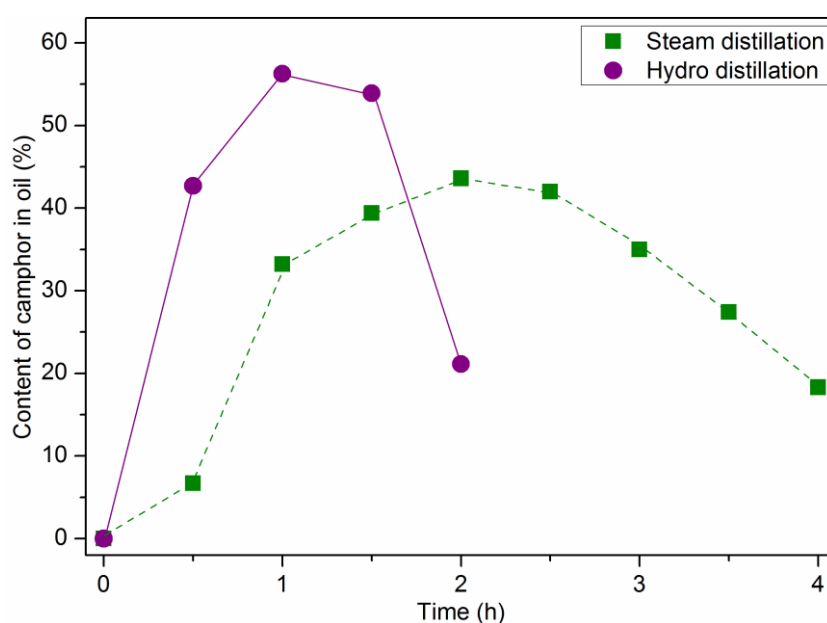


Figure 7.15: Time-dependent content of camphor in the rosemary essential oil obtained by hydro distillation and steam distillation. The yield is given in weight percent of the mass of essential oil collected after the given time.

In addition, the content of camphor in the essential oil is relatively high and the analyses of the different oil fractions show that only the sample of a 0.5 h lasting steam distillation meets the ISO 1342 international standard. Here, the content of camphor is limited to a value from 5 until 15% in the essential oil of Moroccan rosemary. Cohobation of the hydrosol even increases the content of camphor in the essential. This can be a result of the solubility of camphor in water. After the first extraction the hydrosol is saturated with camphor. If this residue is cohobated, no more camphor is soluble due to the saturated water. As a result, more camphor can be extracted.

7.4.4 Influence of hydro distillation on antioxidants

During hydro distillation the rosemary leaves are surrounded for hours by boiling water. As already mentioned, antioxidants are temperature sensitive compounds. Thus, it is important to investigate the influence of hydro distillation on the antioxidant compounds. The content of antioxidants in the hydro distillation water residues was investigated. After hydro distillation, the residual leaves were analyzed on the content of antioxidants using HPLC/UV.

7.4.4.1 Content of antioxidants in hydro distillation water residues

After the hydro distillation of rosemary leaves the remaining water is brown colored. Normally this residue is waste, because the main focus in this method is the essential oil. But the plant material always contains some hydrophilic thus water-soluble compounds which can be dissolved in the water residue during hydro distillation. For this reason it is worth to analyze this residual water on the antioxidant content.

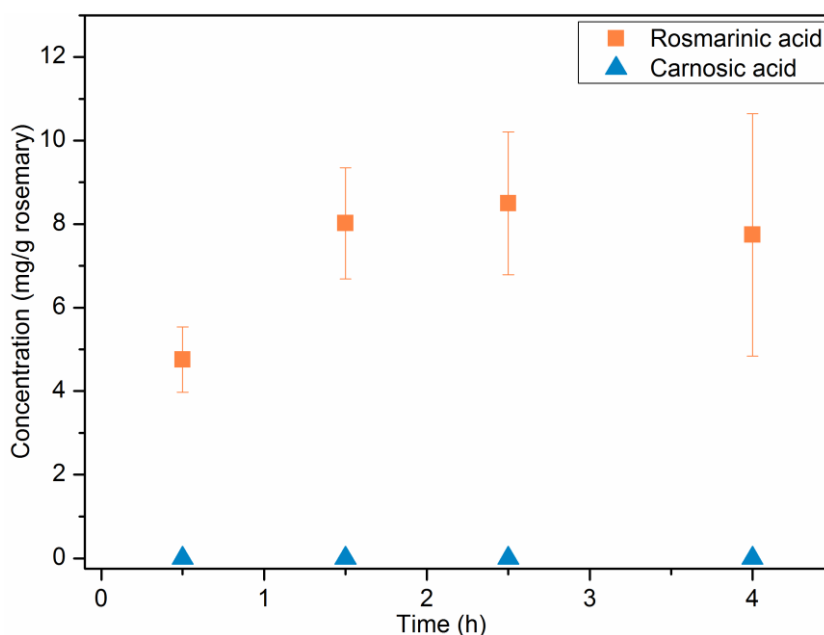


Figure 7.16: Time-dependent mass concentrations of rosmarinic acid and carnosic acid yields obtained by hydro distillation of rosemary leaves. The yield is given in weight percent of the initial mass of rosemary leaves.

Figure 7.16 presents the influence of distillation time on the concentration of rosmarinic acid and carnosic acid in the water residue. It is found that the content of rosmarinic acid in the water residue increases over extraction time. After 2.5 h of distillation a maximum content of 8.5 mg rosmarinic acid per 1 g of dry rosemary leaves is reached. This value is close to the maximum rosmarinic acid amount of 8.9 mg/g in the leaves, which was investigated by Soxhlet extractions. The large standard deviations of the single measurements, especially at longer extraction times, can be explained by the significant variation of some extraction

parameters, for example irregularities in the stirring rate of the suspension and other inevitable inhomogeneities in the process. As expected, no carnosic acid is determined in the water residue. Figure 7.18 shows the chromatogram of the water residue from a 2.5 h lasting hydro distillation. It looks quite similar to the chromatogram of the water Soxhlet extract (see Figure 7.13). In general, compounds with small retention times, thus polar substances, are extracted. It is apparent that only small amounts of carnosol and rosmanol are contained in the water residue.

7.4.4.2 Content of antioxidants in the residual leaves after hydro distillation

After distillation, the residual rosemary leaves were dried and extracted by Soxhlet with methanol to investigate the influence of hydro distillation on the residual content of antioxidants, especially rosmarinic acid and carnosic acid. In Figure 7.17 it is shown that there is still rosmarinic acid left in the rosemary leaves after hydro distillation. But the content decreases from an initial amount of 8.9 mg/g to 2.1 mg/g after 4 h of distillation. The time of the proceeding hydro distillation also influences the content of carnosic acid residual leaves. The initial content of 23.6 mg/g decreases significantly by 16.3 mg/g after 1.5 h of distillation, followed by a small increase to 18.9 mg/g after 4 h.

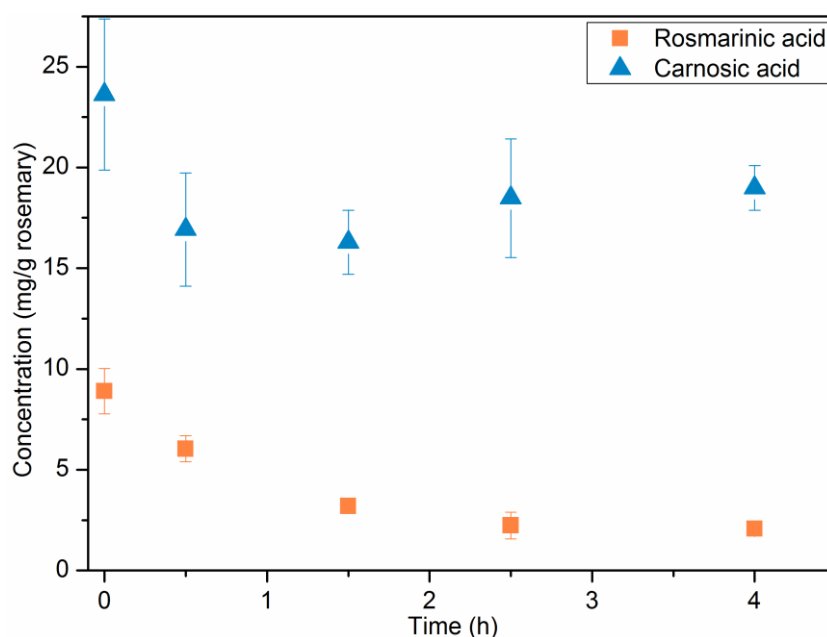


Figure 7.17: Time-dependent mass concentrations of rosmarinic acid and carnosic acid in the residual rosemary leaves after hydro distillation. The content of antioxidants was investigated by Soxhlet extractions with methanol. The yield is given in weight percent of the acids relative to the initial mass of rosemary leaves.

The chromatogram of the Soxhlet extract of the residual leaves (see Figure 7.18) after a 2.5 h lasting hydro distillation is similar to the standard methanol extract (see Figure 7.13). Differences are the lower content of polar compounds, especially rosmarinic acid. Also an

extension of the methyl carnosate, rosmanol and particularly carnosol peak area can be determined. With these results the trend of the antioxidants concentrations in the rosemary leaves during hydro distillation can be explained.

The decrease of rosmarinic acid during hydro distillation is due to its water solubility. The longer the distillation, the lower is the residual amount of rosmarinic acid in the leaves. After 2.5 h a saturation of the solution due to the solubility limit of rosmarinic acid in water is reached. For this reason, there is still some rosmarinic acid left in the leaves after hydro distillation. The trend of carnosic acid is slightly different. First the concentration in the leaves decreases, but this is not based on the solubility of carnosic acid in water. This compound is water insoluble. The decrease of the concentration can be explained by the degradation of carnosic acid to rosmanol and carnosol, which were detected in the water residue and the residual leaves. The subsequent increase of the carnosic acid concentration in the leaves is more or less an artifact, because the results are given in mg of antioxidant per 1 g of rosemary. It has to be mentioned that with increasing hydro distillation time more and more compounds are extracted from the leaves. This leads to a reduction of the mass of the rosemary leaves and thus the remaining compounds get more and more concentrated in the leaves. As the content of carnosic acid is not reduced in the leaves after 1.5 h, the calculated concentration in mg per 1 g of the residual rosemary leaves is hence higher.

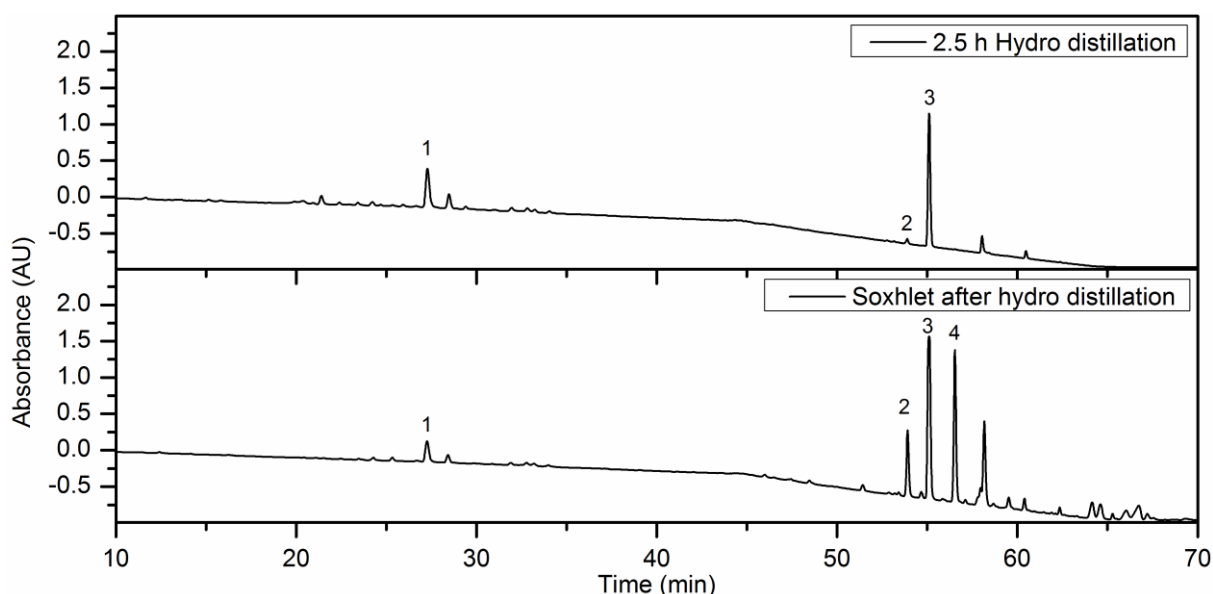


Figure 7.18: HPLC chromatograms of the hydro distillation water residue after 2.5 h and the subsequent Soxhlet extraction of the corresponding residual rosemary leaves with methanol. Peak identification: (1) rosmarinic acid; (2) carnosol; (3) gemfibrozil (IS); (4) carnosic acid;

In comparison, the influence of steam distillation on the antioxidants in rosemary leaves was also determined. To this purpose, defatted rosemary leaves from the company Phytotagante were analyzed. This plant material was extracted for 4 h by steam distillation according to the procedure described in section 7.3.3.3. After distillation, the leaves were dried. The

difference of steam distillation to hydro distillation is that the plant material is not covered by boiling water, but instead surrounded by steam. However, the leaves are exposed to heat for several hours which can induce degradation of antioxidant compounds. It is determined that less antioxidant compounds are contained in the defatted leaves after steam distillation compared to normal rosemary leaves. In detail, 3.94 mg/g of rosmarinic acid and 14.05 mg/g of carnosic acid are left in the defatted leaves. This means that the amount of rosmarinic acid is lowered to 44.3% and 59.4% for carnosic acid related to the initial content. Consequently, steam distillation strongly influences the antioxidant content in the rosemary leaves. Results from literature also show that steam distillation influences the composition of antioxidants in the residual leaves. The degradation of carnosic acid to carnosol and the loss of rosmarinic acid were also determined [61]. Compared to hydro distillation less rosmarinic acid is lost during steam distillation, but more carnosic acid. In summary, it can be said that hydro and steam distillation have a strong influence on the antioxidant content of rosemary leaves. During distillation, antioxidants get lost by solubilization or degradation.

Nevertheless, the residual leaves can be re-processed to extract the remaining antioxidants after hydro distillation. This would be in line with the concept of biorefinery. This concept is defined as “the sustainable processing of biomass into a spectrum of marketable products and energy”. However in future it would be better to focus on alternative extraction methods for essential oils especially in order to minimize the decomposition of antioxidants in the plant material. Another drawback of hydro and steam distillation is the high energy consumption to generate the steam and also to condense the essential oil/steam mixture. In general, it is known that an industrial extraction cycle needs at least 50% of the energy of the whole industrial process [66, 67]. An appropriate option could be microwave-assisted extraction techniques like microwave hydro diffusion and gravity (MHG). With this method, the rosemary essential oil can be extracted within 10 min instead of 240 min for hydro distillation. Another advantage of MHG compared to hydro distillation is the saving in solvent, because no additional water (fresh plants) or only a small amount (dry plants) is needed. The impacts on antioxidants during extraction can probably be decreased with this method. There is also a saving in energy, solvent, waste and time, which would decrease the environmental impact of the extraction process. Minor disadvantages of microwave-assisted distillation are the higher acquisition costs and higher level of safety and attention compared to steam or hydro distillation. Also up-scaling of the microwave-assisted extraction process is not arbitrary possible. Large-scale microwave reactors are suitable to extract up to 100 kg of fresh plant material per batch [32, 66]. This is less plant material compared to steam distillation where 800 kg of rosemary leaves were extracted per batch.

7.4.5 Antioxidant activity of hydro distillation water residues

The previous results showed that there is a large amount of rosmarinic acid and other compounds in the hydro distillation water residue of rosemary leaves. The concentration of rosmarinic acid reaches a maximum value of 0.43 mg/mL after 2.5 h of hydro distillation. But the HPLC analyses also indicated the presence of other water soluble compounds in the water residue. Thus it is worth to investigate the total antioxidant activity in the water residue. DPPH assays are a suitable way to measure the radical scavenging properties of different compounds.

7.4.5.1 Calibration

First of all, different concentrations of a DPPH solution were measured for calibration. It was determined that the absorbance maximum is at a wavelength of 518 nm. When the concentration is plotted as a function of the absorbance, a linear trend can be observed. The exact DPPH concentration of the blank samples can be calculated with the following equation (7.5).

$$\beta_{DPPH} = \frac{A_{DPPH \text{ at } 518 \text{ nm}}}{30.682 \frac{\text{mL}}{\text{mg}}} \quad (7.5)$$

where β_{DPPH} = mass concentration of DPPH [mg/mL], $A_{DPPH \text{ at } 518 \text{ nm}}$ = absorbance maximum of the DPPH blank solution at 518 nm, 30.682 mL/mg = slope of the linear calibration curve.

7.4.5.2 Reference substances

The antioxidant activity of the following pure compounds was investigated: rosmarinic acid, carnosic acid, butylated hydroxyanisole, ascorbic acid and α -tocopherol. First, the kinetic of the reaction was determined. It is necessary to assume a complete reaction of DPPH with the antioxidant. Rosmarinic acid shows a slow reaction kinetic. After approximately 1 h of reaction, the absorbance of the sample at 518 nm stays constant. In contrast, ascorbic acid reacts very fast with the DPPH radical. Here, a complete reaction of the antioxidant is reached after 1 min. To make all the results comparable and dismiss some disturbing factors, the absorbance of the samples was measured after exactly 1 h of reaction time.

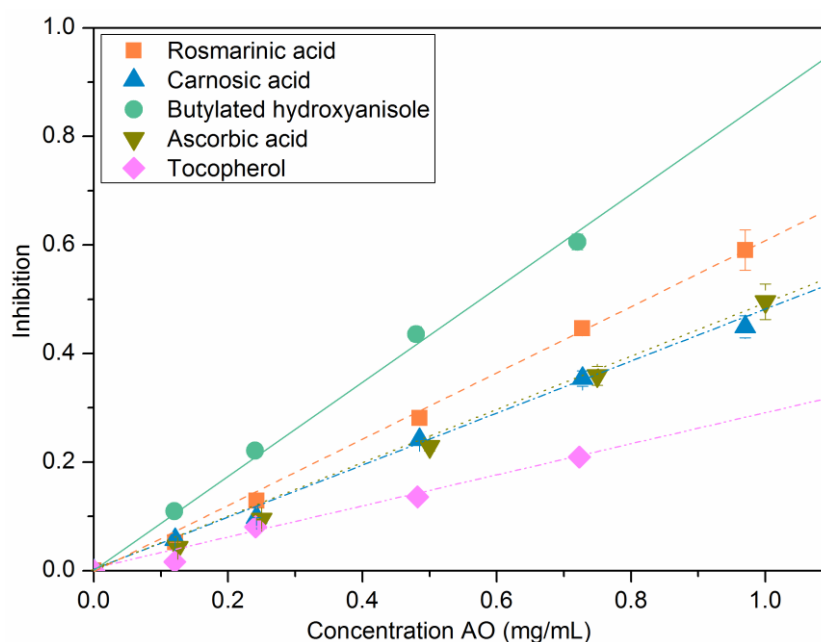


Figure 7.19: Influence of concentration on the inhibition of different compounds: rosmarinic acid, carnosic acid, butylated hydroxyanisole, ascorbic acid and α -tocopherol.

Figure 7.19 shows the influence of mass concentration on the inhibition for different antioxidants. A linear trend between the inhibition and the concentration of the antioxidant solutions can be observed. The larger the slope of the trend line, the more efficient is the antioxidant. At higher antioxidant concentrations the curve reaches a maximum value due to the lack of DPPH. The order of the analyzed antioxidant in ascending antioxidant power in regard to their mass concentration is: α -tocopherol, ascorbic acid, carnosic acid, rosmarinic acid, and butylated hydroxyanisole. But to compare the antioxidant activity of the single molecules these results need to be converted into values which are depended on the amount of substance.

Figure 7.20 shows the influence of the ratio $n(\text{antioxidant})/n(\text{DPPH})$ on the inhibition for different antioxidants. Again, a linear trend of the values can be observed. The larger the slope of the trend line, the higher is the antioxidant activity of the molecule. The value of the slope gives the number of reduced DPPH radical molecules per one antioxidant molecule, whereas the linear extrapolation of the measured point to an inhibition value of 1 provides the stoichiometric value of the reaction. An inhibition of 1 means that all of the DPPH has reacted with the antioxidant.

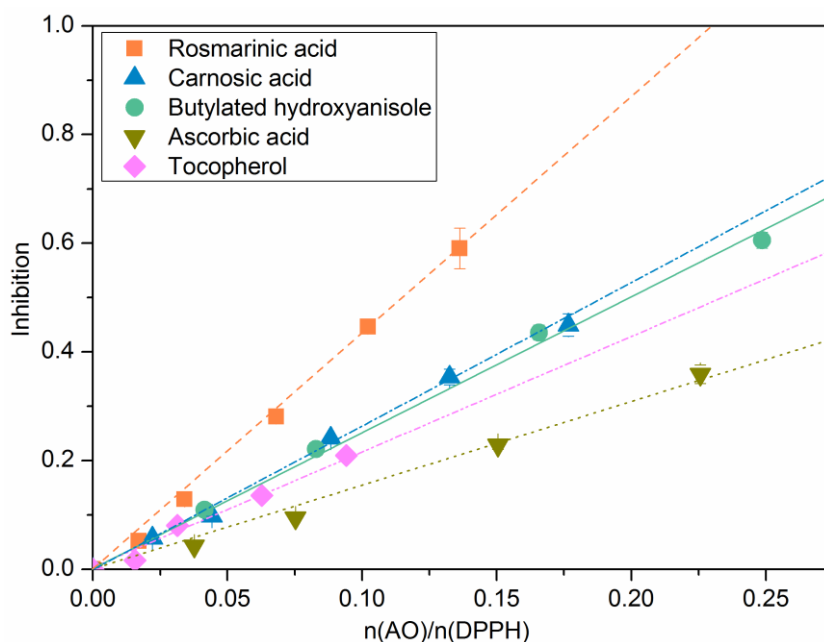


Figure 7.20: Influence of molar ratio of compound to DPPH on the inhibition of different compounds: rosmarinic acid, carnosic acid, butylated hydroxyanisole, ascorbic acid, and α -tocopherol.

The antioxidant power of the compounds in ascending order is as follows: rosmarinic acid, carnosic acid, butylated hydroxyanisole, α -tocopherol, and ascorbic acid. The absolute values of the results are summarized in Table 7.3. The experimentally determined values in this work are in agreement with the literature data [68]. Also a new value for the reaction of carnosic acid with DPPH is described, which has not been specified in literature before. In this reaction, 2.57 DPPH molecules react with one molecule of carnosic acid. The corresponding stoichiometric value was determined to be 0.39.

Table 7.3: Stoichiometric value of the reaction DPPH-AO and number of reduced DPPH molecules per molecule antioxidant of different compounds: rosmarinic acid, carnosic acid, butylated hydroxyanisole, ascorbic acid, and α -tocopherol.

Compound	Stoichiometric Value	Number of reduced DPPH	
		Experimental	Literature
Rosmarinic acid	0.24	4.25	3.33 [68]
Carnosic acid	0.39	2.57	-
Butylated hydroxyanisole	0.40	2.49	2.63 [68]
Ascorbic acid	0.63	1.60	1.85 [68]
α -Tocopherol	0.45	2.21	-

7.4.5.3 Soxhlet extracts

The choice of solvent also influences the antioxidant activity of the Soxhlet extracts, like it can be seen in Figure 7.21. First, it can be noted that the water Soxhlet extracts shows the highest antioxidant activity of the samples, followed by the methanol extract. Soxhlet extracts of rosemary leaves with acetone show the lowest antioxidant power. At first sight, these results are not in agreement with the determined total amount of rosmarinic acid and carnosic acid by HPLC/UV (see 7.4.2.2). There, methanol extracted the highest mass concentration of both antioxidants. As a result, it can be said that methanol extracts the highest amount of antioxidants, in regard to of rosmarinic acid and carnosic acid, but water delivers the extract with the highest total antioxidant activity. This may be explained by the assumption that water extracts antioxidants, which react better respectively in a smaller stoichiometric value (see Table 7.3) with the DPPH radical.

7.4.5.4 Hydro distillation water residues

The previous results already showed that there is a significant amount of antioxidants contained in the residual water of hydro distillations. But only the amount of rosmarinic acid and carnosic acid could be quantitatively determined by HPLC/UV. The chromatograms already showed that there are more compounds in the residue. To quantify them, the water residues of hydro distillation were analyzed by DPPH assays to determine the total antioxidant power. For comparison and classification of the results, the DPPH assays were also carried out for the water, methanol, and acetone Soxhlet extracts. Preliminary to the assays of the samples, the UV/VIS spectra of the pure hydro distillation water residue and Soxhlet extracts were measured. It was found that the absorbance of the extracts does not influence the absorbance of DPPH.

As it can be seen in Figure 7.21, the duration of hydro distillation influences significantly the inhibition of different dilutions of the water residue. As mentioned previously, the bigger the slope of the linear trend line, the greater is the antioxidant activity of the sample. The water residue of a 0.5 h lasting hydro distillation of rosemary leaves shows the smallest antioxidant activity of all samples. With increasing hydro distillation time, the antioxidant activity of the water residue increases. A maximum value is reached after a distillation time of 2.5 h. Afterwards, the antioxidant activity of the hydro distillation water residue decreases. The value of a 4 h lasting hydro distillation is in the range of a distillation time of 1.5 h. This behavior can be explained by the increasing solubilization of antioxidant compounds with increasing hydro distillation time. The decay of the antioxidant power after 2.5 h of hydro distillation is probably due to the decomposition of some antioxidant compounds. These results are in accordance with the previously investigated behavior. It can also be noted that not only rosmarinic acid is responsible for the high antioxidant activity in the hydro distillation

water residue. Other water soluble antioxidants, like rosmanol, methyl carnosate, and unknown compounds also affect the antioxidant activity.

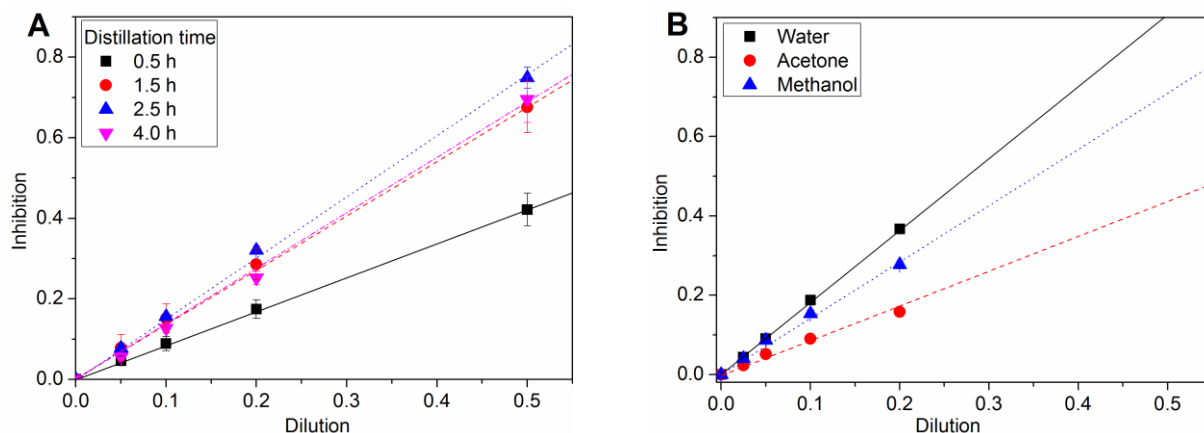


Figure 7.21: (A) Influence of the dilution on the inhibition of hydro distillation water residues gained after 0.5, 1.5, 2.5 and 4.0 h and (B) Soxhlet extracts obtained with different solvents: water, acetone, and methanol.

To classify the antioxidant activity of the hydro distillation water residues, the results are compared with the water, methanol, and acetone Soxhlet extracts. Hydro distillations were carried out with a solid/liquid ratio of 0.05. This means that 0.05 g of rosemary leaves were “extracted” with 1 mL of water. The solid/liquid ratio for Soxhlet extraction was higher with 0.1 g rosemary leaves per 1 mL of solvent. This ratio was taken into account in the results presented in Figure 7.21. Thus, the results respectively dilutions of hydro distillation and Soxhlet extractions are directly comparable.

It can be noted that the water Soxhlet extract has a slightly higher antioxidant activity as the water residue of a 2.5 h lasting hydro distillation. This is predictable and can be explained by the fact that Soxhlet is an exhaustive extraction method, whereas, in hydro distillation the water is finally saturated with the compounds after the establishment of an equilibrium. The antioxidant activity of the water residue of a 1.5 and 4 h lasting hydro distillation is in the same range as a Soxhlet extraction carried out with methanol. Soxhlet extracts obtained with acetone show the lowest antioxidant activity. The value is comparable to the residue of a 0.5 h lasting hydro distillation. It is supposed that the water insoluble antioxidants contained in rosemary leaves have a lower antioxidant activity than the water soluble ones. The main result of these DPPH assays is that almost all of the water soluble antioxidants get lost during hydro distillation and are contained in the residual water.

As already mentioned, this residual water is normally a waste product. The results of HPLC analyses and DPPH assays show clearly that a large amount of antioxidants is contained in this residue. In future, the extraction of antioxidants from natural resources will become mandatory due to the replacement of artificial antioxidants. Here, a possible source of the natural antioxidant rosmarinic acid was identified. For this reason it is necessary to see the

hydro distillation water residue as co-product of the extraction and not as waste product. This would be in line with the concept of biorefinery and green extraction. The approach of these two concepts is to maximize the valorization of raw materials, reduce the energy consumption and use alternative solvents for economic sustainability. The goal of the industrial process to extract rosemary is the fast and moderate recovery of the essential oil from the leaves with a minimum impact on the antioxidants. Microwave hydro diffusion and gravity could be an alternative extraction method. Furthermore, the residual water of hydro distillation which contains a large amount of antioxidants can be used for different applications. This residual water can be taken as additive without any further purification to increase the antioxidant activity of a product or it can be re-extracted to gain the pure antioxidants. At least, the residual leaves can be extracted with a green organic solvent to obtain antioxidants. This process will more and more approach the concept and principles of green extraction of natural products and biorefinery [66, 67].

7.4.6 Antioxidant activity of hydro distillation water residues in microemulsions

The previous results showed that the antioxidant activity of the hydro distillation water residue reaches a maximum value after 2.5 h of extraction. This is originated in the presence of rosmarinic acid and other antioxidant compounds in the water residue. The concentration of rosmarinic acid in the aqueous solution is 0.43 mg/mL. The goal of the following work was to find a possible application for the aqueous residue without any further treatment. This antioxidant water residue can probably be an alternative compound to conventional antioxidants, like ascorbic acid, in beverages. To this purpose, the antioxidant activity of this residue was investigated in different microemulsions. The topic of “antioxidant activity in microemulsions” gained more and more attention in the last years. Although it is still a niche topic and only 53 scientific articles have been published so far [69].

7.4.6.1 System SDS/1-pentanol/*n*-dodecane/water

The first investigated system comprises water, sodium dodecyl sulfate (SDS), 1-pentanol, and *n*-dodecane. The microemulsions were either prepared with pure water or with the hydro distillation water residue of rosemary leaves. The main aim of this study is to investigate if the activity of the antioxidants is influenced by the different structures present in the microemulsion. Preliminarily, it was investigated if the water residue or rather the dissolved antioxidants influence the shape of the phase diagram and the microstructures of the microemulsion, like it is the case by the addition of kosmotropic or chaotropic salts. In addition, DPPH assays were carried out in microemulsions to determine the antioxidant activity. The system SDS/1-pentanol/*n*-dodecane/water was chosen as it is already well-known and described in literature [48]. For instance, the activity of the enzyme horseradish

peroxidase was studied in reverse microemulsion of this system as a function of the microstructure [70].

7.4.6.1.1 Phase diagram

At first, the phase diagram for the system SDS/1-pentanol/*n*-dodecane/hydro distillation water residue was determined at 25 °C and a constant weight ratio of SDS to 1-pentanol (1:2). To this purpose, the hydro distillation water residue of rosemary leaves after 2.5 h of distillation was used as aqueous phase. The resulting phase diagram is illustrated in Figure 7.22. The grey areas represent the microemulsion domain. Here, the solution is clear, slightly yellow, and homogeneous. The color is due to the used brown colored water residue. LC indicates a liquid crystalline area, which was recognized by polarizing filters. These phases appeared birefringent between the cross polarizers. The phase diagram with pure water is presented in literature [48]. The shape of the phase diagram with pure water is very similar to the one with hydro distillation water residue and no significant differences are noticeable between both. The microemulsion domain at the right corner (oil rich) of the phase diagram was detectable, but it was difficult to determine it accurately. For this reason, the area is bordered with a dotted line. But this part of the phase diagram is not significant for the further investigations.

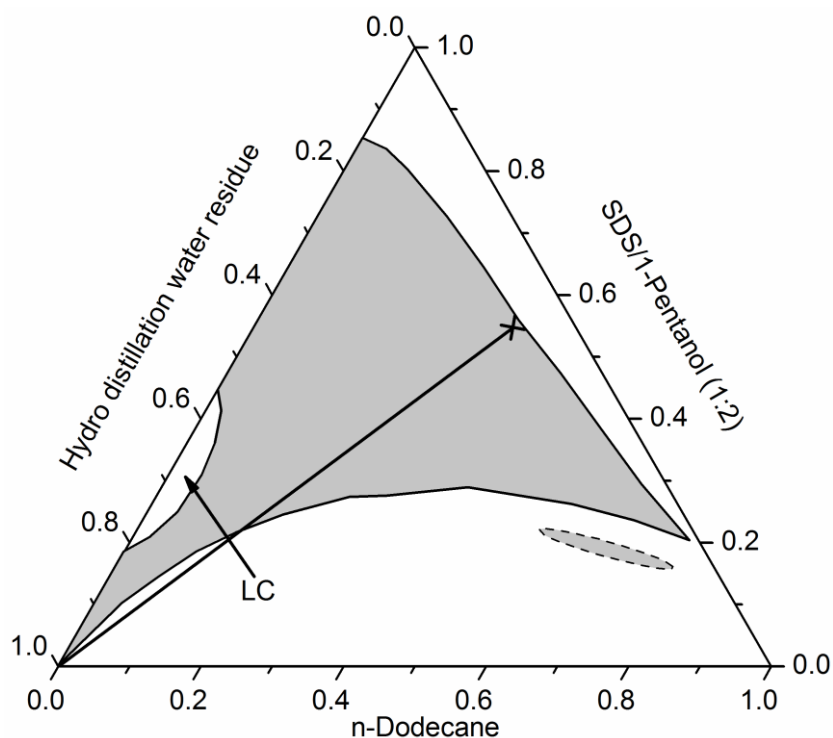


Figure 7.22: Pseudo-ternary phase diagram of SDS/1-pentanol/*n*-dodecane/hydro distillation water residue of rosemary leaves at 25 °C and a constant weight ratio of SDS to 1-pentanol (1:2). The grey areas represent the microemulsion domain. LC indicates a liquid crystalline area. The cross marks the starting point of the conductivity measurements. Also the antioxidant activities were measured in samples with compositions of the microemulsion on the black line.

Although the solutions appear homogenous to the eye, different microstructures can be present in the microemulsion domain. A w/o-microemulsion with inverse micelles is present in the oil-rich domain. With increasing water content, first a bicontinuous microemulsion domain is passed, until the water-rich o/w-microemulsion is reached [48]. The barriers of the microstructures can be determined by conductivity measurements, which are presented in chapter 7.4.6.1.2.

The cross in the phase diagram marks the starting point of the conductivity measurements. Also the antioxidant activities were measured in samples with compositions of the microemulsion on the black line.

7.4.6.1.2 Conductivity measurements

Conductivity measurements are a suitable method to investigate the microstructures in microemulsions. In this part, the influence of the hydro distillation water residue on the partition of the structures compared to the normal system SDS/1-pentanol(1:2)/*n*-dodecane/water is investigated. Both measurements were started in the oil-rich domain of the microemulsion. The experimental path and starting point of the experiments is marked in Figure 7.22. The ratio of surfactant/cosurfactant to oil was constant at 2:3. The measurements were carried out at 25 °C. Water respectively hydro distillation water residue was subsequently added to the microemulsion and the corresponding value of the specific conductivity was recorded.

Figure 7.23 shows the specific conductivity κ as a function of the mass fraction of water and hydro distillation water residue. It can be seen that both curves show the same behavior. The electrical conductivity is nearly zero at the beginning. Here, a w/o-microemulsion with spherical inverse micelles is present. The sodium cations of SDS are located inside the reverse micelles. The micelles are isolated and thus, no charge transfer can occur. Consequently, the system is an insulator. Low values of κ can still be measured, since collisions of reverse micelles occur, which results in a charge transfer at low levels. With increasing water content, a non-linear increase of the conductivity can be observed, which changes in a linear relationship at a certain point. This behavior is well-known and can be explained by the percolative conduction phenomena in microemulsion domains. The increase in the electrical conductivity with increasing water content can be explained by progressive droplet interlinking and clustering processes. After the linear trend, the slope of the curve gradually decreases, until a maximum value of the conductivity is reached. Here, a bicontinuous microemulsion domain is present, where the cross-linked micelles form channels. This maximum is often considered to be the transition of oil-rich to a water-rich microemulsion. With an increasing content of water, the conductivity decreases continuously in a nonlinear manner, which is due to another phase transition. In this area an o/w-microemulsion is formed. The system is made up of oil spheres surrounded by a mixed

surfactant and cosurfactant film surrounded in the continuous water phase. The further decrease of conductivity can be explained with the dilution of sodium cations in the microemulsion. At a certain water content, a separation into two phases occurs and the solution becomes turbid [71-73].

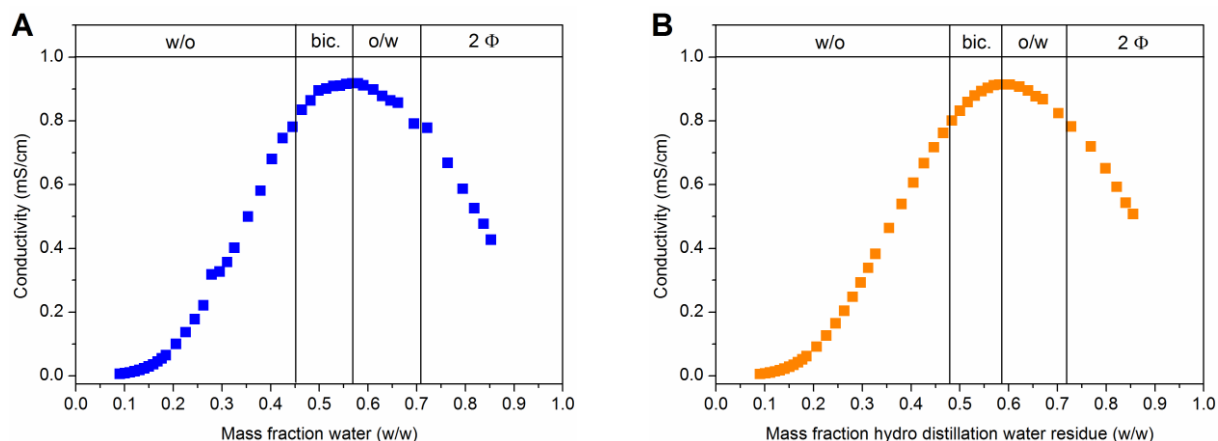


Figure 7.23: The specific conductivity of the microemulsions as a function of (A) water respectively (B) hydro distillation water residue mass fraction for the pseudo ternary system SDS/1-pentanol (1:2)/dodecane/water. In addition the corresponding structures of the microemulsions are shown. The measurements were carried out at 25 °C.

The measurements clearly show that different kinds of microstructures are present in the both microemulsion systems. These structures are dependent on the mass fraction of water or hydro distillation water residue. The borders of different microstructures were identified for the system with pure water. Starting with a low content of water, a w/o-microemulsion with percolative behavior is present up to a water mass fraction of 0.45. By subsequent water addition a bicontinuous domain is reached to a value of 0.57. Here, the conductivity reaches its maximum value of 0.9 mS/cm. Afterwards, a transition of the oil-rich microemulsion to a water-rich domain occurs. From this point the conductivity decreases continuously and an o/w-microemulsion is formed until a water mass fraction of 0.71. Above this water content a separation in two phases occurs and the solution becomes turbid. The system with hydro distillation water residue shows the same behavior. The thresholds for the different microstructures differ only in a very small range from those with pure water. These deviations can be explained by the fact that these transitions of the microstructures do not have sharp boundaries. Nevertheless, these results also show that the incorporation of the hydro distillation water residue does not influence the characteristics of the microemulsion system.

7.4.6.1.3 Antioxidant activity in microemulsions

Previous results showed that the presence of antioxidants in the water phase does not influence the microstructure of the microemulsion. The further aim of this work was to investigate if these microstructures in the microemulsions influence the antioxidant activity of

the hydro distillation water residue. For this purpose, a fast and easy method to measure the antioxidant activity in microemulsions is investigated. The method to measure the antioxidant activity of pure compounds and the hydro distillation water residue with DPPH in methanol solutions was already described. The results were presented in chapter 7.4.5. In this case, this method is not applicable. In literature, a few methods are described to measure the antioxidant activity in microemulsions. However, either electrochemical analyses [74] or inappropriate methods with the DPPH radical are applied. In the last case, DPPH or another dye is dissolved in a solvent, then mixed with an antioxidant containing microemulsion and the absorbance of the sample was measured after a certain time [75-77]. This method is not applicable for the measurements here, because adding a solvent/DPPH solution to the microemulsion would change the properties of the microemulsion. One applicable method is described in literature, where the DPPH radical is dissolved in a microemulsion and the antioxidant in another microemulsion with the same composition. By mixing both microemulsions, the antioxidant activity can be determined [78]. That's why a new method on the basis of the reported technique was established.

Some preliminary tests had to be carried out to ensure the accuracy of the experiments. First of all, UV/VIS spectra of a DPPH solution, the hydro distillation water residue and the microemulsion were recorded. It is determined that the microemulsion or the compounds present in the water residue do not disturb the absorbance of DPPH at 518 nm.

Furthermore, the solubility of DPPH in the microemulsion was investigated in two microemulsion samples with a composition on the black line. One sample contained few *n*-dodecane, whereas the second sample contained a larger amount of the oil. A spade point of DPPH was added to the samples. Both colorless microemulsions turned weakly violet, but the DPPH powder was not completely dissolved. A possible way to enhance the solubility of DPPH in the microemulsion is to put the samples in an ultrasonic bath for a few minutes. Afterwards, both microemulsions got an intensive violet color and the whole DPPH was dissolved.

The next step was to record a calibration curve of DPPH in the microemulsion. To this purpose, the UV/VIS-spectra of samples with different concentrations of DPPH in microemulsion were measured. The concentrations varied from 0.0125 mg/mL up to 0.1 mg/mL. A linear correlation between the absorbance at 518 nm and the DPPH concentration can be observed. The slope of the function is almost identical to one observed for DPPH in methanol (see equation (7.5), page 176). It can be concluded that the microemulsion does not affect the absorbance of DPPH.

Subsequently, two microemulsion samples were prepared, one with hydro distillation water residue (40 wt%) and the other one with millipore water(40 wt%). DPPH was dissolved in the microemulsion with pure water to reach a concentration of 0.1 mg/mL. The aim of this step is, to find the best mixing ratio of the DPPH microemulsion to the water residue-microemulsion.

A defined volume (3.0, 3.5, 3.9, and 3.95 mL) of the DPPH microemulsion was pipetted into a snap cap vial. The water residue-microemulsion was added to every sample obtaining a total volume of the samples of 4 mL. The UV/VIS spectra were measured after 60 min. Only the sample where 3.95 mL of DPPH microemulsion was mixed with 0.05 mL of the tea-microemulsion was violet and an absorbance at 518 nm was measurable. All other samples turned yellow during this time, implying a total reaction of the DPPH radical.

A new analyses method to investigate the antioxidant activity of compounds in microemulsions can be established by summarizing all the previous results. For a better illustration, the method is presented in Figure 7.24. First of all a microemulsion with the desired composition was prepared with pure water. Afterwards, DPPH was dissolved in this microemulsion to gain a concentration of 0.1 mg/mL. The solubility of the dye was enhanced in an ultrasonic bath. The remaining microemulsion without DPPH was used as a zero sample for the UV/VIS measurements. Another microemulsion with the same composition was produced, but with hydro distillation water residue instead of millipore water. 0.05 mL of the hydro distillation water residue microemulsion was mixed with 3.95 mL of DPPH microemulsion in a snap cap vial. The UV/VIS-spectra of the samples were measured after exactly 60 min of reaction time. Finally, the Inhibition I of the DPPH radical was calculated (see equation (7.2), p. 153).

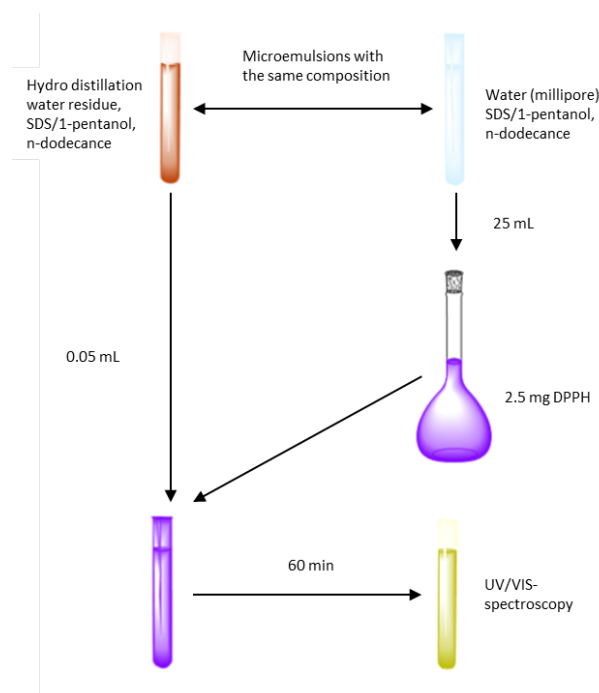


Figure 7.24: Newly established method to determine the antioxidant activity of the hydro distillation water residue in a microemulsion.

To make the results comparable solutions with a defined ratio of hydro distillation water residue is also measured in methanol DPPH solutions. Measurements in microemulsions are carried out with samples on the black line in the phase diagram (Figure 7.22). The ratio of

surfactant/cosurfactant to oil was kept constant and the amount of hydro distillation water residue was changed.

Figure 7.25 shows the percentage of inhibition in microemulsion and methanol solutions in relation to the mass fraction of the hydro distillation water residue. A linear correlation between the inhibition and the concentration of water residue can be observed. In general, the higher the amount of hydro distillation water residue in the sample, the higher is the inhibition of the DPPH radical. It can also be noticed that the inhibition in methanol solutions is slightly higher than in the microemulsions. But the slope of both functions is identical. From this follows, that the efficiency of the antioxidants in microemulsion is equal to the one in methanol solutions. As mentioned previously, the bigger the slope of the linear trend line, the greater is the antioxidant activity of the sample. Consequently the different structures in the microemulsions do not influence the antioxidant activity of the hydro distillation water residue. The measurements in the microemulsion were carried out in all different microstructure domains (w/o-, bicontinuous, and o/w-microemulsion). If the structuring of the microemulsion would influence the antioxidant activity, a deviation from the linear correlation should have been observed.

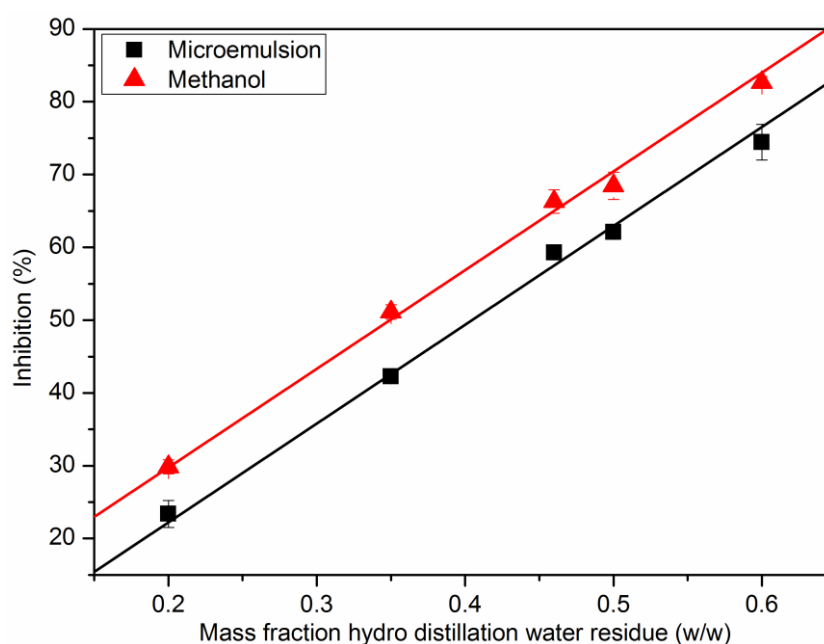


Figure 7.25: Percentage of inhibition in microemulsion (SDS/1-pentanol(1:2)/*n*-dodecane/hydro distillation water residue) and methanol solutions in relation to the mass fraction of hydro distillation water residue.

Nevertheless, there is a difference between methanol solutions and microemulsions. The inhibition in methanol solutions is higher than in microemulsions. A possible explanation of this behavior is that the water soluble antioxidant compounds and DPPH are unequally distributed in the water and oil phase of the microemulsions. Solubility experiments showed that DPPH is only soluble in *n*-dodecane and 1-pentanol, but not at all soluble in pure water.

If the surfactant SDS is added to the water the solubility of DPPH increases, which is due to the formation of micelles and the incorporation of the dye in the inside. The hydro distillation water residue only contains water soluble antioxidant compounds. By preparing a microemulsion with DPPH and the hydro distillation water residue the reactants are partially isolated by the surfactant/cosurfactant interface. An exchange of the reactants has to take place at the interface and thus the radical reaction is slower than in methanol solution. This can also be a consequence due to the higher viscosities of the microemulsion sample. As the reaction kinetic is slowed down in microemulsion, but the UV/VIS spectra of every sample is measured after exactly 60 min, the inhibition in the microemulsion is lower than in methanol solutions. This behavior can perhaps be used for pharmaceutical or nutrition applications to regulate the delivery duration of antioxidant compounds.

7.4.6.2 Antioxidant activity of some essential oils

The further aim of this work was to find a possible application of the hydro distillation water residue in a green microemulsion. The microemulsion should be drinkable and only contain green ingredients, including an essential oil. Therefore, preliminary experiments had to be carried out. In fact, DPPH assays of different essential oils were realized in order to determine a compound with no antioxidant activity. This condition is necessary to be able to measure the antioxidant activity of the hydro distillation water residue in a microemulsion which contains the essential oil. The DPPH assays could not be carried out if the essential oil by itself would already possess antioxidant properties, because this would distort the results.

The investigated essential oils were *trans*-anethole, limonene, linalool, citral (mixture of neral and geranial), α -terpineol, 1,8-cineole, camphor, α -ionone, and nana mint oil. The chemical structures are given in Figure 7.26.

All these compounds are ingredients in different plant respectively their corresponding essential oils. Some of these compounds are used to flavor beverages or other nutrition. *Trans*-anethole is the main compound in the essential oil of star anise. It is mainly used in spirituous beverages, like Ouzo or Pernond and oral care products [79]. Limonene and citral are the main ingredients in lemon peels. Citral is a mixture of the two isomers geranial (Citral A, *trans*-isomer) and neral (Citral B, *cis*-isomer), which are responsible for the characteristic smell of lemons [1]. The essential oil of lemons is often used in soft drinks and perfume industry. Linalool is one of the most commonly used fragrances. It is contained in linaloe oils as a main ingredient, but also in cinnamon oil, orange blossom oil, bergamot oil and many other essential oils. The substance α -terpineol is present in the essential oils of pine-needles and lavender. It is often used in cosmetics and perfumes. Camphor can especially be found in the essential oil of the camphor tree (*Cinnamomum camphora*). This compound is often used in cosmetics and medicine for external application to support the therapy for rheumatism and pulled muscle. The main compound of eucalyptus and bay

leaves oil is 1,8-cineole, also called eucalyptol. It is often used in tooth pastes and mouth rinse, but also in perfume industry. Camphor and 1,8-cineole are both present in the essential oil of rosemary leaves. The fragrance α -ionone is especially used in perfumery due to the flowery scent of violets. The last investigated compound is the essential oil of the Moroccan nana mint (*Mentha spicata* 'Nana'). The main compounds are menthol, menthone and menthyl acetate. The essential oil is applied in oral and dental care products as well as in cosmetics and soap industry [79]. The leaves of this plant are used to prepare the traditional Moroccan mint tea [80]. The most promising compounds for the application in a drinkable microemulsion are limonene, citral, *trans*-anethole, and nana oil, as these essential oils are already used in beverages.

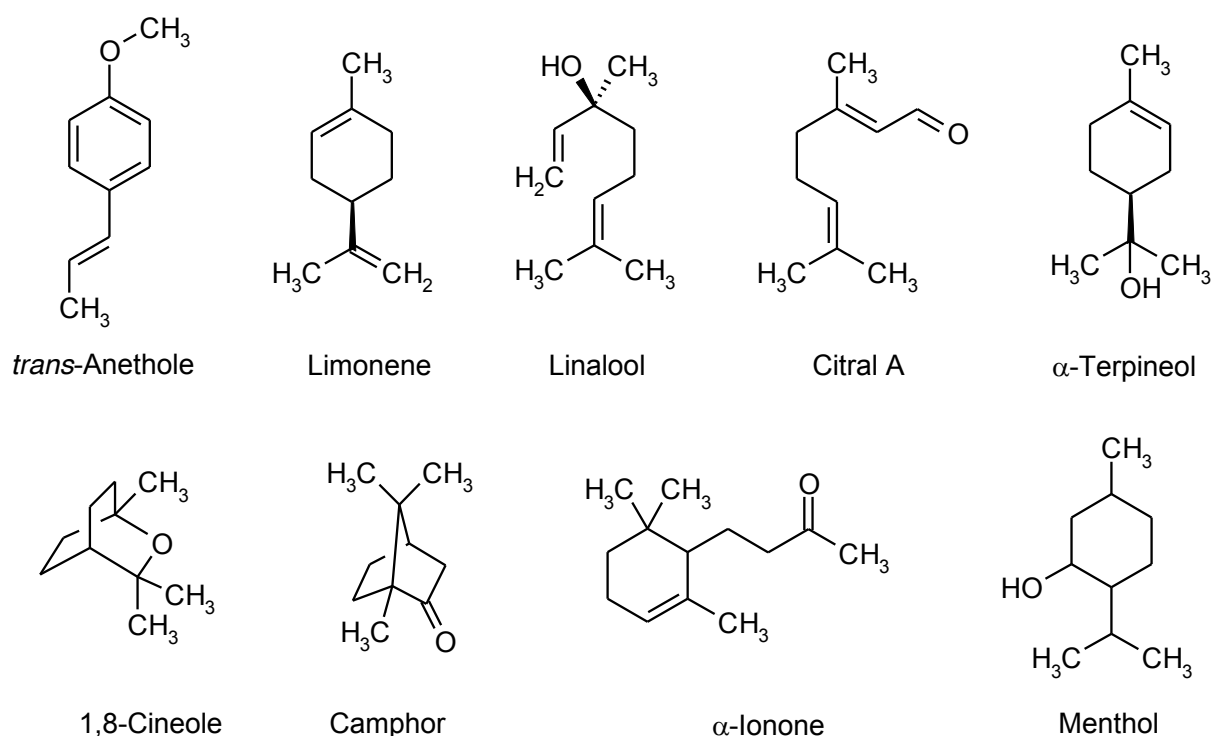


Figure 7.26: Chemical structures of the investigated essential oils: *trans*-anethole, limonene, linalool, citral A (geranial, *trans*-isomer), α -terpineol, 1,8-cineole, camphor, α -ionone, and menthol (as main compound in nana mint oil).

Solutions of each essential oil in methanol were prepared with an approximate concentration of 15 mg/mL and mixed with a 0.1 mg/mL solution of DPPH in methanol. The spectra were recorded after exactly 60 min of reaction time. Figure 7.27 shows the UV/VIS spectra of the different essential oils after the reaction with DPPH.

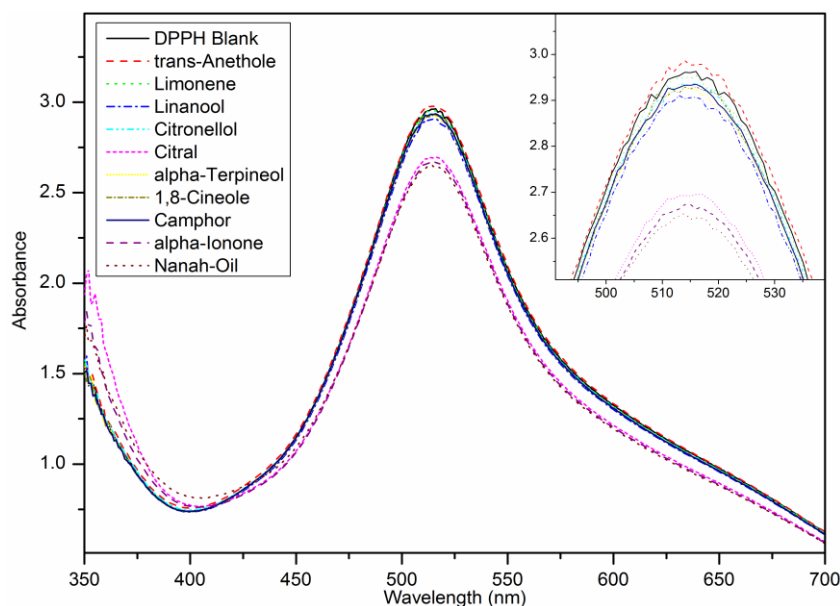


Figure 7.27: UV/VIS spectra of different essential oils after the reaction with DPPH. Investigated compounds are *trans*-anethole, limonene, linalool, citral, α -terpineol, 1,8-cineole, camphor, α -ionone, and menthol (as main compound in Nana mint oil).

The shape and trend of the spectra of limonene, linalool, citronellol, α -terpineol, cineole, camphor, and *trans*-anethole is nearly identical to the one of the pure DPPH solution. This behavior indicates that these compounds have probably no antioxidant properties. Citral, α -ionone, and nana oil show a different behavior. Here, the absorbance maximum decreases slightly at a wavelength of 518 nm. Consequently, these essential oils react with the DPPH radical and thus possess antioxidant activity. These compounds are not applicable for the further investigations, as they would distort the measurements.

7.4.6.3 System TWEEN 60/ethanol/essential oil/water

A new microemulsion system was chosen for a possible application of the hydro distillation water residue of rosemary leaves. The investigated system comprises water, TWEEN® 60, ethanol, and essential oil. The characteristics of this microemulsion with nana oil as oil phase were already investigated by Freyburger A. and Endert C. during their Master theses. The aim of their studies was the preparation of a fully water dilutable beverage concentrate based on a microemulsion with the taste of the Moroccan nana mint tea. The substitution of the nana oil by other essential oils was also investigated in order to create a general beverage concentrate [80, 81].

The main aim of the further study is to incorporate the hydro distillation water residue into the described system and determine the antioxidant activity. As the previous results showed that pure nana oil possesses an antioxidant activity, it is not suitable for DPPH assays. Therefore, limonene, an essential oil without antioxidant properties, was used as oil phase in the

microemulsion. The microemulsions were again either prepared with pure water or the hydro distillation water residue. The effects of the water residue respectively the dissolved antioxidants on the shape of the phase diagram were investigated. In addition, DPPH assays were performed in microemulsions to determine the antioxidant activity.

7.4.6.3.1 Phase diagram

At first, the hydro distillation water residue of rosemary leaves after 2.5 h of extraction was used as aqueous phase. The phase diagram for the system TWEEN® 60/ethanol/limonene/hydro distillation water residue was determined at 25 °C and a constant weight ratio of TWEEN® 60 to ethanol (2:1).

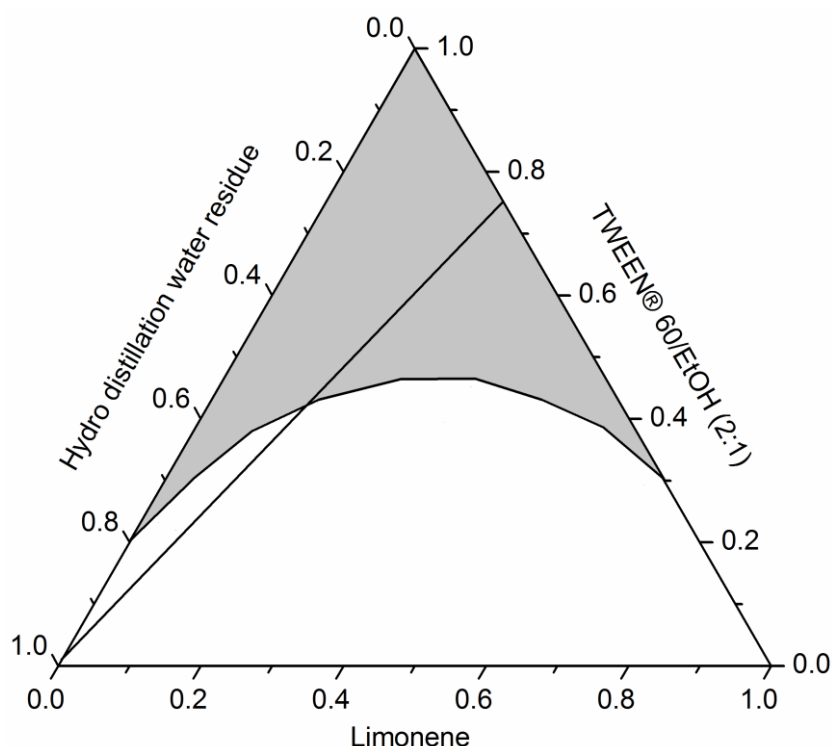


Figure 7.28: Pseudo ternary phase diagram of TWEEN 60®/ethanol/limonene/hydro distillation water residue of rosemary leaves at 25 °C and a constant weight ratio of TWEEN 60® to ethanol (2:1). The grey areas represent the microemulsion domain. The antioxidant activities were measured in samples with compositions of the microemulsion on the black line.

The resulting phase diagram is illustrated in Figure 7.28. The grey areas represent the microemulsion domain. Here the solution is clear, slightly yellow colored and homogeneous. The color is due to the used brown colored water residue. The shape of the phase diagram with limonene is very similar to the one with nana mint oil. A significant difference is the smaller microemulsion domain at the left corner (water rich). As a result, a concentrate with approximately 10 wt% limonene, 10 wt% hydro distillation water residue and 80 wt% surfactant/cosurfactant is not fully dilutable with water. Thus, a phase separation occurs at a

high content of water. In contrast, a beverage concentrate with nana mint oil is fully water dilutable [80, 81].

In addition, a concentrate with the given composition above was prepared. The scent of the beverage is lemon-like and is comparable to the Italian liqueur “limoncello”. The taste of the microemulsion was very soapy, as the surfactant concentration is very high. However, dilution of the concentrate with pure water, did not improve the taste, which was still soapy. The addition of sweeteners to the beverage can help to cover the soapy taste [80, 81]. Furthermore, the application of the hydro distillation water residue of rosemary leaves had no influence on the taste, as the concentration is probably too low in the concentrate.

7.4.6.3.2 Antioxidant activity of drinkable microemulsions

The new established analyses method to investigate the antioxidant activity of compounds in microemulsions described in chapter 7.4.6.1.3 was used for the following experiments. Measurements in the microemulsion domain are carried out with samples with compositions according to the black line in the phase diagram (Figure 7.28). The ratio of surfactant/cosurfactant to the essential oil was kept constant at a value of 1:3 and the amount of hydro distillation water residue was changed. Measurements in microemulsion solutions were only carried out for hydro distillation water residue contents of 20, 30 and 40%. Higher water contents could not be measured, as the samples were right from the preparation turbid, respectively two phasic.

Figure 7.29 shows the percentage of inhibition in microemulsion (TWEEN® 60/ethanol (2:1)/limonene/hydro distillation water residue) and methanol solutions in relation to the mass fraction of hydro distillation water residue. The system shows some equal and different behaviors as the previous investigated microemulsion with SDS/1-pentanol (1:2), *n*-dodecane, and hydro distillation water residue. Again, a more or less linear correlation between the inhibition and the concentration of antioxidant containing water residue can be observed. In general, the higher the amount of the hydro distillation water residue in the sample, the higher is the inhibition of the DPPH radical. But the efficiency of the antioxidants in the microemulsion seems to be better than in methanol solutions, as the slope of the microemulsion samples is larger. As mentioned previously, the bigger the slope of the linear trend line, the greater is the antioxidant activity of the sample. Perhaps, the deviation from the linear behavior is due to the high viscosity of the samples, especially of the samples with 30 and 40% hydro distillation water residue. These microemulsions showed a very high viscosity, which could affect the reaction kinetics of DPPH and the antioxidants.

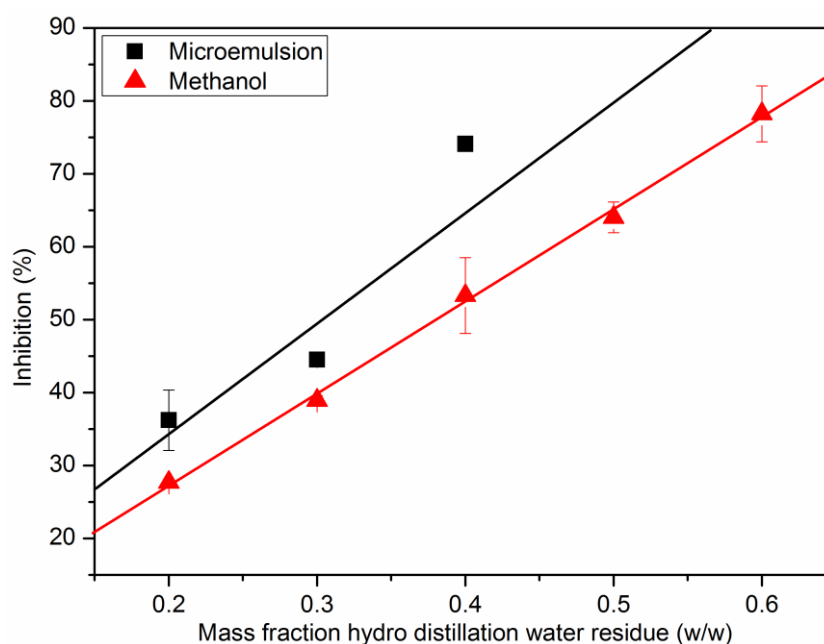


Figure 7.29: Percentage of inhibition in microemulsion (TWEEN[®] 60/ethanol (2:1)/limonene/hydro distillation water residue) and methanol solutions in relation to the mass fraction of hydro distillation water residue.

Nevertheless, there is again a difference between methanol solutions and microemulsions. However, this behavior was very surprising as the inhibition in microemulsions is slightly higher than in methanol solutions. Most likely, this result can be explained by the reaction of limonene with the DPPH radical, although the previous results (Chapter 7.4.6.2) do not confirm this behavior. But the concentration of limonene is significantly higher in the microemulsion than in the test samples from chapter 7.4.6.2. Thus, DPPH reacts with the antioxidants of the hydro distillation water residue and limonene, resulting in a higher inhibition compared to the methanol solutions of the water residue. This is in accordance with results from literature where limonene showed slight activity against the DPPH [82, 83] and other radicals [84, 85]. Concluding, it is possible to introduce the hydro distillation water residue into a green and drinkable microemulsion with limonene as essential oil. Herewith, the antioxidant properties of the beverage can be induced respectively enhanced.

Moreover, the beverage concentrate of the microemulsion with TWEEN[®] 60/ethanol (2:1), nana mint oil and water should be used to incorporate the hydro distillation water residue. As the previous results showed that pure nana oil possesses an antioxidant activity. Hence, the procedure to measure the antioxidant activity had to be adjusted. The question was if the antioxidant properties of the microemulsion with nana mint oil can be increased by the addition of the hydro distillation water residue. A formulation with 10% water respectively hydro distillation water residue, 10 wt% nana mint oil and 80 wt% TWEEN[®] 60/ ethanol was prepared. The ratio of surfactant to cosurfactant was constant at 1:2.

First, DPPH assays were carried out with a microemulsion sample containing nana mint oil, surfactant and pure water. The concentration of DPPH had to be increased to 0.2 mg/mL in the microemulsion to be able to measure appropriate UV/VIS spectra, as the nana mint oil already reacts with the DPPH radical. The other parameters were taken from the previous experiments. A second microemulsion was prepared with the hydro distillation water residue instead of pure water. A big disadvantage of this method is that the absorbance of the pure DPPH solution with a concentration of 0.2 mg/mL is above a value of 6. These spectra are not evaluable and cannot be used for analysis. For that reason, it is not possible to calculate the inhibition. Nevertheless, the measured spectra can be interpreted.

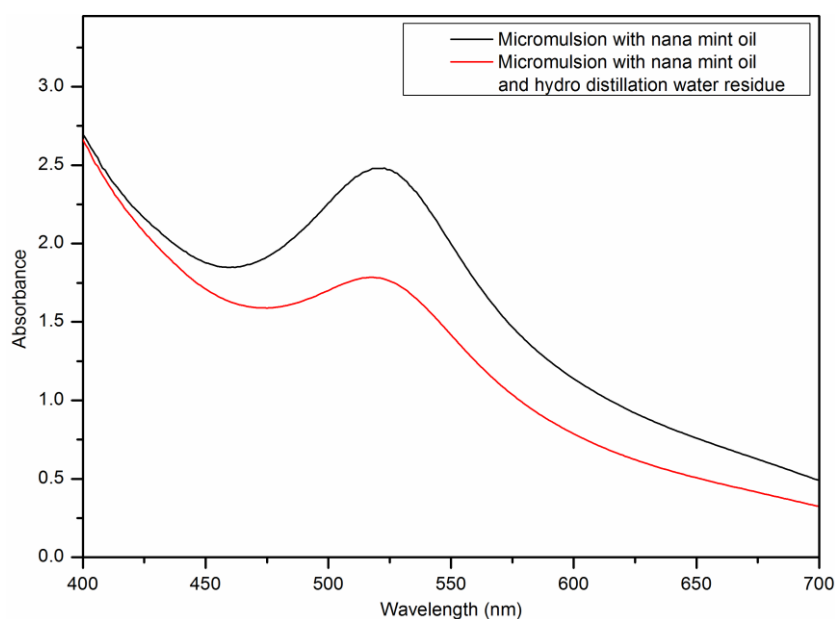


Figure 7.30: UV/VIS spectra of nana mint oil microemulsion with pure water and hydro distillation water residue after the reaction with DPPH.

Figure 7.30 presents the UV/VIS spectra of nana mint oil microemulsion with pure water and hydro distillation water residue after the reaction with a 0.2 mg/mL DPPH solution. The absorbance at 518 nm of both samples decreases from a value of approximately 6. This indicates that both microemulsions possess antioxidant properties due to the presence of nana mint oil. The absorbance after the reaction with DPPH of the sample containing the hydro distillation water residue microemulsion is lower than the one with pure water. This behavior implies an enhancement of the antioxidant activity due to the antioxidants present in the hydro distillation water residue of rosemary leaves. Concluding, it is possible to introduce the hydro distillation water residue into a green and drinkable microemulsion with the essential oil of nana mint in order to increase the antioxidant properties of the beverage. This antioxidant water residue can be also an alternative compound to conventional antioxidants, like ascorbic acid, in beverages.

7.4.7 Extraction with sodium myristate

Recently, it was demonstrated that aqueous solutions of sodium salts from fatty acids can be used to extract selectively nonpolar odorants from iris rhizomes. The method has been patented by Höß *et al.* (Institute of Physical and Theoretical Chemistry II, University of Regensburg). Now, this method should be applied to the extraction of antioxidants from rosemary leaves, especially rosmarinic acid and carnosic acid. The initial aim of this work was to find a new green method to extract simultaneously both antioxidants. By using aqueous solutions, toxic or hazardous solvents can be avoided. Aqueous soap solutions can be promising systems for this project. These soap molecules form aggregates above a certain concentration (cmc = critical micellar concentration), which can enhance the simultaneous extraction of hydrophobic and hydrophilic compounds. Especially sodium myristate, the salt of the saturated C14-fatty acid myristic acid is investigated. It is a natural amphiphilic constituent partially occurring in nearly every plant. Also rosemary leaves contain a small amount of myristic acid [26]. Thus, the idea is to use a chemical contained in the plant for plant extraction processes.

The results of this section are part of an inventor's notification, as the established method should be applied for a patent, with the topic "Selective extraction of hydrophobic antioxidant compounds from plant material by aqueous micellar solutions".

7.4.7.1 Adjustment of extraction procedure

Preliminary extraction experiments of rosemary leaves were carried out with a 1.5 wt% sodium myristate solution. Note, however, the critical micellar concentration (cmc) of sodium myristate is about 0.1 wt% and thus much lower than the used concentrations [86]. Extractions were performed with different durations (1, 2, 4, and 24 h) and a temperature of 45 °C. A temperature of 45 °C is necessary to have a clear and homogenous micellar solution. Sodium myristate has a Krafft temperature of approximately 42 °C, at which it gets soluble in water [87]. After centrifugation of the suspension, the supernatant was mixed with the internal standard solution, filtrated and analyzed by HPLC/UV without any further preparation. The results of the analyses revealed two general problems. On the one hand, it was not possible to extract carnosic acid with these experimental parameters. The recovery of rosmarinic acid from the leaves was practicable, but the extraction yield was very low with 3.32 mg rosmarinic acid per 1 g of rosemary. On the other hand, the results showed that more rosmarinic acid can be extracted within 2 h than within 4 h. This observation indicates that a degradation of the compounds may occur. Another effect supports this hypothesis. In fact, the concentration of rosmarinic acid in the sample decreased during three independent HPLC measurements. This has become noticeable as the peak area of rosmarinic acid decreased from the first to the third injection of the same sample.

By measuring the pH-value with a pH meter, it was determined that the pH-value of all sodium myristate solutions is approximately 9.7. This high pH value is typical for soaps in aqueous media. For this reason, some simple experiments with rosmarinic acid and carnosic acid standard solutions (0.5 mg/mL) were carried out. To this purpose, the pH of these solutions was adjusted to a value of 10 with 0.1 M NaOH. A change of color was observed in both solutions, which indicates a chemical reaction of the compounds. The colorless solution of rosmarinic acid turned immediately dark yellow after the addition of NaOH. After neutralization of the mixture with formic acid, the solution stayed light yellow. This observation indicates a nonreversible reaction or decomposition of rosmarinic acid. Carnosic acid showed the same behavior. The prior light yellow solution turned orange after the addition of NaOH. After neutralization, the mixture maintains a light red color.

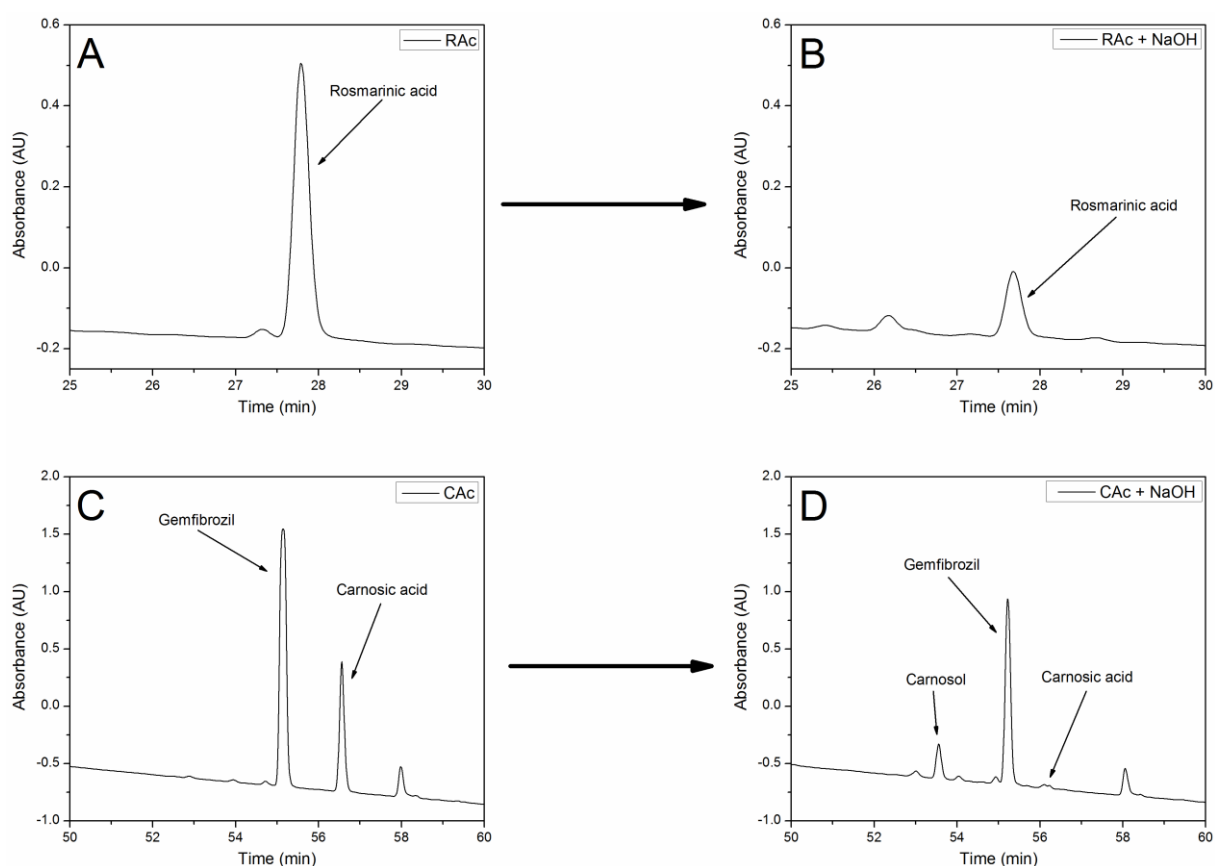


Figure 7.31: HPLC/UV chromatograms of the antioxidants before and after the addition of a 0.1 M NaOH solution. (A) Rosmarinic acid (RAC) standard solution (0.2 mg/mL) (B) Rosmarinic acid after the addition of NaOH (C) Carnosic acid (CAC) standard solution (0.2 mg/mL) with the internal standard gemfibrozil (D) Carnosic acid solution after the addition of NaOH with the internal standard gemfibrozil.

These solutions were analyzed by HPLC/UV. The chromatograms (Figure 7.31) of the antioxidants confirm the results of the visual observations. It was determined that the peak height of rosmarinic acid, with a retention time (r.t) of 27.71 min, decreases after the addition of sodium hydroxide. Also, the appearance of some other peaks can be observed, which can

be assigned to potential degradation products of rosmarinic acid. A conceivable reaction can be the hydrolysis of the ester group and the resulting formation of the yellow compound caffeic acid. The influence of alkaline pH value on carnosic acid is more significant. The chromatograms show that the peak of carnosic acid (r.t. = 56.09 min) vanishes almost completely. Also, the formation of the degradation product carnosol (r.t. = 54.04 min) and some other unknown compounds can be observed. It also seems that the alkaline pH value decreases the concentration of the internal standard gemfibrozil (r.t. = 55.21 min).

Summing up, the extraction conditions and procedure have a negative influence on the desired antioxidants. According to that, the extraction method had to be adjusted. After extraction and centrifugation, 500 μ L of the supernatant were taken and immediately acidified with 100 μ L formic acid to decrease the pH value and prevent degradation of the antioxidant compounds. This approach results in the precipitation of myristic acid and maybe carnosic acid, because both compounds are insoluble in water at room temperature. For this reason, 500 μ L of the internal standard in methanol (90%) were added to ensure the complete solubilization of the antioxidants. This adapted procedure was used for all further experiments.

7.4.7.2 Influence of extraction time and solid-liquid ratio

As already mentioned, the extraction time has a strong influence on the antioxidant yield. For all experiments, 3 wt% solutions of sodium myristate were used. It was observed that the colorless solution immediately turned green after the addition of rosemary. After a few minutes, the mixtures became brown and with increasing extraction time steadily darker. The extraction time refers to the stirring time of the samples at 45 °C in the oil bath. It has to be mentioned that extraction is not promptly stopped because of the subsequent centrifugation which lasts additionally 10 min.

Figure 7.32 shows the influence of time on the extraction yield of the antioxidants. The recovery of rosmarinic acid is almost completed after 5 min of extraction. The extraction efficiency increases slightly within 30 min and an amount of 10.33 mg rosmarinic acid per 1 g of rosemary. This value is correlated to the total amount of rosmarinic acid contained in the normal rosemary leaves. However, a longer extraction time does not influence the yield significantly. By contrast, carnosic acid shows a different behavior. The highest amount of 9.94 mg/g can be extracted after 5 min, which is 42% of the total content in the leaves. With longer extraction times, the yield of carnosic acid decreases significantly to 4.67 mg/g after 60 min, which is due to the decomposition of the antioxidant, generated by the alkaline pH value. After 4 h of extraction no more carnosic acid is detectable. Considering everything, the best extraction duration is 5 min.

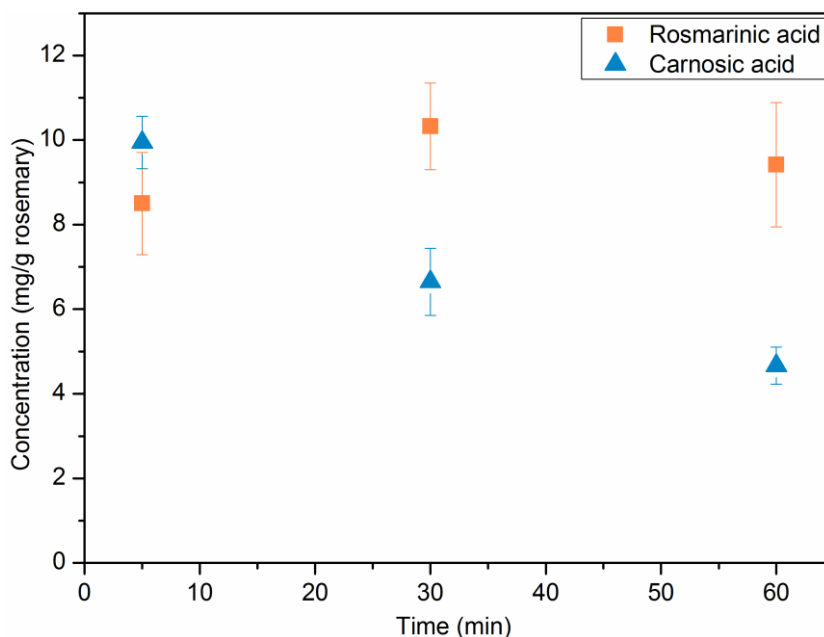


Figure 7.32: Mass concentration of rosmarinic acid and carnosic acid yield obtained by micellar extraction for different durations. A 3 wt% solution of sodium myristate was used for every extraction.

In addition, the solid-liquid ratio of rosemary leaves to micellar solution was varied. The standard solid-liquid ratio was 1/20. Experiments were also carried out with a ratio of 1/40. The experiments were performed with normal grinded rosemary leaves at 45 °C in a water bath for 5 min. It was determined that the extraction yield of carnosic acid and rosmarinic acid decreases with an increasing solid-liquid ratio. In detail, only 7.36 mg/g of carnosic acid and 5.02 mg/g of rosmarinic acid can be extracted. In addition, it was observed that the peak of carnosol in the chromatograms of these extractions is relatively high. This observation indicates an easier degradation of carnosic acid at a solid-liquid ratio of 1/40. Lower solid-liquid ratios were not investigated because of the more complicated reworking process. In summary, the best solid-liquid ratio for the extraction of rosemary leaves with aqueous sodium myristate solutions is 1/20.

7.4.7.3 Influence of concentration of sodium myristate

Besides the extraction time, also the concentration of sodium myristate solution influences the yield of antioxidants significantly. The extraction time for these experiments was always 5 min. Also a control sample with water was prepared. Figure 7.33 shows the influence of the sodium myristate concentration on the extraction yield of rosmarinic acid and carnosic acid.

It is determined that the yield of rosmarinic acid rises with increasing concentration of sodium myristate. A nearly exhaustive recovery of 8.97 mg rosmarinic acid per 1 g of rosemary leaves can be achieved with a 4 wt% aqueous solution of sodium myristate within 5 min. Carnosic acid shows quite the same behavior. The yield of carnosic acid is raised by an increasing soap concentration. The maximum amount which can be extracted with a 4 wt%

sodium myristate solution is 12.57 mg carnosic acid per 1 g rosemary. This is about 53% of the total carnosic acid amount in the leaves. The control sample shows that carnosic acid cannot be extracted with pure water. Whereas only a small amount of rosmarinic acid is recovered.

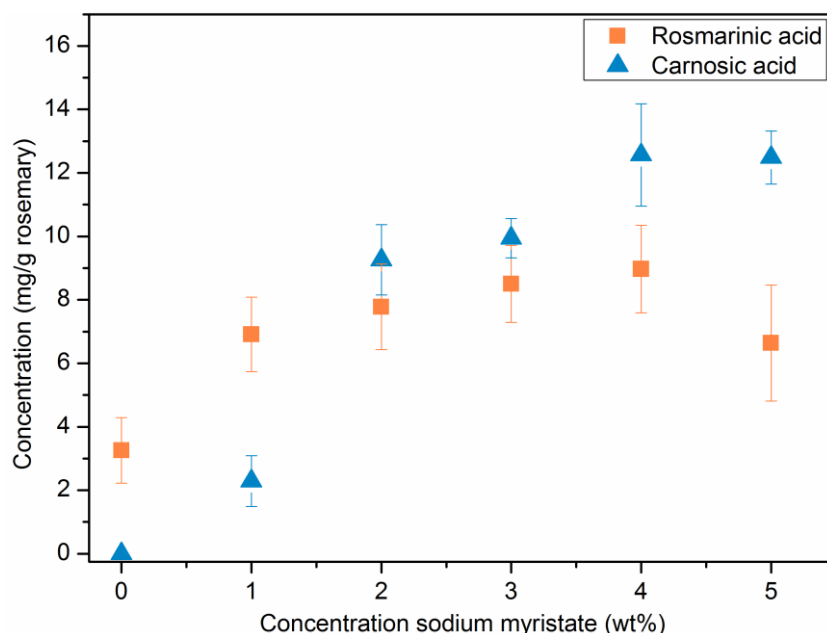


Figure 7.33: Mass concentration of rosmarinic acid and carnosic acid yields obtained by micellar extraction with varying concentrations of sodium myristate. Extraction time was always 5 min at 45 °C stirred in a water bath.

This leads to the presumption that the extraction of both antioxidants, the water-soluble rosmarinic acid and the water insoluble carnosic acid, is certainly related to the further formation of structures in the solution with increasing soap concentration. Note, however, the cmc of sodium myristate is about 0.1 wt% and thus much lower than the used concentrations [86]. Therefore, the formation of mixed micelles (soap plus antioxidants) is probable.

7.4.7.4 Influence of pH value and base

The previous results showed that the pH value of the sodium myristate influences the stability of the antioxidants. For this reason it has been investigated if the high pH value (9.7) of the micellar soap solution has a significant influence on the extraction yield of the antioxidants, especially carnosic acid. To this purpose, extraction of grinded rosemary leaves were carried out with sodium hydroxide solutions with pH values of 9, 11, 13, and 14. The experiments were also carried out for 5 min at 45 °C to make them comparable to the micellar extraction. Right after the addition of rosemary leaves to the sodium hydroxide solution, the first difference can be observed. The small rosemary particles swim initially at the water surface and the color of the solutions turns from yellow to brown. The color of the sodium hydroxide extract solution is also getting darker with rising pH. This is in contrast to

the sodium myristate solutions, where the rosemary leaves are immediately in solution and the color becomes green. Another observation is that the sodium hydroxide solutions form stable foams after 5 min of extraction. Also, a solid precipitates after the neutralization of the extract solution with formic acid.

The extracts were also analyzed by HPLC/UV to determine the exact extraction yield of the antioxidants. The influence of the pH value on the extracted concentration of rosmarinic acid and carnosic acid is plotted in Figure 7.34. The diagram shows that the extraction yield of rosmarinic acid increases with rising pH until a value of 13 is reached. In contrast at higher pH values the yield decreases slightly. In turn, the extraction yield of carnosic acid shows an unexpected trend. The extracted concentration increases significantly at pH values higher than 11. For instance, at a pH value of 13, about 4.04 mg/g of the commonly non water-soluble carnosic acid can be extracted. This is 20 times the amount, which can be extracted with pure water. The extraction yield can be increased up to 7.68 mg/g at a pH value of 14.

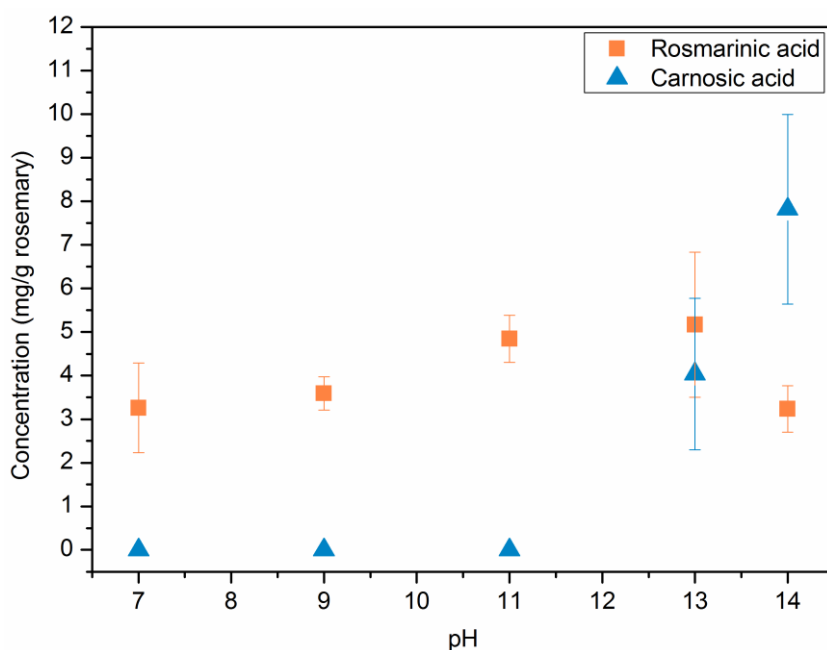


Figure 7.34: Influence of pH value on the extraction yield of the antioxidants rosmarinic acid and carnosic acid. Extractions were carried out within 5 min at 45 °C stirred in a water bath.

The macroscopic observations and the HPLC results indicate again that the alkaline pH value of the extraction solution results in a certain transformation of the compound. A possible explanation can be the formation of carnosic acid to carnosate at high pH. This molecule has a strong similarity to the cholic acid respectively the salt molecule cholate. Sodium cholate, a bile salt, is soluble in water. Above the cmc of 15 mM, cholate can form micelles in solution [88]. This behavior is also conceivable for the carnosate. Thus, carnosate is soluble in water and can form micelles. These micelles are able to extract and solubilize other compounds. This behavior is also described for bile acids and their salts. The solubility

of a bile acid can be enhanced by the addition of a bile salt above the cmc of ladder [89]. After the neutralization with an acid, carnosic acid is formed. The compound is not anymore soluble in the aqueous solution and finally precipitates as a solid.

In addition, the formation of choline salts of phenolic acids was reported in literature. The solubility of these choline-based salts in water is three orders of magnitude higher than the one of the respective acidic precursors [90]. For this reason, extractions with choline hydroxide were carried out for 5 min at 45 °C. The idea is that the extraction with choline hydroxide leads to the formation of choline carnosate and hence increases the yield of carnosic acid. The behavior of the extraction solution after the addition of rosemary leaves is quite similar to the sodium hydroxide samples. Only the color of the solution becomes darker brown and it seems to be more viscous. The extract also shows foam formation. The extraction yield of both antioxidants is higher with choline hydroxide than sodium hydroxide at a pH value of 14. In detail, 4.68 mg/g of rosmarinic acid and 10.31 mg/g of carnosic acid can be extracted with choline hydroxide. These higher values can indicate the formation of choline carnosate.

But the yields with bases as extraction solvent are still below the values of micellar extraction with sodium myristate. On the one hand, the high pH value enhances the extraction efficiency, but on the other hand, the yield of the antioxidants decreases over time. Thus, the extraction process is somewhat dependent on pH, but the extraction yield is significantly influenced by the sodium myristate concentration.

7.4.7.5 Influence of particle size and ultrasound-assisted extraction

Another attempt to increase the extraction yield of the antioxidants was to minimize the particle size of the rosemary leaves. A fine and homogenous powder of rosemary leaves was obtained by grinding the leaves in liquid nitrogen. Also, the influence of ultrasound-assisted extraction was investigated. It is expected that ultrasound enhances the extraction efficiency by accelerating the extraction equilibration. Therefore, the samples were put in the ultrasonic bath for 5 min at 45 °C. Sodium myristate solutions with a concentration of 3 wt% were used for all these experiments.

Figure 7.35 shows the influence of the particle size of the rosemary leaves and the influence of ultrasound-assisted extraction on the extraction yield of rosmarinic acid and carnosic acid. It is illustrated that the extraction efficiency of rosmarinic acid is more or less neither influenced by the particle size nor by ultrasound-assisted extraction. The yield of carnosic acid is more influenced by these factors. If normal grinded rosemary leaves are used, ultrasound can increase the extraction yield for carnosic acid from 9.55 mg/g up to 13.44 mg/g. A smaller particle size of the rosemary leaves actually decreases the extracted amount of carnosic acid.

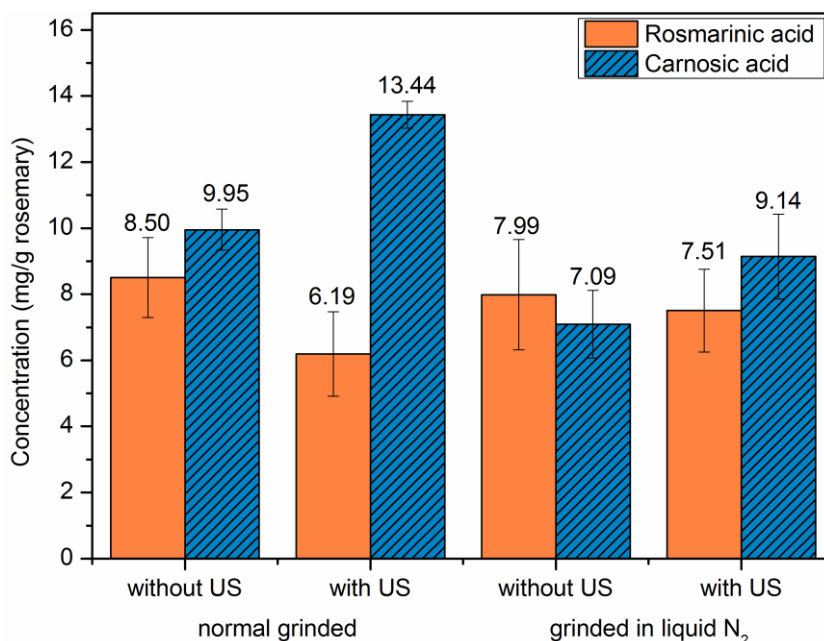


Figure 7.35: Influence of the rosemary leaves particle size and ultrasound-assisted (US) extraction on the extraction yield of antioxidants. All extractions were carried with sodium myristate solutions (3 wt%) for 5 min at 45 °C

Ultrasound-assisted extraction of the fine powder does not significantly change respectively more or less decrease the extraction yield. This behavior can possibly explained by the fact that carnosic acid is more adsorbed on the rosemary leaves surface due to the smaller particle size. For this reason, the mass transfer kinetics of the antioxidant to the solvent is slowed down [91, 92]. Taking everything into account, the best way to extract rosemary with aqueous sodium myristate solutions is to take normal grinded leaves and assist the extraction by ultrasound.

7.4.7.6 Extraction with best parameters

In the previous chapters a lot of different extraction parameters were investigated. The results of the best extraction methods are summarized in Figure 7.36. In addition, further extractions were carried out which combine the best parameters of the previous results in one experiment.

The best yield was achieved by extractions of normal grinded rosemary leaves with an aqueous 4 wt% sodium myristate solution within 5 min in an ultrasonic bath at 45 °C. In detail, 7.27 mg/g of rosmarinic acid (82% of the total amount) and 12.81 mg/g of carnosic acid (54%) can be extracted with these parameters. The results of the pH-dependent extractions also show that both antioxidants can be extracted with aqueous alkaline solutions instead of micellar solutions. For example, a 1 M sodium hydroxide solution with a pH-value of 14 can extract 3.23 mg/g of rosmarinic acid and 7.68 mg/g of carnosic acid. If choline

hydroxide is used as a base, the extraction yield can actually be increased up to 10.31 mg/g for carnosic acid and 7.27 mg/g for rosmarinic acid.

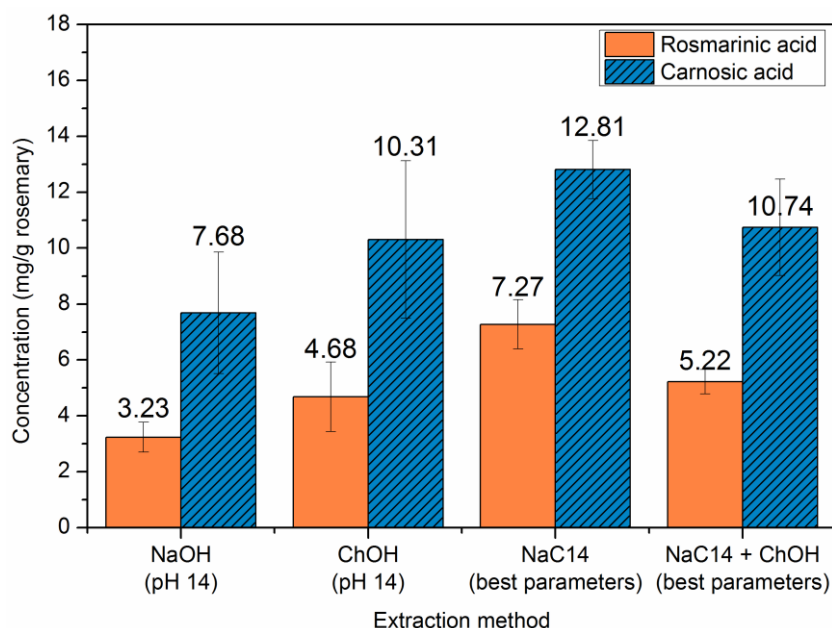


Figure 7.36: Overview of the different investigated extraction methods and the corresponding extraction yield of rosmarinic acid and carnosic acid. All experiments were carried out for 5 min and 45 °C.

The idea came up if a combination of sodium myristate and choline hydroxide can increase the extraction yield. Unfortunately, the yield decreases compared to extractions with aqueous sodium myristate solutions. The extracted concentrations of 10.74 mg/g of carnosic acid and 5.22 mg/g of rosmarinic acid are in the range of a pure choline hydroxide solution with a pH value of 13.6. A possible explanation of this observation can be that the high pH-value of the extraction solution accelerates the decomposition of the antioxidant compounds. In summary, it can be noticed that the extraction of antioxidants with aqueous sodium myristate solutions provides the highest extraction yields.

7.4.7.7 Alternative surfactants

Due to the fact that especially carnosic acid cannot be extracted exhaustively with aqueous sodium myristate solutions, alternative surfactants respectively soaps were investigated. Experiments were carried out with potassium myristate (KC14), potassium stearate (KC18), and a self-prepared sodium myristate solution (NaC14 (techn.)). Sodium myristate can be easily produced by adding an appropriate amount of sodium hydroxide to an aqueous myristic acid solution at 60 °C. The reaction is completed at the point when a homogenous clear solution is obtained. The pH value of a 4 wt% solution was measured to be 9.5. Potassium stearate was obtained from the company Stéarinerie Dubois. The purity of the fine white powder is 97.5%. An advantage of this compound is the lower price compared to

sodium myristate. The used Potassium stearate is a technical mixture of potassium salts of the saturated fatty acids myristic acid (C_{14}), palmitic acid (C_{16}), and stearic acid (C_{18}). The white powder contains 60% potassium stearate and 30% salts of the other fatty acids. The trade name of this product is Ligastar KA M from the company Peter Greven.

In addition, further extractions were attempted to be carried out with sodium stearate, but the soap is not soluble in water at 45 °C. A clear homogenous solution can be obtained over 65 °C. This high temperature can accelerate the decomposition of the antioxidants. For this reason, the soap was not used for the extraction of rosemary leaves. The trade name of the soap is Ligastar NA R/D from the company Peter Greven. Sodium stearate is a technical mixture of sodium salts of the saturated fatty acids palmitic acid (C_{16}) and stearic acid (C_{18}). The white powder contains 60% sodium stearate and 30% salts of the other fatty acids.

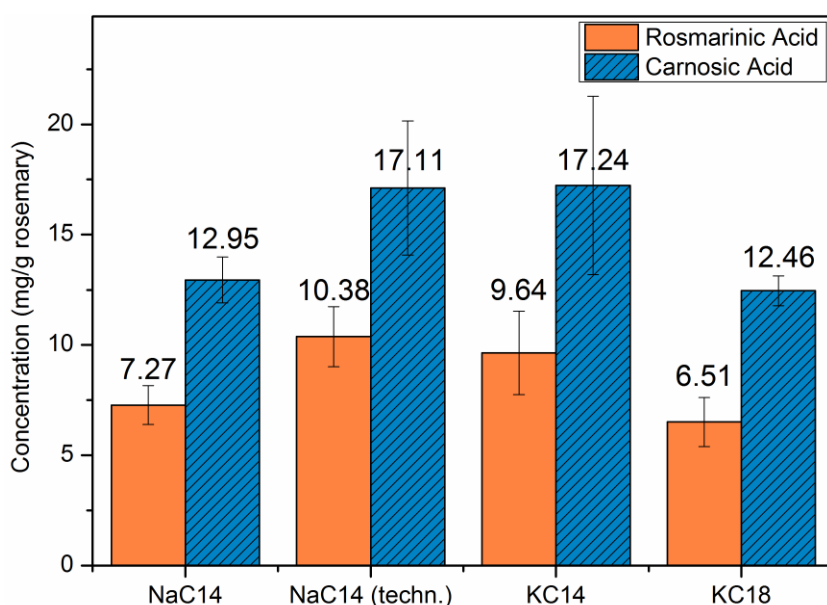


Figure 7.37: Overview of the different investigated surfactants and the corresponding extraction yield of rosmarinic acid and carnosic acid. For the experiments a 4 wt% solution of sodium myristate (NaC14), a technical sodium myristate solution (NaC14 (techn.)), potassium myristate (KC14), and potassium stearate (KC18) was used. All extractions were carried out for 5 min and 45 °C in an ultrasonic bath.

All extractions of normal grinded rosemary leaves were carried out with aqueous 4 wt% soap solutions within 5 min in an ultrasonic bath at 45 °C. The extraction yields of the different surfactant solutions are summarized in Figure 7.37. It is shown that sodium myristate and potassium stearate achieve almost the same extraction efficiency of rosmarinic acid and carnosic acid. The yield of both antioxidants can be increased by using aqueous solutions of potassium myristate. With potassium myristate the extracted concentration of carnosic acid can be increased up to 17.24 mg/g and 9.64 mg/g of rosmarinic acid. This is correlated to an exhaustive extraction of rosmarinic acid and 73% of the total amount of carnosic acid in rosemary leaves. A further advantage of potassium myristate is the lower Krafft temperature

compared to the sodium salt. Thus, extractions can be performed at lower temperatures, which will have a positive influence on the decomposition of the antioxidant compounds.

7.4.7.8 Alternative extraction method

Further investigations focused on the goal to extract selectively carnosic acid with aqueous solutions. Currently, carnosic acid is extracted, besides other compounds, with organic solvents like ethanol or acetone. The major disadvantage of these solvents is their extreme flammability. Therefore, an alternative method to extract carnosic acid from rosemary leaves was established.

Previous results showed that carnosic acid is soluble respectively extractable at high pH values. For this reason, extractions of rosemary leaves were realized with a 0.1 M sodium hydroxide solution at a pH value of 13. The extractions were carried out for 5 min in an ultrasonic bath at room temperature. The solution turned brown and foam formation was observed. The suspension was subsequently filtrated through a paper filter in order to remove the residual leaves. The aqueous solution was acidified with formic acid to obtain a low pH value and a solid precipitates. The suspension was again filtrated, obtaining a yellow solution and a white solid. The solid was dried in the compartment drier at 40 °C. The mass of the extracted precipitate is 3.6% of the initial rosemary leaves weight. The yellow aqueous solution and the white solid were analyzed by HPLC/UV in order to determine the content of carnosic acid. It was found out that the aqueous solution only contains rosmarinic acid and other water soluble compounds, but no carnosic acid. More important is the analysis of the precipitate. Here, the major compound should be carnosic acid, due to the extraction at a high pH value and the subsequent precipitation by acidifying the solution. Actually, carnosic acid is present in the solid, but only in a mass ratio of approximately 3%. This indicates that other compounds were extracted at high pH values, which precipitate again at low pH values. Possible substances are the saponins ursolic and oleanolic acid, which are also contained in rosemary leaves [22]. However, it has to be mentioned that the extraction of carnosic acid was not exhaustive and only 1.04 mg/g were recovered. But one result led to the implementation of further investigations, as it is possible to separate rosmarinic acid and other water soluble compounds from carnosic acid with this extraction procedure, which is described in the following chapter.

7.4.7.9 Selective extraction of carnosic acid

A further possible method to recover selectively carnosic acid from rosemary leaves is the extraction with aqueous sodium myristate solutions. For this reason, extractions of normal rosemary leaves were realized with a 4 wt% sodium myristate solution in an ultrasonic bath for 5 min at 45 °C. The suspensions were subsequently centrifuged for 10 min. A defined volume of the supernatant was acidified with formic acid. The low pH value of the aqueous

solution results in the precipitation of a white solid. The suspension was filtrated, obtaining a brown solution and a white solid. The precipitate was dried for 1 h in the compartment drier at 40 °C. Also, extractions with acetone were carried out to compare the selectivity of both solvents. To this purpose, normal rosemary leaves were extracted with acetone in an ultrasonic bath for 5 min at 45 °C. The solvent was evaporated under a nitrogen stream after the filtration of the suspension, obtaining a green solid. The white solid and brown solutions of the micellar extraction, as well as the green solid obtained by acetone extraction were analyzed by HPLC/UV.

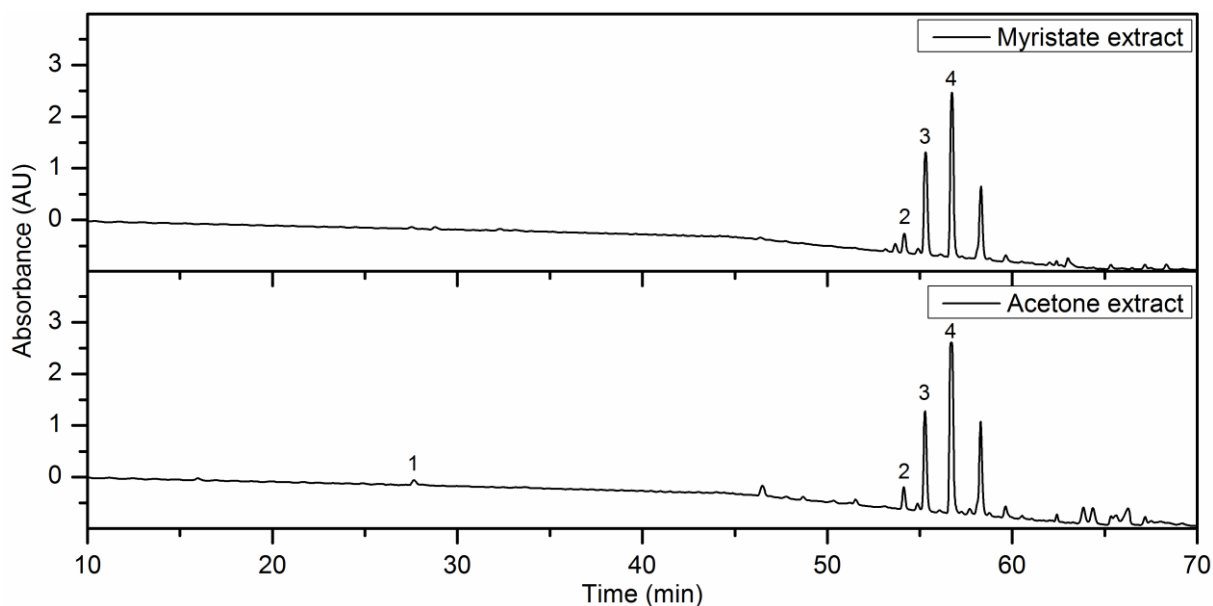


Figure 7.38: HPLC chromatograms of a sodium myristate and acetone extract. Peak identification: (1) rosmarinic acid; (2) carnosol; (3) gemfibrozil (IS); (4) carnosic acid;

Figure 7.38 presents the chromatograms of the dissolved precipitates of a sodium myristate and acetone extract obtained by HPLC/UV. Both extracts contain mainly carnosic acid and carnosol. The aqueous phase of the micellar extraction only contains rosmarinic acid and other water soluble compounds, but no carnosic acid. For a better validity of the extraction selectivity and classification of the compounds, the samples were additionally analyzed by HPLC coupled with a mass spectrometer (HPLC/MS). It is examined that the acetone extract contains mainly rosmarinic acid, rosmanol, carnosol, carnosic acid, methyl carnosate, and a triterpenoid (probably ursolic or oleanolic acid). Whereas the precipitate of the micellar extraction only contains carnosic acid and the degradation products carnosol and methyl carnosate, as well as a high amount of myristic acid. Deductive, it can be concluded that a better selective extraction of carnosic acid can be achieved with aqueous sodium myristate solutions compared with acetone extraction. But the micellar extract contains a high amount of myristic acid.

In addition, the total mass yield of both extraction method related to the initial weight of rosemary leaves was determined, which is 16.7% for acetone and 38.6% for sodium myristate. The reason for the significant higher mass extraction yield of the myristate solution is the high content of myristic acid in the extract respectively precipitate. However, the much more important property of the extract is the content of carnosic acid, which is 2.0% in the micellar extract and 13.3% in the acetone extract.

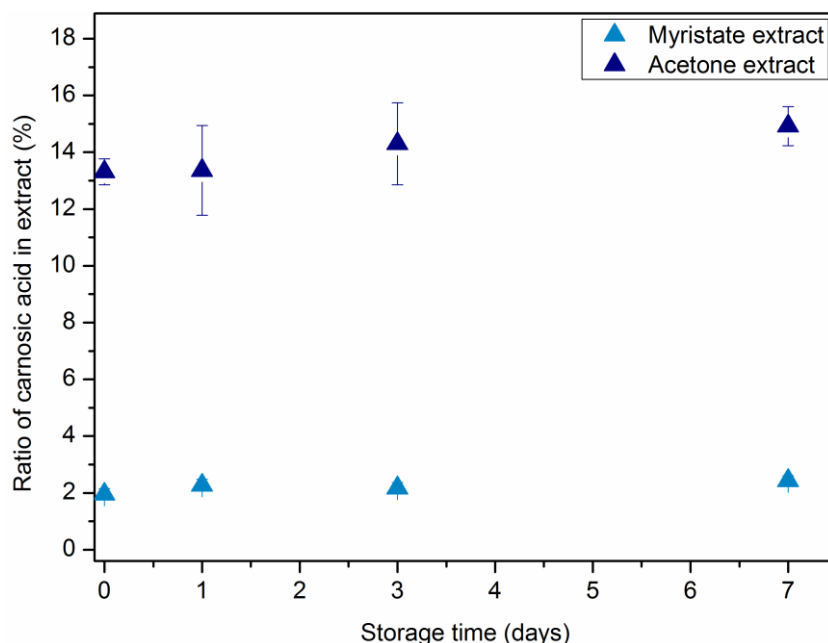


Figure 7.39: Ratio of carnosic acid in myristate and acetone extract. The samples were analyzed after different storage times (room temperature, without light exposure) to investigate the stability of the antioxidant in the extract over time.

Furthermore, the stability of carnosic acid in the micellar and acetone was investigated over time. The samples were stored at room temperature and without light exposure and subsequently analyzed after different storage times. Figure 7.39 shows the ratio of carnosic acid in the myristate and acetone extract as a function of the storage time. It can be seen that the content of carnosic acid increases slightly in both extracts. This is probably due to the fact that the extracts were not completely dry at the beginning. However, a decrease of the carnosic acid is not observable. Thus, carnosic acid is stable in both extracts over seven days of storage.

In addition, another method to extract selectively carnosic acid from rosemary leaves was investigated. To this purpose, a combination of maceration and percolation with water was used to remove rosmarinic acid and other water soluble compounds from the rosemary leaves. The aqueous extract solution was colored yellow/brown, whereas the leaves got a brown/dark green color. Micellar extractions of these pretreated leaves were realized according to the previous described method. The extract solution was again acidified with formic acid. The suspension was filtrated, obtaining a colorless solution and a white solid. It

can be determined that the aqueous solution of the micellar extraction contains no rosmarinic acid or other water soluble compounds. Apart from that, the precipitate of the micellar extraction only contains the antioxidant carnosic acid and its degradation products carnosol and methyl carnosate, as well as a high amount of myristic acid. Thus, the composition of the precipitate from pretreated leaves shows no differences to the one obtained from normal rosemary leaves. These experiments show that it is not necessary to remove rosmarinic acid or other water soluble compounds before the extraction with aqueous sodium myristate solutions.

It can be concluded that a more selective extraction of carnosic acid can be achieved with aqueous sodium myristate solutions compared to acetone. Surprisingly, by means of the investigated method fewer by-products are contained in the precipitate of the micellar extract compared to the acetone extract. But the content of carnosic acid is relatively low with 2.0% in the extract, due to the high amount of myristic acid. It was also demonstrated that the pretreatment of the rosemary leaves in order to remove water soluble compounds is not necessary. With the described technique, extractions can be carried out with a non-flammable, non-toxic, and green solvent. Compared to conventional extraction methods of rosemary leaves, this is a significant saving in time and energy as no distillation respectively removal of the solvent is necessary. The stability of carnosic acid is the same as in acetone extract. In future, the yield of the micellar extraction should be increased, which can be achieved by using an alternative soap like potassium myristate instead of sodium myristate. A further advantage of the potassium salt is that extractions can be performed at lower temperatures. These extract can be used as food additive without further treatment, as only green compounds respectively plant substances. A possible disadvantage of this new extraction method could be the smaller amount of carnosic acid in the final extract. Therefore, a method has to be established to increase the content of carnosic acid.

7.4.7.10 Regeneration of the extract

A further goal was to concentrate the carnosic acid in the precipitate of the sodium myristate extract. To this purpose, the precipitate was dried after neutralization and filtration. The extract was dissolved in a small amount of ethanol. In detail, 3 mL ethanol was added to 0.1 g of extract. After a further filtration step, the extract was put in a freezer at -20 °C. Myristic acid precipitates at this low temperature, whereas carnosic acid is still dissolved in ethanol. After filtration of the solution, the excessive ethanol is evaporated under a nitrogen stream to obtain the pure extract. HPLC analyses show that the ratio of carnosic acid was increased up to 8.4%. If this step is performed several times, a further concentration of carnosic acid in the extract can be achieved.

Consequently, it is possible to extract carnosic acid from rosemary leaves by the neutralization of an aqueous micellar sodium myristate solution. The ratio of carnosic acid in

the extract can be increased by dissolving the precipitate in ethanol and subsequent precipitation of myristic acid at -20 °C. The precipitated and recovered myristic acid can be re-used for further extractions.

7.5 Conclusion

The preliminary aim of this work was to investigate the influence of hydro and steam distillation on the antioxidant compounds present in rosemary leaves. In addition, a possible application of the waste water after hydro distillation was sought. Furthermore, an alternative method, micellar extraction, to obtain antioxidants from rosemary leaves was investigated. The main focus of the research involved the two antioxidants carnosic acid and rosmarinic acid.

Before starting the extraction experiments, it was necessary to have suitable and efficient analyses methods. The solvent extracts containing antioxidants were analyzed by HPLC/UV. It was found out that the compound gemfibrozil is a suitable compound for internal standard calibration. By means of this compound it was for the first time possible to determine simultaneously the content of rosmarinic acid and carnosic acid in rosemary extracts. The volatile essential oil of rosemary leaves was analyzed by GC/FID.

In the first part of this chapter, the effect of hydro distillation on the antioxidant compounds contained in Moroccan rosemary leaves was investigated. For characterization, methanol is an appropriate solvent for Soxhlet extraction to determine simultaneously the content of rosmarinic acid (water soluble) and carnosic acid (insoluble in water) in the rosemary leaves, which is 8.9 mg/g for rosmarinic acid and 23.6 mg/g for carnosic acid. The time of hydro distillation affects significantly the antioxidants in the leaves. On the one hand, a maximum amount of rosmarinic acid is present in the water residue after 2.5 h of hydro distillation. Also the antioxidant activity of the residual water determined by DPPH assays increases with rising hydro distillation time. Moreover, the concentration of rosmarinic acid decreased again with increasing distillation time. On the other hand, the long exposure of heat during hydro distillation influences the residual antioxidants in the leaves, especially carnosic acid. Actually, the content of rosmarinic acid in the residual leaves after a 4 h lasting hydro distillation is reduced by up to 76% and 36% for carnosic acid.

Normally, the aqueous residue of hydro distillation is a waste product and is disposed. In future, the recovery of antioxidants from natural resources becomes more and more important due to the replacement of synthetic antioxidants. Here, a possible source of the natural antioxidant rosmarinic acid was identified. For this reason it is necessary to see the hydro distillation water residue as co-product of the extraction and not as waste product. This residue can be taken as additive without any further purification to increase the antioxidant

activity of a product or it can be re-extracted to gain the pure antioxidants. This would be in line with the concept of biorefinery and green extraction.

The goal of the second part of this main chapter was to find an application for the hydro distillation water residue without any further purification. Therefore, the antioxidant activity of this residue was investigated in different microemulsions. The main aim of this study was to find out if the microstructure in microemulsions influences the activity of the antioxidant compounds. The water residue of a 2.5 h lasting hydro distillation was taken for all investigations, as this residue has the highest antioxidant activity. Preliminary, the water residue was introduced to the system SDS, 1-pentanol, and *n*-dodecane. It was determined that the hydro distillation water residue does not influence the shape of the phase diagram and the microstructures of the microemulsion, compared to pure water. Moreover, a method was developed to carry out DDPH assays in microemulsions. It was found that the microstructures in different regions of the microemulsion do not influence the antioxidant activity. In addition, these results were compared with common DPPH measurements in methanol solutions. It was investigated that the efficiency of the antioxidants in the microemulsions is equal to the one in methanol solutions. But the inhibition in methanol solutions is higher than in microemulsions. A possible explanation of this behavior is that the water soluble antioxidant compounds and DPPH are unequally distributed in the water and oil phase of the microemulsions. As a consequence, the reaction kinetic is slowed down in microemulsions. This behavior can probably be used for pharmaceutical or nutrition applications to regulate the delivery duration of antioxidant compounds.

Another microemulsion system was chosen for the possible application of the hydro distillation water residue. The investigated system consisted of water, TWEEN[®] 60, ethanol, and limonene, which is a drinkable and green microemulsion. The hydro distillation water residue of rosemary leaves was introduced to this system in order to enhance its antioxidant activity. The results showed the same behavior as the previous investigated microemulsion. Concluding, it was possible to introduce the water residue into a green and drinkable microemulsion with limonene as essential oil in order to induce the antioxidant properties of the beverage.

Afterwards, the market-ready beverage concentrate of a microemulsion with TWEEN[®] 60/ ethanol (2:1), nana mint oil, and water was used to incorporate the hydro distillation water residue. The results implied an enhancement of the antioxidant properties in the beverage concentrate due to the antioxidant compounds present in the hydro distillation water residue. Concluding, it is possible to introduce the hydro distillation water residue into a green and drinkable microemulsion with the essential oil of nana mint in order to increase the antioxidant properties of the beverage. Thus, this antioxidant water residue can be an alternative to common antioxidants, like ascorbic acid, in conventional beverages. The water

residue does not influence the smell and taste of the beverage concentrate, as only a small amount of the residue is necessary to have a sufficient antioxidant activity.

In the last part of this chapter an alternative green method for the extraction of antioxidants from rosemary leaves was investigated. The goal was to extract simultaneously the water-soluble rosmarinic acid and the water insoluble carnosic acid with aqueous micellar solutions. Extractions were carried out with aqueous solutions of the sodium myristate, which is the salt of the saturated C₁₄-fatty acid myristic acid. Different parameters like extraction time, soap concentration, pH-value, particle size of rosemary leaves, and ultrasound-assisted extraction were investigated. The best yield was obtained when grinded rosemary leaves were extracted with a 4 wt% sodium myristate solution in an ultrasonic bath at 45 °C. The extraction process was stopped after 5 min by acidifying the soap solution with formic acid, which results in the precipitation of myristic acid. By means of this method, the total amount of rosmarinic acid and three-quarter of the water insoluble carnosic acid can be extracted. An almost exhaustive extraction of carnosic acid can be achieved by using the alternative soap potassium myristate. Compared to conventional extraction methods of rosemary leaves, this is a significant saving in time and energy as no distillation or removal of the solvent is necessary.

In addition, an alternative processing method to obtain specifically carnosic acid was invented. Therefore, the white precipitate was removed after the micellar extraction and acidification of the solution and analyzed. This solid contains carnosic acid and its degradation products carnosol and methyl carnosate, as well as a high amount of myristic acid. Hence, a more selective extraction of carnosic acid can be achieved with aqueous sodium myristate solutions compared to acetone. It was examined that the extracts obtained by acetone contained mainly rosmarinic acid, rosmanol, carnosol, carnosic acid, methyl carnosate, and a triterpenoid (probably ursolic or oleanolic acid). By means of the investigated method fewer by-products are contained in the precipitate of the micellar extract compared to the acetone extract. But the content of carnosic acid was 2.0% in the micellar extract due to the high amount of myristic acid, whereas 13.3% of carnosic acid was present in the acetone extract. The stability of carnosic acid is identical in both extracts over seven days of storage.

A minor disadvantage of the micellar extraction method was the lower content of carnosic acid in the final extract. For that reason, the precipitate was dissolved in ethanol and subsequently put in a freezer at -20 °C. Myristic acid precipitated at this low temperature, whereas carnosic acid was still dissolved in ethanol. After the filtration of the solution, the excessive ethanol was evaporated under a nitrogen stream obtaining the pure extract. With this method the content of carnosic acid in the extract can be significantly increased. Thus, a new green extraction method was invented which allows a selective extraction of carnosic acid with a non-flammable, non-toxic, and green aqueous micellar solution.

7.6 References

- [1] M. Wichtl, *Teedrogen und Phytopharmaka* - ein Handbuch für die Praxis auf wissenschaftlicher Grundlage 5. ed, **2009**, Stuttgart: Wiss. Verl.-Ges.
- [2] N. Nakatani, *BioFactors*, **2000**, 13, 141-146.
- [3] N. Ito, S. Fukushima, A. Haqlwara, M. Shibata, and T. Ogiso, *J. Natl. Cancer Inst.*, **1983**, 70, 343-352.
- [4] C. Leclercq, D. Arcella, and A. Turrini, *Food Chem. Toxicol.*, **2000**, 38, 1075-1084.
- [5] N. Ito, S. Fukushima, and H. Tsuda, *Crit. Rev. Toxicol.*, **1985**, 15, 109-50.
- [6] M.L. Presti, S. Ragusa, A. Trozzi, P. Dugo, F. Visinoni, A. Fazio, G. Dugo, and L. Mondello, *J. Sep. Sci.*, **2005**, 28, 273-80.
- [7] E. Stahl and W. Schild, *Pharmazeutische Biologie (Drogenanalyse II: Inhaltsstoffe und Isolierungen)*, **1981**, Stuttgart, New York: Gustav Fischer.
- [8] R. Hänsel and O. Sticher, *Pharmakognosie - Phytopharmazie*, 9. ed, **2010**, Heidelberg: Springer.
- [9] M. Marin, V. Koko, S. Duletić-Laušević, P.D. Marin, D. Rančić, and Z. Dajic-Stevanovic, *S. Afr. J. Bot.*, **2006**, 72, 378-382.
- [10] A.K. Genena, H. Hense, A. Smânia Junior, and S.M.d. Souza, *Ciênc. Tecnol. Aliment.*, **2008**, 28, 463-469.
- [11] M. Moss, J. Cook, K. Wesnes, and P. Duckett, *Intern. J. Neuroscience*, **2003**, 113, 15-38.
- [12] A. Ismail, Z. Marjan, and C. Foong, *Food Chem.*, **2004**, 87, 581-586.
- [13] M.P. Kähkönen, A.I. Hopia, H.J. Vuorela, J.-P. Rauha, K. Pihlaja, T.S. Kujala, and M. Heinonen, *J. Agric. Food Chem.*, **1999**, 47, 3954-3962.
- [14] H. Lindberg Madsen and G. Bertelsen, *Trend. Food Sci. Tech.*, **1995**, 6, 271-277.
- [15] P.J. Hidalgo, J.L. Ubera, M.T. Tena, and M. Valcárcel, *J. Agric. Food Chem.*, **1998**, 46, 2624-2627.
- [16] M.J. del Bano, J. Lorente, J. Castillo, O. Benavente-Garcia, J.A. del Rio, A. Ortuno, K.W. Quirin, and D. Gerard, *J. Agric. Food Chem.*, **2003**, 51, 4247-53.
- [17] J.C. Luis and C.B. Johnson, *Span. J. Agric. Res.*, **2005**, 3, 106.
- [18] S. Tewtrakul, H. Miyashiro, N. Nakamura, M. Hattori, T. Kawahata, T. Otake, T. Yoshinaga, T. Fujiwara, T. Supavita, S. Yuenyongsawad, P. Rattanasuwon, and S. Dej-Adisai, *Phytother. Res.*, **2003**, 17, 232-9.
- [19] A. Mazumder, N. Neamati, S. Sunder, J. Schulz, H. Pertz, E. Eich, and Y. Pommier, *J. Med. Chem.*, **1997**, 40, 3057-63.
- [20] J. Bauer, S. Kuehn, J.M. Rollinger, O. Scherer, H. Northoff, H. Stuppner, O. Werz, and A. Koeberle, *J. Pharmacol. Exp. Ther.*, **2012**, 342, 169-76.
- [21] A.E. Moran, A.M. Carothers, M.J. Weyant, M. Redston, and M.M. Bertagnolli, *Cancer Res.*, **2005**, 65, 1097-1104.
- [22] R. Hänsel, H. Hager, S. Greiner, G. Heubl, K. Keller, H. Rimpler, E. Stahl-Biskup, and G. Schneider, *Hagers Handbuch der Pharmazeutischen Praxis: Drogen P-Z Folgeband 2*, **2013**, Berlin, Heidelberg: Springer.
- [23] J. Pollier and A. Goossens, *Phytochemistry*, **2012**, 77, 10-15.

- [24] J. Liu, *J. Ethnopharmacol.*, **2005**, 100, 92-94.
- [25] J. Liu, *J. Ethnopharmacol.*, **1995**, 49, 57-68.
- [26] S. Dallali, M. Llovera, J. Eras Joli, S. Houcine, and R. Canela-Garayoa, *Anal. Lett.*, **2015**, 49, 467-476.
- [27] C. Boutekedjiret, F. Bentahar, R. Belabbes, and J.M. Bessiere, *Flavour Fragr. J.*, **2003**, 18, 481-484.
- [28] S. Catty, *Hydrosols: the next aromatherapy*, **2001**, Rochester: Healing Arts Press.
- [29] P.W. Atkins and J. de Paula, *Physikalische Chemie*, 4. ed, **2006**, Weinheim: Wiley-VCH.
- [30] E. Reverchon and F. Senatore, *Flavour Fragr. J.*, **1992**, 7, 227-230.
- [31] A. Basile, M.M. Jiménez-Carmona, and A.A. Clifford, *J. Agric. Food Chem.*, **1998**, 46, 5205-5209.
- [32] N. Bousbia, M. Abert Vian, M.A. Ferhat, E. Petitcolas, B.Y. Meklati, and F. Chemat, *Food Chem.*, **2009**, 114, 355-362.
- [33] C. Bicchi, A. Binello, and P. Rubiolo, *Phytochem. Anal.*, **2000**, 11, 236-242.
- [34] S.S. Chang, B. Ostric-Matijasevic, O.A.L. Hsieh, and C.-L. Huang, *J. Food Sci.*, **1977**, 42, 1102-1106.
- [35] M.T. Tena, M. Valcarcel, P.J. Hidalgo, and J.L. Uebera, *Anal. Chem.*, **1997**, 69, 521-6.
- [36] O. Celiktas, E. Bedir, and F. Sukan, *Food Chem.*, **2007**, 101, 1457-1464.
- [37] E. Ibanez, A. Kubatova, F.J. Senorans, S. Cavero, G. Reglero, and S.B. Hawthorne, *J. Agric. Food Chem.*, **2003**, 51, 375-82.
- [38] S. Birtic, P. Dussort, F.X. Pierre, A.C. Bily, and M. Roller, *Phytochemistry*, **2015**, 115, 9-19.
- [39] M.C. Díaz-Maroto, M.S. Pérez-Coello, E. Sánchez-Palomo, and M.A. González Vinas, *J. Sens. Stud.*, **2007**, 22.
- [40] A. Szumny, A. Figiel, A. Gutiérrez-Ortiz, and Á.A. Carbonell-Barrachina, *J. Food Eng.*, **2010**, 97, 253-260.
- [41] J.A. Larrauri, P. Rupérez, and F. Saura-Calixto, *J. Agric. Food Chem.*, **1997**, 45, 1390-1393.
- [42] M.C.S.G. Blanco, L.C. Ming, M.O.M. Marques, and O.A. Bovi, *Acta Hort.*, **2002**, 569, 99-103.
- [43] Y. Zhang, J.P. Smuts, E. Dodbiba, R. Rangarajan, J.C. Lang, and D.W. Armstrong, *J. Agric. Food Chem.*, **2012**, 60, 9305-14.
- [44] E. Ibáñez, A. Oca, G. de Murga, S. López-Sebastián, J. Tabera, and G. Reglero, *J. Agric. Food Chem.*, **1999**, 47, 1400-1404.
- [45] H. Yan, L. Wang, X. Li, C. Yu, K. Zhang, Y. Jiang, L. Wu, W. Lu, and P. Tu, *Biomed. Chromatogr.*, **2009**, 23, 776-81.
- [46] C. Popovici, I. Saykova, and B. Tylkowski, *e-Rev. Génie Ind.*, **2009**, 4, 25-39.
- [47] M.H.H. Roby, M.A. Sarhan, K.A.-H. Selim, and K.I. Khalel, *Ind. Crop. Prod.*, **2013**, 43, 827-831.
- [48] M. Clausse, L. Nicolas-Morgantini, A. Zradba, and D. Touraud, *Microemulsion Systems - Surfactant Science Series*, Vol. 24, **1987**, New York: Dekker.

- [49] N. Troncoso, H. Sierra, L. Carvajal, P. Delpiano, and G. Gunther, *J. Chromatogr. A*, **2005**, 1100, 20-5.
- [50] S.A. Hassan, K. Lam, M. El sherbiney, T. Haikal, M. Mantawy, M. Siddiqui, and S. Al-Jassabi, *Int. J. Pharm. Sci. Letters*, **2012**, 2, 37-43.
- [51] S. Başkan, N. Öztekin, and F.B. Erim, *Food Chem.*, **2007**, 101, 1748-1752.
- [52] V.R. Meyer, *Practical High-Performance Liquid Chromatography*, 5. ed, **2013**: Wiley.
- [53] J.K. Swadesh, *HPLC: Practical and Industrial Applications*, 2. ed, **2000**: CRC Press.
- [54] Safety Data Sheet: Diethyl ether, Sigma-Aldrich, Version: 18.06.2015
- [55] E.R. Chamorro, S.N. Zambón, W.G. Morales, A.F. Sequeira, and G.A. Velasco, *Study of the Chemical Composition of Essential Oils by Gas Chromatography*, in *Gas Chromatography in Plant Science, Wine Technology, Toxicology and Some Specific Applications*, D.B. Salih, Editor. **2012**, InTech: Rijeka, Shanghai.
- [56] D. Frohne and U. Jensen, *Systematik des Pflanzenreichs: unter besonderer Berücksichtigung chemischer Merkmale und pflanzlicher Drogen*, 5. ed, **1998**, Stuttgart: Wissenschaftliche Verlagsgesellschaft.
- [57] P.J. Marriott, R. Shellie, and C. Cornwell, *J. Chrom. A*, **2001**, 936, 1-22.
- [58] Safety Data Sheet: 1,8-Cineole, A. Aesar, Version: 27.08.2014
- [59] Safety Data Sheet: Camphor, A. Aesar, Version: 05.11.2015
- [60] *Europäisches Arzneibuch*, 7. ed, **2011**, Stuttgart: Deutscher Apotheker Verlag.
- [61] L. Almela, B. Sanchez-Munoz, J.A. Fernandez-Lopez, M.J. Roca, and V. Rabe, *J. Chromatogr. A*, **2006**, 1120, 221-9.
- [62] M.M. Ozcan and J.C. Chalchat, *Int. J. Food Sci. Nutr.*, **2008**, 59, 691-8.
- [63] I. Mizrahi, M.A. Juarez, and A.L. Bandoni, *J. Essent. Oil Res.*, **1991**, 3, 11-15.
- [64] D.E. Gibson, G.P. Moore, and J.A. Pfaff, *Am. J. Emerg. Med.*, **1989**, 7, 41-43.
- [65] A.F.d.N. (AFNOR), *Huile essentielle de Romarin (Rosmarinus officinalis L.)*, **2001**: Paris.
- [66] F. Chemat, M.A. Vian, and G. Cravotto, *Int. J. Mol. Sci.*, **2012**, 13, 8615-27.
- [67] N. Rombaut, A.-S. Tixier, A. Bily, and F. Chemat, *Biofuels, Bioprod. Bioref.*, **2014**, 8, 530-544.
- [68] W. Brand-Williams, M.E. Cuvelier, and C. Berset, *LWT-Food Sci. Technol.*, **1995**, 28, 25-30.
- [69] *Count of publications "antioxidant activity microemulsion"*, Cited: 08.12.2015 Available from: scifinder.cas.org.
- [70] P. Bauduin, D. Touraud, W. Kunz, M.P. Savelli, S. Pulvin, and B.W. Ninham, *J. Colloid Interface Sci.*, **2005**, 292, 244-54.
- [71] M. Clausse, J. Peyrelasse, J. Heil, C. Boned, and B. Lagourette, *Nature*, **1981**, 293, 636-638.
- [72] M.L. Klossek, D. Touraud, and W. Kunz, *Green Chem.*, **2012**, 14, 2017.
- [73] M. Sahimi, *Applications of Percolation Theory*, **1994**, London: Tayler & Francis.
- [74] E. Kuraya, S. Nagatomo, K. Sakata, D. Kato, O. Niwa, T. Nishimi, and M. Kunitake, *Anal. Chem.*, **2015**, 87, 1489-1493.

- [75] S. Kim, W.K. Ng, S. Shen, Y. Dong, and R.B.H. Tan, *Colloids Surf. A*, **2009**, 348, 289-297.
- [76] W.L.S. Sim, M.Y. Han, and D. Huang, *J. Agric. Food Chem.*, **2009**, 57, 3409-3414.
- [77] C. Dima, G. Coman, M. Cotârlet, P. Alexe, and Ș. Dima, *AUDJG - Food Technology*, **2013**, 37, 39-49.
- [78] J. Balogh, L. Marques, and A. Lopes, *Nonionic Model Microemulsions to Study Interactions with Active Components and Antioxidant Activity*, in *Microemulsions - An Introduction to Properties and Applications*, D.R. Najja, Editor. **2012**, InTech: Rijeka, Shanghai.
- [79] L. Roth and K. Kormann, *Duftpflanzen Pflanzendüfte - Ätherische Öle und Riechstoffe*, **1997**, ecomed verlagsgesellschaft AG & Co. KG: Landsberg.
- [80] A. Freyburger, *Investigation and Development of a concentrated fully water dilutable lecithin-based microemulsion for food application*, Master Thesis, **2013**, Department of Physical and Theoretical Chemistry at University of Regensburg
- [81] C. Endert, *Optimization of a Fully Water Dilutable Beverage Concentrate Based on a Microemulsion*, Master Thesis, **2015**, Department of Physical and Theoretical Chemistry at University of Regensburg
- [82] S.A. Yang, S.K. Jeon, E.J. Lee, N.K. Im, K.H. Jhee, S.P. Lee, and I.S. Lee, *Journal of clinical biochemistry and nutrition*, **2009**, 44, 253-9.
- [83] M.R.M. Junior, T.A.A.R.e. Silva, G.C. Franchi, A. Nowill, G.M. Pastore, and S. Hyslop, *Food Chem.*, **2009**, 116, 8-12.
- [84] D. Grosjean, E.L. Williams, E. Grosjean, J.M. Andino, and J.H. Seinfeld, *Environ. Sci. Technol.*, **1993**, 27, 2754-2758.
- [85] T. Braure, Y. Bedjanian, M.N. Romanias, J. Morin, V. Riffault, A. Tomas, and P. Coddeville, *The journal of physical chemistry. A*, **2014**, 118, 9482-90.
- [86] A.N. Campbell and G.R. Lakshminarayanan, *Can. J. Chem.*, **1965**, 43, 1729-1737.
- [87] X. Wen and E.I. Franses, *J. Colloid Interface Sci.*, **2000**, 231, 42-51.
- [88] P. Ekwall, T. Rosendahl, and N. Löfman, *Acta Chem. Scand.*, **1957**, 11, 590-598.
- [89] M.C. Carey, *J. Hepatol.*, **1984**, 4, 66S-71S.
- [90] T.E. Sintra, A. Luís, S.N. Rocha, A.I.M.C. Lobo Ferreira, F. Gonçalves, L.M.N.B.F. Santos, B.M. Neves, M.G. Freire, S.P.M. Ventura, and J.A.P. Coutinho, *ACS Sustainable Chem. Eng.*, **2015**, 3, 2558-2565.
- [91] S. Both, R. Ditz, M. Tegtmeier, U. Jenelten, and J. Strube, *Process Engineering and Product Design for Green Extraction*, in *Green Extraction of Natural Products*. **2015**, Wiley-VCH Verlag GmbH & Co. KGaA. 37-70.
- [92] M. Kassing, U. Jenelten, J. Schenk, and J. Strube, *Chem. Eng. Technol.*, **2010**, 33, 377-387.

8 Conclusion

The main objective of this thesis was to invent new extraction methods and optimize existing extraction methods in regard to the principles of green extraction and biorefinery.

First of all, an alternative extraction method of iris rhizomes was investigated to obtain iris butter. The research was focused on a fast, selective, and environmentally friendly extraction of irones, the main odorants in iris rhizomes. To this purpose, supercritical fluid extraction (SFE) with carbon dioxide was performed. It was observed that the extracts of SFE contained up to 30% of irones. This is three times the amount compared to conventional iris butter obtained by steam distillation. Consequently, a more valuable extract can be produced by SFE compared to conventional techniques.

Furthermore, the extraction of antioxidant compounds (rosmarinic acid and carnosic acid) from rosemary leaves was investigated. The first approach was the optimization of an existing extraction method (hydro distillation). In detail, it was found that the aqueous residue of the distillation contains a significant amount of antioxidants. In regard to the concept of biorefinery, this residue can be an alternative to common antioxidants, like ascorbic acid, in conventional beverages.

In the final part, an alternative green extraction method of antioxidants from rosemary leaves was presented. In particular, micellar extractions, with different salts of fatty acids, are performed. It was shown that almost the total amount of rosmarinic acid and three-quarter of the water insoluble carnosic acid can be extracted by means of a 4 wt% sodium myristate within 5 min. In addition, an alternative processing method of the extract was invented in order to recover selectively the carnosic acid. This is the first process used to obtain carnosic acid by extractions with aqueous solutions.

To conclude, two new green extraction methods were investigated in this thesis, which provide high valuable products. No toxic or harmful solvents were used. Moreover, both extraction techniques were performed at relatively low temperatures and within few minutes. This leads to a significant decrease of energy consumption, compared to conventional extraction techniques. Further, no waste products are produced as all arisen compounds can be re-used in subsequent extractions or applied elsewhere.

In future, it is preferable to apply the invented extraction techniques in an industrial scale. These methods can also be used for the selective extraction of hydrophobic and thermal-labile ingredients, like antioxidants or fragrances, from other plant materials. The development of these new green and sustainable extraction processes can be an approach to manage the growing demand of plant-based extracts and products.

A Definition of technical terms and natural compounds

Technical terms:

Absolutes: Essential oil (especially expensive oil from blossoms), manufactured by dissolving of concretes in ethanol, precipitation of insoluble compounds (waxes, paraffin) at low temperature, filtration or centrifugation of sparingly soluble compounds and distillation of ethanol in vacuum. It is also called absolue. Examples: jasmine absolue, rose absolue, mimosa absolue [1].

Concretes: Plant extracts (especially expensive extracts from blossoms), manufactured by extraction with low-boiling solvents (e.g. petroleum ether, benzine, hexane), containing the simultaneous extracted waxes, paraffin, and other sparingly in ethanol soluble compounds. The solvent is recovered by distillation. It should be as pure as possible and free of disturbing odorants. Examples: jasmine concrete, rose concrete, mimosa concrete [1].

Essential oil: Mixtures of several compounds gained by distillation of plant material. It is highly volatile. Some essential oils are recovered by mechanical processes: e.g. lemon oil from peels by rasping, pressing and centrifugation. There are over 200 important essential oils from seeds, roots, leafs, wood, herbs, fruit-peels and resins [1].

Enfleurage: Extraction of natural odorants, mainly from blossoms, by cold adsorption of blossom oils in odorless fats (e.g. beef, mutton or pork fat, occasional also petroleum jelly). Glass plates, coated on both sides with fat, are sprinkled with flowers and hung in a special rack. The sprinkling of flowers is repeated several times, resulting in an enrichment of the fragrance in the fat. The so-called pomade is obtained. The absolue d'Enfleurage is produced by the elution with ethanol. Example: jasmine [1].

Hydrosol: In steam distillation, the distilled and condensed water phase is called hydrosol. If this hydrosol is recycled and taken to carry out another steam or hydro distillation the process is called cohobation [2].

Resinoids: Concentrated, non-aqueous extract of dried plant material. Sometimes commercially products, which contain a higher proportion of solvent to facilitate further processing, are called resinoids. It is not a pure extract such as concretes and absolutes [1].

Natural compounds:

Antioxidants: An antioxidant is a molecule that inhibits or slows down the oxidation of other molecules. Thereby, an antioxidant prevents the start of an oxidative chain reaction or interrupts the continuation by quenching free radicals. In addition it can be distinguished between natural antioxidants, like ascorbic acid (vitamin C), and synthetic ones, like butylated hydroxytoluene (BHT) [3, 4].

Flavonoids: Flavonoids are a class of plant secondary metabolites, with the general molecule structure as it can be seen in Figure A.1. It can be further distinguished between isoflavonoids and neoflavonoids, which are distinguished from flavonoids by the position of the phenyl and/or ketone group. Furthermore, these main structures can contain additional functional groups (e.g. hydroxyl, carbonyl, and aldehyde) [5].

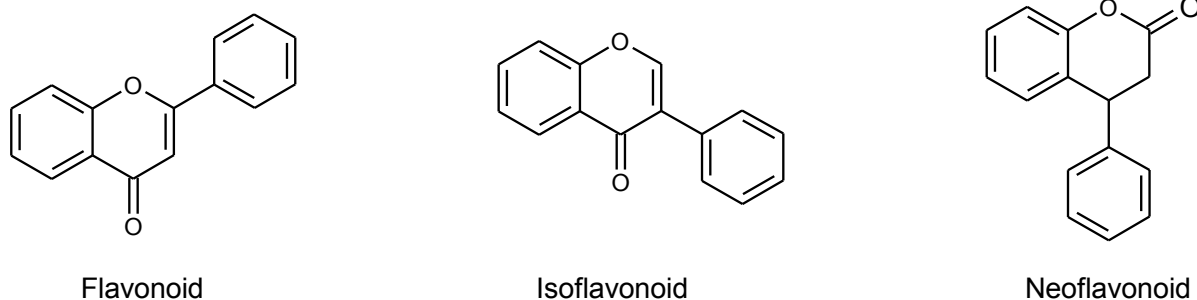


Figure A.1: Chemical structures of flavonoids, isoflavonoids, and neoflavonoids.

Saponins: Saponins are amphiphilic glycosides which can be found in various plant species. The molecule consists of one or more hydrophilic glycoside part combined with a lipophilic triterpene or steroid derivative. Most of the saponins are natural surfactants, which lower the surface tension of water and form stable foams. However, they taste bitter and are toxic for fish [6].

Terpenes: Terpenes are hydrocarbons, whereas terpenoids contain additional functional groups (e.g. hydroxyl, carbonyl, and aldehyde). They cover a great range of diverse compounds: up to 25000 terpenoids have been identified. They often possess flavoring properties. Terpenoids are mainly known as major components of essential oils. Isoprene (C_5H_8) is the building block of terpenoids. Terpenoids are classified according to the number of isoprene units. The main classes are listed in with some structures represented in [7]

Table A.1: Classification of terpenes with corresponding number of C-atoms and examples.

Type	Number of C-atoms	Examples
Monoterpene	10	linalool, limonene, pinene
Sesquiterpene	15	farnesol, bisabolene
Diterpene	20	phytol, retinol, taxadiene
Sesterterpene	25	geranylfarnesol
Triterpene	30	sapogenin
Tetraterpene	40	β -carotene, xanthophyll

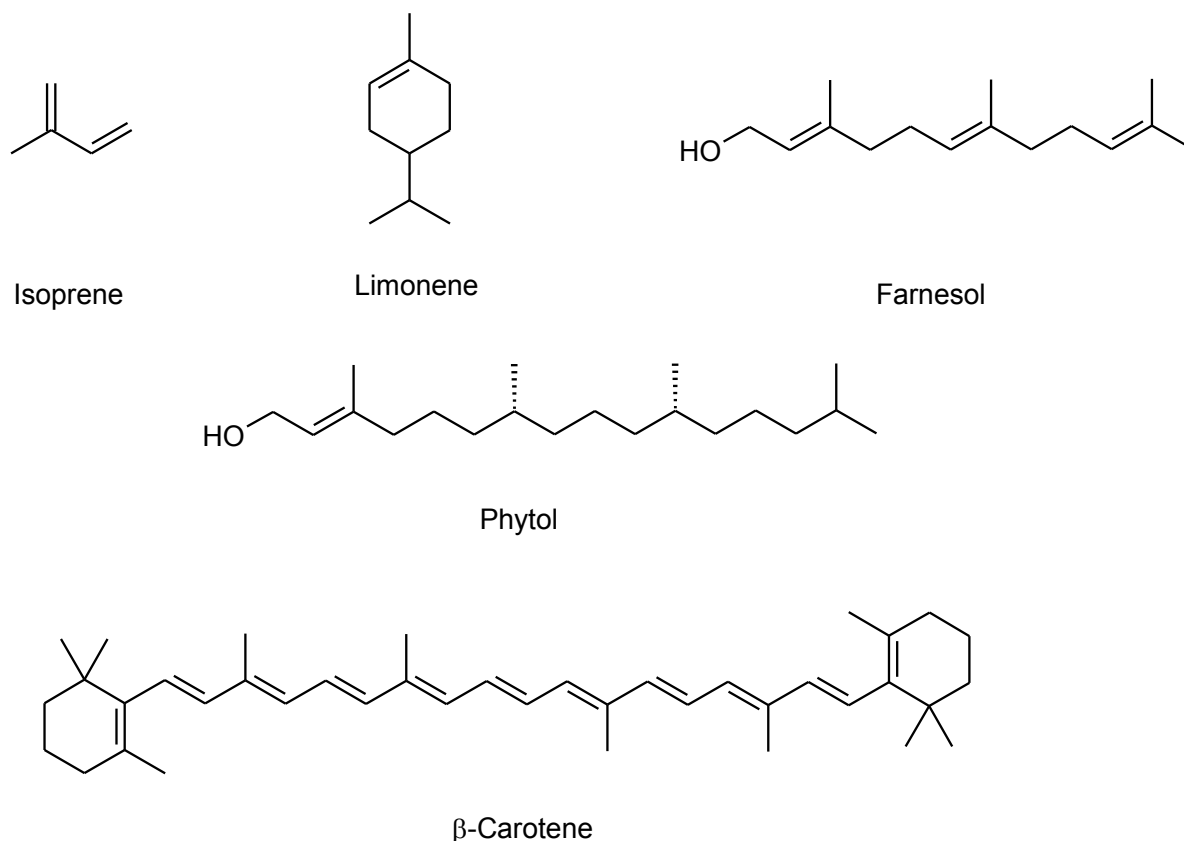


Figure A.2: Chemical structure of different terpenoids.

References

- [1] L. Roth and K. Kormann, *Duftpflanzen Pflanzendüfte - Ätherische Öle und Riechstoffe*, **1997**, ecomed verlagsgesellschaft AG & Co. KG: Landsberg.
- [2] S. Catty, *Hydrosols: the next aromatherapy*, **2001**, Rochester: Healing Arts Press.
- [3] M.P. Kähkönen, A.I. Hopia, H.J. Vuorela, J.-P. Rauha, K. Pihlaja, T.S. Kujala, and M. Heinonen, *J. Agric. Food Chem.*, **1999**, 47, 3954-3962.
- [4] D.L. Madhavi, S.S. Deshpande, and D.K. Salunkhe, *Food Antioxidants: Technological: Toxicological and Health Perspectives*, **1995**, New York: Marcel Dekker.
- [5] IUPAC, *Flavonoids (isoflavonoids and neoflavonoids)*, in *Compendium of Chemical Terminology*, A.D. McNaught and A. Wilkinson, Editors. **1997**, Blackwell Scientific Publications: Oxford.
- [6] K. Hostettmann and A. Marston, *Saponins*, **2005**, New York: Cambridge University Press.
- [7] F. Chemat and J. Strube, *Green Extraction of Natural Products*, 1. ed, **2015**, Weinheim: Wiley-VCH Verlag GmbH & Co. KGaA.

List of figures

Figure 2.1: Procedure of (A) steam and (B) hydro distillation of plant material to obtain the essential oil.....	4
Figure 2.2: Sketch of a Soxhlet extraction apparatus for the exhaustive extraction of plant material.....	7
Figure 2.3: Selection of solvents which are suitable for different plant ingredients [7].	8
Figure 2.4: Phase diagram of carbon dioxide. Data from [54-57].	15
Figure 2.5: Simplified flow scheme of a supercritical fluid extraction unit with the most important sections.....	19
Figure 3.1: Schematic representation of nanodroplets formed in (A) o/w-microemulsions and (B) w/o-microemulsions. Adapted from [13].	30
Figure 3.2: A typical ordering of cations and anions in “Hofmeister Series” with their most important properties and effects. Adapted from [19].....	31
Figure 4.1: Presentation of the curve according to the equation of Van Deemter depending on the height of a theoretical plate H and the linear velocity u of the mobile phase.....	36
Figure 4.2: General chromatogram with the retention times of the mobile phase (t_m), the total (t_r) and net (t_s) retention time of a compound X and the integrated area of a peak.	37
Figure 4.3: Simplified scheme of a high-performance liquid chromatography (HPLC) system.	39
Figure 4.4: Simplified scheme of a gas chromatography (GC) system.	42
Figure 4.5: Reaction between the DPPH radical (violet) and an antioxidant yielding the neutralized DPPH molecule (orange). The corresponding UV/VIS spectra are also shown. A significant decrease of the absorbance at 518 nm appears during the reaction and can be used to follow the reaction.	45
Figure 5.1: Sketch of the supercritical fluid extraction unit "LAB SFE 100 mL – 4368".	47
Figure 5.2: Engineering plan of the supercritical fluid extraction unit "LAB SFE 100 mL – 4368".	48
Figure 5.3: Home screen of the CO ₂ pump (P200) with configuration options and actual values.	50
Figure 5.4: Picture of the (A) 0.1 L (A40) and (B) 1 L (A41) extraction vessel with different connection options for the pipes. Normally, (1) is used as inlet at the bottom and (2) as outlet	

of the vessel. The lateral outlet (3) is used if the mixer is used during extraction. Also the sapphire windows (4) of the A41-vessel can be seen..... 53

Figure 5.5: (A) Back pressure regulator valve (BPR400) and (B) normal valve to control manually the pressure in the extraction unit. 54

Figure 5.6: Picture of the (1) first and (2) second separator and (3) the regulating valve MRV501. Additionally, the draining valves of both separators (4, 5) are shown. 55

Figure 5.7: Starting window of the software Labview™ with the different steps that should be performed before starting an experiment. 57

Figure 5.8: Window of software to adjust the value of the temperature in the oven (1) and the separators (2). The flow value of CO₂ can be entered in (3). 59

Figure 5.9: (A) Installation of the vessel lid (1) with a lip seal (2), sintered disc (3), snap ring (4), and filter paper (5). (B) Mounted lid of the extraction vessel A40. 60

Figure 5.10: (A) Pipes and dip tube of the separator to be removed for recovery of the extract. (B) Connection pipe in oven. 62

Figure 5.11: Development of pressure and temperature in the extraction vessel (A40), first separator (S50), and second separator (S51). In addition, the flow of CO₂ in g/min is plotted. 63

Figure 5.12: Dismounting procedure of the back pressure regulation valve (BPR400). 64

Figure 6.1: Full picture of an *Iris germanica* L. plant with blossoms, leafs, roots and the rhizome. 69

Figure 6.2: Chemical structures of isoflavones present in *Iris germanica* and *Iris pallida* rhizomes [1]. 70

Figure 6.3: Formation of different irone isomers (*cis*- α -irone, *trans*- α -irone, β -irone, *cis*- γ -irone) due to oxidation of their precursors iridals (iripallidal, iriflorental). 71

Figure 6.4: Overview of the current procedure to extract iris rhizomes and obtain iris butter. (A) iris plant; (B) fresh iris rhizome; (C) peeled and dried iris rhizome; (D) milled iris rhizomes; (E) iris butter; 74

Figure 6.5: HPLC chromatogram of a Soxhlet extract obtained from iris rhizomes. Peak identification: (1) acetovanillone; (2) isoflavones and irone related compounds; (3) α -ionone (IS); (4) irones; (5) iridals and iridal esters; 84

Figure 6.6: Section of HPLC chromatograms of a technical irone mixture (Sigma-Aldrich) and iris butter (Phytotgante) with the assignment of the different irone isomers. 85

Figure 6.7: Chemical structures of *cis*- α -irone and the potential internal standard compounds *trans*-anethole and α -ionone. 86

- Figure 6.8: Determination of the response factor of irones with α -ionone for internal standard calibration by HPLC/UV. The slope of the graph indicates the response factor (yellow block). β correlates to the mass concentration of irones and α -ionone and a is the determined peak area of the compounds. 87
- Figure 6.9: GC chromatogram of a Soxhlet extract obtained from iris rhizomes. Peak identification: (1) α -ionone (IS); (2) irones; (3) myristic acid (IS); (4) other fatty acids and compounds; 89
- Figure 6.10: Section of GC chromatograms of a technical irone mixture and iris butter with the assignment of different irone isomers..... 89
- Figure 6.11: Determination of the response factor of irones with α -ionone for internal standard calibration by GC/FID. The slope of the graph indicates the response factor (yellow block). β correlates to the mass concentration of irones and α -ionone and a is the determined peak area of the compounds..... 90
- Figure 6.12: TLC-sheet of a technical irone mixture (1) and methanol extract of iris rhizomes (2) stained with an anisaldehyde/ sulfuric acid solution. The violet spot corresponds to irones..... 92
- Figure 6.13: Investigation of the residual moisture of Iris 2011 rhizomes. The values were determined by the mass loss of grinded rhizomes in a compartment drier at 45 °C. A maximum value of 5.20% is reached after 48 h..... 93
- Figure 6.14: Time-dependent mass loss of water (millipore) and irones (technical mixture of *cis*- and *trans*- α -irone from Sigma-Aldrich) in the compartment drier at 45 °C..... 94
- Figure 6.15: Soxhlet extractions of *Iris germanica* L. rhizomes with different solvents. Comparison of the irone content in the rhizomes, total mass extraction yield and the content of irones in the extract for methanol (MeOH), ethanol (EtOH), acetone, ethyl acetate (EtAc), a mixture of EtAc/EtOH (70/30 v/v), and methyl *tert*-butyl ether (MTBE). 96
- Figure 6.16: External appearance of different single iris rhizomes and the corresponding total irone peak area determined by GC/FID..... 98
- Figure 6.17: Irone content of 1 year (Iris 2015.1), 2 years (Iris 2015.2) and 3 years (Iris 2011) stored *Iris germanica* rhizomes before and after the artificial oxidation by sodium nitrite..... 99
- Figure 6.18: HPLC chromatograms and corresponding irone yields of the ultrasound-assisted solvent extraction of iris rhizomes with hexane, methyl-THF, and methanol. Peak identification: (1) acetovanillone; (2) α -ionone (IS); (3) irones (*cis*- α - and *cis*- γ -irone); (4) butylated hydroxytoluene (BHT); 101

Figure 6.19: HPLC chromatograms of a common iris butter obtained by steam distillation and a commercial CO₂-extract (Flavex). Peak identification: (1) acetovanillone; (2) α -ionone (IS); (3) *cis*- γ -irone; (4) *cis*- α -irone; 103

Figure 6.20: Schematic drawing of the supercritical fluid extraction unit with different components of the unit (black boxes) and corresponding variable parameters (red boxes). 104

Figure 6.21: Mass extraction yield in the first (S50) and second (S51) separator obtained by SFE with CO₂ at 60 °C in dependence of the pressure in the extraction vessel..... 106

Figure 6.22: Total extraction yield of irones obtained by SFE in dependence of the CO₂ density in the extraction vessel. Extractions were carried out for 2 h with CO₂ at 60 °C and 40 °C at different pressure values. 106

Figure 6.23: HPLC chromatograms and corresponding irone yields of the first (S50) and second (S51) separator obtained by SFE with CO₂. The experiment was carried out for 2 h at 60 °C and 300 bar in the extraction vessel. Peak identification: (1) acetovanillone; (2) α -ionone (IS); (3) irones (*cis*- α - and *cis*- γ -irone);..... 107

Figure 6.24: Overview of the investigated parameters during DoE and corresponding calculated *b*-values for the total irone yield. The dotted line represents the level of significance. 116

Figure 6.25: Variation of pressure during static pressure extraction of iris rhizomes in the extraction vessel (A40), the first separator (S50), and the second separator (S51) of the SFE-unit..... 119

Figure 6.26: HPLC chromatograms and corresponding irone yields of the first (S50), and the second (S51) separator, as well as the purge solution (Purge) after the experiment and the Soxhlet extract (Soxhlet) of the residual rhizomes after SFE. Extractions were carried at a static pressure. Peak identification: (1) acetovanillone; (2) α -ionone (IS); (3) irones (*cis*- α - and *cis*- γ -irone); 120

Figure 6.27: Variation of pressure during dynamic pressure extraction of iris rhizomes in the extraction vessel (A40), the first separator (S50), and the second separator (S51) of the SFE-unit..... 121

Figure 6.28: HPLC chromatograms and corresponding irone yields of the first (S50), and the second (S51) separator, as well as the purge solution (Purge) after the experiment and the Soxhlet extract (Soxhlet) of the residual rhizomes after SFE. Extractions were carried at with a dynamic pressure. Peak identification: (1) acetovanillone; (2) α -ionone (IS); (3) irones (*cis*- α - and *cis*- γ -irone); 122

- Figure 6.29: HPLC chromatograms and corresponding irone yields of the first (S50), and the second (S51) separator obtained by SFE with ethanol as cosolvent. Peak identification: (1) acetovanillone; (2) α -ionone (IS); (3) irones (*cis*- α - and *cis*- γ -irone);..... 125
- Figure 6.30: Irone yields of the first (S50) and second (S51) separator obtained by SFE with CO₂ at 100 bar in dependence of the CO₂-density in the extraction vessel. The corresponding temperatures and the supercritical (sc) or liquid (l) state of CO₂ are also given..... 127
- Figure 6.31: Chromatograms and corresponding irone yields of the first (S50) and second (S51) separator, as well as the purge solution (Purge) after the experiment and the Soxhlet extract (Soxhlet) of the residual rhizomes after SFE. Extractions were carried out at a temperature of 60 °C and pressure of 100 bar in the extraction vessel. Peak identification: (1) acetovanillone; (2) α -ionone (IS); (3) irones (*cis*- α - and *cis*- γ -irone);..... 128
- Figure 6.32: Irone yield of SFE in depending on different pretreatment aqueous solutions (water, sodium myristate, acetic acid). 130
- Figure 7.1: Pictures of (A) fresh and (B) dried leaves of *Rosmarinus officinalis* L..... 142
- Figure 7.2: Chemical structures of the main essential oil compounds (camphor, 1,8-cineole, α -pinene, borneol, α -terpineol) present in rosemary leaves..... 143
- Figure 7.3: Chemical structures of the main antioxidants (carnosic acid, carnosol, rosmanol, rosmarinic acid) and flavones (genkwanin, luteolin, diosmetin) present in rosemary leaves. 144
- Figure 7.4: HPLC chromatogram of a methanol Soxhlet extract of rosemary leaves. Peak identification: (1) rosmarinic acid; Carnosic acid and carnosol are probably present at retention times between 40 and 50 min..... 157
- Figure 7.5: Determination of the linear function of rosmarinic acid for external calibration. The concentration of rosmarinic acid is plotted against the corresponding peak area. By means of the slopes and intercept of the graph, the rosmarinic acid concentration of an extract sample can be calculated..... 158
- Figure 7.6: Chemical structures of potential internal standard molecules (butylated hydroxyanisole, butylated hydroxytoluene, coumarin, gemfibrozil). 159
- Figure 7.7: HPLC chromatograms of different potential internal standards, rosmarinic acid and carnosic acid at detection wavelengths of 204 nm and 285 nm. Peak identification: (1) rosmarinic acid; (2) carnosic acid; (3) BHA; (4) BHT; (5) coumarin; (6) gemfibrozil 160
- Figure 7.8: Determination of the response factors of rosmarinic acid (K_{CAC}) and rosmarinic acid (K_{RAC}) with gemfibrozil for internal standard calibration. The slopes of the graphs indicate the corresponding response factors of the antioxidants. β correlates to the mass

concentration of the antioxidants and gemfibrozil, whereas, a is the determined peak area of the compounds. 162

Figure 7.9: GC/FID chromatogram of rosemary essential oil obtained by hydro distillation. Separation was achieved on a nonpolar HP-5 column. Peak identification: (1) 1,8-cineole; (2) camphor; 163

Figure 7.10: Determination of the linear functions of 1,8-cineole and camphor for external calibration. The concentrations of the essential oils are plotted against the corresponding peak areas. By means of the slopes and intercept of the graph, the concentrations of 1,8-cineole and camphor in an extract sample can be calculated. 164

Figure 7.11: Investigation of the residual moisture of normal rosemary leaves. The values were determined by the mass loss of grinded leaves in a compartment drier at 40 °C. A maximum value of 3.48% is reached after 48 h. 166

Figure 7.12: Mass concentration of rosmarinic acid and carnosic acid yields obtained by Soxhlet extraction lasting 4 h with different solvents: water, methanol and acetone. Concentrations are given in mg of antioxidant per 1 g of rosemary leaves. 167

Figure 7.13: HPLC chromatograms of Soxhlet extracts from rosemary leaves obtained by different solvents: water, methanol and acetone. Peak identification: (1) rosmarinic acid; (2) carnosol; (3) gemfibrozil (IS); (4) carnosic acid; 168

Figure 7.14: (A) Differential and (B) total extraction yield of essential oil gained by hydro distillation and steam distillation at different times. The yield is given in weight percent of the initial mass of rosemary leaves. 170

Figure 7.15: Time-dependent content of camphor in the rosemary essential oil obtained by hydro distillation and steam distillation. The yield is given in weight percent of the mass of essential oil collected after the given time. 171

Figure 7.16: Time-dependent mass concentrations of rosmarinic acid and carnosic acid yields obtained by hydro distillation of rosemary leaves. The yield is given in weight percent of the initial mass of rosemary leaves. 172

Figure 7.17: Time-dependent mass concentrations of rosmarinic acid and carnosic acid in the residual rosemary leaves after hydro distillation. The content of antioxidants was investigated by Soxhlet extractions with methanol. The yield is given in weight percent of the acids relative to the initial mass of rosemary leaves. 173

Figure 7.18: HPLC chromatograms of the hydro distillation water residue after 2.5 h and the subsequent Soxhlet extraction of the corresponding residual rosemary leaves with methanol. Peak identification: (1) rosmarinic acid; (2) carnosol; (3) gemfibrozil (IS); (4) carnosic acid; 174

Figure 7.19: Influence of concentration on the inhibition of different compounds: rosmarinic acid, carnosic acid, butylated hydroxyanisole, ascorbic acid and α -tocopherol.	177
Figure 7.20: Influence of molar ratio of compound to DPPH on the inhibition of different compounds: rosmarinic acid, carnosic acid, butylated hydroxyanisole, ascorbic acid, and α -tocopherol.....	178
Figure 7.21: (A) Influence of the dilution on the inhibition of hydro distillation water residues gained after 0.5, 1.5, 2.5 and 4.0 h and (B) Soxhlet extracts obtained with different solvents: water, acetone, and methanol.....	180
Figure 7.22: Pseudo-ternary phase diagram of SDS/1-pentanol/ <i>n</i> -dodecane/hydro distillation water residue of rosemary leaves at 25 °C and a constant weight ratio of SDS to 1-pentanol (1:2). The grey areas represent the microemulsion domain. LC indicates a liquid crystalline area. The cross marks the starting point of the conductivity measurements. Also the antioxidant activities were measured in samples with compositions of the microemulsion on the black line.....	182
Figure 7.23: The specific conductivity of the microemulsions as a function of (A) water respectively (B) hydro distillation water residue mass fraction for the pseudo ternary system SDS/1-pentanol (1:2)/dodecane/water. In addition the corresponding structures of the microemulsions are shown. The measurements were carried out at 25 °C.	184
Figure 7.24: Newly established method to determine the antioxidant activity of the hydro distillation water residue in a microemulsion.	186
Figure 7.25: Percentage of inhibition in microemulsion (SDS/1-pentanol(1:2)/ <i>n</i> -dodecane/hydro distillation water residue) and methanol solutions in relation to the mass fraction of hydro distillation water residue.	187
Figure 7.26: Chemical structures of the investigated essential oils: <i>trans</i> -anethole, limonene, linalool, citral A (geranial, <i>trans</i> -isomer), α -terpineol, 1,8-cineole, camphor, α -ionone, and menthol (as main compound in nana mint oil).	189
Figure 7.27: UV/VIS spectra of different essential oils after the reaction with DPPH. Investigated compounds are <i>trans</i> -anethole, limonene, linalool, citral, α -terpineol, 1,8-cineole, camphor, α -ionone, and menthol (as main compound in Nana mint oil).	190
Figure 7.28: Pseudo ternary phase diagram of TWEEN 60®/ethanol/limonene/hydro distillation water residue of rosemary leaves at 25 °C and a constant weight ratio of TWEEN 60® to ethanol (2:1). The grey areas represent the microemulsion domain. The antioxidant activities were measured in samples with compositions of the microemulsion on the black line.....	191

- Figure 7.29: Percentage of inhibition in microemulsion (TWEEN® 60/ethanol (2:1)/limonene/hydro distillation water residue) and methanol solutions in relation to the mass fraction of hydro distillation water residue..... 193
- Figure 7.30: UV/VIS spectra of nana mint oil microemulsion with pure water and hydro distillation water residue after the reaction with DPPH. 194
- Figure 7.31: HPLC/UV chromatograms of the antioxidants before and after the addition of a 0.1 M NaOH solution. (A) Rosmarinic acid (RAc) standard solution (0.2 mg/mL) (B) Rosmarinic acid after the addition of NaOH (C) Carnosic acid (CAc) standard solution (0.2 mg/mL) with the internal standard gemfibrozil (D) Carnosic acid solution after the addition of NaOH with the internal standard gemfibrozil. 196
- Figure 7.32: Mass concentration of rosmarinic acid and carnosic acid yield obtained by micellar extraction for different durations. A 3 wt% solution of sodium myristate was used for every extraction. 198
- Figure 7.33: Mass concentration of rosmarinic acid and carnosic acid yields obtained by micellar extraction with varying concentrations of sodium myristate. Extraction time was always 5 min at 45 °C stirred in a water bath. 199
- Figure 7.34: Influence of pH value on the extraction yield of the antioxidants rosmarinic acid and carnosic acid. Extractions were carried out within 5 min at 45 °C stirred in a water bath. 200
- Figure 7.35: Influence of the rosemary leaves particle size and ultrasound-assisted (US) extraction on the extraction yield of antioxidants. All extractions were carried with sodium myristate solutions (3 wt%) for 5 min at 45 °C..... 202
- Figure 7.36: Overview of the different investigated extraction methods and the corresponding extraction yield of rosmarinic acid and carnosic acid. All experiments were carried out for 5 min and 45 °C. 203
- Figure 7.37: Overview of the different investigated surfactants and the corresponding extraction yield of rosmarinic acid and carnosic acid. For the experiments a 4 wt% solution of sodium myristate (NaC14), a technical sodium myristate solution (NaC14 (techn.)), potassium myristate (KC14), and potassium stearate (KC18) was used. All extractions were carried out for 5 min and 45 °C in an ultrasonic bath..... 204
- Figure 7.38: HPLC chromatograms of a sodium myristate and acetone extract. Peak identification: (1) rosmarinic acid; (2) carnosol; (3) gemfibrozil (IS); (4) carnosic acid; 206
- Figure 7.39: Ratio of carnosic acid in myristate and acetone extract. The samples were analyzed after different storage times (room temperature, without light exposure) to investigate the stability of the antioxidant in the extract over time. 207

Figure A.1: Chemical structures of flavonoids, isoflavonoids, and neoflavonoids.	220
Figure A.2: Chemical structure of different terpenoids.....	221

List of tables

Table 2.1: Physical properties of solvents in different states of aggregation [59].....	16
Table 4.1: Eluotropic series for common HPLC solvents, arranged by increasing eluting power with silica gel as stationary phase. Adapted from [3].	40
Table 5.1: Maximum operating conditions (pressure, temperature) of different process parts.	65
Table 6.1: Isomeric distribution of irones in iris butter of <i>Iris germanica</i> L. and <i>Iris pallida</i> Lam. from literature, with the corresponding odor [1, 6, 67].	76
Table 6.2: Overview of the different used iris rhizomes. The storage time refers to the value which was current at the delivery date. The name of the samples includes the year of delivery.	77
Table 6.3: Overview of the actual irone content and isomer distribution in iris rhizomes of different species and varying storage times.	97
Table 6.4: Summary of the examined characteristic parameters of iris rhizomes from different species and varying storage time.....	100
Table 6.5: Overview of performed experiments for this sub-chapter. Parameters of the experiments were extraction time, flow of CO ₂ , temperature and pressure in the extraction vessel (A40), first (S50), and second (S50) separator.....	105
Table 6.6: Overview of investigated factors (X_i) of the parameters and their corresponding maximum (+1) and minimum (-1) values.....	109
Table 6.7: First line to establish the Hadamard matrix for the design of experiments with the number of maximum investigable parameters (n) and number of experiments (m). (+) indicates the maximum value and (-) the minimum value of a parameter.	109
Table 6.8: Matrix of experiments and effects obtained by circular permutation of the first line of the Hadamard matrix by Plackett and Burman. (+) indicates the maximum value and (-) the minimum value of the factor (X_i) of the parameter.	110
Table 6.9: Schedule of experiments which have to be carried out based on the Hadamard matrix (matrix of experiments). Y_j represents the response of each experiment, thus the extraction yield.....	111
Table 6.10: Overview of the extraction yields (mass extraction yield and irone yield: total, separator 1 [S50] and separator 2 [S51]) obtained for every experiment.....	111

Table 6.11: Summary of the performed experiments according to the Hadamard matrix (matrix of experiments) with the corresponding total irone yield (response Y_j) and calculated b-values (b_j) of the investigated parameters.	113
Table 6.12: Overview of the extraction yields (mass extraction yield and irone yield: total, separator 1 [S50] and separator 2 [S51]) obtained for the experiment No. 8 from the matrix of experiments.	114
Table 6.13: Overview of investigated factors (X_i) of the parameters and their corresponding maximum (+1) and minimum (-1) values. The best values are marked green if they are significant for the extraction and stripped green if they are not significant.	116
Table 6.14: Overview of parameters of the experiment with ethanol as modifier: extraction time, flow of CO ₂ , flow of ethanol (EtOH), temperature and pressure in the extraction vessel (A40), first (S50), and second (S50) separator.	124
Table 6.15: Overview of realized experiments for this sub-chapter. Parameters of the experiments were extraction time, flow of CO ₂ , temperature and pressure in the extraction vessel (A40), first (S50), and second (S50) separator.	126
Table 7.1: Response factors K_{AO} of carnosic acid and rosmarinic acid for different internal standards (BHA, BHT, coumarin, gemfibrozil) in dependence on the detection wavelenth. Suitable K-values are marked green, whereas inappropriate values are marked red.	161
Table 7.2: Summary of the examined characteristic parameters of normal and defatted rosemary leaves.	169
Table 7.3: Stoichiometric value of the reaction DPPH-AO and number of reduced DPPH molecules per molecule antioxidant of different compounds: rosmarinic acid, carnosic acid, butylated hydroxyanisole, ascorbic acid, and α -tocopherol.	178
Table A.1: Classification of terpenes with corresponding number of C-atoms and examples.	220

List of publications

Posters

- (1) **Alexander Wollinger**, Elodie Perrin, Jamal Chahboun, Valérie Jeannot, Nadine Payrot, Didier Touraud and Werner Kunz - Extraction and Quality of Essential Oil from *Rosmarinus officinalis*-Leaves and Detection of Rosmarinic Acid Distillation Water Residues, Gemeinsames Jahrestreffen der ProcessNet-Fachgruppen February 26th-28th, 2014, TU München, Freising/Weißenstephan
- (2) **Alexander Wollinger**, Theresa Höß, Didier Touraud, Werner Kunz – Extraction of *Iris germanica* L., 33èmes Journées Internationales Huiles Essentielles Extraits, September 24th – 25th, 2014, Digne les Bains, France
- (3) Neslihan Aslan, **Alexander Wollinger**, Didier Touraud and Werner Kunz - Antioxidant Activity of Hydro Distillation Water Residues from *Rosmarinus officinalis* L. in Microemulsions, 33èmes Journées Internationales Huiles Essentielles Extraits, September 24th – 25th, 2014, Digne les Bains, France
- (4) **Alexander Wollinger**, Didier Touraud and Werner Kunz - Extraction of *Iris germanica* L. with supercritical CO₂, Jahrestreffen der ProcessNet-Fachgruppe “Phytoextrakte – Produkte und Prozesse” 2015, February 23rd, 2015, Maritim Hotel Bonn, Germany
- (5) **Alexander Wollinger**, Didier Touraud and Werner Kunz - Extraction of *Iris germanica* L. with supercritical CO₂, International Workshop on Alternative Solvents for Extraction, Purification and Formulation - WAS, June 4, 2015, Avignon, France

Papers

- (1) **Alexander Wollinger**, Elodie Perrin, Jamal Chahboun, Valérie Jeannot, Didier Touraud, Werner Kunz - Antioxidant activity of hydro distillation water residues from *Rosmarinus officinalis* L. leaves determined by DPPH assays (accepted in *Comptes Rendus Chimie*)
- (2) **Alexander Wollinger**, Valérie Jeannot, Didier Touraud, Werner Kunz - Antioxidant activity of hydro distillation water residues from *Rosmarinus officinalis* L. leaves in microemulsions (in preparation)

Inventor's notification for a patent

- (1) **Alexander Wollinger**, Theresa Höß, Didier Touraud, Werner Kunz – Selektive Extraktion von hydrophoben Antioxidantien aus Pflanzen mit Hilfe von wässrigen Mizellaren Lösungen

Declaration

Hiermit erkläre ich, dass ich die vorliegende Dissertation ohne unzulässige Hilfe Dritter und ohne Benutzung anderer als der angegebenen Hilfsmittel angefertigt habe. Die aus anderen Quellen direkt oder indirekt übernommenen Daten und Konzepte sind unter Angabe des Literaturzitats gekennzeichnet. Die Arbeit wurde bisher weder im In- noch Ausland in gleicher oder ähnlicher Form einer anderen Prüfungsbehörde vorgelegt.

Regensburg, 29. Februar 2016

(Wollinger Alexander)